PRESTRESSED CONCRETE BEAMS INTERMIXED WITH STEEL BEAMS FOR BRIDGE WIDENING

(FINAL REPORT)

by

Robert N. Bruce, Jr.
James C. O'Hara
and
P. Michael Lynch

for

State of Louisiana
Department of Transportation and Development
Louisiana Transportation Research Center

In cooperation with
U. S. Department of Transportation
Federal Highway Administration

State Project No. 736-10-45

May 1987

Civil Engineering Department
Tulane University
New Orleans, Louisiana

METRIC CONVERSION FACTORS*

To Convert from	To	Multiply by
	Length	
foot	meter (m)	0.3048
inch	millimeter (mm)	25.4
yard	meter (m)	0.9144
mile (statute)	kilometer (km)	1.609
	Area	
square foot	square meter (m^2)	0.0929
square inch	square centimeter (cm^2)	6.451
square yard	square meter (m^2)	0.8361
	Volume (Capacity)	
cubic foot	cubic meter (m^3)	0.02832
gallon (U.S. liquid)**	cubic meter (m^3)	0.003785
gallon (Can. liquid)**	cubic meter (m^3)	0.004546
ounce (U.S. liquid)	cubic centimeter (cm^3)	29.57
	Mass	
ounce-mass (avdp)	gram (g)	28.35
pound-mass (avdp)	kilogram (kg)	0.4536
ton (metric)	kilogram (kg)	1000
ton (short, 2000 lbs)	kilogram (kg)	907.2
	Mass per Volume	
pound-mass/cubic foot	kilogram/cubic meter (kg/m^3)	16.02
pound-mass/cubic yard	kilogram/cubic meter (kg/m^3)	0.5933
pound-mass/gallon (U.S.)**	kilogram/cubic meter (kg/m^3)	119.8
pound-mass/gallon (Can.)**	kilogram/cubic meter (kg/m^3)	99.78
	Temperature	
deg Celsius (C)	kelvin (K)	$t_K=(t_C+273.15)$
deg Fahrenheit (F)	kelvin (K)	$t_K=(t_F+459.67)/1.8$
deg Fahrenheit (F)	deg Celsius (C)	$t_C=(t_F-32)/1.8$

*The reference source for information on SI units and more exact conversion factors is "Metric Practice Guide" ASTM E 380.

**One U.S. gallon equals 0.8327 Canadian gallon.

ABSTRACT

The object of this research was to investigate the behavior, under various conditions, of a typical bridge span in which prestressed concrete beams and steel beams are used in the same span. The bridge investigated was the westbound I-10 Bonnabel Overpass in Metairie, Louisiana, in which steel beams were used in the original construction, and prestressed concrete beams were used for a subsequent widening. The steel girders were installed with intermediate diaphragms at the third points, but the concrete girders do not have intermediate diaphragms at all. It was felt that the use of prestressed concrete girders in combination with steel girders could lead to potential problem areas related to camber growth of the prestressed concrete girders, different coefficients of thermal expansion between concrete and steel, different stiffnesses for the concrete and steel, different support techniques for concrete and steel, and effects related to distribution of live load.

The investigation consisted of three main parts: the adaptation of a commercially available computer program, MSC/NASTRAN, to a mixed girder span; field testing of a typical span as a means of evaluating the computer program; and using the MSC/NASTRAN program to identify but not to solve potential problem areas.

The results of this investigation indicate that the MSC/NASTRAN computer program can be used successfully to predict live load span deflections for HS20-44 truck loads as well as overload truck cranes on mixed girder spans, provided that the computer input data is accurately defined.

The results indicate that the MSC/NASTRAN computer program has limitations in calculating the response of a mixed girder span to ambient thermal conditions, the main limitation being the definition of the temperature input data required by the computer program.

In the mixed girder system, the computer solution indicates that camber growth can have a marked effect on the maximum moment in the adjacent concrete and steel girders. For the assumed amount of camber growth (1/4"), the resulting moment increase in the concrete girder adjacent to the steel girder is quite large and of the same order of magnitude as the AASHTO design moment due to live loads.

For the mixed girder system, the maximum moment due to live load in the concrete girder adjacent to the steel girders will be greater than the moment in the interior concrete girders. In this case the moment in the adjacent concrete girder exceeds the AASHTO design value when loaded with side-by-side HS20-44 trucks by 25-45%, depending on the assumed conditions of the slab.

Concrete diaphragms which are installed for the purpose of distributing moments between girders are more effective at midspan than at the one-third span location. However,

the diaphragms modeled herein would not be effective in distributing moments because the end connections are too flexible. Care should be exercised in placing rigid diaphragms between the adjacent concrete and steel girders because of the probability of camber growth. An increase in rigidity in this case would further increase the moment due to camber growth in the adjacent concrete girder.

For the mixed girder system the combination of live load and camber growth may cause severe overloading of the concrete girder adjacemt to the steel girder. In the case of the Bonnabel Overpass, the computer results show that an HS20-44 truck live load and a 1/4" camber growth acting together will cause the maximum moment in the adjacent concrete girder to be approximately 100% greater than the AASHTO design value.

The report of the investigation makes the recommendation that the MSC/NASTRAN computer program be kept active and current and at the disposal of the State and the University. The report recommends further investigation of the combined effects of live load and camber growth in a mixed girder span, and further investigation of the combined effects of live load and thermal load.

Consideration should be given to a future investigation addressing in more detail the live load distribution and its relationship to AASHTO specifications.

TABLE OF CONTENTS

Page

1. INTRODUCTION

1.1 Object and Scope. 1
1.2 Background. 1
1.3 Outline of Investigation. 2
1.4 Acknowledgements. 4
1.5 Notation. 5

2. DESCRIPTION OF FIELD TESTS

2.1 Introduction. 6
2.2 Nominal HS20-44 Truck Test. 6
2.3 Overload Truck Crane Test 8
2.4 Thermal Deflection Test 11
2.5 Neoprene Bearing Pad Test 13
2.6 Measurement of Slab Thickness 13
2.7 Determination of Concrete Strength. 13

3. COMPARISON OF COMPUTER PREDICTIONS TO FIELD TESTS

3.1 Introduction. 32
3.2 Overload Truck Crane Test 33
3.3 Nominal HS20-44 Truck Test. 36
3.4 Thermal Deflection Test 37

4. INVESTIGATION OF MIXED GIRDER SUPPORT SYSTEM

4.1 Introduction. 56
4.2 Camber Growth 57
4.3 Temperature Effects 60
4.4 Live Load Distribution. 65
4.5 Concrete Diaphragms 74
4.6 Rolled Beams with Cover Plates. 77
4.7 Non-Composite Rolled Beams. 79
4.8 Bearing Movement Effects. 80
4.9 Combined Effects. 84

5. SUMMARY AND RECOMMENDATIONS

5.1 Summary 118
5.2 Recommendations 122

APPENDIX A

A.1 Introduction. 123
A.2 Description of Program. 124

LIST OF FIGURES

No.		Page
1	Nominal HS20-44 Loading Positions.	15
2	Location of Dial Indicators for Nominal HS20-44 Loading.	16
3	Live Load Deflections at Midspan for Nominal HS20-44 Loading Position 1 and Position 2.	17
4	Longitudinal Live Load Deflections for Nominal HS20-44 Loading Position 1	18
5	Longitudinal Live Load Deflections for Nominal HS20-44 Loading Position 2	19
6	Measured Wheel Loads for Overload Truck Crane.	20
7	Overload Truck Crane Loading Positions No. 1, No. 2, and No. 3.	21
8	Location of Dial Indicators for Overload Truck Crane Tests.	22
9	Live Load Deflections at Midspan for Overload Position No. 1	23
10	Live Load Deflections at Midspan for Overload Position No. 2	24
11	Live Load Deflections at Midspan for Overload Position No. 3	25
12	Longitudinal Live Load Deflections for Overload Position No. 1	26
13	Longitudinal Live Load Deflections for Overload Position No. 2	27
14	Longitudinal Live Load Deflections for Overload Position No. 3	28
15	Measured Vertical Deflections vs. Ambient Temperature.	29
16	Measured Longitudinal Deflections vs. Ambient Temperature.	30
17	Load Deflection Relationship for Neoprene Bearing Pad. . .	31
18	Span Transverse Centerline Computer Predicted vs. Measured Deflections for Overload Position No. 1	44

19	Span Transverse Centerline Computer Predicted vs. Measured Deflections for Overload Position No. 2	45
20	Span Transverse Centerline Computer Predicted vs. Measured Deflections for Overload Position No. 3	46
21	Computer Predicted vs. Measured Longitudinal Deflections for Overload Position No. 1.	47
22	Computer Predicted vs. Measured Longitudinal Deflections for Overload Position No. 2.	48
23	Computer Predicted vs. Measured Longitudinal Deflections for Overload Position No. 3.	49
24	Span Transverse Centerline Computer Predicted vs. Measured Deflections for Nominal HS20-44 Loading Position No. 1 and No. 2	50
25	Computer Predicted vs. Measured Longitudinal Deflections for Nominal HS20-44 Loading Position No. 1	51
26	Computer Predicted vs. Measured Longitudinal Deflections for Nominal HS20-44 Loading Position No. 2	52
27	Comparison of Temperature Induced Vertical Deflections as a Function of the Time of Day	53
28	Computer Predicted Deflections Across Transverse Centerline After Four Hours of Sunshine vs. Measured Deflections at Noon.	54
29	Computer Predicted Longitudinal Deflections as a Function of Temperature vs. Measured Longitudinal Deflections.	55
30	Layout of Model Span	87
31	Effect of Camber Growth on Moment at Midspan in Adjacent Concrete and Steel Composite Girders	88
32	Lateral Stress in Top and Bottom Fibers of Slab at Midspan Due to 1/4 in. Camber Growth.	89
33	Lateral Stresses in Slab Due to Ambient Temperature Changes	90
34	Longitudinal Stresses in Slab Due to Ambient Temperature Changes	91
35	Live Load Location for Determining Longitudinal Moment in Girders.	92

36 Live Load Location for Determining Lateral Moment in Slab 93

37 Moment in Girders at Midspan Due to HS20-44 Truck Load - Design Concrete Properties. 94

38 Moment in Girders at Midspan Due to HS20-44 Truck Load - Field Concrete Properties 95

39 Moment in Girders at Midspan Due to Two HS20-44 Trucks Side by Side - Design Concrete Properties, Uncracked Slab. 96

40 Moment in Girders at Midspan Due to Two HS20-44 Trucks Side by Side - Field Concrete Properties, Uncracked Slab. 97

41 Moment in Girders at Midspan Due to Two HS20-44 Trucks Side by Side - Field Concrete Properties, Both Old and New Slab Cracked. 98

42 Moment in Girders at Midspan Due to 220 k Overload Truck Crane - Design Concrete Properties. 99

43 Moment in Girders at Midspan Due to 220 k Overload Truck Crane - Field Concrete Properties 100

44 Typical Distribution of Wheel Loads to Grid Points for Moments in Slab Due to HS20-44 Truck Load 101

45 Variation of Moment in Slab Caused by HS20-44 Truck Load at Selected Locations 102

46 Variation of Maximum Moment in Slab as a Function of HS20-44 Truck Wheel Location. 103

47 Variation of Moment in Slab Caused by 220 k Overload Truck Crane at Selected Positions 104

48 Variation of Maximum Moment in Slab as a Function of 220 k Overload Truck Crane Wheel Location 105

49 Details of Diaphragms 106

50 Effect of Diaphragms at Third Span on Maximum Moment in Girder G-3 for HS20-44 Truck Load and 220 k OTC. 107

51 Effect of Diaphragms at Midspan on Maximum Moment in Girder G-3 for HS20-44 Truck Load and 220 k OTC. 108

52 Effect of Diaphragms at Third Span on Stresses in Slab for HS20-44 Truck Load and 220 k OTC 109

53 Typical Stress Distribution in Bottom Fibers of Girder G-6 Using Rolled Beams with Cover Plates 110

54 Effect of Length of Cover Plate on Maximum Stress in Bottom Fibers of Flange of Beam at End of Cover Plate . . . 111

55 Typical Moment Distribution for Girder G-6 When Using Rolled Beams with Cover Plates. 112

56 Vertical Deflection of Slab at Midspan Due to Camber Growth When Loaded with Dead Weight of Slab. 113

57 Effect of 0.1 in. Consolidation of Neoprene Pad on Lateral Stresses in Slab at End of Span 114

58 Combined Effect on the Moment at Midspan in Composite Girder Due to Dual HS20-44 Truck Load, 1/4 in. Camber Growth, and 0.1 in. Neoprene Pad Consolidation. 115

59 Combined Effect on the Lateral Stresses in Bottom Fibers of Slab at Midspan Due to Dual HS20-44 Truck Load, Three Hours of Sunshine, 1/4 in. Camber Growth, 0.1 in. Neoprene Pad Consolidation, and 30 F Temperature Increase of Steel Girders 116

60 Combined Effect on the Longitudinal Stresses in the Bottom Fibers of the Slab at Midspan Due to Dual HS20-44 Truck Load, Three Hours of Sunshine, 1/4 in. Camber Growth, 0.1 in. Neoprene Pad Consolidation, and 30 F Temperature Increase of Steel Girders. 117

A-1 Simple Bridge Model. 142

A-2 Bridge Model Grid Pattern. 143

A-3 Bridge Model Selected Elements 144

1. INTRODUCTION

1.1 Object and Scope

The object of the research reported herein is to determine the effects of using prestressed concrete and steel girders in combination in the same span. In order to accomplish this objective, a three-dimensional finite element computer program is used to model an existing bridge that incorporates a mixed girder support system; i.e., the I-10 Bonnabel Overpass located in Metairie, Louisiana. The computer model, loaded to measure deflections and stress levels, is used in combination with field measurements on the actual overpass field loaded by the same amount.

1.2 Background

Many of the bridges built in the U.S. in the late 1950's and throughout the 1960's were designed and constructed with steel plate girders and/or steel wide-flanged sections which support the deck. In the widening of certain bridges, the option to support the additional width with prestressed concrete girders is desirable. However, it is possible that the use of prestressed concrete girders in combination with steel girders can introduce problem areas:

1. The prestressed concrete girders are subject to camber growth, whereas the steel girders are not.
2. Concrete and steel reach ambient temperature at different stages.

3. The prestressed concrete girders normally are stiffer than the steel girders.
4. The AASHTO specifications which prescribe the transverse distribution of live load on a span were developed for same type support members, and may not be valid for a combined system of supports.
5. The present criteria for the design of bridge decks is based on a uniform deflection pattern; i.e., a cylinder rather than a dish.

Examination of the above potential problem areas is desirable.

1.3 Outline of Investigation

The I-10 Bonnabel Overpass in Metairie, Louisiana, is an existing bridge that incorporates a mixed girder support system; i.e., a combination of steel girders and prestressed concrete girders in the same span. This bridge is modeled in a three-dimensional finite element program as provided by the MacNeal Schwendler Corporation MSC/NASTRAN Program. Central to the research is the adaptation of the MSC/NASTRAN Program to the mixed girder support system. The investigation is in three parts, the first involving the adaptation of the computer program to the existing simple span bridge, the second involving field measurements for this bridge to verify the accuracy of the computer program, and the third involving the use of the computer program to

examine potential problems inherent in the use of prestressed concrete beams intermixed with steel beams. The investigation includes the following items:

I. Adaptation of MSC/NASTRAN Computer Program
   1. Acquisition, installation, and verification of MSC/NASTRAN computer program.
   2. Literature search to determine the existence of input packages.
   3. Development of input data for support system consisting of mixed girders, including:
      a) selection of elements and nodes,
      b) temperature variations and camber growth,
      c) grid point constraints,
      d) development of stiffness matrix, and
      e) establishment of output requirements.
   4. Operation of program to obtain data for existing bridge span for mixed girder support system.

II. Field Measurements
   1. Field testing of mixed girder support system.
   2. Analysis of results and comparison to MSC/NASTRAN Program.

III. Investigation of Mixed Girder Support System

1. Investigation of stresses and deflections under conditions of:

   a) live load for HS20-44 and overload truck

   b) maximum expected camber growth

   c) extreme temperature variations

   d) bearing movement differential

   e) addition of diaphragms

2. Evaluation of existing AASHTO specifications with respect to mixed girder support systems.

1.4 Acknowledgements

The work on the project was conducted by the Department of Civil Engineering of Tulane University for the Louisiana Department of Transportation and Development in cooperation with the Federal Highway Administration.

On the part of the Louisiana Department of Transportation and Development, the work was done under the administrative direction of Mr. S. C. Shah, Research and Development Engineer. Mr. Louis A. Garrido, Bridge Design Engineer; and Mr. Norval P. Knapp, Structural Design Engineer, contributed greatly to the investigation.

On the part of the Federal Highway Administration, the work was supervised by Mr. Mitchell D. Smith, Division Bridge Engineer.

On the part of Tulane University, the work was conducted under the administrative supervision of Dr. John L. Niklaus, Head of the Department of Civil Engineering; and Dr. Hugh A. Thompson, Dean of the School of Engineering.

Special appreciation is expressed to Mr. Fred Grilletta of the B & G Crane Service, Inc. for providing required equipment for the field tests. The manuscript was prepared by Mrs. Renee Ladmirault, and graphics were prepared by Mr. Charles H. McGee.

1.5 Notation

For reference purposes, girders are numbered across the transverse direction of the span tested, from south to north. Girders G-1, G-2, and G-3, are the three prestressed concrete girders on the south; girders G-4 through G-9 are the steel girders; and girder G-10 is the prestressed concrete girder on the north.

2. DESCRIPTION OF FIELD TESTS

2.1 Introduction

The existing I-10 Bonnabel Overpass incorporates a mixed girder support system; i.e., a combination of steel girders and prestressed concrete girders in the same span. The bridge provides the opportunity for the conduct of various load tests that can be used to determine the ability of the MSC/NASTRAN Program to predict the behavior of the mixed girder bridge. Principal among the field investigations are tests of load versus deflection for service load and for overload. Thermal deflection tests are also described in this section. In addition, it was necessary to conduct tests of the neoprene bearing pads, as well as determinations of slab thickness and concrete strength.

2.2 Nominal HS20-44 Truck Test

In an effort to provide the HS20-44 loading proposed, two trucks were placed back-to-back on a single span of the Bonnabel Overpass. The trucks were intended to provide a load approximately equivalent to the HS20-44 loading, and this equivalent load is designated as the nominal HS20-44 load in this report. The field test consisted of loading the span in two positions, as shown in Fig. 1. Each loading position has the two trucks back-to-back, as indicated in the figure, and centered longitudinally on the span. The

girder designation is indicated on Fig. 1. In the first position, the trucks are transversely centered over girders G-4 and G-5. In the second position, the trucks are transversely centered over girders G-2 and G-3. Axle loads and distance between axles are shown on Fig. 1. Loads were positioned and applied during a two-hour period beginning approximately at 3:00 a.m. on Sunday, May 26, 1985.

For the span tested, Fig. 2 shows the location of dial gages used to measure vertical and horizontal deflections. Dial gages designated as "V" measured vertical deflections. Dial gages designated as "R" measured horizontal lateral movement of individual girders and served to indicate any torsional motions. In general, the dial gages used were Starrett Dial Indicators Type 655-441J graduated to 0.001 in. with a range of 1.000 in. All dial indicators were zeroed under the existing dead load, so that dead load deflection was not measured. The deflections measured, recorded, and presented are for live load only. Transverse deflection patterns and longitudinal deflection patterns are plotted as a function of load position for each of the two loading positions described above.

Fig. 3 indicates live load deflections across a transverse section of the span at the middle of the span for loading position No. 1; i.e., the two trucks transversely centered over the two steel girders that are adjacent to the prestressed concrete girders. Fig. 3 also indicates live load deflections across the same transverse section for

loading position No. 2; i.e., the two trucks transversely centered over the two concrete girders that are adjacent to the steel girders.

Fig. 4 indicates longitudinal deflection patterns along four girders -- G-2, G-3, G-4, and G-5 -- for loading position No. 1. The deflections are for live load only.

Fig. 5 indicates longitudinal deflection patterns along the same four girders -- G-2, G-3, G-4, and G-5 -- for loading position No. 2.

Relative deflection values of adjacent girders may be noted from the figures.

The dial indicators designated as "R" did not indicate significant torsional motions.

2.3 Overload Truck Crane Test

The live load utilized in the overload test was provided by a Link-Belt wire rope truck crane model HC-258, with the weight of the crane and components applied with the crane in the "Upper Facing Rear" configuration, so that the nominal front axle load is 107,845 lbs. and the nominal rear axle load is 112,505 lbs. Actual wheel loads were determined by weighing the truck crane on June 12, 1985, four days before the test on June 16, 1985. Wheel loads as measured are indicated in Fig. 6. It may be noted from Fig. 6 that front and rear axle loads are approximately equal.

Six sets of deflection measurements were observed and recorded for six different positions of overload. Deflection measurements were recorded for the following positions:

SET	PURPOSE	CONFIGURATION
1	Initial Zero Reading	Load Off of Bridge
2	Load on Adjacent Span W	Load Position No. 1
3	Load on Test Span	Load Position No. 1
4	Load on Test Span	Load Position No. 2
5	Load on Test Span	Load Position No. 3
6	Final Zero Reading	Load Off of Bridge

Each loading position has the overload truck crane centered longitudinally on the span. Load position No. 1 has the overload truck crane transversely centered above girder G-5 as shown in Fig. 7. Load position No. 2 has the overload transversely centered above girder G-2 as shown in Fig. 7. Load position No. 3 has the overload transversely centered above girder G-8 as also shown in Fig. 7.

Fig. 8 shows the location of dial gages used to measure vertical and horizontal deflections. Dial gages designated as "V" measured vertical deflections. Dial gages designated as "R" measured horizontal lateral movement of individual girders and served to indicate any torsional motions. Dial gages designated as "B" measured movement of the support

system. In general, the dial gages used were the same that were used in the service load (nominal HS20-44) test. All dial indicators were zeroed under existing dead load, so that dead load deflection was not measured. The deflections reported are for live load (overload) only. Transverse deflection patterns and longitudinal deflection patterns are plotted as a function of load position for each of the three positions of load on the test span.

Fig. 9 indicates live load deflections across a transverse section of the span at the middle of the span for overload position No. 1; i.e., with the truck crane transversely centered above girder G-5.

Fig. 10 indicates live load deflections across the same transverse section for loading position No. 2; i.e., the overload transversely centered above girder G-2.

Fig. 11 indicates live load deflections across the same transverse section for loading position No. 3; i.e., with the overload transversely centered above girder G-8.

Fig. 12 indicates longitudinal deflection patterns along four girders -- G-2, G-3, G-4, and G-5 -- for loading position No. 1. The deflections are for live load (overload) only.

Fig. 13 indicates longitudinal live load deflection patterns along four girders -- G-2, G-3, G-4, and G-5 -- for loading position No. 2.

Fig. 14 indicates longitudinal live load deflection patterns along the same four girders -- G-2, G-3, G-4, and

G-5 -- for loading position No. 3.

For different loading positions, relative deflection of adjacent girders may be noted from the figures.

Dial indicators designated as "R" did not indicate significant torsional motions.

2.4 Thermal Deflection Test

In an effort to determine the field response of the bridge span to temperature change, temperature readings and bridge span deflections were measured over a twenty four hour period in November 1985. Both vertical and longitudinal deflections were measured for night time conditions, conditions of bright sunshine, and for conditions in between. Deflections were measured with dial gages graduated to 0.001 in. Vertical deflections were measured by dial gages located at the midspan of girders G-2, G-3, G-4, and G-5. The change in girder length was measured by dial gages located at each end of girder G-2, G-3, G-4, and G-5 in a manner to record the change in length of the bottom of each girder. The change in the distance between adjacent bent caps, located at the east end and the west end of the instrumented span, was measured by dial gages located so as to measure the movement of the bent cap relative to the ground. It should be noted that all interior bent caps are common to two adjacent spans. This is reflected in the motion of the bent caps, as shown in Fig. 16.

Fig. 15 indicates vertical deflections at midspan for girders G-2, G-3, G-4, and G-5 during the daily cycle. Direct sunshine on the bridge deck, expressed in terms of time of day, was considered an important cause of deflections. Thus, time of day is also indicated on the figure. The figure indicates a "zero" deflection for the early morning hours from 4:00 a.m. - 7:00 a.m., with deflections increasing upward as the sun rises and direct sunshine hits the bridge deck. It can be seen that the maximum vertical mid span movement during the twenty-four hour cycle is approximately equal to 0.13 in.

Fig. 16 indicates longitudinal deflections for various values of ambient temperature during the daily cycle. Time of day is also indicated in the figure. Change in girder length (measured at the bottom of the girder) is plotted as a function of ambient temperature, for a concrete girder G-3 and for a steel girder G-4. The change in the distance between adjacent bent caps, east end and west end of span, is plotted as a function of ambient temperature. Bent cap movements were measured relative to the ground. All deflection values were obtained with dial gages graduated to 0.001 in. Analysis of the temperature effects is given in Section 4.3. The interrelationship between distortions of the neoprene bearing pads and temperature variations is discussed in Section 4.8.

2.5 Neoprene Bearing Pad Test

The concrete girders in the Bonnabel Overpass are end-supported on compressible neoprene bearing pads. A typical neoprene pad, similar to those in use on the span investigated, was tested in the laboratory and found to have the load-deflection relationship shown in Fig. 17. The analysis presented in Section 4.8 of this report is adjusted to allow for the compressibility of the neoprene pads.

2.6 Measurement of Slab Thickness

By means of a nine-point grid on the original slab, a nine-point grid on the widened south portion of the bridge deck, and a three-point grid on the widened north portion of the bridge deck, slab thicknesses were measured under conditions of no traffic. Measurements were made to the nearest 0.01 ft. by means of a surveyor's level. The average thickness of the original deck slab was found to be 6.50 in. The average thickness of the slab on both widened portions of the bridge deck was found to be 7.44 in. All thickness values pertain only to the span tested and were used as input to the computer program.

2.7 Determination of Concrete Strength

Reports indicate that the concrete used in the prestressed girders was approximately 6500 psi equivalent 28- day compressive strength. The expected gain in strength over an eight-year period is approximately 38% for the Type

I cement used in the girders. It is reasonable to expect that the present strength of the concrete in the prestressed girders is approximately 8970 psi. An average of 33 nondestructive tests with a calibrated Schmidt impact hammer indicated a present average strength of 8460 psi for the concrete in the girders.

Reports indicated that the deck concrete was approximately 4000 psi equivalent 28-day compressive strength in the original structure. Nondestructive tests with the Schmidt impact hammer indicated a present average strength of 8040 psi for the deck concrete.

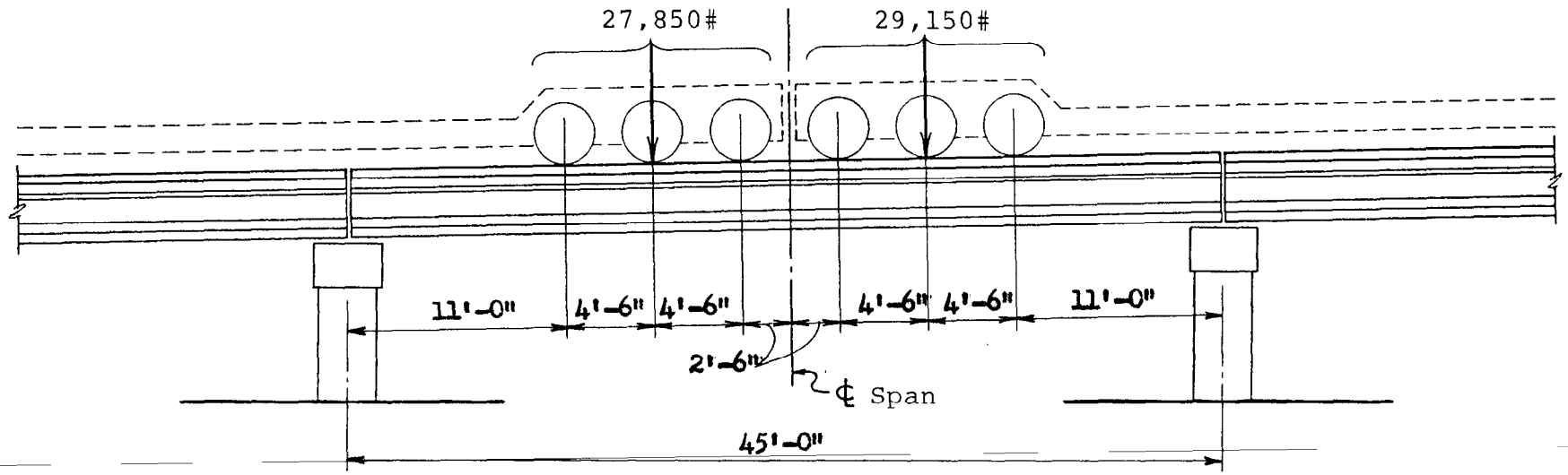

Longitudinal Elevation Looking North

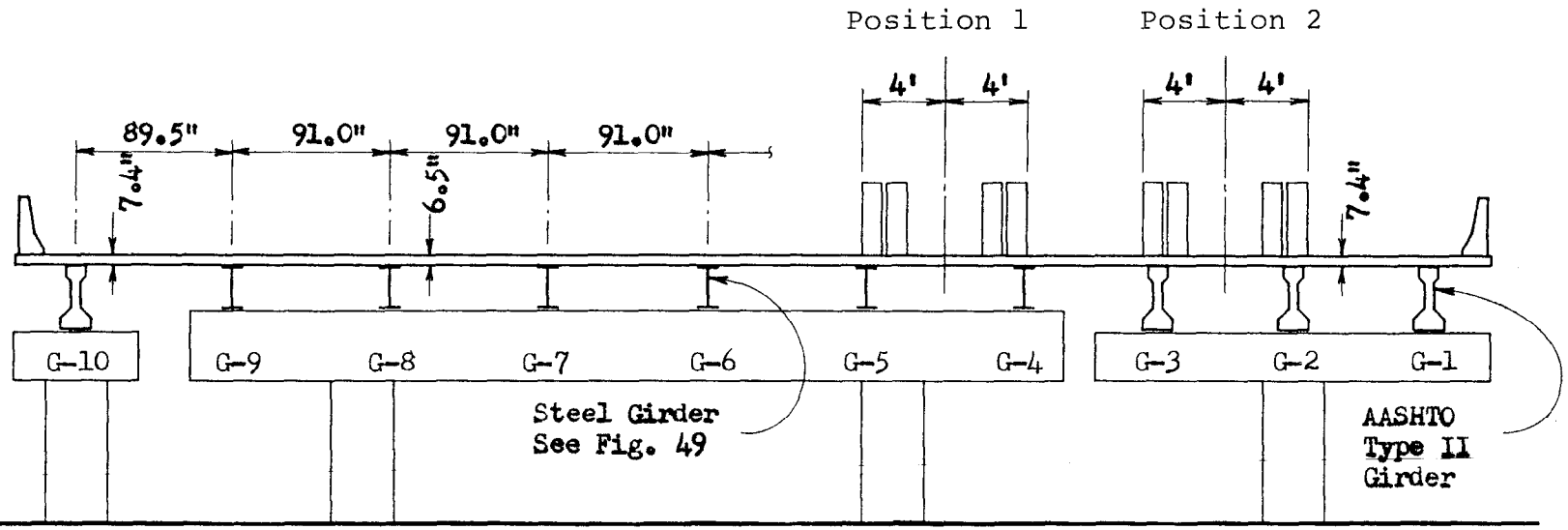

Transverse Section Looking East

FIG.1 NOMINAL HS20-44 LOADING POSITIONS

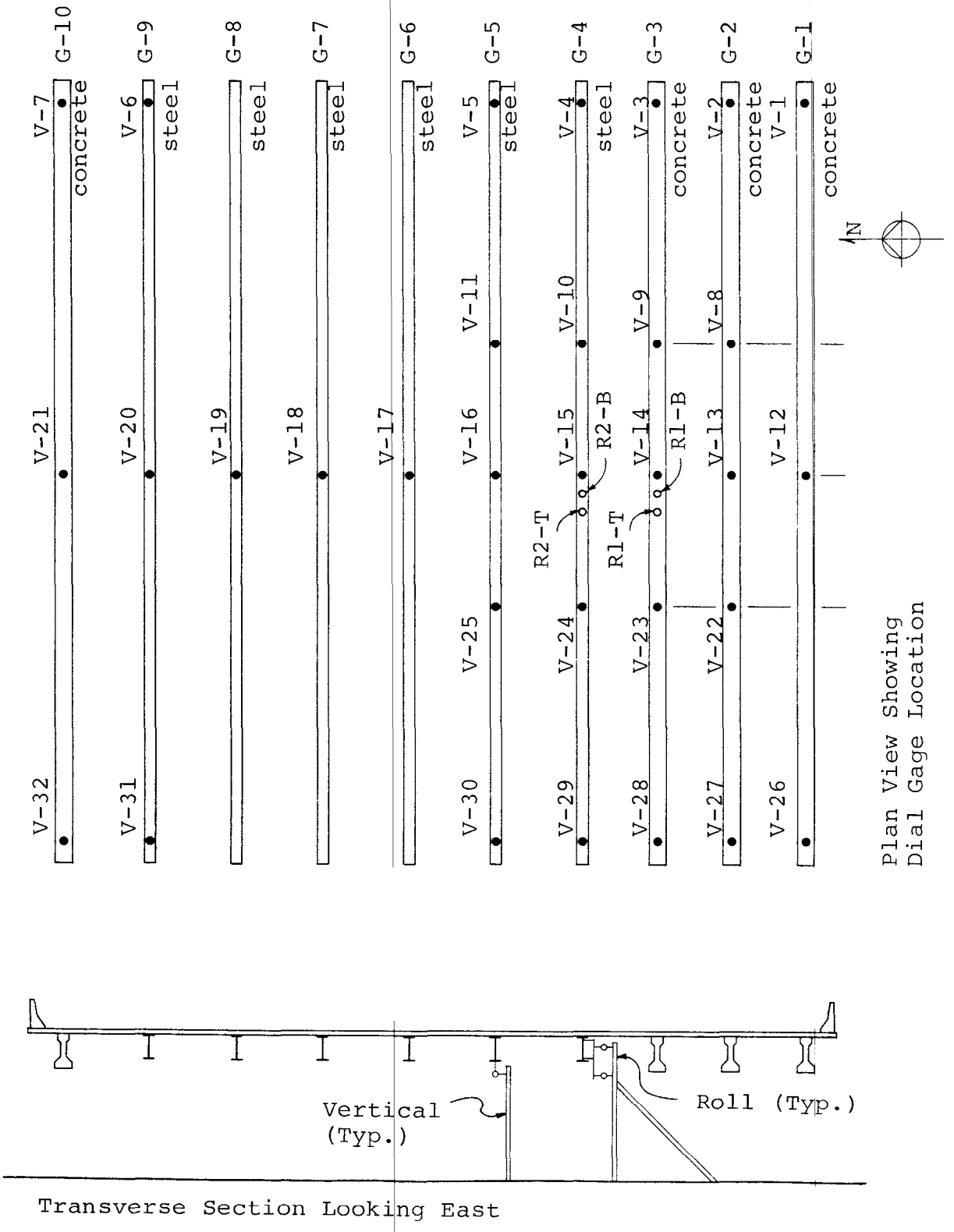

FIG. 2 LOCATION OF DIAL INDICATORS FOR NOMINAL HS20-44 LOADING

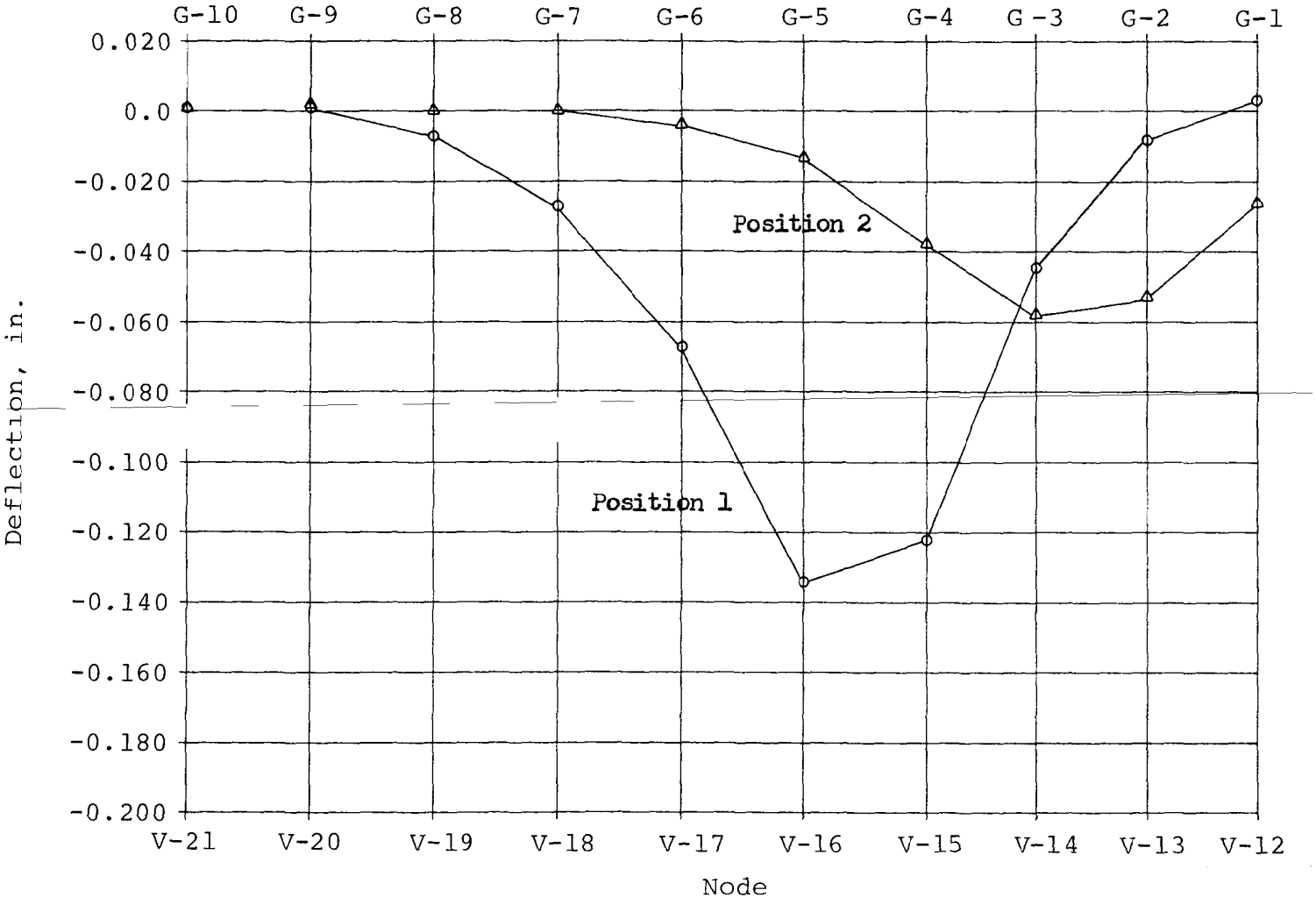

FIG. 3 LIVE LOAD DEFLECTIONS AT MIDSPAN FOR NOMINAL HS20-44 LOADING POSITION 1 AND POSITION 2

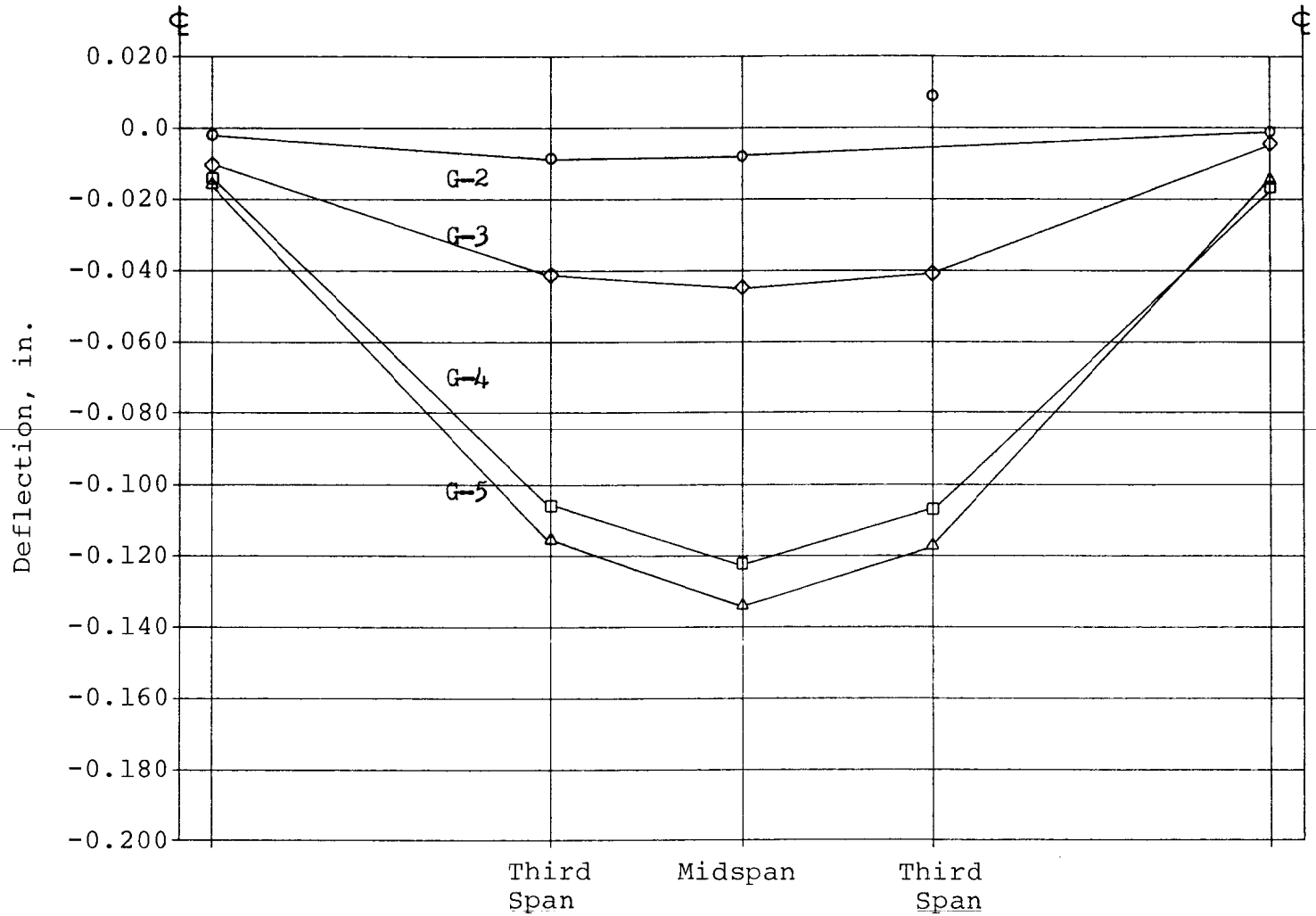

FIG. 4 LONGITUDINAL LIVE LOAD DEFLECTIONS FOR NOMINAL HS20-44 LOADING POSITION 1

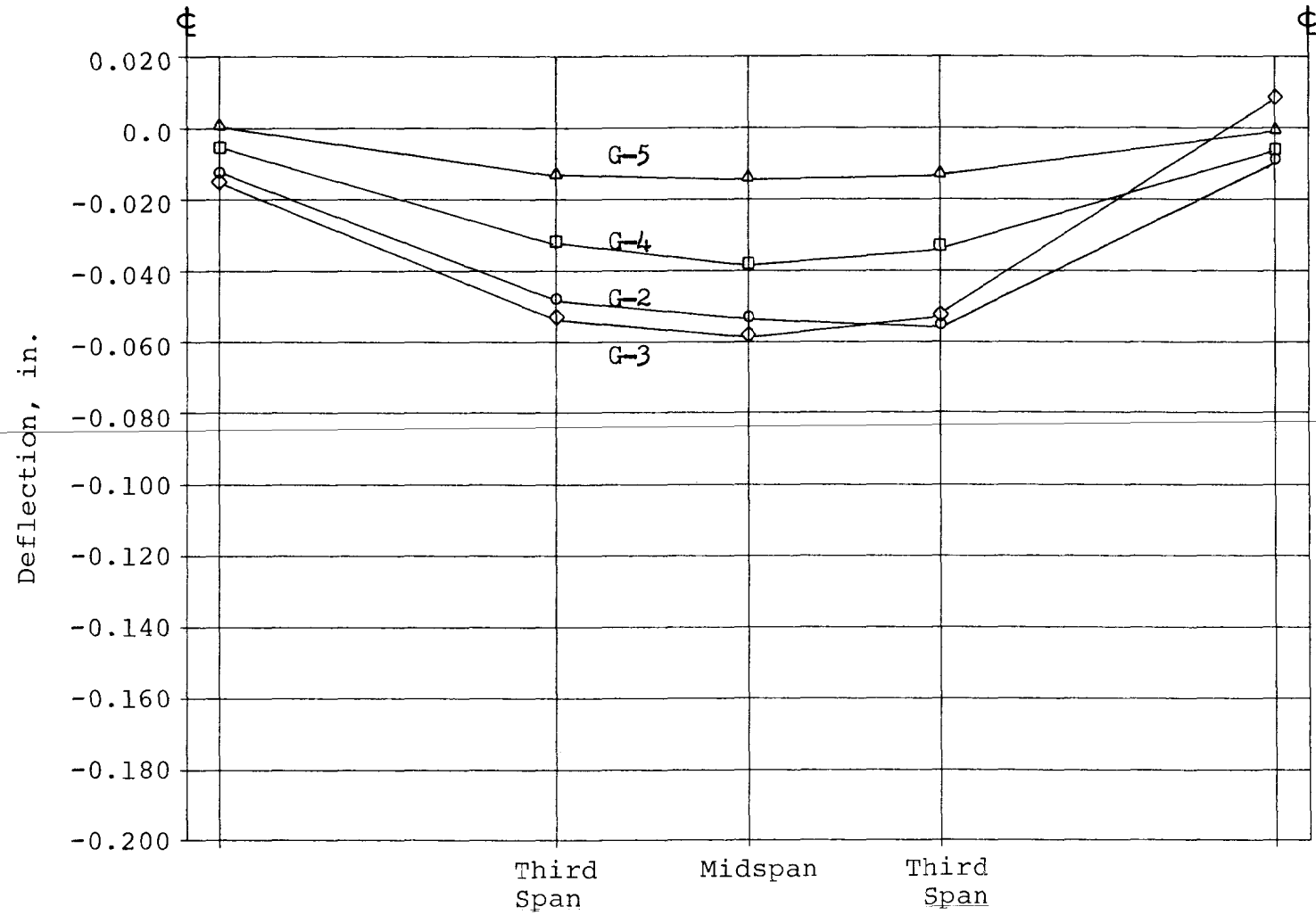

FIG. 5 LONGITUDINAL LIVE LOAD DEFLECTIONS FOR NOMINAL HS20-44 LOADING POSITION 2

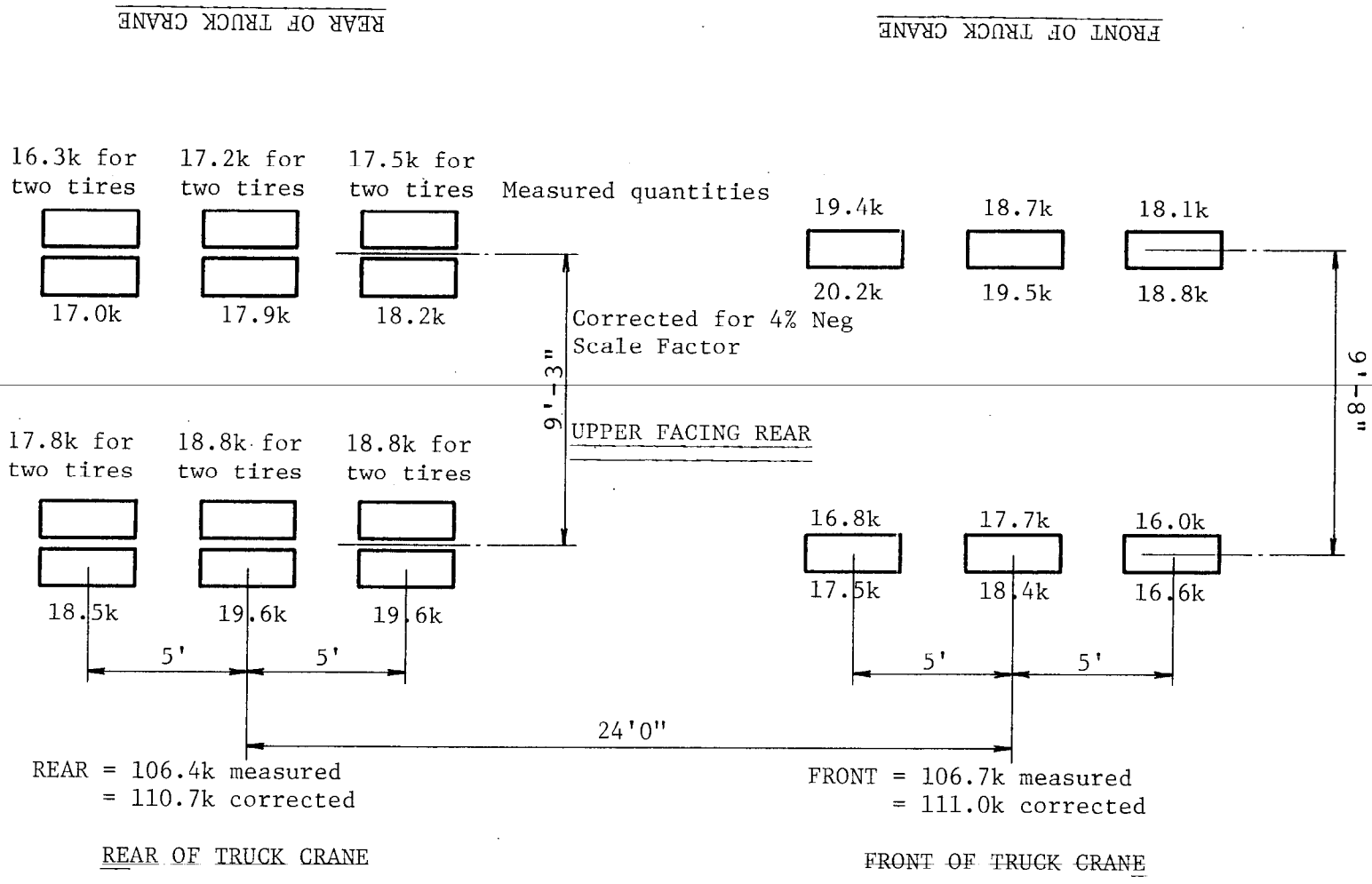

FIG. 6 MEASURED WHEEL LOADS FOR OVERLOAD TRUCK CRANE

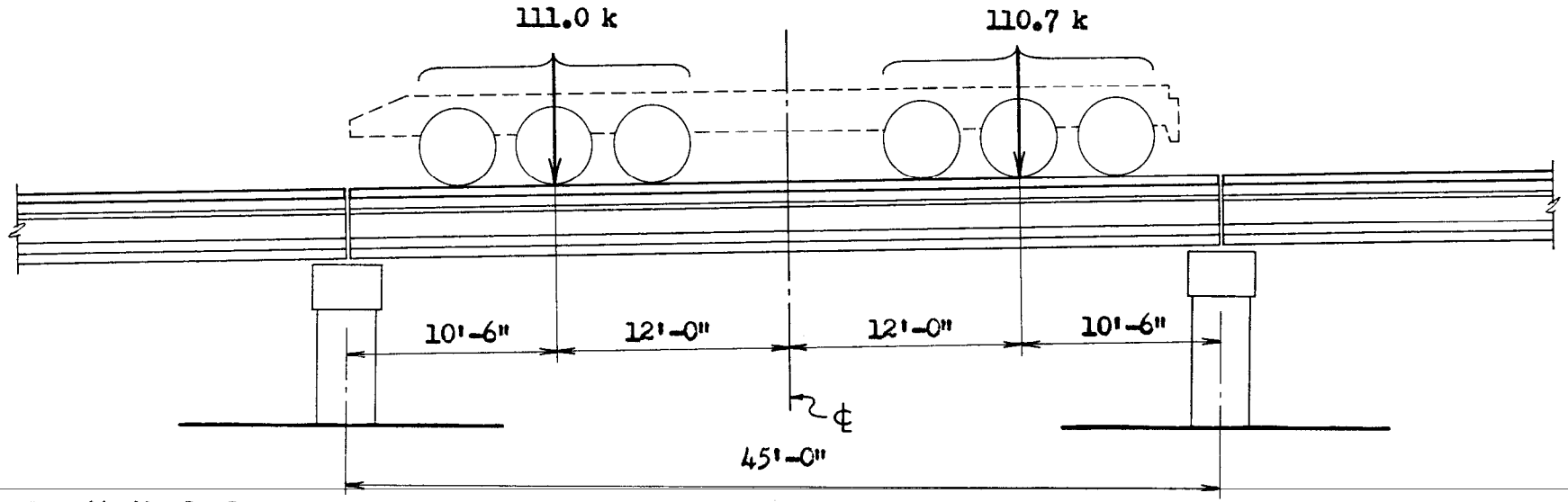

Longitudinal Elevation Looking North

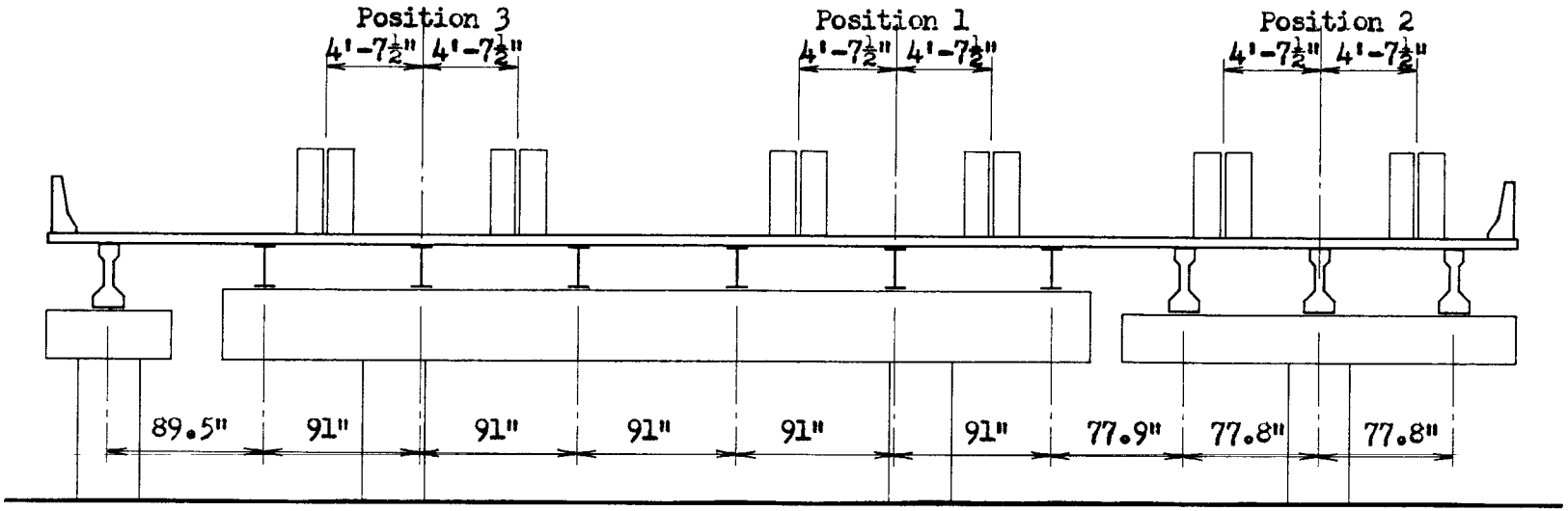

Transverse Section Looking East

FIG. 7 OVERLOAD TRUCK CRANE LOADING POSITIONS NO. 1, NO. 2, AND NO. 3

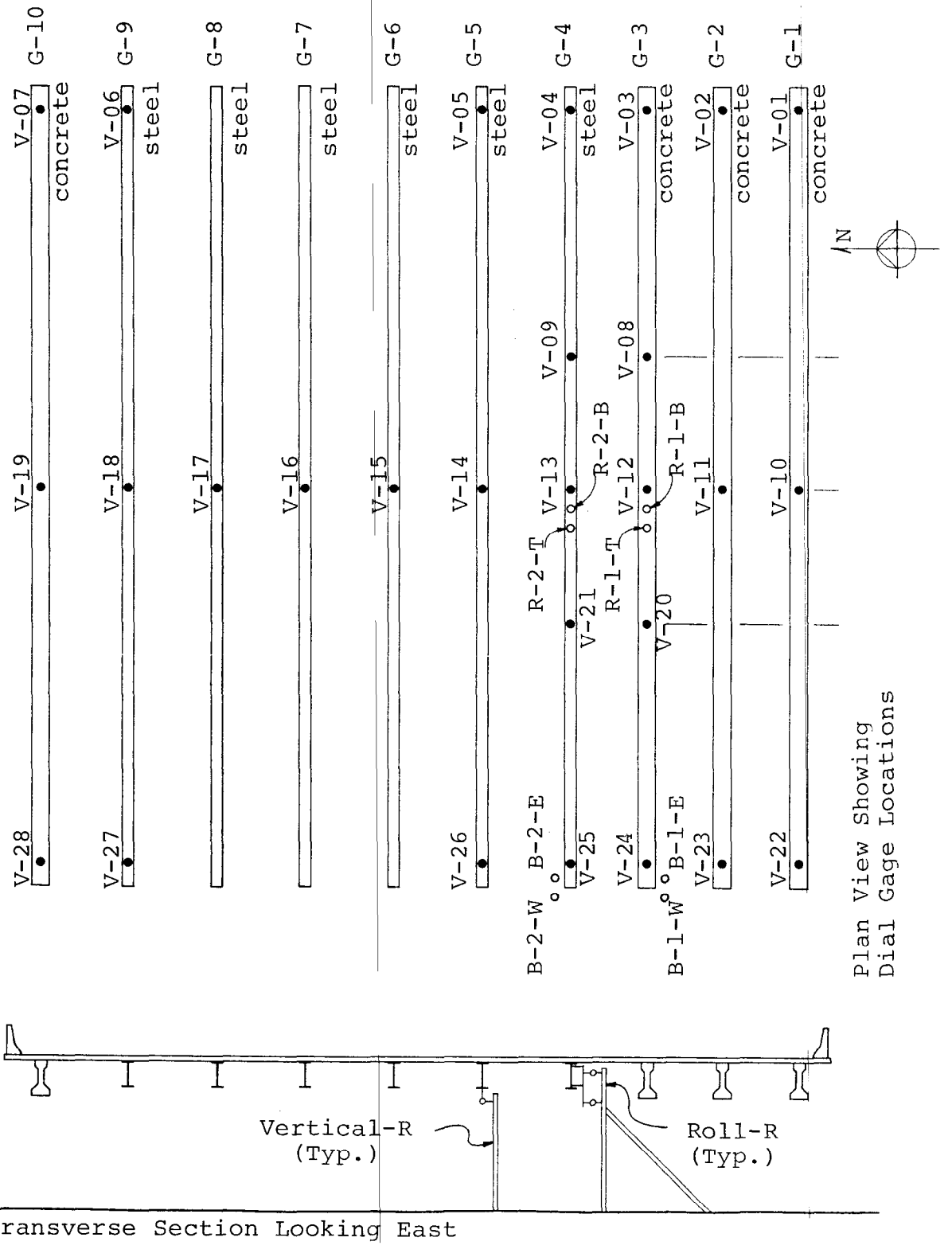

FIG. 8 LOCATION OF DIAL INDICATORS FOR OVERLOAD TRUCK CRANE TESTS

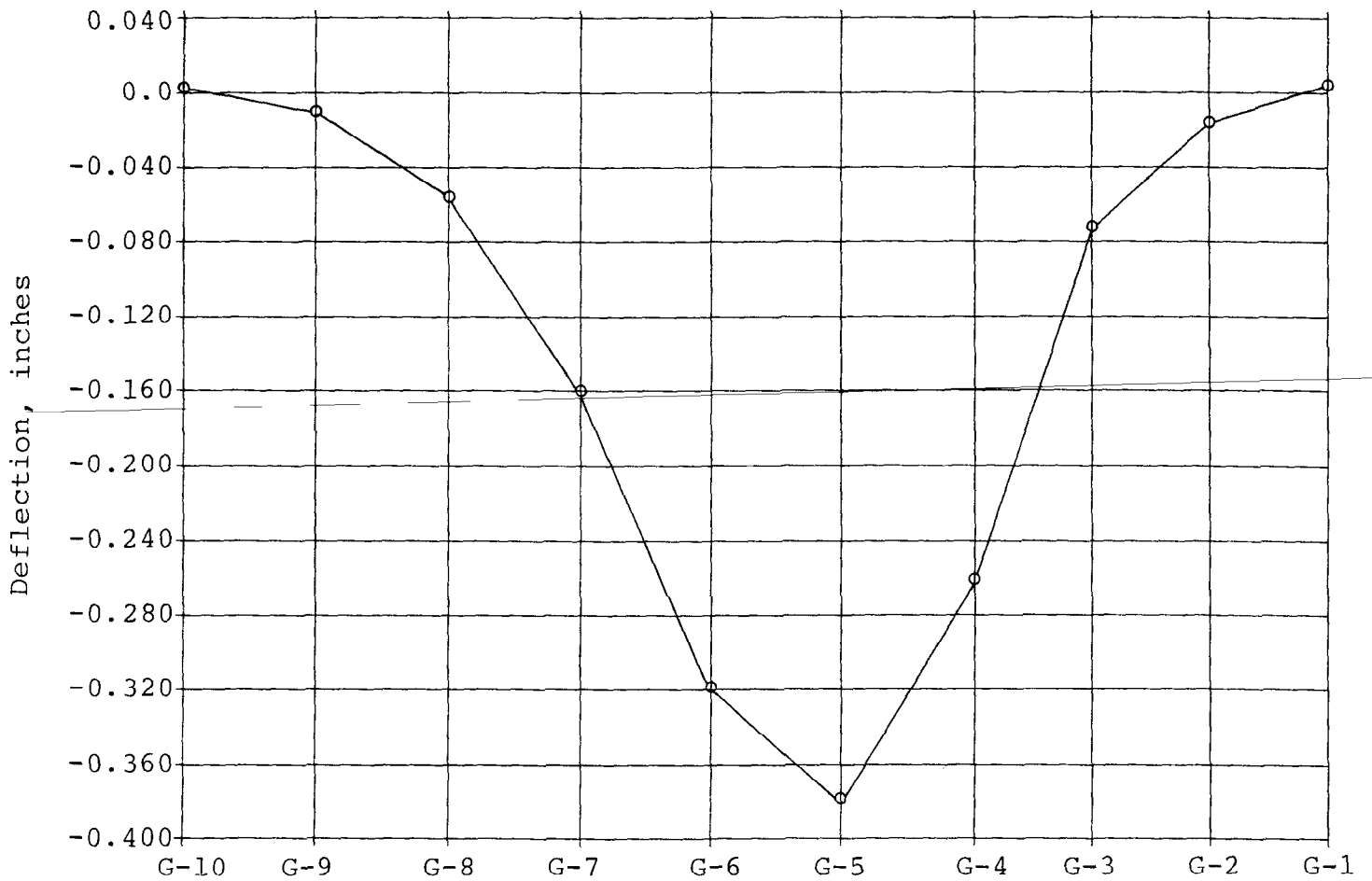

FIG. 9 LIVE LOAD DEFLECTIONS AT MIDSPAN FOR OVERLOAD POSITION NO. 1

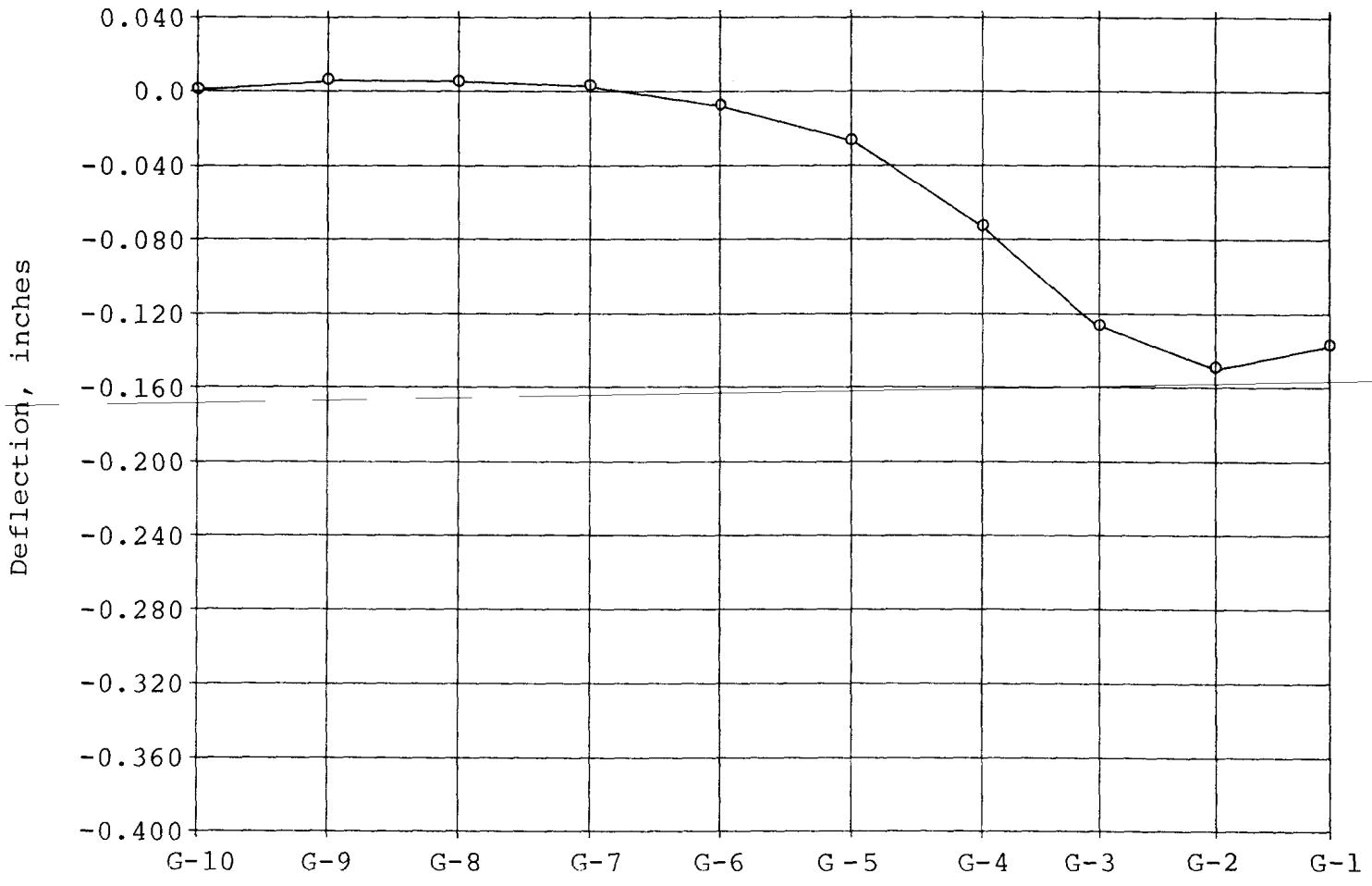

FIG. 10 LIVE LOAD DEFLECTIONS AT MIDSPAN FOR OVERLOAD POSITION NO. 2

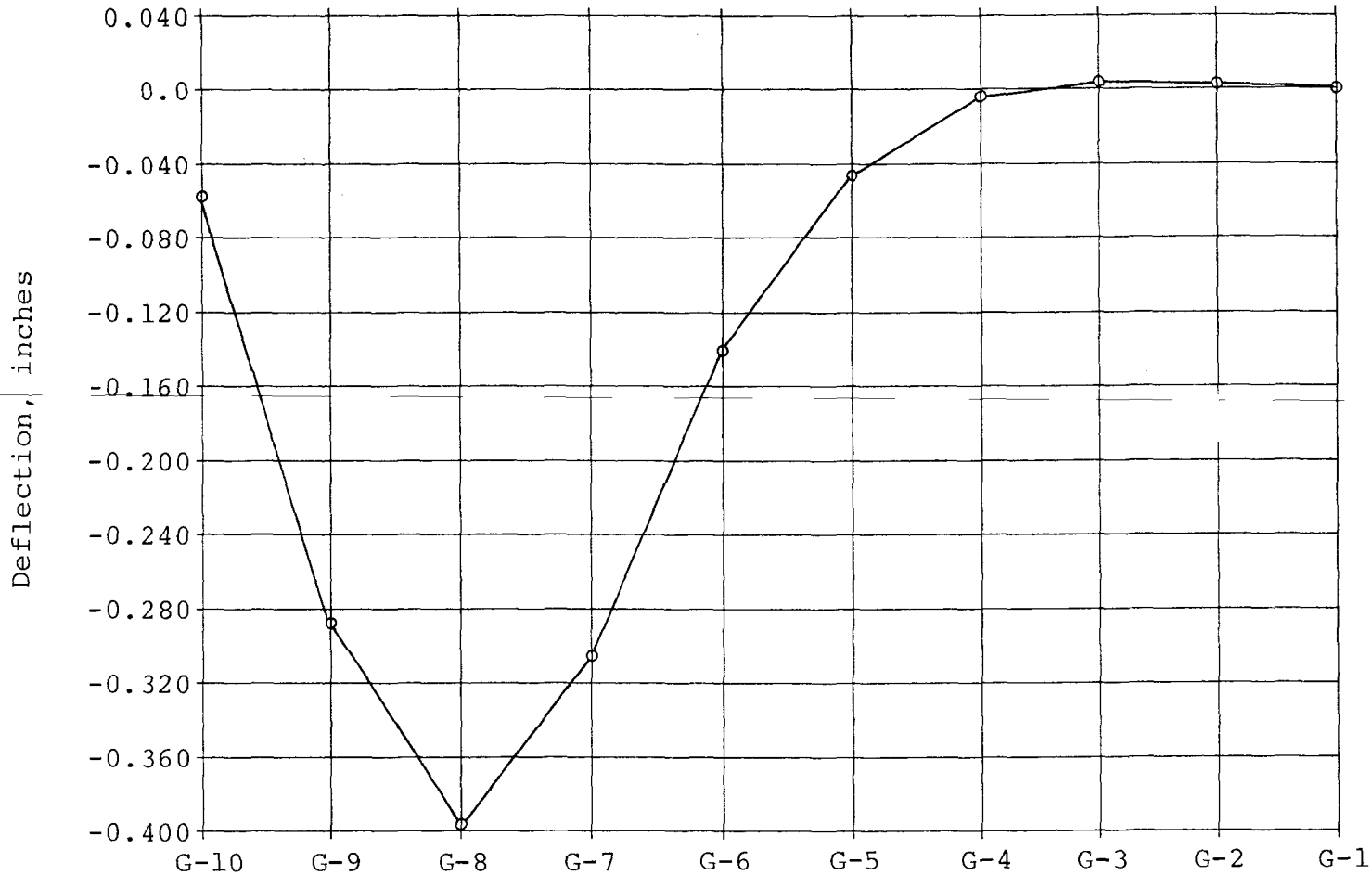

FIG. 11 LIVE LOAD DEFLECTIONS AT MIDSPAN FOR OVERLOAD POSITION NO. 3

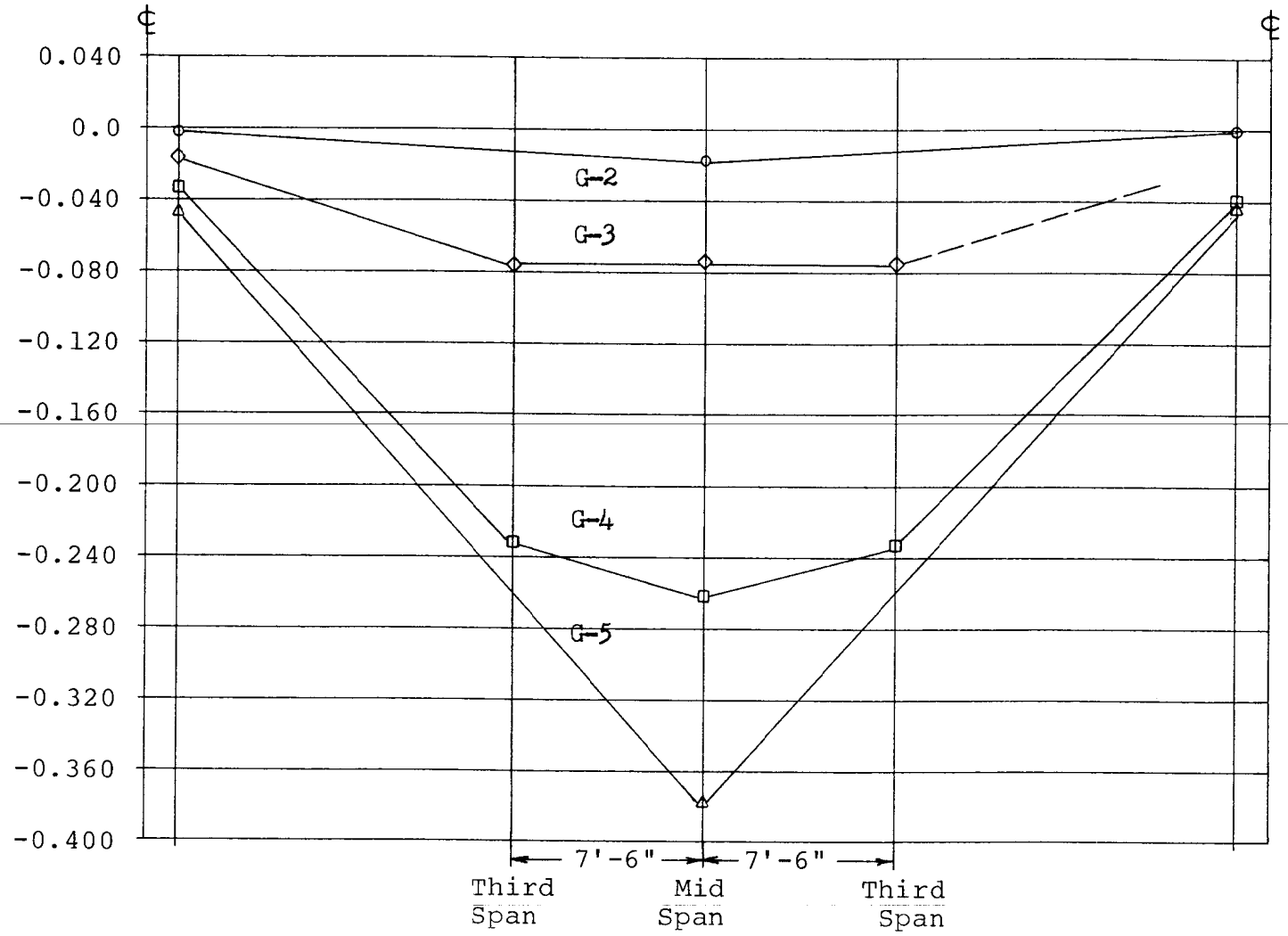

FIG. 12 LONGITUDINAL LIVE LOAD DEFLECTIONS FOR OVERLOAD POSITION NO. 1

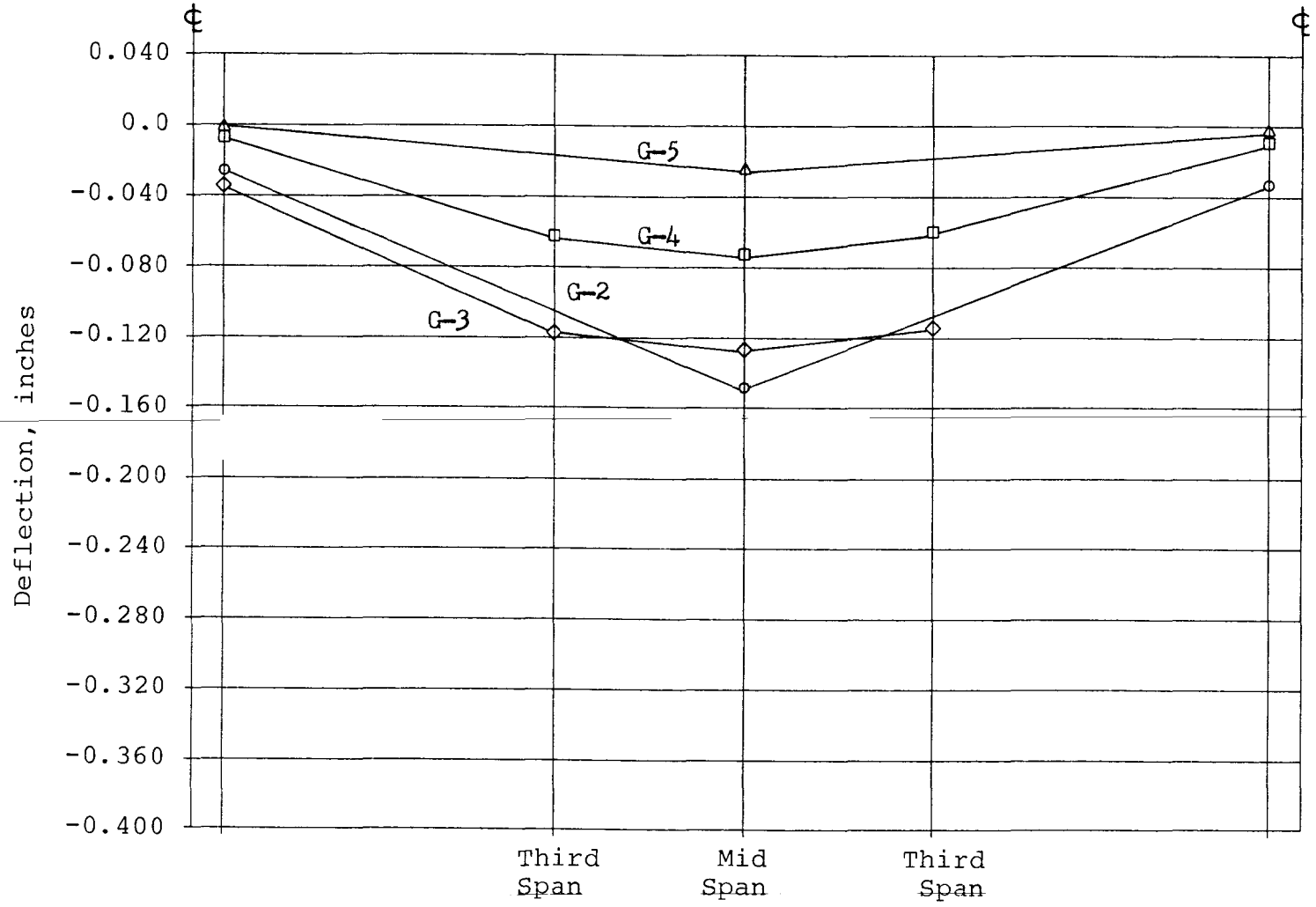

FIG. 13 LONGITUDINAL LIVE LOAD DEFLECTIONS FOR OVERLOAD POSITION NO. 2

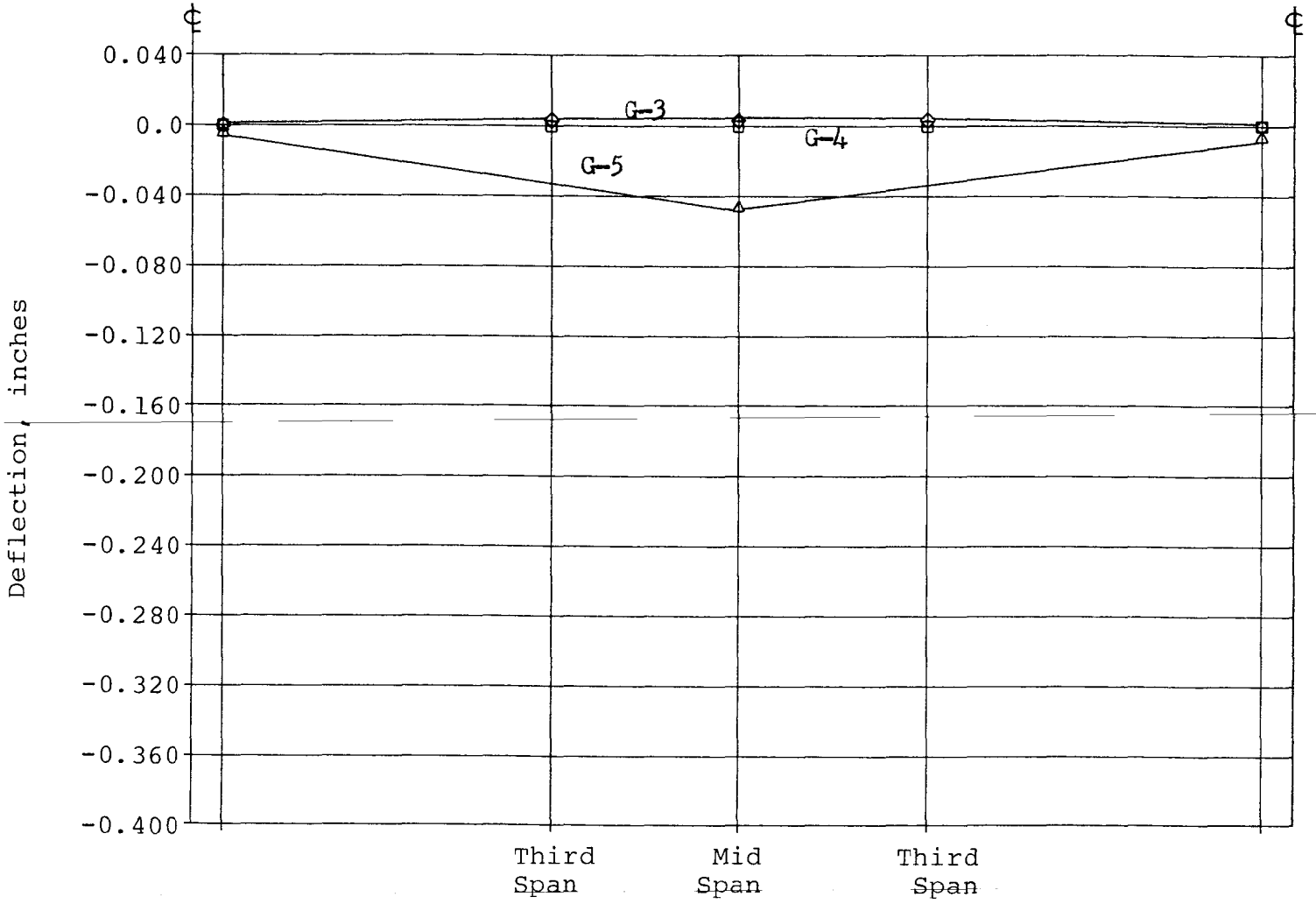

FIG. 14 LONGITUDINAL LIVE LOAD DEFLECTIONS FOR OVERLOAD POSITION NO. 3

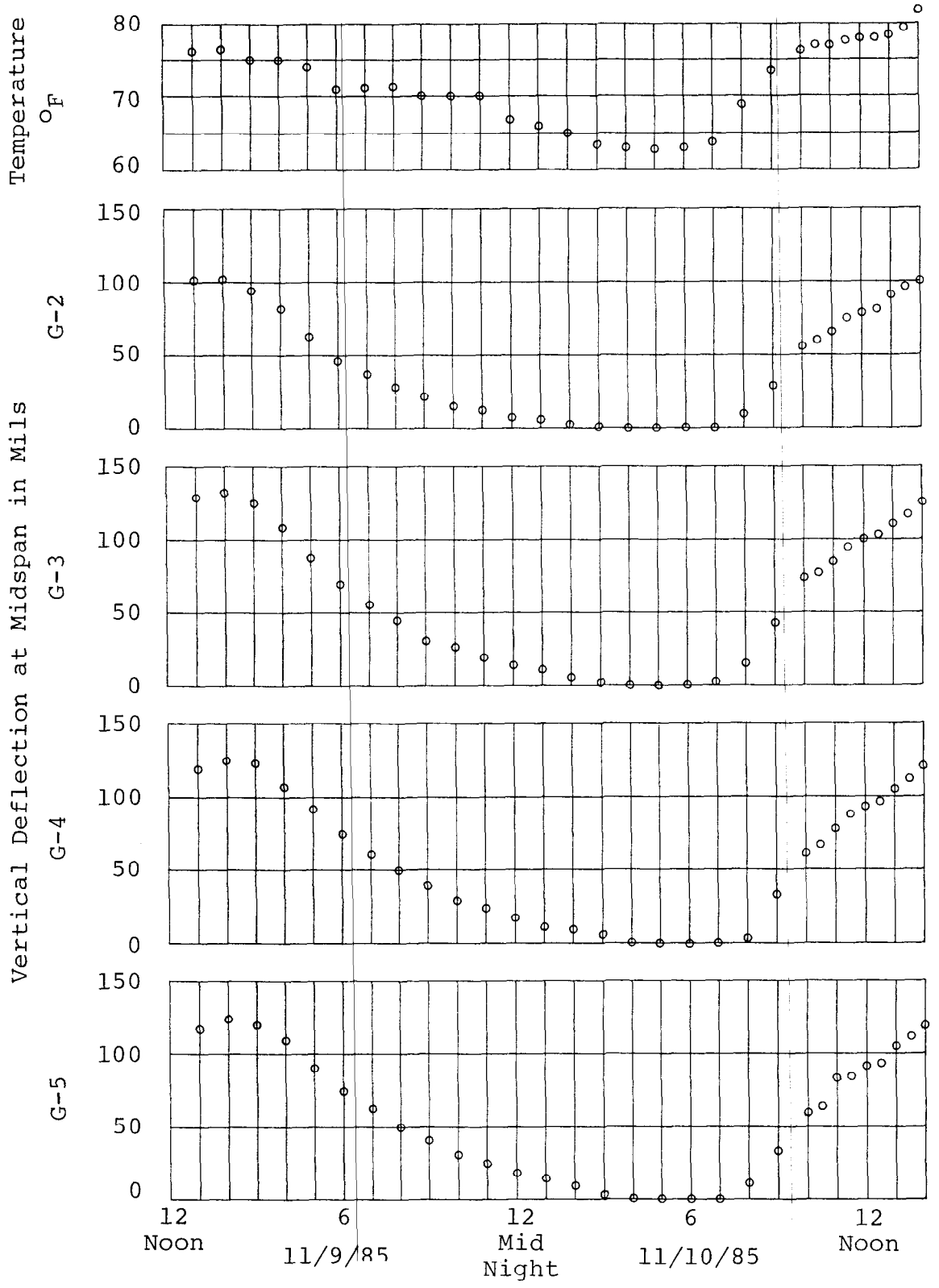

FIG. 15 MEASURED VERTICAL DEFLECTIONS VS. AMBIENT TEMPERATURE

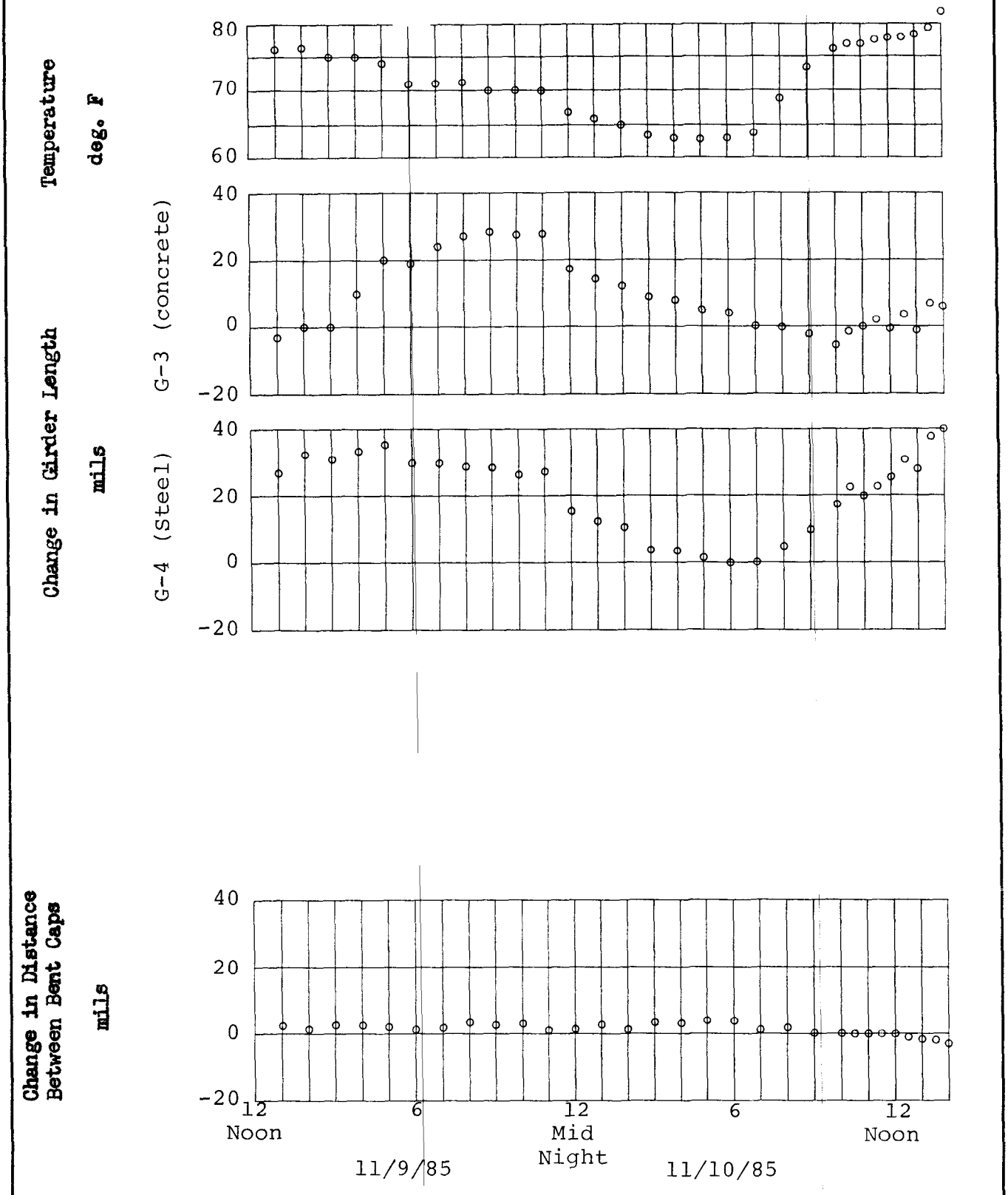

FIG. **16** MEASURED LONGITUDINAL DEFLECTIONS VS. AMBIENT TEMPERATURE

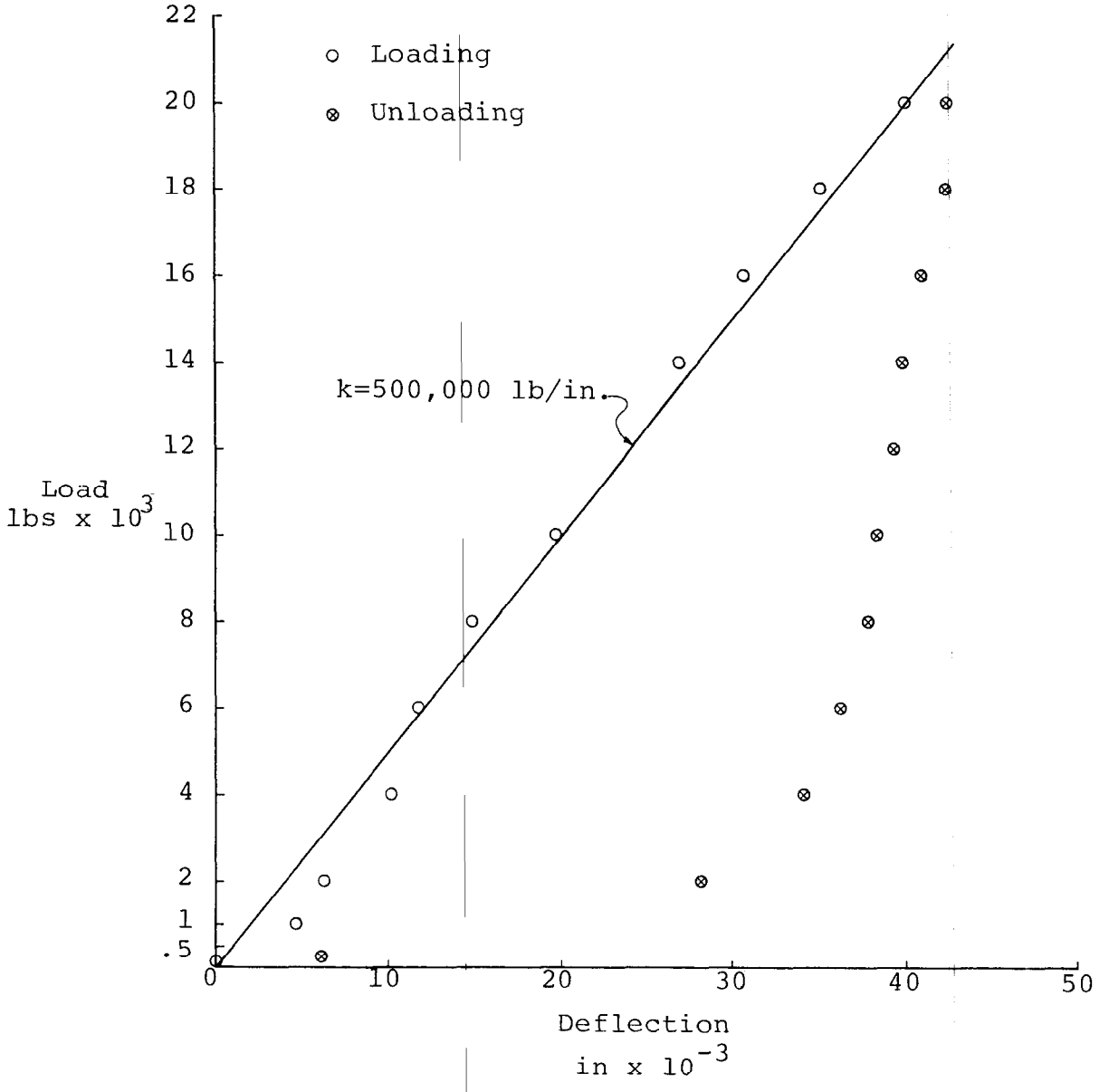

FIG. 17 LOAD DEFLECTION RELATIONSHIP FOR NEOPRENE BEARING PAD

3. COMPARISON OF COMPUTER PREDICTIONS TO FIELD TESTS

3.1 Introduction

In this section computer results obtained using the NASTRAN computer program are compared to the field test results. The model of the Bonnabel Overpass as developed in Appendix A is used for the comparison. Three loading situations are considered. These situations are: loading caused by the overload truck crane, loading caused by two trucks back-to-back, as shown in Fig. 1, and loading caused by temperature variations.

The steps in developing the input data deck for modeling a particular structure are to select the physical grid layout, select the appropriate connecting elements, specify material properties and end fixity conditions, and apply the appropriate loading situations. In developing the files for this comparison, the selection of the grid layout and the connecting elements are the same as discussed in Appendix A. The grid layout used has a fine mesh in the region between the concrete and steel girders. The fine mesh grid layout is not necessary insofar as obtaining an accurate comparison with field test data but is used in order to obtain greater detail.

In this chapter the approach is to develop the basic model or input file to NASTRAN for the Bonnabel Overpass loaded with the overload truck crane. This model is

adjusted to investigate the effect of certain material properties and end fixity conditions. The "best fit" configuration is then loaded with loads corresponding to two trucks back-to-back, as shown in Fig. 1, in order to verify the final model. Finally, the "best fit" model is "loaded" thermally and compared with the thermal deflection data.

3.2 Overload Truck Crane Tests

In this section the comparison of the computer results to the deflection data from the overload truck crane tests will be described. The discussion addresses data presented in part on Figs. 18, 19 and 20 for loading positions No. 1, No. 2 and No. 3, respectively.

While it should be obvious that the data represent discrete deflections of individual girders, and not continuous deflection curves, the data points are connected with straight lines to facilitate better visualization of the results.

The first computer model discussed is one for which the concrete slab is assumed to be uncracked and to have isotropic section properties. Young's Modulus for the concrete is taken to be 5.4×10^6 psi for the slab and 5.6×10^6 psi for the prestressed concrete girders. These values are based on the concrete strength tests discussed in Section 2.7. The slab is assumed to be a monolithic section and all diaphragms are assumed to have rigid end connections.

It can be seen from examination of the figures, particularly Figs. 18 and 20, that the agreement is not as good as might be expected. The maximum deflection values obtained from the computer solution are significantly less than the measured maximum values, and the model predicts that more of the load is being transferred laterally to adjacent girders than was actually found in the field tests. It is further noted that the agreement appears to be poorer for the region having steel girders, i.e., the original section, than it is for the widened section having concrete girders.

Computer runs were made simulating cracked slab conditions for the old slab; i.e., the section of slab over the steel girders. It is reasoned that a cracked slab would not affect the longitudinal stiffness because the entire slab is in longitudinal compression but it would affect the lateral stiffness because the slab is in reverse bending transversely. Orthotropic slab material properties were input into the computer to simulate a condition where the lateral stiffness of the old slab is 50% of the longitudinal stiffness of the slab. This condition is accomplished in the NASTRAN computer program by assigning Young's Modulus for the slab to be orthotropic where E_y (lateral) = 0.5 E_x (longitudinal). The results of these computer runs are shown on the same graphs as mentioned above.

It can be seen from examination of the graphs that the agreement obtained using orthotropic slab properties is

better than that obtained using isotropic properties; however, the agreement is still not exceptional. The maximum deflection values obtained from the computer solutions are less than the measured values, and the computer predicts that more of the load is being transferred laterally to adjacent girders than was actually measured.

Computer runs were made in which all the diaphragms were assumed to have pinned end connections and the slab was assumed to be uncracked. As can be seen, this configuration did not give quite as good a fit as the previous configuration.

Computer runs were made in which all of the diaphragms between girders are assumed to have pinned connections and the slab is also assumed to be cracked with $E_y = 0.5\ E_x$.

It can be seen by examining the graphs that this computer configuration gives very good agreement with the field test results. The maximum deflection is within 3% and the shape of the computer curve is very similar to that of the measured curve. Figs. 21, 22, and 23 show a comparison of the longitudinal deflection data using the cracked slab and pinned diaphragm model.

It is not believed worthwhile to attempt to adjust the computer input results to obtain a more exact fit of the field test results. Further adjustment would involve varying the degree of cracking assumed for the slab and the amount of fixity assumed for the diaphragm ends, which at best would hold for this particular span. It is believed,

This is the model which gave the best agreement with the overload truck crane field test results, as discussed in the previous section.

The results of the comparison under the nominal HS20-44 truck load are shown by Figs. 24, 25 and 26. It can be seen that the computed deflections agree very closely with the field test results. The maximum calculated deflections are within 5% of the maximum measured deflections and the shapes of the calculated and experimental deflection curves are similar.

3.4 Thermal Deflection Tests

In this section the results of the thermal deflection tests are discussed and certain computer results are compared with the field test data.

The NASTRAN computer program allows thermal loads to be applied by specifying temperature distributions in the structural elements. In terms of the model of the Bonnabel Overpass, a temperature gradient can be imposed through the slab from top to bottom and temperature changes can be imposed on the girders. However, the heat transfer analysis required to define these temperatures over a full diurnal cycle is beyond the scope of this investigation.

The computer comparison will be limited to a specific period of time during the field tests for which it is believed the element temperatures can be approximately specified. This is the period in the morning from sunrise

until about noon. Before this period there was a relatively long predawn period of approximately constant conditions.

This section also contains some observations relative to the effect of temperature variation on the Bonnabel Overpass.

3.4.1 Computer Comparison of Thermal Deflections

It can be seen from the thermal field test data that there is a period of several hours between about midnight and dawn when the temperature is approximately constant and the test span reaches a more or less stable condition. After sunrise, the structure starts to deflect upward at mid-span and continues to rise for several hours. An attempt has been made to model the overpass during this period using the NASTRAN computer program. As mentioned previously, defining the thermal loads for this situation is difficult and at best the results presented herein are only approximate; however, it is believed that some significant information is obtained.

During the period after the sun rises, the major thermal load on the span is caused by the radiant energy exchange on the top of the deck. Radiant energy is received both from direct sunshine and from sun rays reflected from the sky. This latter radiant energy is primarily reflected from water vapor and carbon dioxide. The amount of radiant energy received increases as the morning progresses, barring shading by clouds. Radiant energy is lost by the top of the

deck due to reradiation. As the deck heats up the amount of energy lost also increases. During the morning period the temperature of the top surface of the deck is slightly higher than ambient so that there is a small loss in thermal energy due to convection.

An average heat input to the top of the deck was estimated and this heat input was used to calculate temperature profiles through the slab at one hour intervals for four hours. These temperature profiles were used to specify the temperature gradients in the slab elements of the NASTRAN program.

During the same period of time the ambient temperature increased from approximately $63^{\circ}F$ to $80^{\circ}F$, which would cause the temperature of the girders to increase. The concrete girders have considerably more thermal mass than the steel girders, which means they will change temperature much more slowly. It is estimated that during the four-hour period under consideration the steel girders would increase in temperature in the order of five degrees, while the concrete girders would change only about one degree total. Temperatures for the steel and concrete girders are estimated at one-hour intervals for the four-hour period, and these values are used to specify the bulk temperature of the elements representing the girders.

The NASTRAN program is used to calculate the deflections caused by the thermal loads discussed above. The results are shown on Fig. 27. Fig. 28 shows the

computed deflections across mid-span after four hours of sunshine and the measured deflections at noon.

Considering the approximations made when defining the thermal inputs into the slab and girders, the agreement between the computer results and the field test data is close. It is believed that this agreement confirms the adequacy of the thermal input model used, this model being a relatively large heat input into the top of the slab and relative small heat input into the girders beneath the slab. The estimate that the rate of change of temperature of the steel girders is five times that of the concrete girders appears to be approximately correct for this configuration.

Changing the relative lateral stiffness of the slab, i.e., cracked versus uncracked, did not change the computer results noticeably. Thus the thermal test results can not be used to gain additional insight into the cracked condition of the slab.

The computer program used for the above analysis also calculated the change in length of the girders at the bottom fibers, as a function of temperature. These values can be compared with the measured values, as shown on Fig. 29. While the agreement between computer results and the field test data is far from ideal, the trends and overall effects appear to be similar.

In the predawn hours the vertical position of the span has become constant, and the lengths of both the concrete and steel girders are decreasing very slightly. This

probably indicates that the overall temperature of the span is uniform and almost constant. When the sun rises and the span starts to arch up at mid-span, the girders will be concave downward, which would tend to shorten the bottom fibers of the girders. On the other hand, the ambient temperature is increasing, which will cause the girders to increase in temperature and thus become longer. As mentioned above, the temperature of the steel girders will change more rapidly than the concrete girder. This result is observed in Fig. 29, where the length of the bottom fibers of the concrete girder, G-3, is remaining relatively constant and the length of bottom fibers of the steel girder, G-4, is increasing significantly.

It is believed that the NASTRAN computer program can accurately represent structures under thermal loading provided the temperature distributions can be specified and the structure can be correctly modeled. However, in the case of an overpass span subjected to atmospheric variations, as in the case herein, the program has some serious limitations. Even if the environmental conditions could be precisely defined, the heat transfer calculations required to specify element temperature distributions are formidable.

3.4-2 Girder-Bent Cap Motion

The longitudinal deflection measurements taken during the thermal field tests give some insight into the overall motion of the overpass. The results indicate that the

overpass expands and contracts as a unit and the motion of the bent caps and columns supporting the concrete girders are a function of the overall overpass design rather than being a function of the expansion and contraction of the individual simple span.

Fig. 29 shows the field measurements for the length of the concrete girder along the bottom fibers. The length measurement was made at approximately the same elevation as the neoprene bearing pad, thus the change in girder length relates to the relative motion of the neoprene pads. It can be seen that the concrete girder bottom fiber length is a minimum in the morning daylight hours and in the afternoon increases in length to reach a maximum in the early evening, with the total change in length being approximately 0.03 inches.

During the thermal deflection test discussed in Section 2.4, the longitudinal movements of the ends of girder G-3 with respect to the bent caps were measured. These measurements, shown on Fig. 16, show that as the concrete girder expands, the west end of the girder moves west with respect to the west bent cap and the east end of the girder moves east with respect to the east bent cap. The magnitude of each motion is approximately the same on each end indicating that the span maintains an approximately centered position between the bent caps.

Measurements of the motion of the bent caps with respect to the ground indicate that the bent caps are more

or less moving together; as the concrete girder length is increasing, both bent caps for the span investigated are moving east and as the length decreases both bent caps for the span investigated move back to the west. Further, measurements can be combined to obtain the net change in distance between the bent caps. As shown by the bottom curve of Fig. 29, the distance between the bent caps changes by only a small amount.

It is believed that the above motion as observed in the field can be explained by considering two apparent facts; namely, the neoprene bearing pads act as approximately linear springs in the longitudinal or shear direction, and each span of the overpass experiences more or less the same environmental conditions. Thus as each span expands and contracts by approximately the same amount, the longitudinal forces exerted by the spans on either side of a bent cap approximately balance out each other. If the abutments at each end of the overpass were perfectly rigid and each span reacted exactly the same, the bent caps would not move at all. However, differences in the environmental conditions of the spans, differences in thermal and elastic properties of the spans and differences in support stiffnesses may cause unbalanced loading on the bent caps.

Thus, it is believed that when neoprene bearing pads are used, the longitudinal loads on the supports are influenced to a great extent by the overall design of the structure and can not be determined by considering a single span.

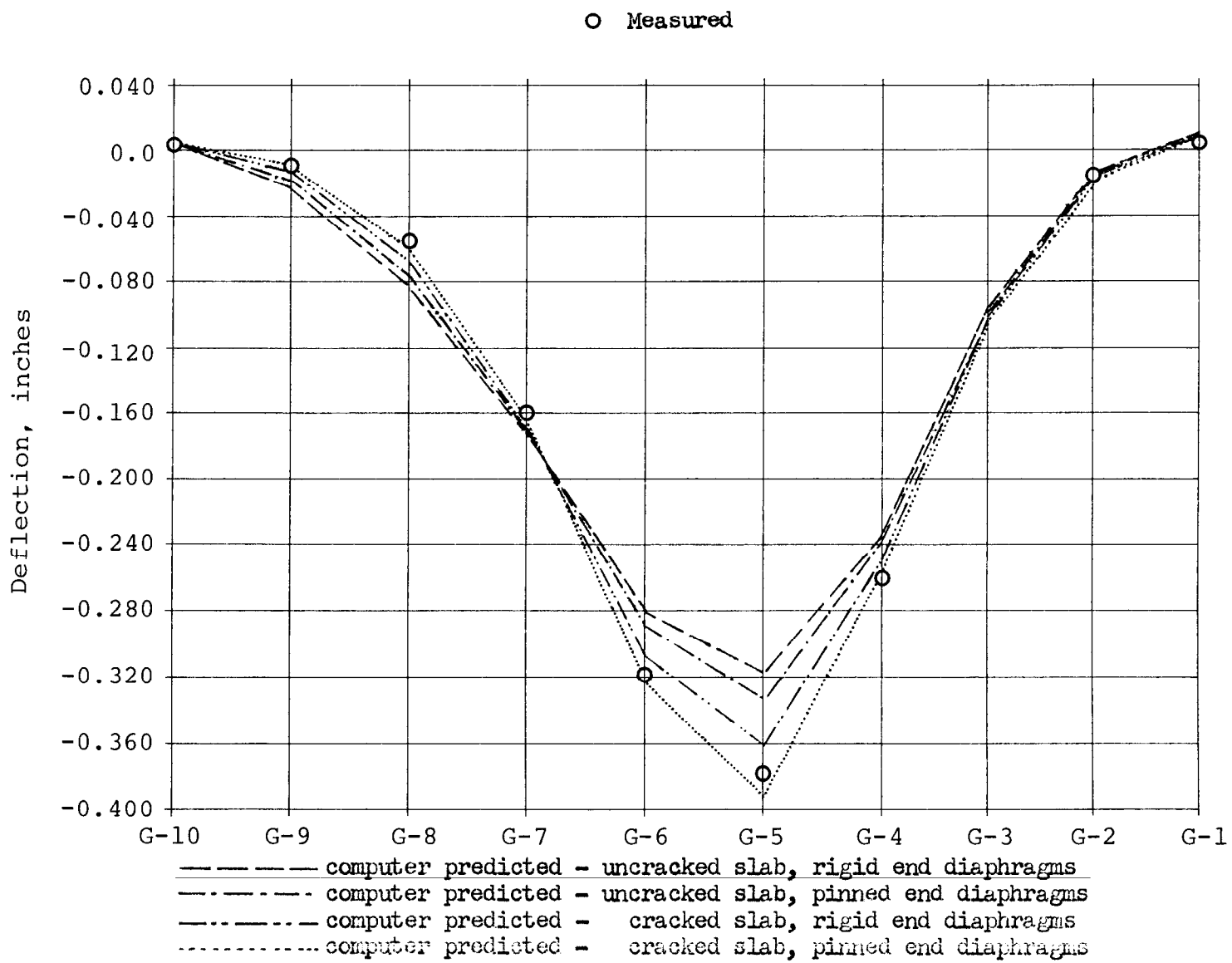

FIG. 18 SPAN TRANSVERSE CENTERLINE COMPUTER PREDICTED VS MEASURED DEFLECTIONS FOR OVERLOAD POSITION NO. 1

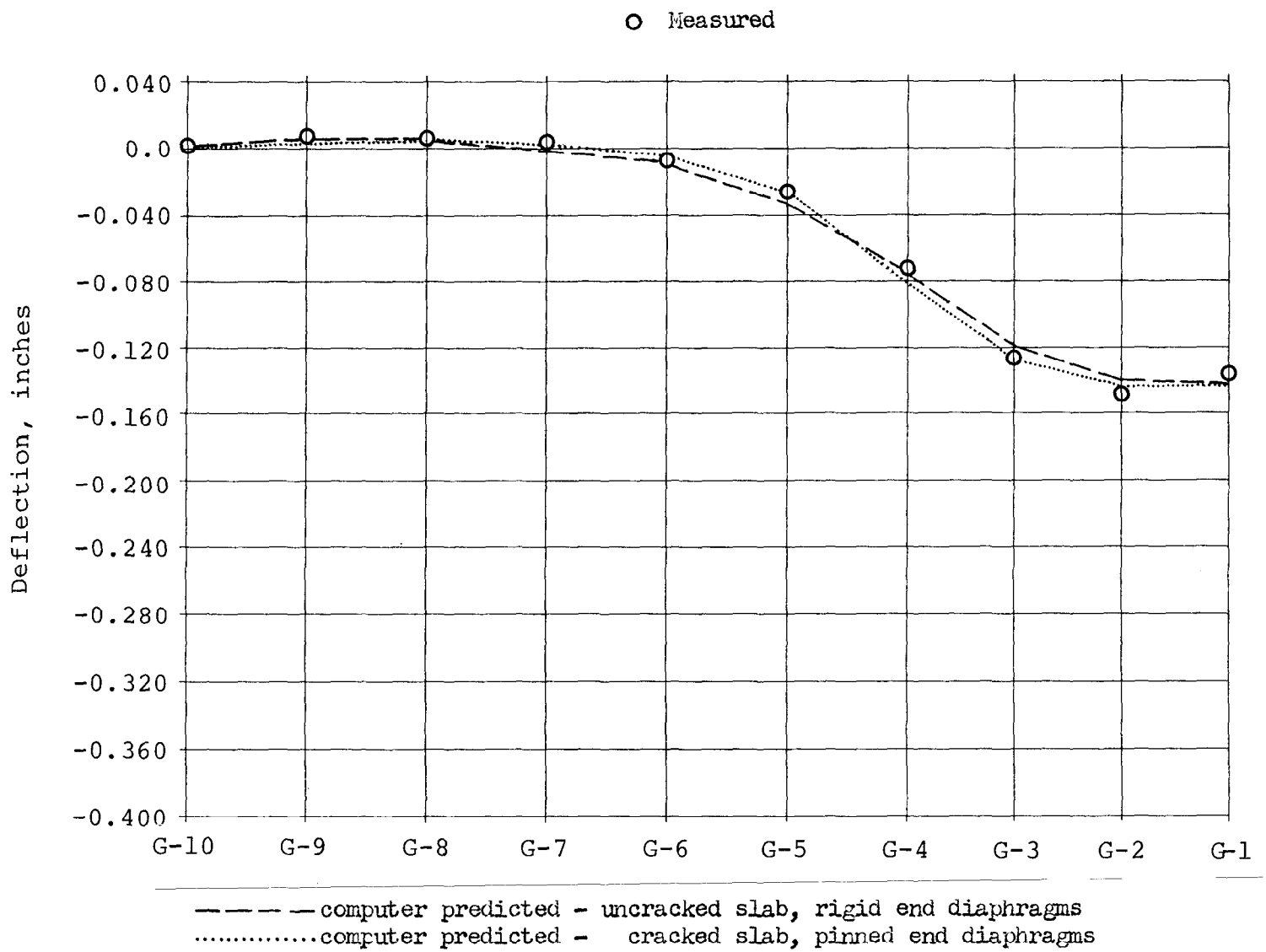

FIG. 19 SPAN TRANSVERSE CENTERLINE COMPUTER PREDICTED VS. MEASURED DEFLECTIONS FOR OVERLOAD POSITION NO. 2

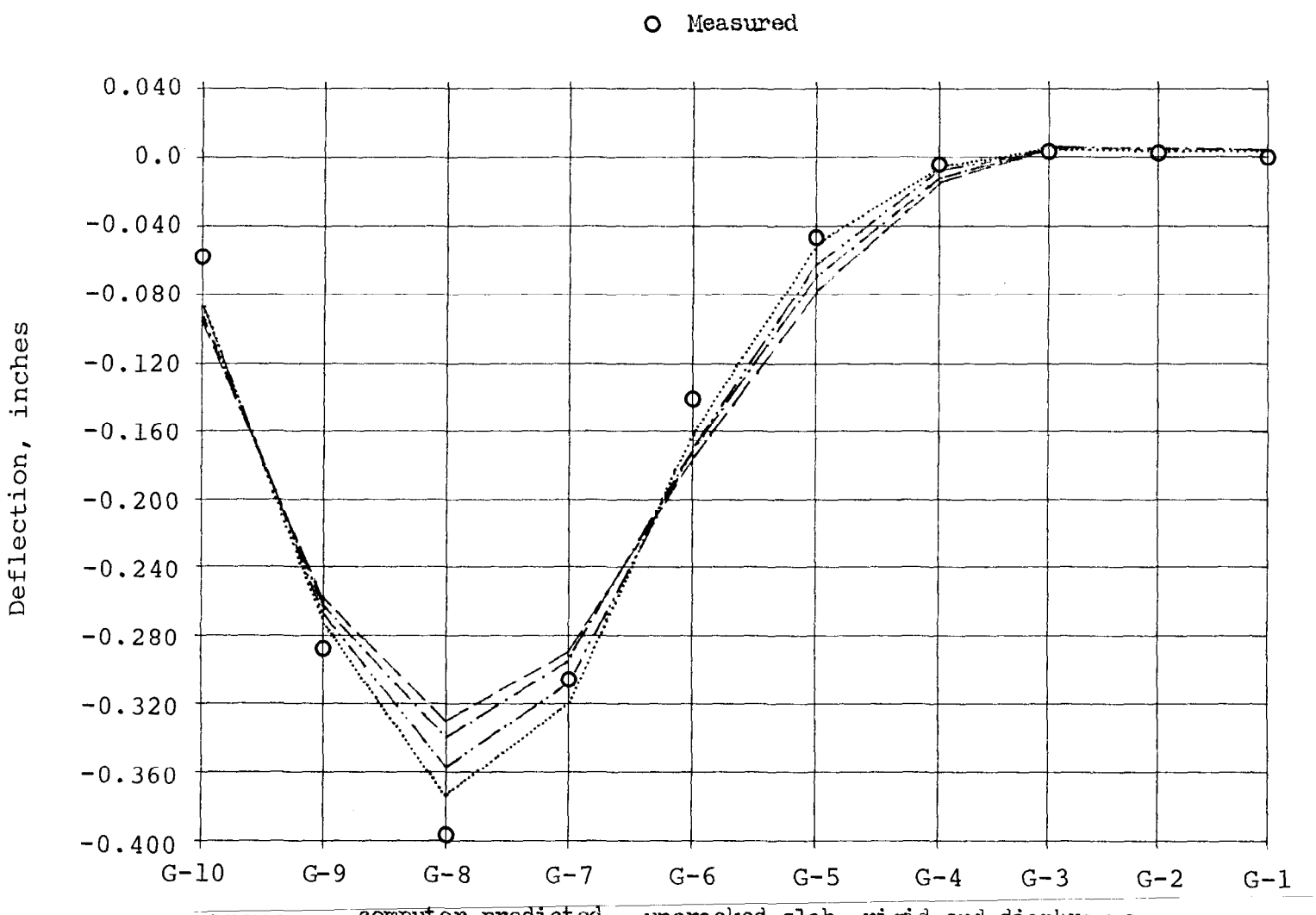

FIG. 20 SPAN TRANSVERSE CENTERLINE COMPUTER PREDICTED VS. MEASURED DEFLECTIONS FOR OVERLOAD POSITION NO. 3

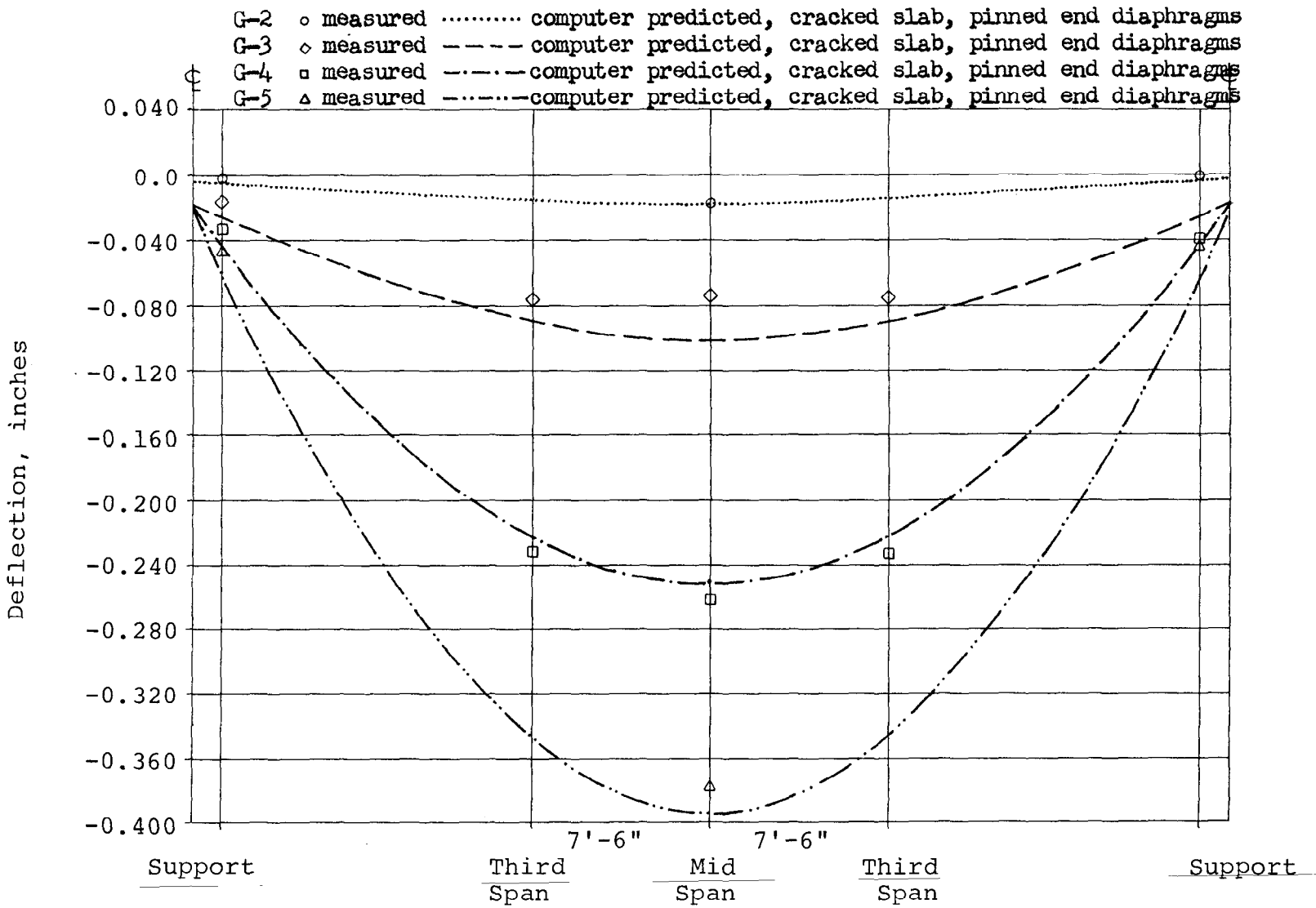

FIG. 21 COMPUTER PREDICTED VS. MEASURED LONGITUDINAL DEFLECTIONS FOR OVERLOAD POSITION NO. 1

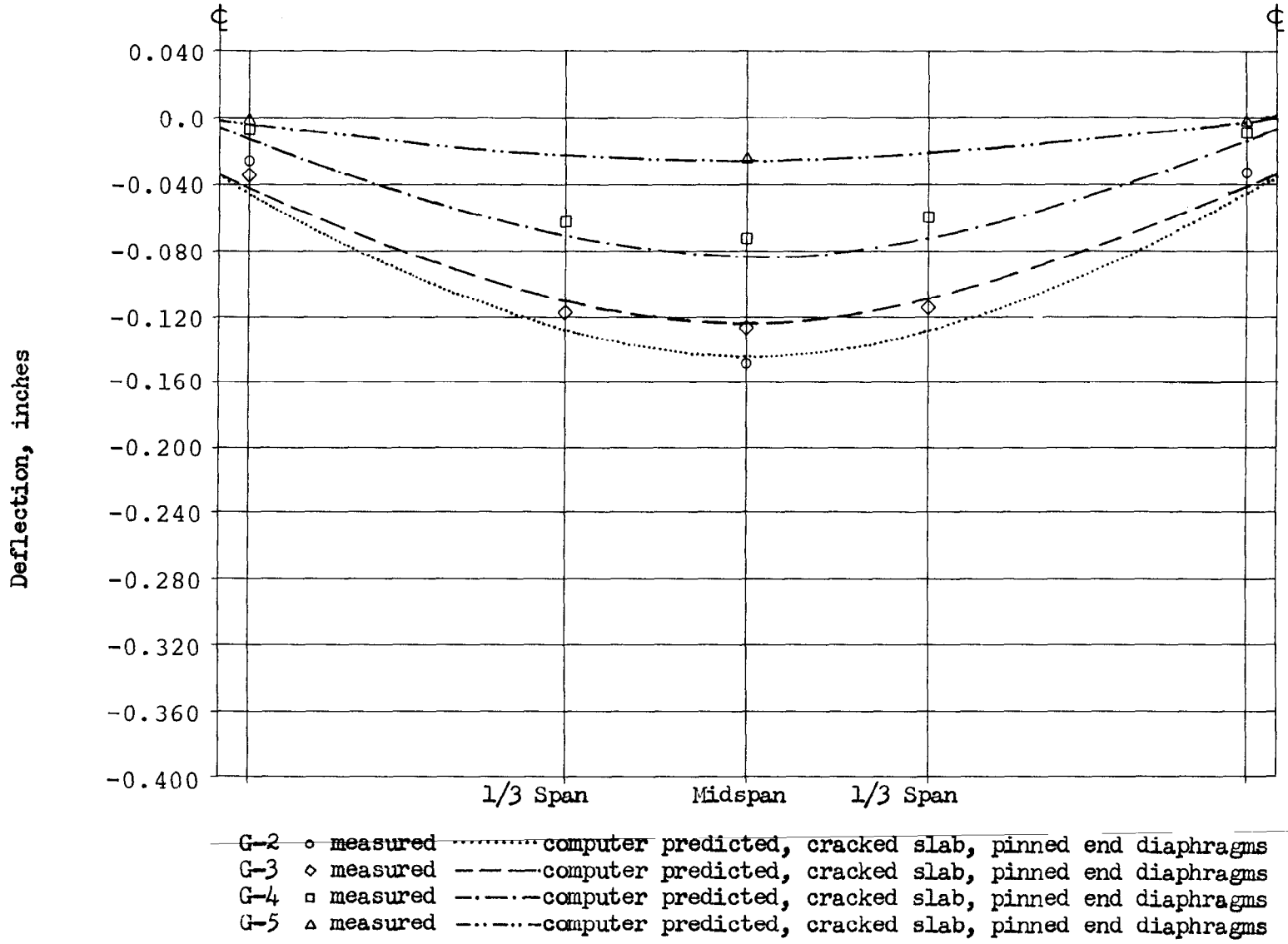

FIG. 22 COMPUTER PREDICTED VS. MEASURED LONGITUDINAL DEFLECTIONS FOR OVERLOAD POSITION NO. 2

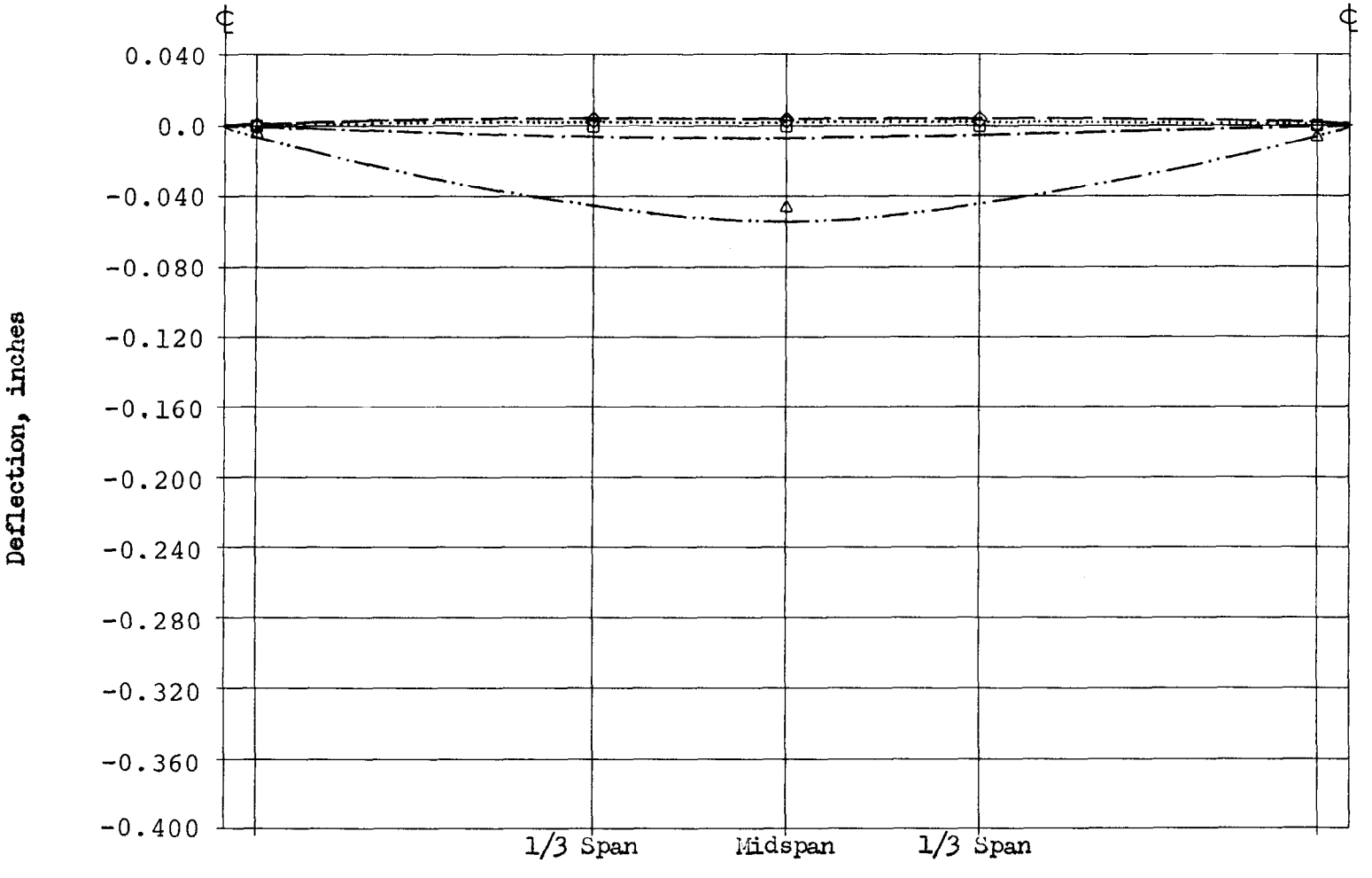

G-2 ○ measured ·····computer predicted, cracked slab, pinned end diaphragms
G-3 ◇ measured — — —computer predicted, cracked slab, pinned end diaphragms
G-4 □ measured —·—·—computer predicted, cracked slab, pinned end diaphragms
G-5 △ measured —··—··—computer predicted, cracked slab, pinned end diaphragms

FIG. 23 COMPUTER PREDICTED VS. MEASURED LONGITUDINAL DEFLECTIONS FOR OVERLOAD POSITION NO. 3

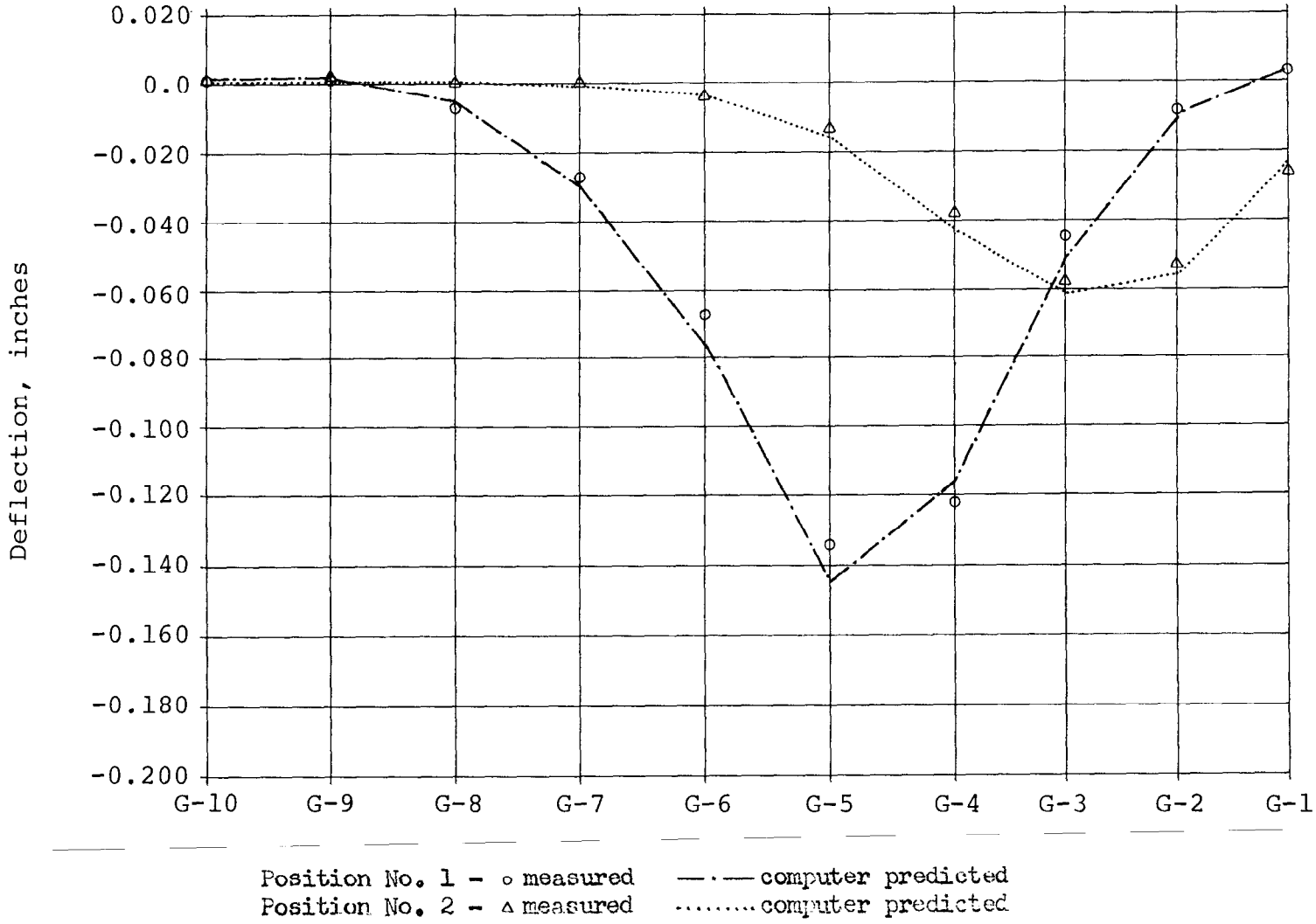

FIG. 24 SPAN TRANSVERSE CENTERLINE COMPUTER PREDICTED VS. MEASURED DEFLECTIONS FOR NOMINAL HS20-44 LOADING POSITION NO. 1 AND NO. 2

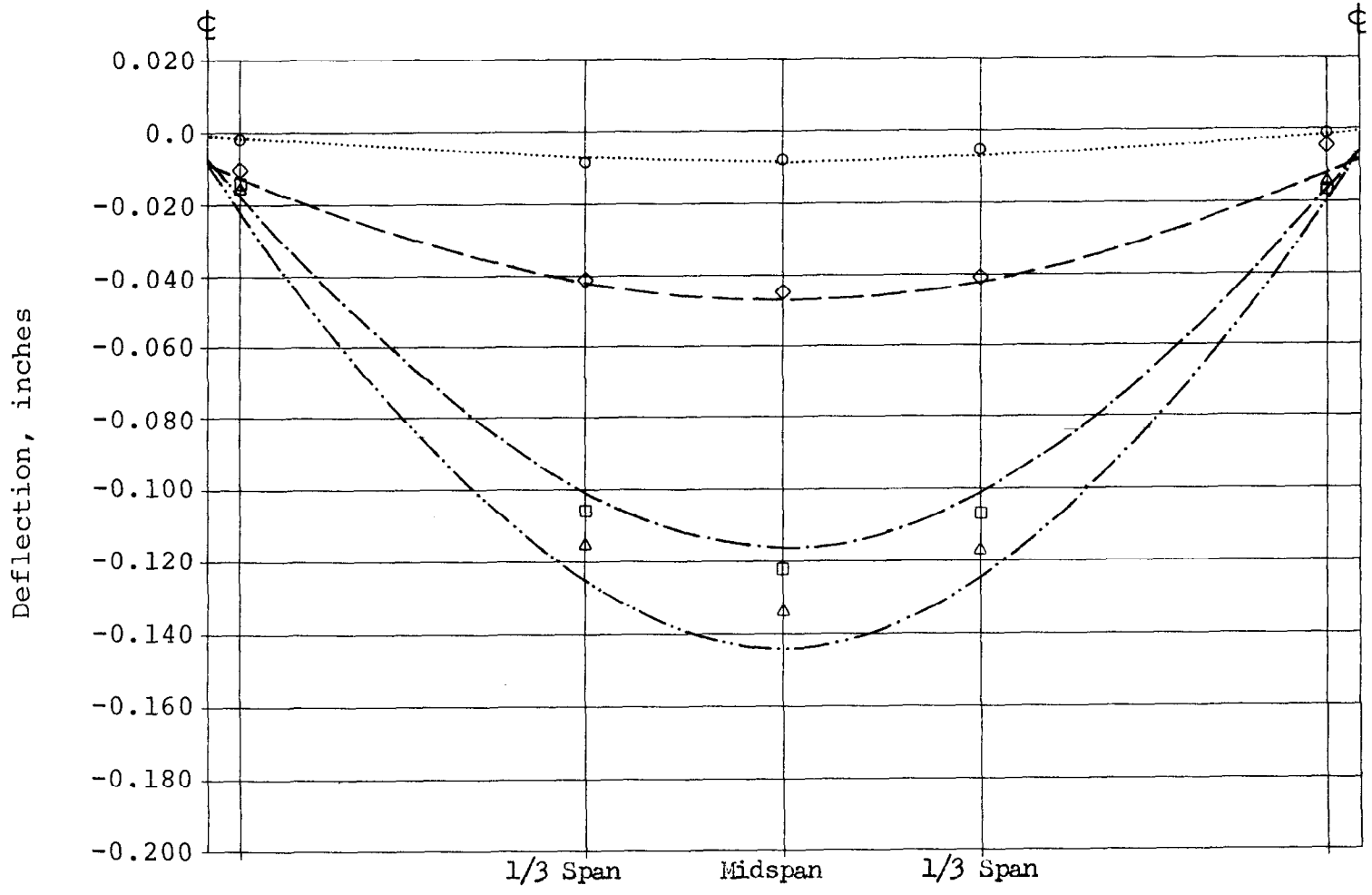

FIG. 25 COMPUTER PREDICTED VS. MEASURED LONGITUDINAL DEFLECTIONS FOR NOMINAL HS20-44 LOADING POSITION NO. 1

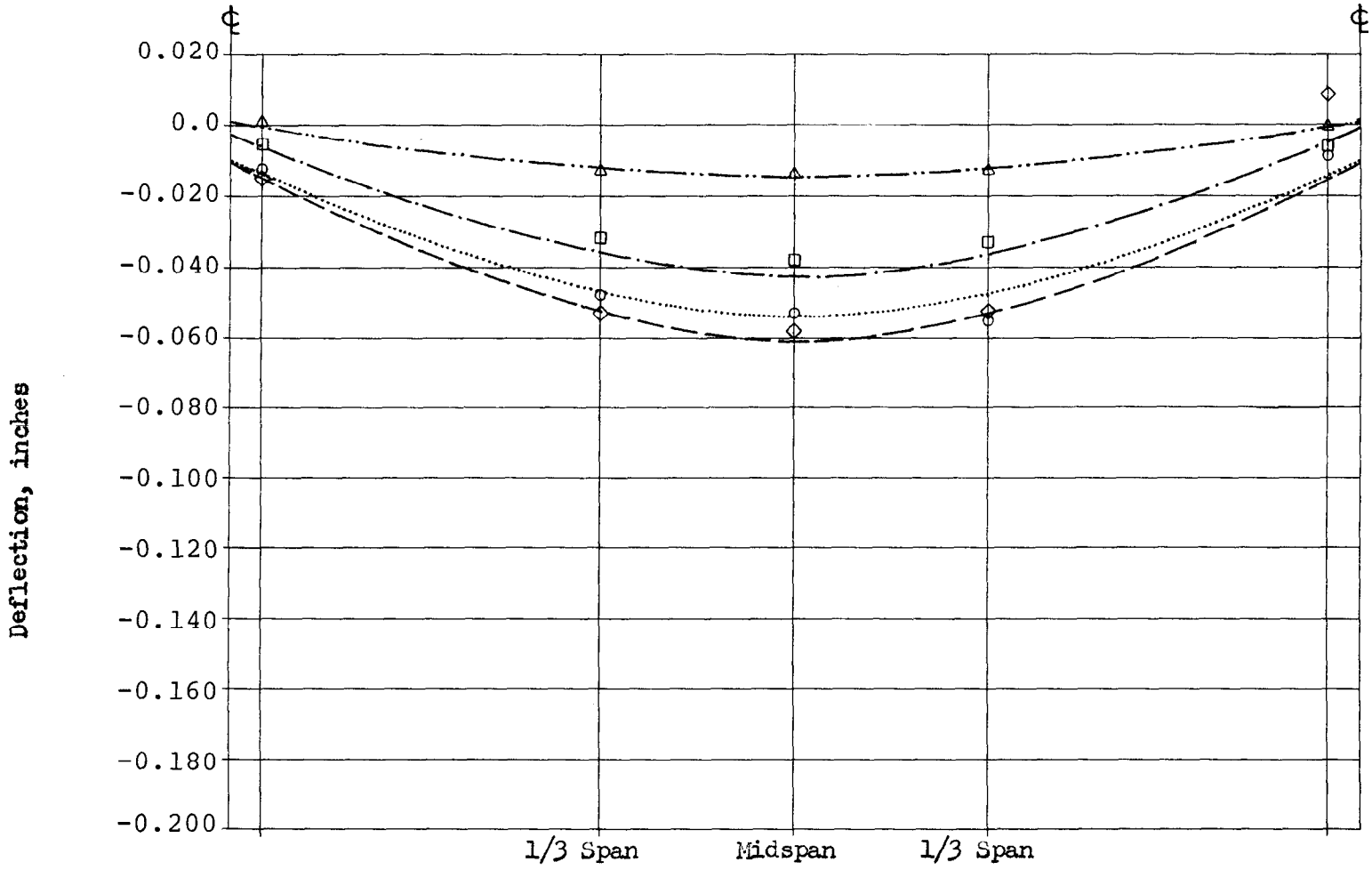

G-2 ○ measured ····· computer predicted, cracked slab, pinned end diaphragms
G-3 ◇ measured – – – computer predicted, cracked slab, pinned end diaphragms
G-4 □ measured –·–·– computer predicted, cracked slab, pinned end diaphragms
G-5 △ measured –···– computer predicted, cracked slab, pinned end diaphragms

FIG. 26 COMPUTER PREDICTED VS. MEASURED LONGITUDINAL DEFLECTIONS FOR NOMINAL HS20-44 LOADING POSITION NO. 2

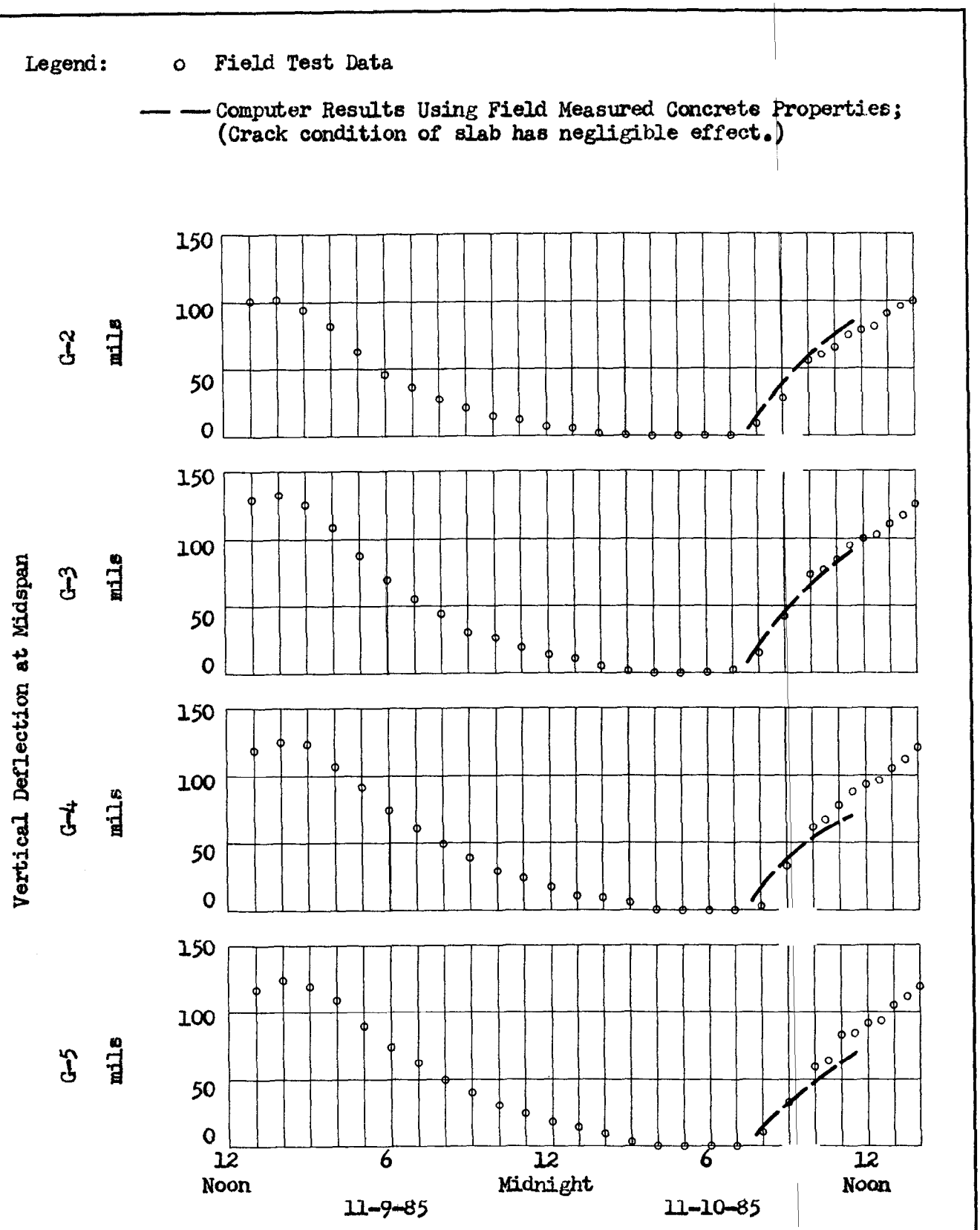

FIG. 27 COMPARISON OF TEMPERATURE INDUCED VERTICAL DEFLECTIONS AS A FUNCTION OF THE TIME OF DAY

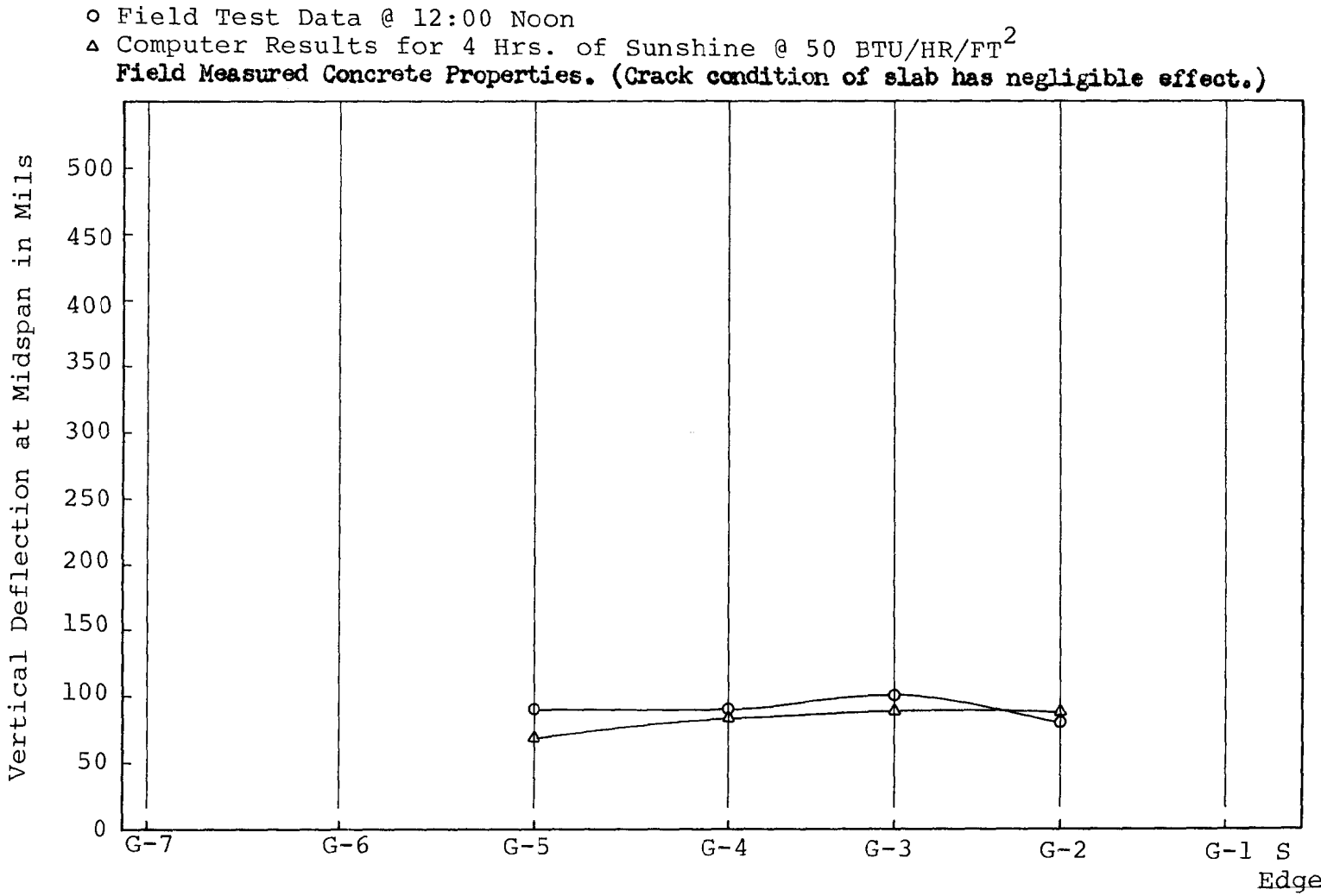

FIG. 28 COMPUTER PREDICTED DEFLECTIONS ACROSS TRANSVERSE CENTERLINE AFTER FOUR HOURS OF SUNSHINE VS. MEASURED DEFLECTIONS AT NOON

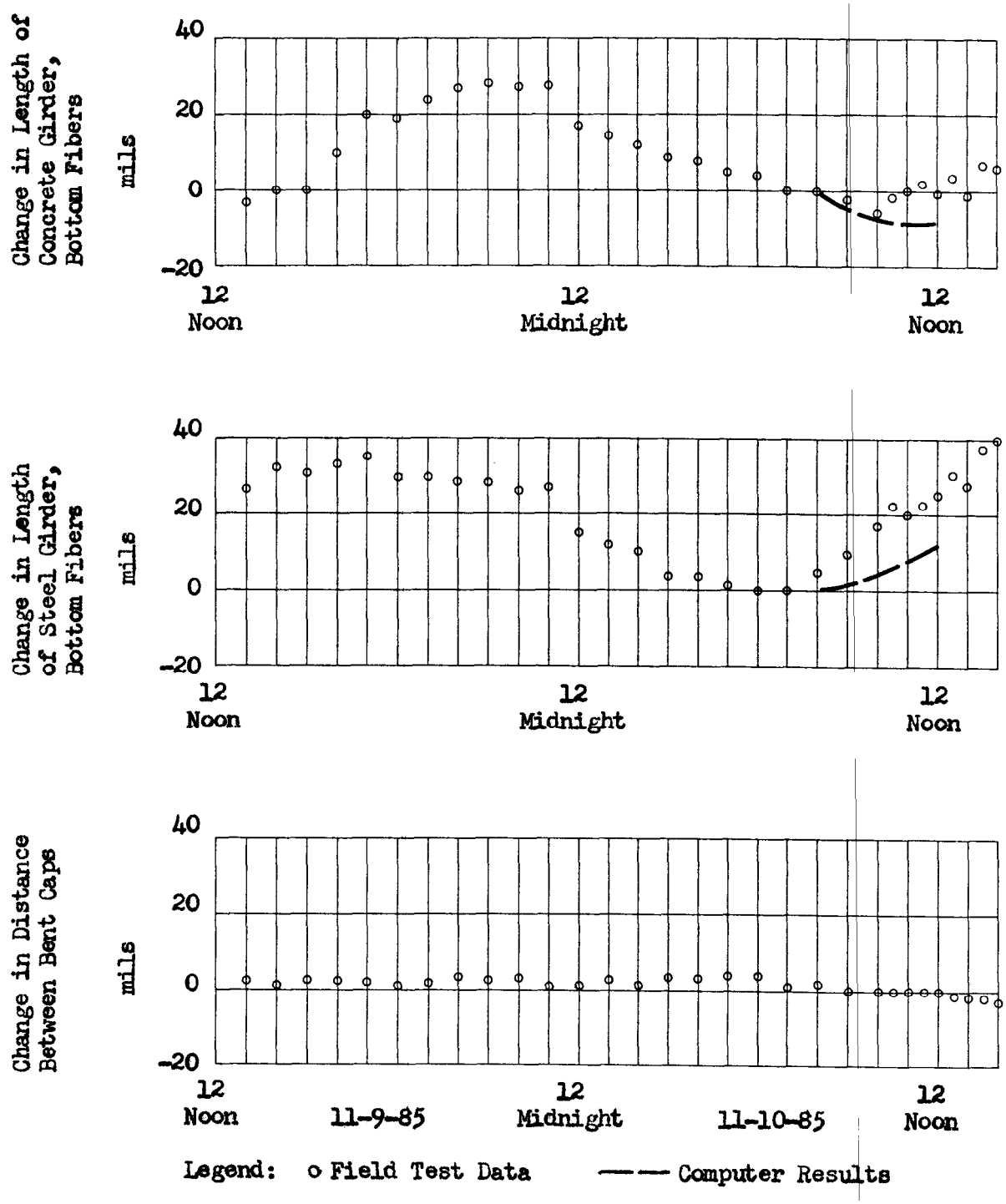

FIG. 29 COMPUTER PREDICTED LONGITUDINAL DEFLECTIONS AS A FUNCTION OF TEMPERATURE VS. MEASURED LONGITUDINAL DEFLECTIONS

4. INVESTIGATION OF MIXED GIRDER SUPPORT SYSTEM

4.1 Introduction

The computer model developed herein is used to investigate potential problem areas associated with mixed girder systems. The areas investigated are: camber growth, temperature effects, live load distribution, concrete diaphragms, rolled beams with cover plates, non-composite rolled beams and bearing movement effects. Finally, the combination of the above areas as appropriate are considered.

It is not the intent of these investigations to probe each area in great breadth nor to offer solutions to any problems uncovered but rather to determine on a gross scale which of the above effects could be a potential problem area.

The cases studied are limited to configurations similar to the Bonnabel Overpass and the computer models used are variations of the model developed for the Bonnabel Overpass. In all cases the model had a 45-ft, simply supported span with six steel girders in the interior, three concrete girders on the south side and one concrete girder on the north side. Also, in all cases symmetry about the mid-span is assumed. This means that the computer model is written for only half the span and a boundary condition of zero rotation about the lateral axis (y-axis) is applied at the

mid-span. The general layout of the model is shown on Fig. 30. The symmetry assumption saved considerable programming and machine time. In only one instance is the assumption suspected of affecting the results; that being when applying the HS20-44 live load to the determination of slab moments. In that situation the effect is investigated and is discussed under Section 4.4.

The following sections describe the model and loading configuration used and the results obtained for each of the potential problem areas investigated.

In this section when the term moment in a girder is used it means the moment about the lateral (y-direction) axis at mid-span in the composite girder-slab system. The term moment in the slab means the moment per unit width of slab about the longitudinal (x-direction) axis at mid-span.

4.2 Camber Growth

When camber growth occurs in prestressed concrete girders, they tend to arch in the center region. If these girders are located alongside steel girders which do not arch, then additional moments and stresses are caused in the concrete girders adjacent to the steel girders and in the section of slab between the concrete and steel girders. In this section these additional moments and stresses are investigated using the NASTRAN computer program.

The amount of camber growth to be expected for these prestressed girders was estimated using the AASHTO

prediction method. Fabrication and installation records were not available for individual girders, and thus camber growth was estimated based on average or specified values. The estimated camber growth based on this information is 1/4" at mid-span. Since this value is at best an average for many girders, it was decided to make computer runs simulating camber growths at mid-span of 1/8", 1/4" and 3/8".

The method used to simulate camber growth is to utilize the thermal aspects of the MSC/NASTRAN program. As discussed earlier, the bar element allows lateral thermal gradients across the element. In this case a positive thermal gradient is applied from bottom to top of the bar elements representing the concrete girders. When the girder is acting alone, the amount of arching at midspan is dependent only upon the magnitude of the temperature gradient imposed. On the other hand, when the girder is acting as a part of a composite beam with the slab in place, it is significant as to whether the gradient causes the bottom of the girder to contract or the top of the girder to expand. The model believed to best represent camber growth is one for which the top fibers of the girder experience little or no net creep and the bottom fibers experience the greatest compressive creep.

Thus the procedure for simulating camber growth is to first determine the linear temperature gradients required to cause 1/8", 1/4" and 3/8" growth at midspan, respectively,

for single girders acting alone. These gradients are then applied to the bar elements representing concrete girders in the total model and the bulk or average temperatures of the elements are specified so that the top of the girders will be at ambient or initial temperature.

As camber growth occurs in concrete girder G-3, which is adjacent to steel girder G-4, girder G-3 will carry a greater share of the dead weight of the slab, while girder G-4 will carry a lesser share of the dead weight of the slab. Also, the net shortening of the concrete girder caused by the compressive creep is being restrained by the slab and adjacent steel girder. This action causes a net tensile force on the girder in the axial direction, which decreases the amount of prestress compression in the bottom fibers of the girder.

Computer runs were made to investigate the stresses and moments in the adjacent concrete and steel girders caused by camber growth. Because of thermal and three dimensional effects as discussed above, there is no "simple moment" applicable to each individual girder. However, in order to compare the results obtained with applicable AASHTO design criteria, an equivalent moment is defined as being the moment required in order to cause the same stress in the bottom fiber of the respective girder. These moments are shown in Fig. 31. It will be observed that the computer program predicts that the moment at mid-span in the concrete girder increases significantly, while the moment in the

steel girder decreases significantly. The initial moments shown, i.e., the moments at zero camber growth, represent the moments due to the dead weight of the slab.

It should be pointed out that no correction has been made to the amount of camber growth caused by the added dead weight of the slab.

The lateral stresses at mid-span in the top and bottom fibers of the slab caused by camber growth are also shown on Fig. 32. It can be seen that the stresses are large near the girders and tend to be smaller in the center region of the slab. This is an advantage because, as will be seen later, the maximum stresses caused by live loads occur in the center region of the slab. Nevertheless, these moments and stresses are of significant magnitude, especially when it is observed that they are not considered in the design process.

4.3 Temperature Effects

The NASTRAN computer program is used to investigate the effect of ambient thermal changes upon the stresses in the section of slab between the concrete and steel girders and the stress in the adjacent concrete girder. Three conditions were investigated; these were a sudden increase in ambient temperature, a sudden decrease in ambient temperature, and a period of bright sunshine on the slab.

When a sudden change of the ambient temperature occurs, the various components of the structure will start to undergo a temperature change. The rate of change of the

bulk or average temperature is dependent upon the ratio of the surface area exposed to the atmosphere to the thermal mass of the component; the thermal mass being the product of the physical mass and the specific heat capacity. In the case of the Bonnabel Overpass, the rate of change in temperature of the steel girders would be five to ten times that of the slab and of the concrete girders. It is estimated that for normal diurnal changes in ambient temperature, the temperature of the steel girders will follow the ambient temperature to within a few degrees, while the concrete girders and slab will only change temperature by a total of a few degrees. This estimate does not include the effect on the slab of bright sunshine. This effect is considered later.

Since the purpose of these investigations is to identify gross problem areas rather than provide exact results, assumed values of 30°F sudden temperature increase and 40° sudden temperature decrease for the steel girders are used. These two conditions are modeled in the NASTRAN computer program by using the thermal expansion characteristics of the CBAR element. That is, a uniform bulk temperature change is imposed upon the bar elements representing the steel girders.

When a temperature increase is imposed on the steel girders, they will expand, tending to cause the center of the span to deform downward or sag near mid-span. On the other hand, the concrete girders which have experienced much

less bulk temperature increase will still be in their cambered profile. This condition will cause lateral moments and lateral stresses in the section of slab between the concrete and steel girders. The relative expansion of the steel girders will also cause a stretching of the slab and adjacent concrete girder in the longitudinal direction, which will cause longitudinal tension stresses in the slab and in the bottom fibers of the concrete girders.

The results of the computer study for the slab are shown on Figs. 33 and 34. Fig. 33 addresses lateral stresses and Fig. 34 addresses longitudinal stresses. It can be seen that for a $30^{o}F$ temperature increase maximum lateral tensile stresses of approximately 120 psi are caused in the top of the slab near girder G-3. The maximum longitudinal stress caused by this condition is approximately 150 psi in the bottom of the slab near girder G-4.

The computer analysis also shows that when a $30^{o}F$ sudden temperature increase is imposed on the steel girders, a tensile stress of approximately 240 psi is superimposed on the bottom fibers of concrete girder G-3.

When a temperature decrease is imposed on the steel girders, an opposite deflection occurs. The steel girders contract, tending to cause the span to arch upward near mid-span. This condition will likewise cause moments and lateral stresses in the section of slab between the concrete and steel girders. Referring to Fig. 33 again, it can be

seen that a $40^{\circ}F$ temperature decrease causes a lateral tensile stress of approximately 120 psi in the bottom of the slab near girder G-3 and a lateral tensile stress of approximately 180 psi in the top of the slab near girder G-4.

The contraction of the steel girder will cause the slab and concrete girders to be in longitudinal compression throughout, thus having minimal effect.

The stresses caused by temperature increases and decreases, as calculated in this section, probably represent extreme cases, because temperature changes of perhaps $50^{\circ}F$ in a one-hour period would be required. On the other hand, the calculations do show that these effects are significant when compared to the AASHTO design criteria. The design values are indicated on the graph.

When a span is subjected to a period of constant ambient temperature and no sunshine as might occur in the early morning hours, the slab and other components tend to reach a uniform temperature. If bright sunshine then impinges upon the deck, the slab will experience a radiant heat input, which will start to heat the top layer of the slab. With time, the heat will be conducted through the slab. After about three hours of sunshine on a slab of this thickness, the thermal gradient from top to bottom will be most severe and the temperature difference between the top and the bottom will be a maximum.

The thermal gradient was calculated for a constant radiant heat input of 50 Btu/hr/ft^2. This value is believed to be close to the maximum value which would be experienced in the early daylight hours. The calculated thermal gradient was imposed in the thickness direction of the quad4 plate elements used to model the slab.

Figs. 33 and 34 give the results of the computer analysis of this situation. The thermal expansion on the top of the slab places the bottom fibers of the slab in tension. It can be seen that both the lateral and longitudinal tensile stresses in the bottom of the slab are uniform across the section of slab between the concrete and steel girders, the lateral stress being about 100 psi and the longitudinal stress being about 70 psi. The stress in the longitudinal direction is less because the girders tend to restrain the expansion of the slab.

Sunshine on the top of the slab will cause small compressive stresses in the bottom fibers of the concrete girders.

It would appear from examining the graphs that the stresses caused by sunshine are not affected by the mixed girder configuration. However, these stresses do appear to be significant. In the lateral direction, the stress caused by sunshine is approximately 25% of the modulus of rupture and in the longitudinal direction the stress is approximately 20% of the modulus of rupture as given in the AASHTO specifications.

All of the computer results presented in this section are for the uncracked slab configuration and design concrete properties.

4.4 Live Load Distribution

The longitudinal moments in the girders at mid-span and the lateral moments in the section of slab between the steel and concrete girders caused by live loads were investigated.

Three different live load configurations were considered for determining the moments in the girders: a single AASHTO HS20-44 truck, dual lane AASHTO HS20-44 trucks and the 220k overload truck crane (OTC). Two different live load configurations were considered for determining the moments in the slab: a single AASHTO HS20-44 truck and the OTC. Since the maximum slab moments are primarily dependent on the tire print, it is not considered necessary to consider both the single and dual lane configurations for slab moment calculations.

For determining moments in the girders, the loads were centered on the span, as shown on Fig. 35, and for determining moments in the slab, the loads were placed with one wheel set at center span, as shown in Fig. 36. There are no significant differences in the girder moments caused by the two configurations, except as discussed below.

In order to facilitate use of the symmetrical computer model, certain wheel loads which would have negligible effect were omitted. For the case of finding moments in the

girders, the load due to the front wheels of the HS20-44 tractor truck were assumed to be negligible, because they are located very nearly over the support points. For the case of finding the moments in the slab, some loads were neglected for the basic investigation. The effect of this assumption was investigated and is discussed later.

For the case of calculating the moments in the slab due to the 220 k OTC, the load caused by all three opposite end axles was neglected. Two axles are off the span under consideration and the third axle is very near the support points.

The basic NASTRAN data deck for the Bonnabel Overpass with certain modifications, was used for this investigation. The only significant modification was to change the grid spacing in the longitudinal direction (x-coordinate) so that the vehicle axles were directly over the line of grid points.

Design properties of the concrete were used in the live-load investigation, except for a few runs made specific-ally to determine the effect of the concrete properties. Design concrete strengths were taken as 3000 psi for the slab and 5000 psi for the prestressed girders. Using the AASHTO equation, the corresponding values for Young's Modulus are 3.3×10^6 psi for the slab and 4.3×10^6 psi for the prestressed girders.

Two sets of computer runs were made for the purpose of investigating the effect of concrete properties. For these

runs concrete strengths more representative of those found in the field were used. Strengths of 6,800 psi for the slab and 8,500 psi for the prestressed girders were assumed, yielding values of Young's modulus of 5.0×10^6 psi for the slab and 5.6×10^6 psi for the prestressed girders. Poisson's ratio was assumed to be 0.15 in all cases.

4.4.1 Girder Moments HS20-44 Truck

Computer runs were made simulating the placing of a single HS20-44 truck at several different positions laterally across the span in the vicinity of the interface between the concrete and steel girders. All runs were made with the truck trailer centered on the span longitudinally, as illustrated on Figure 36. The longitudinal grid spacing was selected such that the wheel sets of the trailer would be over the line of the grid points. Further, in positioning the truck in the lateral direction, positions were chosen such that the wheel located between the concrete and steel girders would be directly over a grid point. For plate type elements point loads can be placed only at grid points; thus, for those cases where the wheel did not fall over a grid point, the wheel load was distributed to adjacent grid points assuming a linear distribution. The results of the computer study for the single HS20-44 truck are shown by the graphs of Figs. 37 and 38. These graphs show plots of the moment in the composite girders at mid-span as a function of position of a single HS20-44 truck

across the span. Results are shown for both design concrete properties and field measured concrete properties. An uncracked slab is assumed for both cases.

The magnitude of the moment at mid-span acting on the composite girder is a function of the vertical location of the lateral axis about which moments are taken. This is because there are longitudinal axial stresses in the girders caused by the interaction between girders. The moments in the girders as given herein are the moments about the neutral axis of each girder, calculated by assuming the composite section to be made up of the girder and the portion of the slab out to the mid-point between the adjacent girder on either side. The vertical location of the neutral axes will thus vary with type girder and with concrete properties. The moments for girders G-2 through G-5 are shown. These are the two concrete and two steel girders adjacent to the concrete-steel girder interface. Note that girder G-3, which is the concrete girder closest to the steel girders, carries approximately 12% more load than girder G-2.

On the other hand, the stiffer concrete girder tends to protect the nearest steel girder G-4. Girder G-4 carries about 20% less load than girder G-5. It is interesting to note that the maximum moment in steel girder G-5 is approximately the same as that in concrete girder G-2, even though the spacing of the steel girders is approximately 16% greater than that of the concrete girders.

A series of computer runs was made with two HS20-44 trucks side-by-side, simulating dual lane loading. The two trucks had a center-to-center spacing of 10 feet. As in the case of the single HS20-44 truck, the dual trucks were positioned at several different lateral locations in the vicinity of the interface between the concrete and steel girders. All computer runs were made with the truck trailers centered on the span longitudinally, as illustrated on Fig. 35.

Comments given in the previous discussion relative to load distribution at grid points and the neutral axes for girder moments are also applicable for this discussion.

The results of the study for the dual lane loading are given on the graphs of Figs. 39, 40 and 41. These graphs show plots of the moment in the composite girders at mid-span as a function of lateral position of the HS20-44 trucks. Results are shown for three concrete configurations: design concrete properties and uncracked slab, field concrete properties and uncracked slab, and field concrete properties and cracked slab. It can be seen that the maximum moment in girder G-3 exceeds the AASHTO design specification value in all cases, by approximately 28%, 35% and 45% respectively for the three concrete configurations given.

The results show that for dual lane loading the moment in girder G-2 also exceeds the AASHTO design value by a

significant amount. It appears that this girder is experiencing edge or end effects.

The data shows that the concrete girder protects the adjacent steel girder, G-4, causing it to carry much less than its share of the load.

4.4.2 Girder Moments - 220 k OTC:

Computer runs were made simulating placing of a 220 k OTC at several different positions laterally across the span in the vicinity of the interface between the concrete and steel girders. All runs were made with the OTC centered or straddling mid-span in the longitudinal direction, as indicated on Fig. 35. The OTC has three wheel sets or axles on both the front and rear and the longitudinal grid spacing was again selected so that each axle of the vehicle would be over a line of grid points. The OTC has a transverse wheel spacing of 10 ft, which means that when the wheels along one side are positioned over the region between the concrete and steel girders, the wheels on the other side may be outside the fine grid region and consequently these wheels may not be over a line of grid points. In this case a linear distribution was used to distribute the load to the neighboring grid points.

The results of the computer study are shown by the graphs of Figs. 42 and 43. The graphs show moments in the composite girders at mid-span as a function of position of the 220 k OTC centerline across the span. Results are shown

for design concrete properties and for field measured concrete properties. An uncracked slab is assumed in both cases. It can be seen that girder G-3, the concrete girder next to the steel girders, carries about 10% to 15% more load than the adjacent concrete girder G-2.

Also it can be seen that the concrete girder again protects the nearest steel girder, G-4, causing girder G-4 to carry about 25% less load than G-5.

4.4.3 Slab Moments - HS20-44 Truck:

Computer runs were made to investigate the moments in the section of the slab between the concrete and steel girders caused by a single HS20-44 truck load. The output was limited to the moments along mid-span. The truck was positioned longitudinally, with one wheel set over mid-span, as shown on Fig. 36, and was positioned at several locations across the span.

For cases involving the determination of slab moments, it was decided that the load of the wheel on the section of slab between the concrete and steel girders would be modeled using a uniform pressure load. The longitudinal grid spacing was thus selected so that the plate elements along mid-span would be approximately the size of the tire contact area given in the AASHTO specification. The details of a typical loading case are shown by Fig. 44. It will be noted that two additional lines of longitudinal grid points have been included so as to better define the moment curves.

Four runs were made to investigate the effect of neglecting the remaining wheels of the tractor-trailer configuration. The worst configuration was assumed to be the case where the rear wheels of the tractor are over mid-span, the front wheels of the tractor are 14 feet ahead of mid-span, and the rear wheels of the trailer are 14 feet before mid-span. Since the computer model required symmetrical loading, the above configuration was approximated by averaging the 4 k front wheel load of the tractor and the 16 k rear wheel load of the trailer and placing 10 k at each wheel location to either side of mid-span. This case could then be simulated by the symmetrical computer model by placing 10 k at the location of the front wheels, as they are shown on Fig. 36. The results of the computer study relative to moments in the slab caused by the HS20-44 truck load are shown by the graphs of Figs. 45 and 46. The significant output from the NASTRAN computer program for this situation is stress in the slab top and bottom fibers. Flexural theory was used to convert these stresses to equivalent moments per unit width assuming design concrete properties and a full depth uncracked slab.

Fig. 45 shows how the moment varies across the section of slab between the concrete and steel girders for several representative loading positions. The maximum lateral moment resulting from each loading position was determined graphically and cross plotted to obtain the graph of Fig. 46.

This second graph shows the maximum moment as a function of the position of the truck wheel across the slab.

It can be noted that the presence of the additional wheel loads 14 feet forward and aft of the mid-span wheel load increases the moment in the slab by approximately 5%.

The maximum moment in the slab is seen to be very near 3400 ft-lb/ft, which would be the design value based on the AASHTO specifications. This would indicate that the present slab design criteria, as given in Section 3.24.3.1 of the 1985 AASHTO specifications, are adequate for spans similar to the Bonnabel Overpass when loaded with an HS20-44 truck.

4.4.4 Slab Moments - 220 k OTC:

Computer runs were made to investigate the moments in the section of slab between the concrete and steel girders caused by the 220 k OTC. The OTC was positioned longitudinally with the center axle of one of the three-axle sets over mid-span and was positioned at several locations laterally across the span.

The load of the wheel which is located at mid-span and on the section of slab between the concrete and steel girders was again modeled using a uniform pressure load. The details of this loading were described in the previous section.

All loads due to the wheels on the opposite end of the OTC were neglected, because two axles are off the span under

investigation and the third is approximately over the supports.

The results of the computer study relative to the moments in the slab caused by the 220 k OTC is shown by the graphs of Figs. 47 and 48. As described earlier, the moments were obtained from stress data output.

Fig. 47 shows how the moment varies across the section of slab between the concrete and steel girders for two representative loading positions. The remaining loading position data were omitted to avoid confusion. The maximum moment resulting from each loading position was determined graphically and cross plotted to obtain the graph of Fig. 48. This graph shows the maximum moment as a function of the position of the OTC wheel across the slab.

It can be seen that the maximum moment in the slab is approximately 4700 ft-lb/ft, and it occurs when the wheels on the opposite side are over the concrete girders. The value of 4700 ft-lb/ft is approximately 40% higher than the value obtained using the AASHTO criteria.

4.5 Concrete Diaphragms

A series of computer runs was made in order to determine the effect on girder moments and slab stresses of adding diaphragms between the concrete girders and between the concrete and steel girders. Two configurations for diaphragm locations were considered. These were placing diaphragms at the third spans and placing diaphragms at the

mid-spans. The existing Bonnabel Overpass and the basic computer model have diaphragms at the third span between the steel girders.

The designs of the diaphraghms used are shown on Fig.49. Between the concrete girders, a cast reinforced concrete diaphragm is used. The diaphragm is attached to the girders by means of a 1" diameter tie rod. Between the concrete and steel girders, a C15 x 33 steel channel diaphragm is used. On the concrete girder end, the channel is bolted to a steel angle bracket, which is in turn bolted to the concrete girder. On the steel girder end, the channel is bolted to a steel plate, which has been welded to the steel girder.

In order to obtain an estimate of the end fixity conditions which should be used to represent the actual field situation, a uniform moment along the diaphragm was assumed. For this situation it is estimated that the angular rotation at each end resulting from the type end connection is in the order of four times the angular deflection that occurs along the remainder of the diaphragm. It is thus deduced that the effective stiffness of the diaphragms is at most one fourth of the stiffness of a rigid end diaphragm. For the steel diaphragms the rotation could be much higher if the bolts slide in the slotted bolt holes. Sliding of the bolts in the bolt holes is not considered in the analysis. Computer runs were made for three different diaphragm end connection configurations and for no diaphragms. The three end connection configurations

represent a very rigid condition, a very flexible condition and an intermediate condition. The intermediate condition is believed to approximate the actual situation. The computer inputs for the three configurations were, respectively, diaphragms with full section moments of inertia and rigid end connections, diaphragms with full section moments of inertia and pinned end conditions, and diaphragms with one quarter of the full section moment of inertia and rigid end connections.

The effects of adding the diaphragms on the maximum moments in girder G-3 are shown by Figs. 50 and 51. It can be seen that as the load is positioned at various locations across the span, there will be a maximum moment value for each diaphragm configuration. It can be seen that the effect of the increasing diaphragm stiffness is to reduce the maximum moment in the girder. If the diaphragm could be installed with perfectly rigid end connections, the maximum moment would be reduced by 10%-12%; however, under actual end fixity conditions the reduction is believed to be less than 10% and may be as low as 5%.

It can be observed that from the standpoint of reducing the moments in girder G-3, one diaphragm at midspan is just as effective as two diaphragms located one at each third span point.

It was found that the diaphragms have even less effect on the slab stresses. This can be seen in Fig. 52, which shows that the maximum stress in the slab is reduced about

8% by diaphragms with perfectly rigid end connections but is only reduced about 4% for the case believed to represent the actual end conditions.

4.6 Rolled Beams with Cover Plates

The computer input data deck representing the Bonnabel Overpass was modified so that all steel beams would be rolled beams with welded coverplates. The rolled beam used was a W 24 x 62 with a section major moment of inertia of 1540 in^4 and a section cross section area of 18.0 in^2. The coverplate was 1/2" x 9" plate.

The span was loaded using the 220 k overload truck crane (OTC), assuming 18.3 k per wheel. The vehicle was centered longitudinally over mid-span. Three lateral loading positions were considered; these being the vehicle centered over (straddling) girder G-6, the vehicle centered between girders G-5 and G-6, and the north wheels of the vehicle directly over girder G-6. Although the differences were small, the case where the vehicle is centered over the girder gave the maximum stresses in the bottom fibers of the girder, and this is the case presented.

Fig. 53 shows a typical curve of stress distribution in the bottom fibers along the length of the girder. The magnitude of the stress along the center portion of the girder is approximately constant and independent of the overall length of the coverplate. At each end of the

coverplate there will be a step increase in stress as shown on the graph.

Computer runs were made for a range of coverplate lengths. Fig. 54 shows how the peak stress at the end of the coverplate varies with coverplate length. It will be noted that for the case of the Bonnabel Overpass symmetrically loaded with the 220 k OTC, the coverplates must be almost 400 inches long (75% of total length) before the stress level at the end of the coverplate drops below the value at mid-span.

Fig. 55 shows the moment distribution along the composite section made up of the steel girder and the associated strip of the concrete slab. The moments acting on this composite section are not values which can be obtained as a direct output from the NASTRAN computer program. To obtain these moments it is necessary to define a composite section and determine a neutral axis location in the traditional manner. The stress data output from the computer can then be used to "work backwards" to obtain the moment distribution for the composite section.

On the stress and moment curves of Figs. 53 and 55 there are two values for each location (some are coincident). This is because the computer model for the girder is made up of a number of bar elements and the NASTRAN program gives output stresses for each end of each bar. Thus for each location where two bar elements attach to a single grid point, two stress values are given.

4.7 Non-Composite Rolled Beams

In this investigation the NASTRAN input data deck for the Bonnabel Overpass is modified so that all steel girders are replaced with non-composite rolled beams. The purpose of this investigation is to determine if camber growth in the concrete girders will cause the slab to separate from the non-composite steel girders. The beams are W27 x 146 with a section major moment of inertia of 5430 in^4 and a cross-section area of 42.7 in^2.

The non-composite configuration is modeled by using a double row of GRID points along each steel girder, one row being attached to the slab and the other row being attached to the girders. Corresponding grid points between the slab and girders are connected using a rigid RBAR element. This element can be programmed so that the grid points are rigidly connected in the vertical direction but are free to move relative to each other in the lateral and longitudinal direction and in the three rotational directions. (MSC has developed a non-linear element called CGAP which allows modeling of surfaces which may come into contact. Documentation was not available on this element in time for it to be used on this project).

The modified model is loaded to simulate camber growth by the same method used in Section 4.2. Fig. 56 shows the vertical deflection of the slab at mid-span caused by camber growth. Curves are shown on the graph for camber growths of 1/4 inch and 3/8 inch. Also shown on the graph is a

dotted line indicating the relative position the slab over the steel girders would have prior to the slab being poured. This line represents the fact that steel girders will deflect downward approximately 0.3 inches when the slab is poured. Thus the slab over the steel girders must be raised by that amount before the slab loses contact with the non-composite girders.

It can be seen from the graph that a camber growth of 3/8 inch will cause the slab in the vicinity of G-4 to raise up by only about 0.2 inches; thus the slab will not lose contact with the non-composite steel girder. It appears that a camber growth of approximately 5/8 inch would be required before the slab lifted off the adjacent non-composite girder.

5.8 Bearing Movement Effects

The original Bonnabel Overpass was constructed using self-lubricated bronze bearing shoes to support the steel girders. These shoes allow sliding motion in the longitudinal direction, rocking motion about the lateral axes and are inelastic in the vertical direction. When the Bonnabel Overpass was widened, neoprene pads were used to support the prestressed concrete girders. These pads, compared to the bronze shoes, are considered to be less rigid in the vertical direction and to impose higher loads on the supporting structure in the longitudinal direction.

The purpose of this section is to investigate some of the consequences of using the neoprene pads.

As was discussed in Section 3.5, a new neoprene pad representative of those used in the Bonnabel Overpass widening was tested in compression. The elastic constant in the vertical direction for this new pad was found to be 0.5 x 10^6 lb/in. Also, the new pad has an uncompressed thickness of 1.1 inches. The dead load on each of these pads when in service is approximately 23,000 pounds, which would cause a compression of about 0.05 inches, so that the thickness of the pads under load would be about 1.05 inches. It was found, however, that the neoprene pads which were installed at the time of the widening are presently about 0.9 inches in thickness, indicating that these pads have experienced considerable creep and consolidation.

Examination of the load test data of sections 2.2 and 2.3 show that both the supports for the steel girders and the supports for the concrete girders are deflecting vertically under load. Elastic constants were deduced from these results to be used in the computer comparison of Sections 3.2 and 3.3. The values used were 1.4 x 10^6 pounds per inch for the steel girder supports and 1.0 x 10^6 pounds per inch for the concrete girder supports. It is noted that the elastic constant of 1.0 x 10^6 pounds per inch for the concrete girder supports includes the effect of both the soil elasticity and the neoprene pad elasticity, and yet it is still twice the elastic constant of a new neoprene pad.

This indicates that the elastic constants of the in-place pads have increased several fold.

One of the most severe consequences of having used the neoprene pads would result from the more than 0.1 inches consolidation of the pad. Assuming the bent caps did not move vertically, this would mean the concrete girders have moved vertically with respect to the steel girders and would thus place a significant bending load on the slab. This load would be the greatest at the end of the span. A computer analysis was made to investigate the effect of this bending. Fig. 57 shows the computed lateral stress in the top and bottom fibers of the slab at the end of the span due to imposing a 0.1 inch vertical displacement downward on girders G-1, G-2 and G-3. It can be seen that the tension stresses in both the top and bottom of the slab are large and are nearing the magnitude which would cause cracks, even without the effect of any other loading.

The computer program was also used to investigate the longitudinal forces on the bent caps caused by thermal contraction and expansion of the span superstructure. The magnitude of these forces are directly dependent on the amount of relative movement of the bent caps and the shear modulus of the neoprene pad. The results of Section 3.4 show that the distance between adjacent bent caps is very nearly constant and the span remains centered between the caps. Thus for this analysis it can be assumed that the neoprene pad supports are fixed.

As discussed above, the elastic constant of the in-place pads appears to have increased several fold, and thus Young's modulus would be much larger than the value for virgin neoprene. This means that the shear modulus has also increased several fold.

In this investigation the properties of new neoprene are used to obtain a base value for the longitudinal forces on the bent caps. Runs were made for $+40^{\circ}F$ and $-40^{\circ}F$ temperature change of the entire span superstructure. It was found that a temperature change of $40^{\circ}F$ causes a longitudinal force of 10,000 pounds at each neoprene pad. The resulting stresses in the bottom fibers of the concrete girders would be 30 psi tension for a $40^{\circ}F$ temperature decrease and 30 psi compression for a $40^{\circ}F$ temperature increase.

Again, these are the forces and stresses assuming virgin neoprene properties. The longitudinal force and stress would be approximately proportional to the shear modulus, thus it is believed that the actual values would be several times the value given above.

It is suspected that the neoprene pads are not performing as intended. The pads have consolidated significantly, possibly causing cracking of the slab near the ends of the span and the pads may have become more or less inelastic, causing abnormally high longitudinal forces on the bent caps.

4.9 Combined Effects

In this section the effects on girder moments and slab stresses of combined loading are considered. The loads used consist of linear combinations of the individual loads as appropriate, which are discussed in earlier sections of this chapter. It is not the intent of this section that all combinations be studied nor that the maximum moments and stresses due to combined loading be determined, but rather to present representative combinations to indicate whether or not problem areas may exist.

The loading situations which the computer solutions indicate as having large effects on girder moments are live loads and camber growth. Neoprene pad consolidation has a lesser effect on girder moments. Computer solutions were obtained for the moments at mid-span due to these combined loads using the Bonnabel Overpass Model, with an uncracked slab configuration and design concrete properties. Girder moments were determined for two combined loading situations: for dual HS20-44 trucks liveload and 1/4" camber growth; and for dual HS20-44 trucks live load, 1/4" camber growth and -0.1" neoprene pad consolidation.

As was discussed in section 4.2, three dimensional and thermal effects make it necessary to further define the meaning of the moment in the composite girder. The term "moment in girder" as used in this section means the equivalent moment which would produce the same stress in the bottom fibers of the girders.

The computer results for the two load cases described above are shown on Fig. 58. The moments at mid-span in girders G-2 through G-5 are plotted versus the lateral position of the dual HS20-44 trucks centerline. It can be seen that the moment in girder G-3, the concrete girder adjacent to the steel girders, is very large, being approximately twice the AASHTO design value given by S/5.5. Note that these moment values do not include the effect of the initial weight of the slab but only the effect of live load, camber growth and pad consolidation.

It can be seen from the graph that the effect on girder moment of neoprene pad consolidation is relatively small and only affects girders G-3 and G-4. Pad consolidation causes a slight decrease in the maximum moment in G-3 and a slight increase in G-4. It will also be observed that the moment in G-4 is negative for some loading situations and reaches a maximum value of only one third of the design value, even when the dual HS20-44 trucks are directly over that girder.

As was discussed in Section 4.2, no correction is made for the effect on camber growth of the added dead weight caused by camber growth. Nevertheless, the computer solution indicates that a combination of live loads and camber growth could cause serious overloading in the adjacent concrete girder for mixed girder configurations.

A series of computer runs was made to determine the effect on slab tensile stresses of a combination of all those loads believed to be significant. The loads which

cause tensile stresses in the bottom fibers of the slab are live load, sunshine on the slab, camber growth, neoprene pad consolidation, and expansion of the steel girders due to temperature increase. All of these loads were input into the computer and an output was obtained which combines dual HS20-44 live load, 3 hours of sunshine, 1/4" camber growth, -0.1" neoprene pad consolidation and 30^{o}F temperature increase of steel girders. The results of these computer runs for one HS20-44 loading position are shown in Figs. 59 and 60. Fig. 59 shows the lateral stress in the bottom fibers of the slab along the mid-span, and Fig. 60 shows the longitudinal stress in the bottom fibers of the slab along mid-span. It can be observed that at a location underneath the tire print, the tensile stress in the lateral direction exceeds the AASHTO specified value for modulus of rupture for plain concrete.

The tension stresses discussed above are caused primarily by live load and sunshine and are thus not unique to the mixed girder situation. The sunshine loading situation used herein assumes a rather modest heat input rate, and it is believed probable that conditions conducive to causing cracking of the bottom of the slab frequently occur over the entire span. This belief is corroborated by the comparison of computer predictions with field test results, as discussed in Sections 3.2 and 3.3.

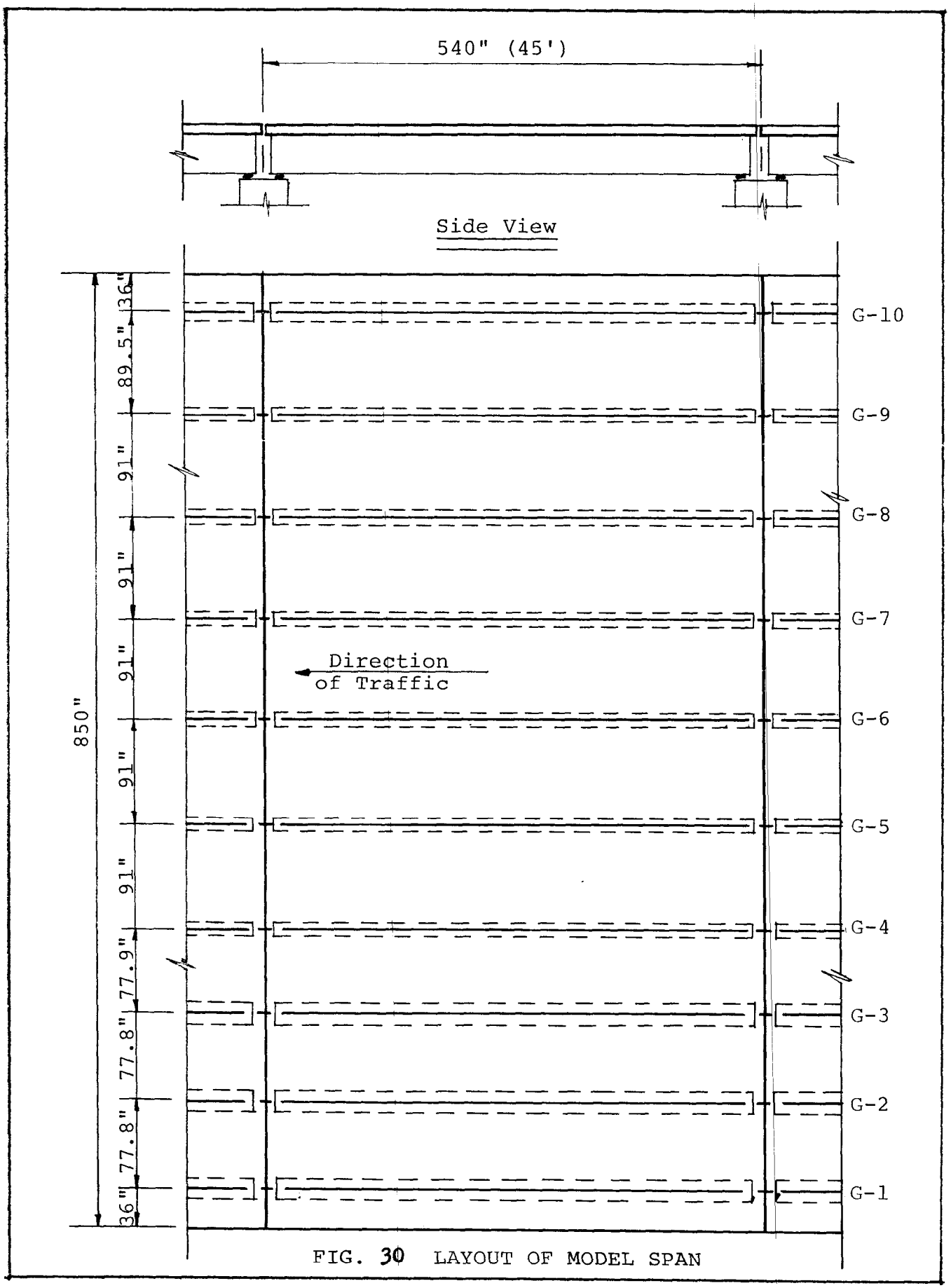

FIG. 30 LAYOUT OF MODEL SPAN

Note: See Section 4.2 for definition of moment as plotted on this figure.

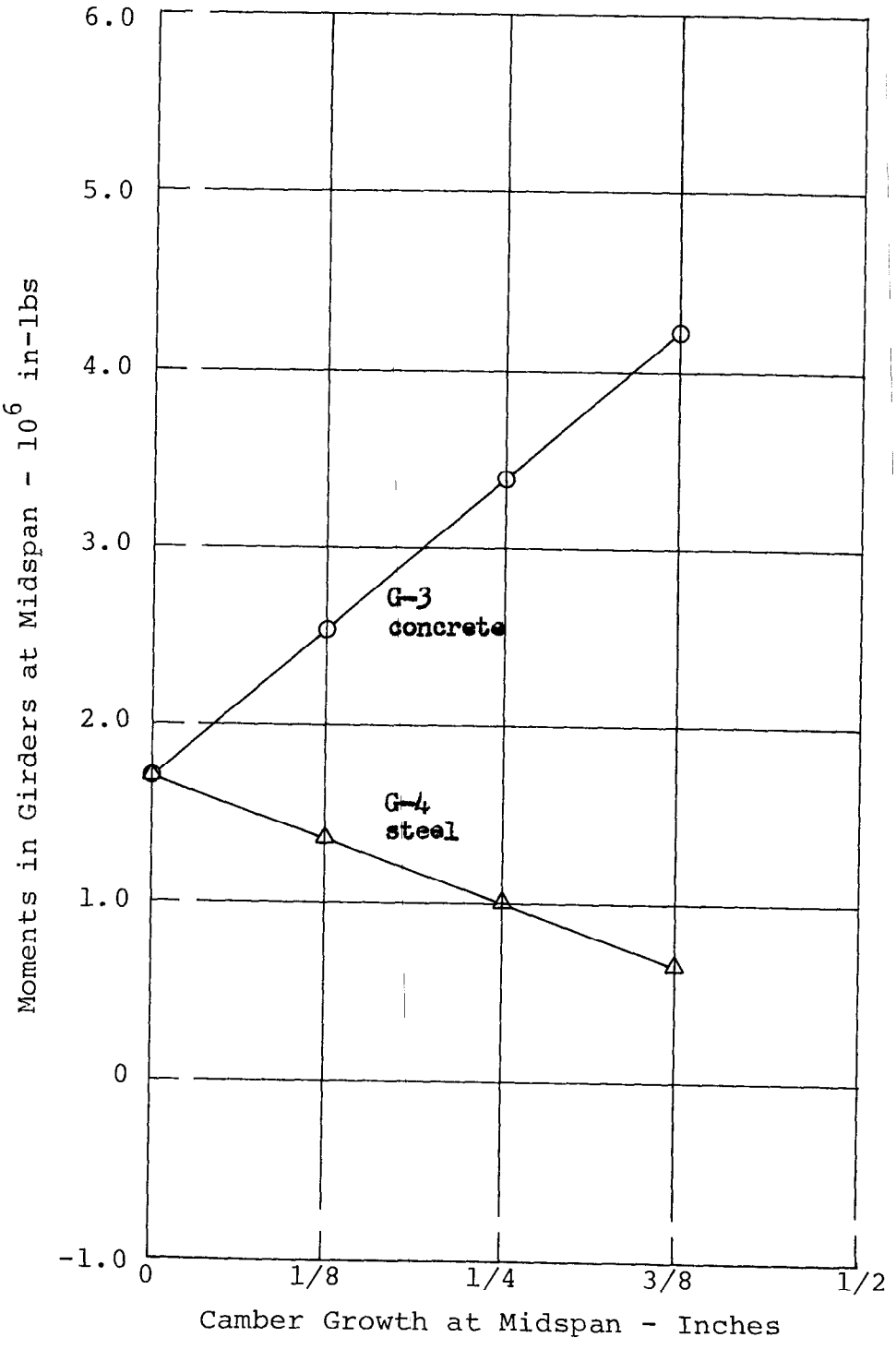

FIG. 31 EFFECT OF CAMBER GROWTH ON MOMENT AT MIDSPAN IN ADJACENT CONCRETE AND STEEL COMPOSITE GIRDERS

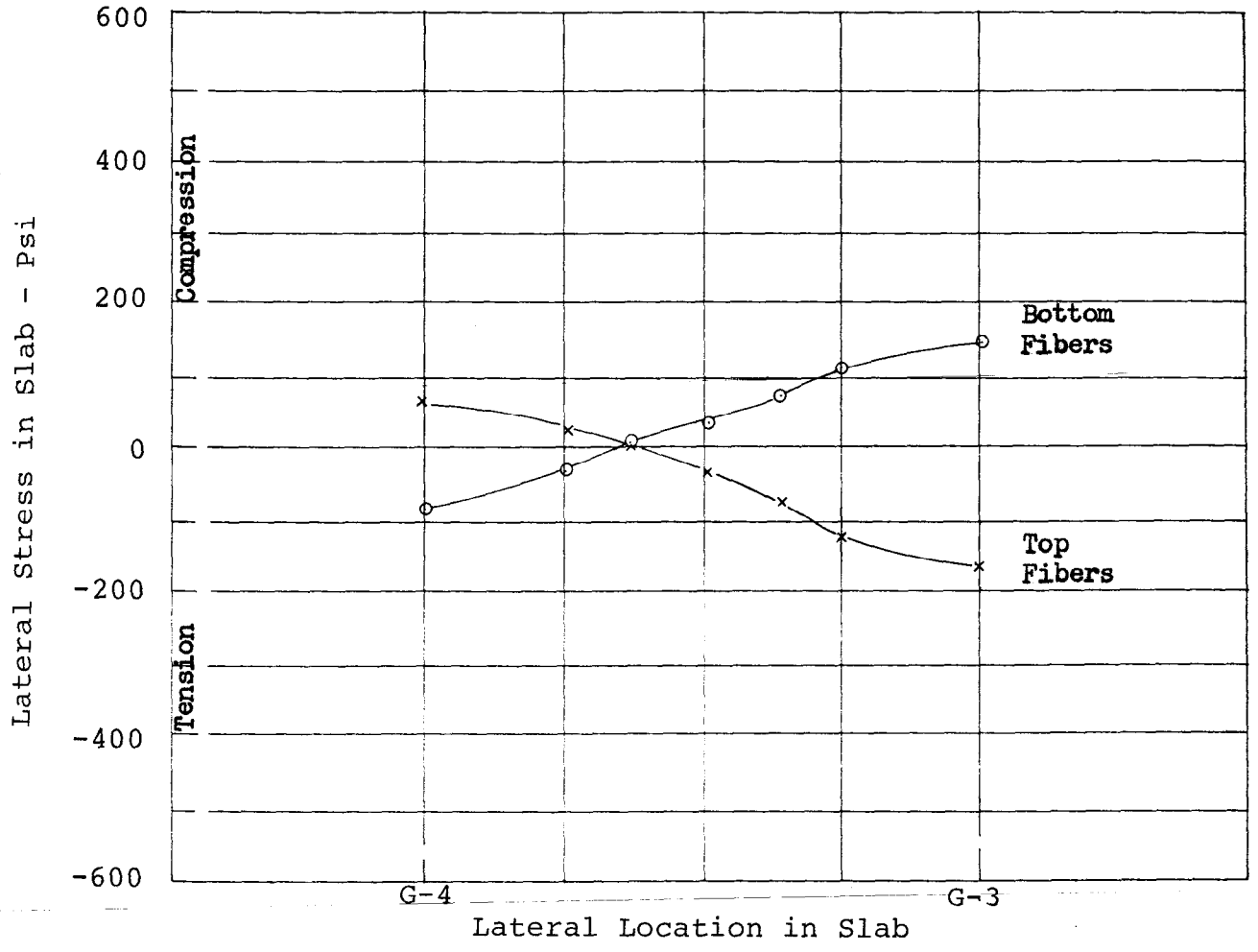

FIG. 32 LATERAL STRESS IN TOP AND BOTTOM FIBERS OF SLAB AT MIDSPAN DUE TO 1/4 IN. CAMBER GROWTH

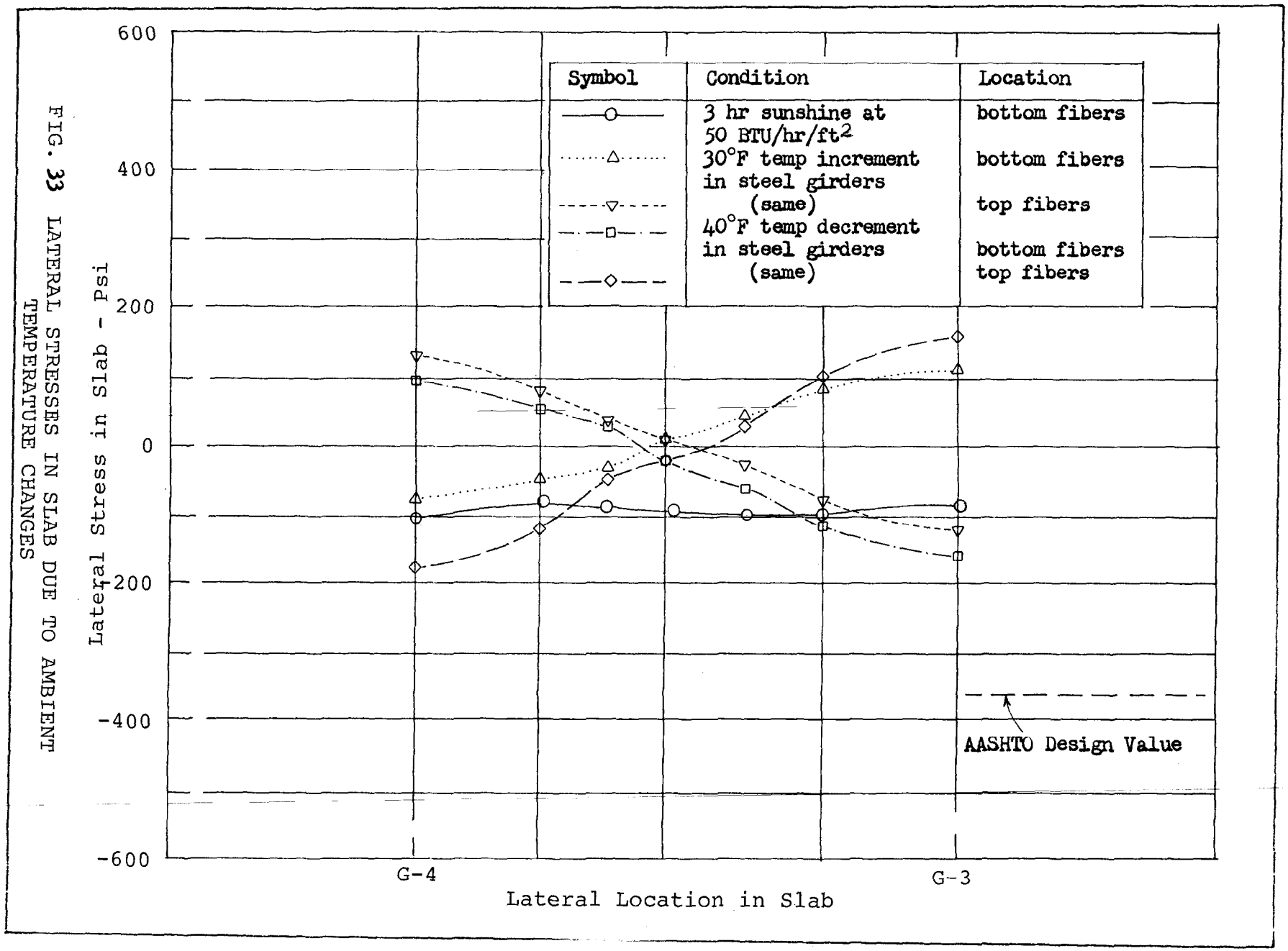

FIG. 33 LATERAL STRESSES IN SLAB DUE TO AMBIENT TEMPERATURE CHANGES

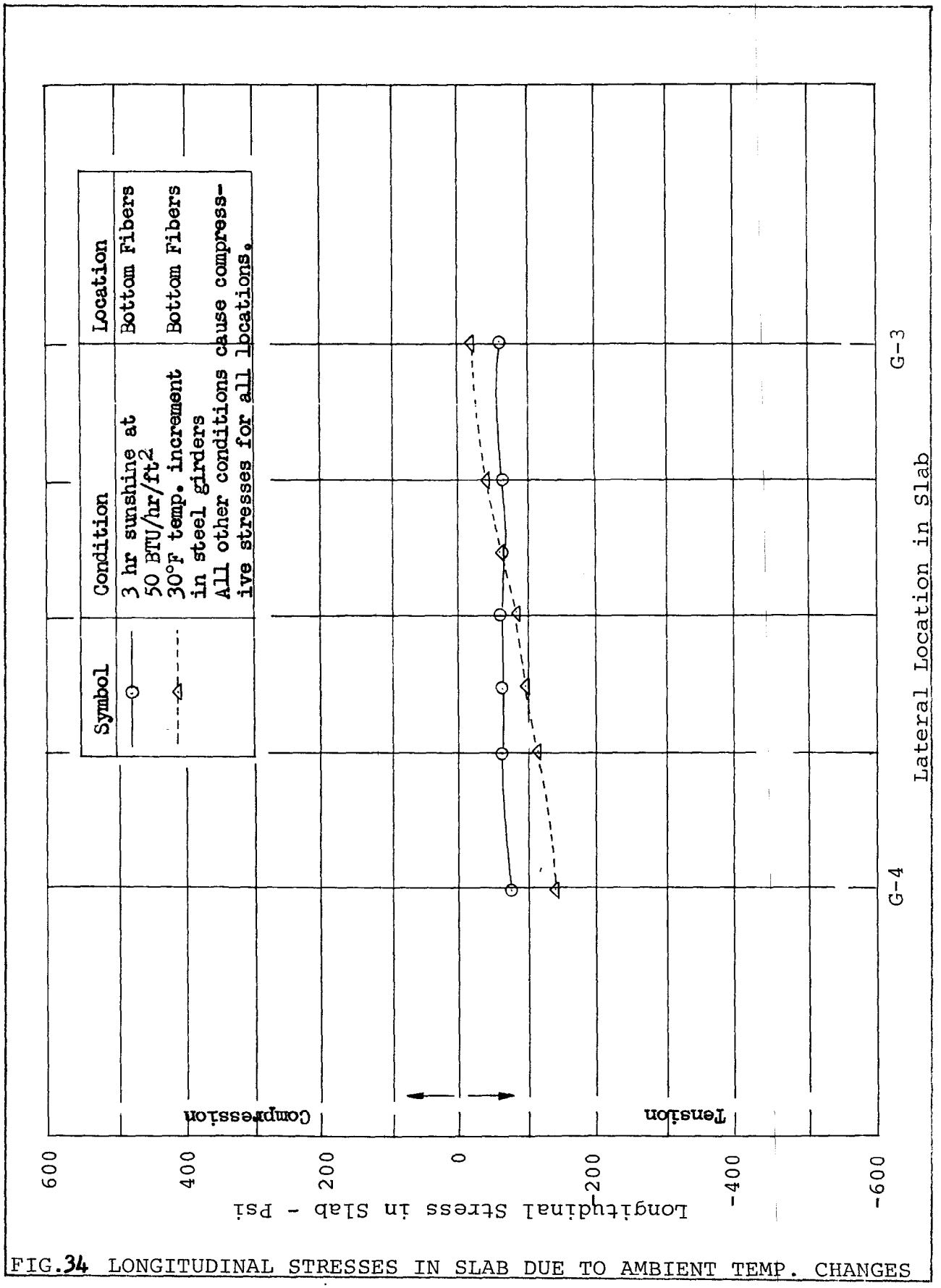

FIG.34 LONGITUDINAL STRESSES IN SLAB DUE TO AMBIENT TEMP. CHANGES

Note: There is no significant difference in the maximum girder moment caused by the load configuration shown on this figure, and that shown on Fig. 36.

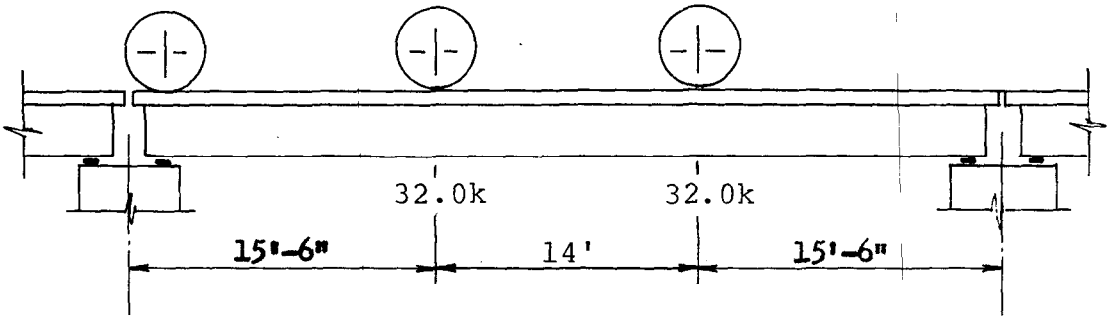

(1) HS20-44 Truck

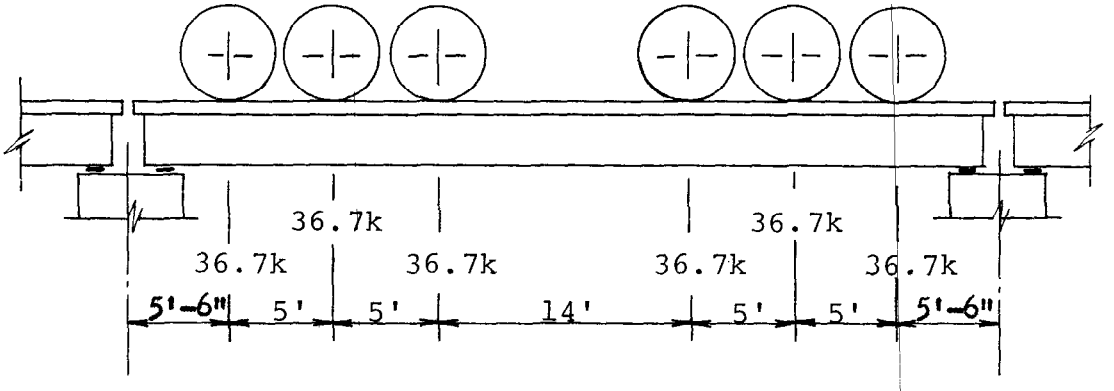

(2) 220k Overload Truck Crane

FIG. 35 LIVE LOAD LOCATION FOR DETERMINING LONGITUDINAL MOMENT IN GIRDERS

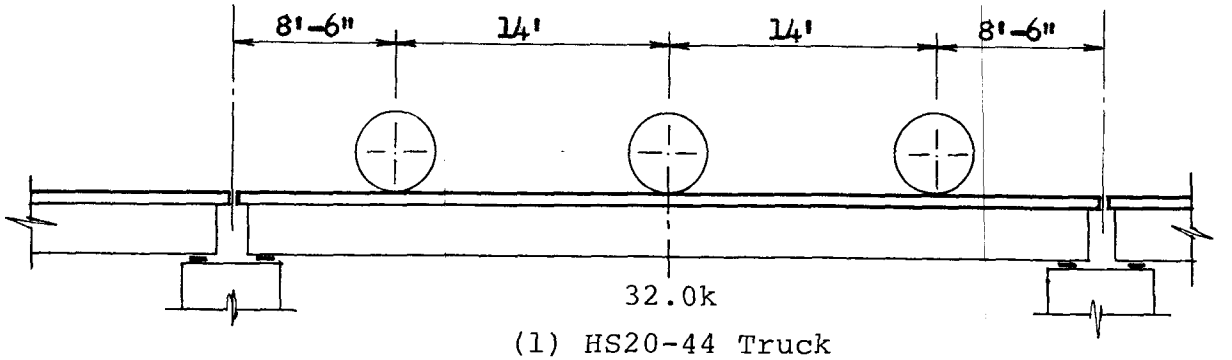

(1) HS20-44 Truck

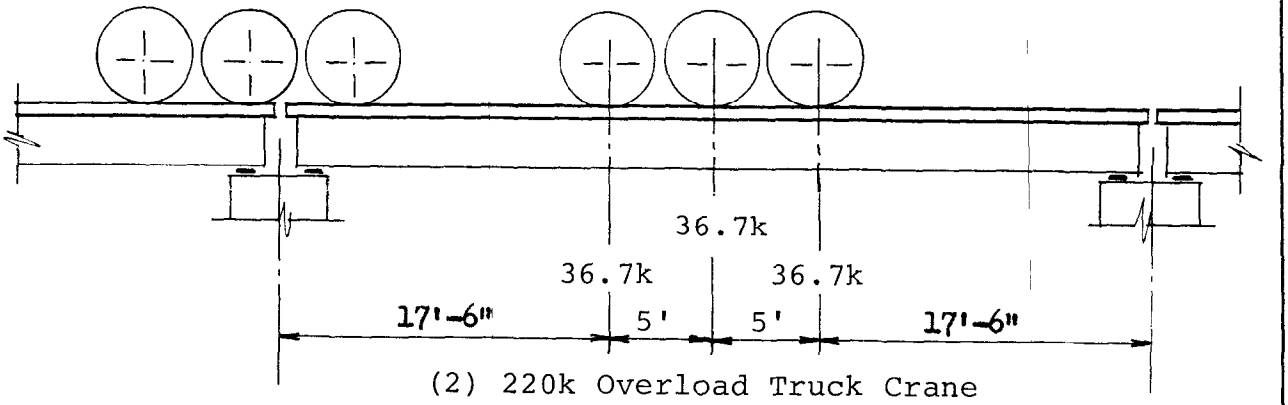

(2) 220k Overload Truck Crane

FIG. 36 LIVE LOAD LOCATION FOR DETERMINING LATERAL MOMENT IN SLAB

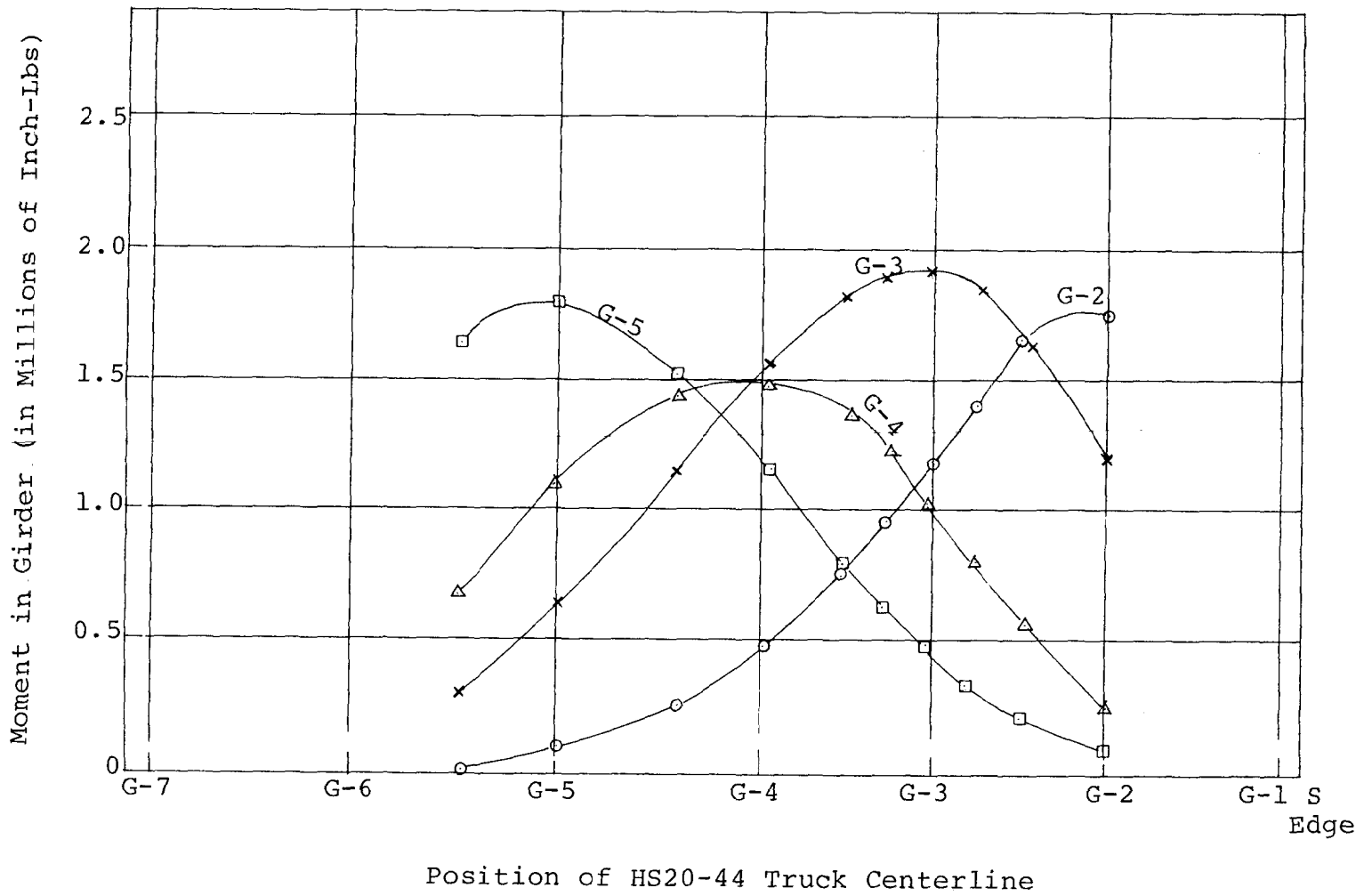

FIG. 37 MOMENT IN GIRDERS AT MIDSPAN DUE TO HS20-44 TRUCK LOAD - DESIGN CONCRETE PROPERTIES
- UNCRACKED SLAB

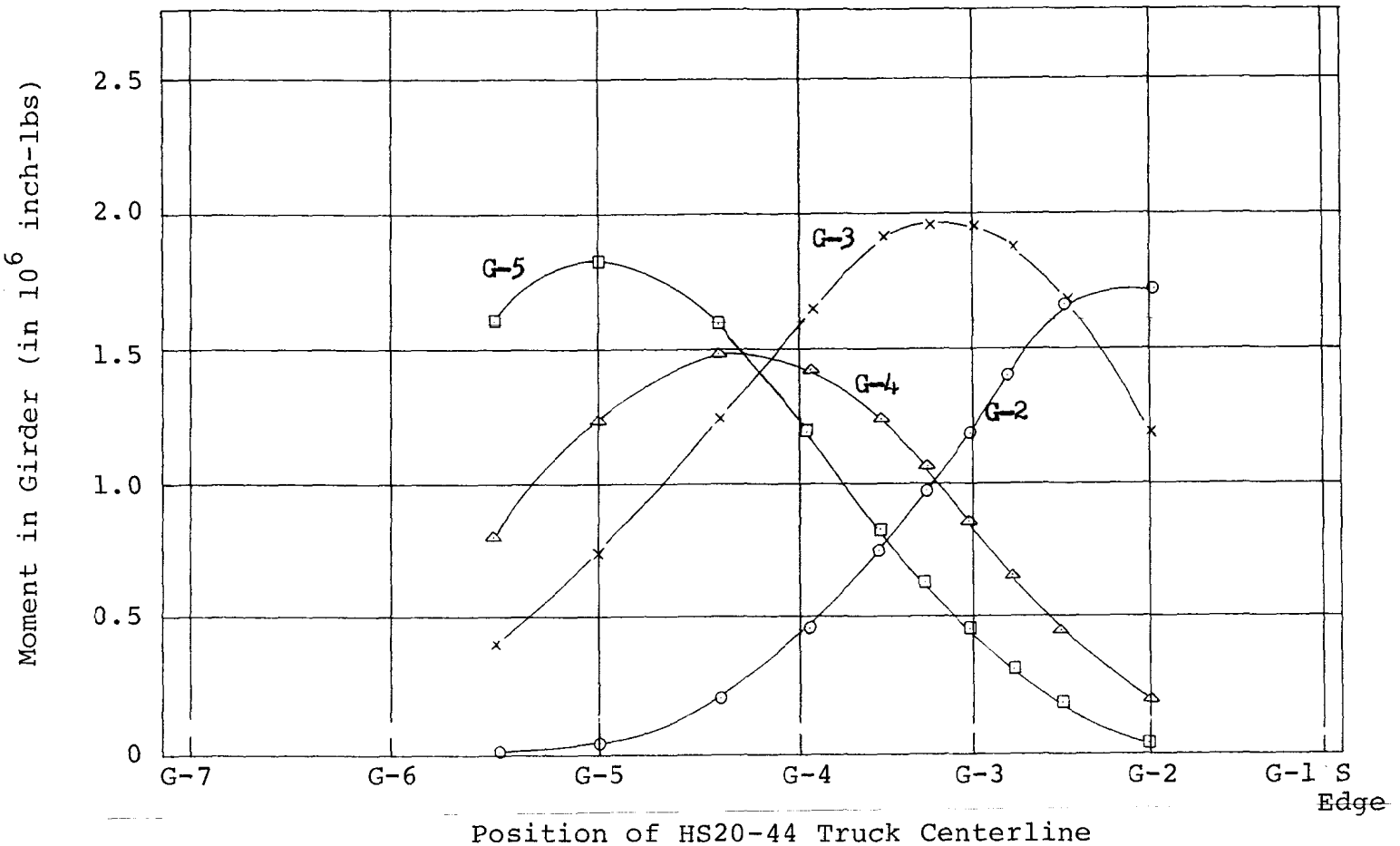

FIG. 38 MOMENT IN GIRDERS AT MIDSPAN DUE TO HS20-44 TRUCK LOAD - FIELD CONCRETE PROPERTIES - UNCRACKED SLAB

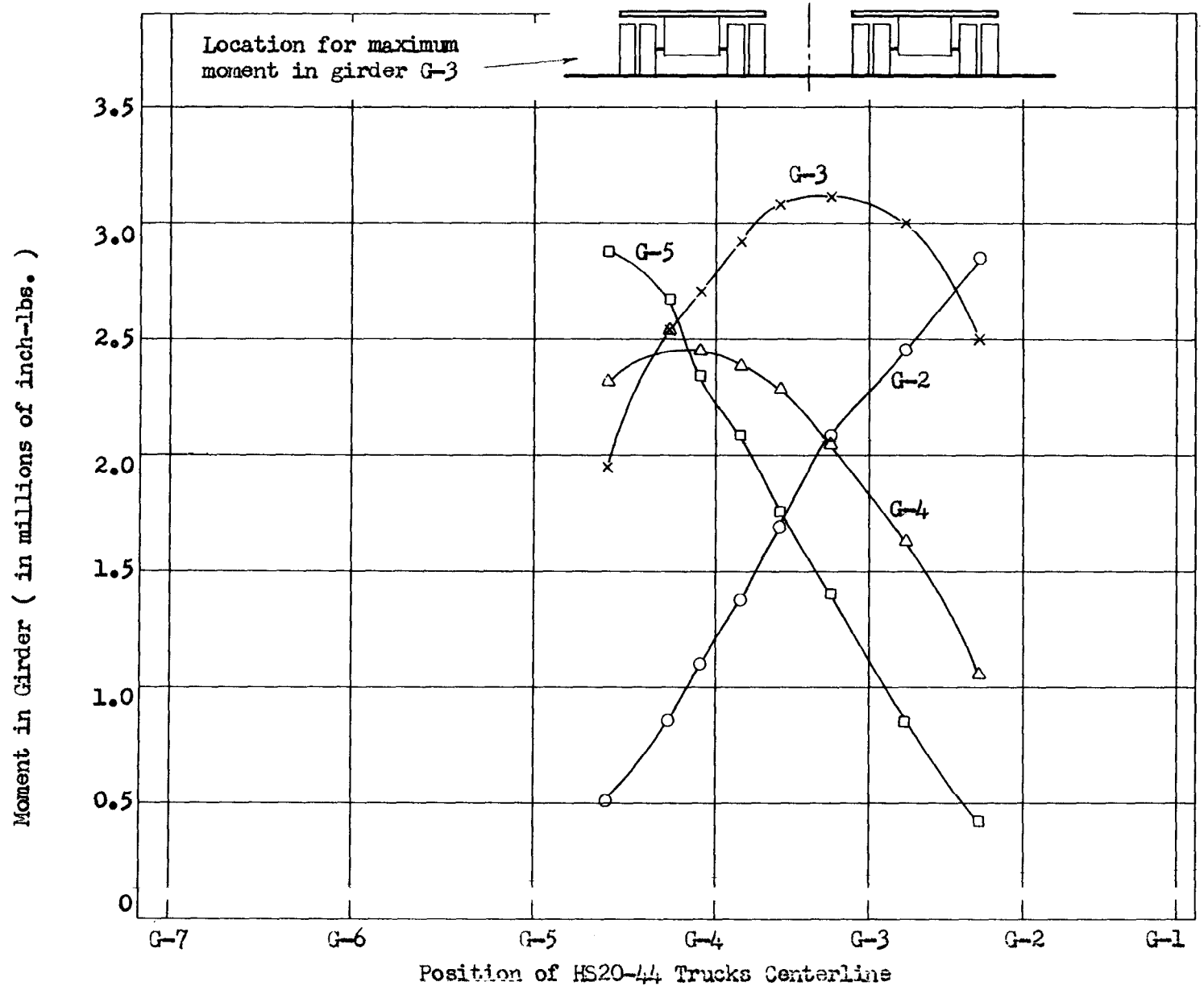

FIG. 39 MOMENT IN GIRDERS AT MIDSPAN DUE TO TWO HS20-44 TRUCKS SIDE BY SIDE - DESIGN CONCRETE PROPERTIES UNCRACKED SLAB

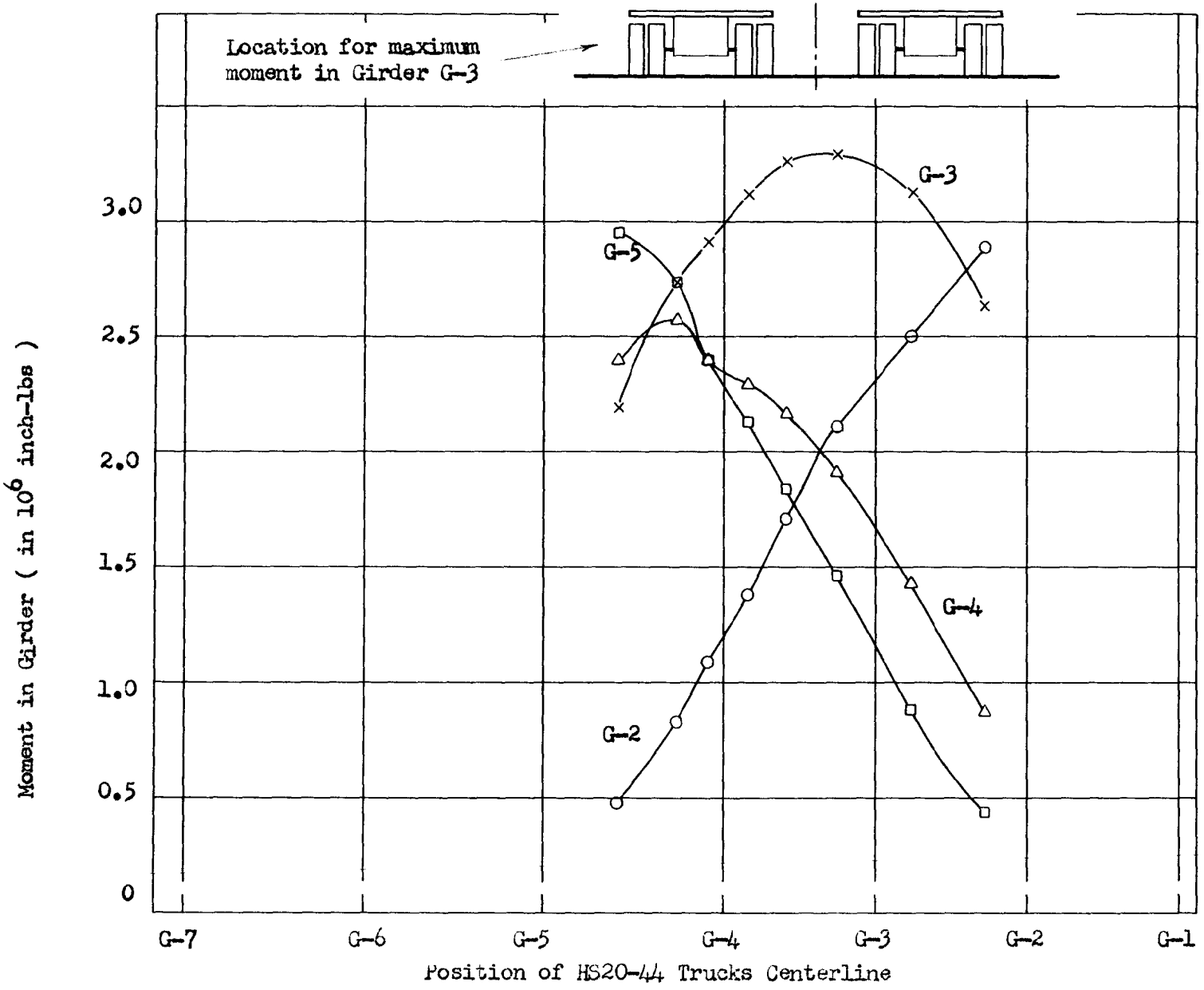

FIG. 40 MOMENT IN GIRDERS AT MIDSPAN DUE TO TWO HS20-44 TRUCKS SIDE BY SIDE - FIELD CONCRETE PROPERTIES UNCRACKED SLAB

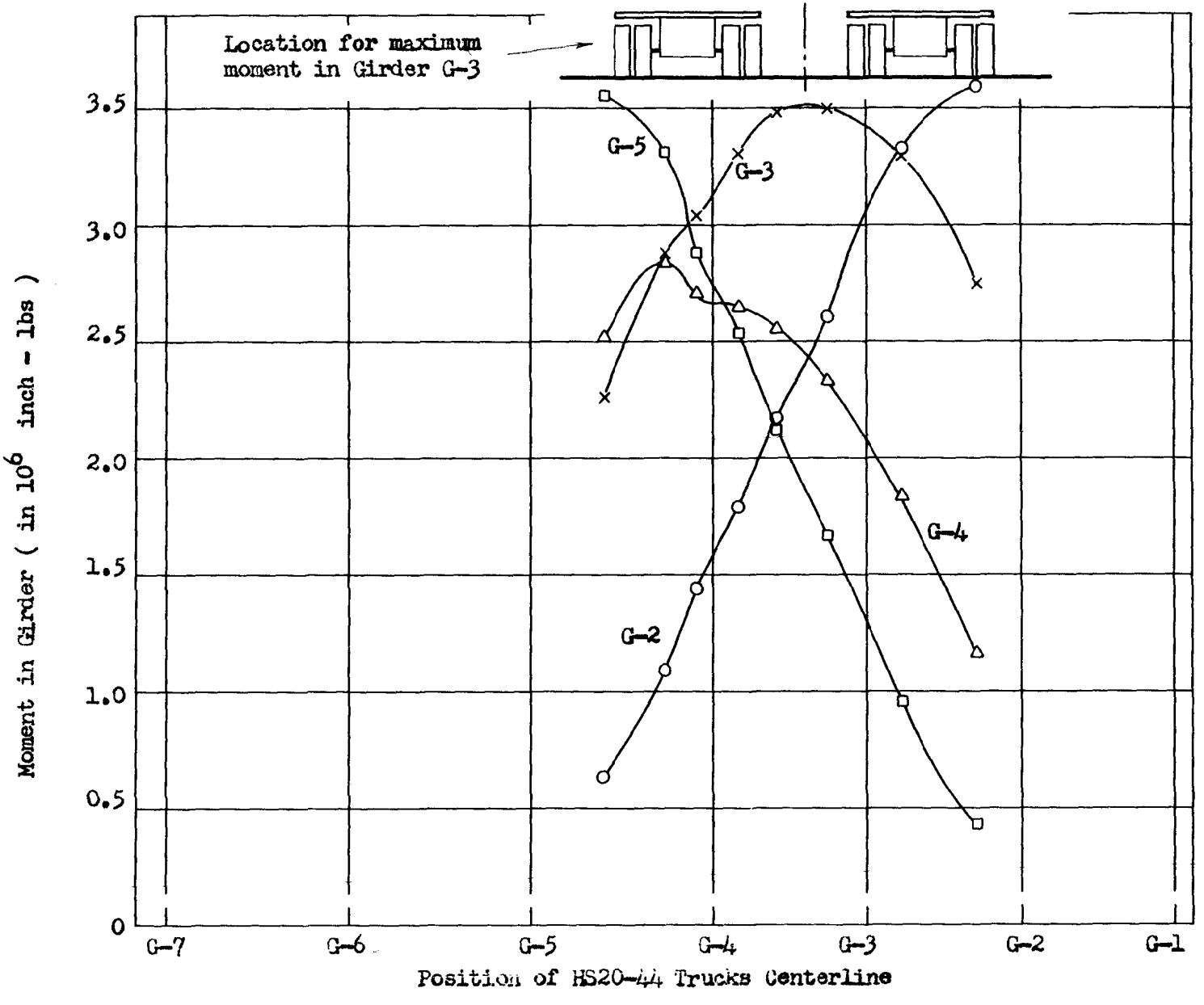

FIG. 41 MOMENT IN GIRDERS AT MIDSPAN DUE TO TWO HS20-44 TRUCKS SIDE BY SIDE - FIELD CONCRETE PROPERTIES BOTH OLD AND NEW SLAB CRACKED

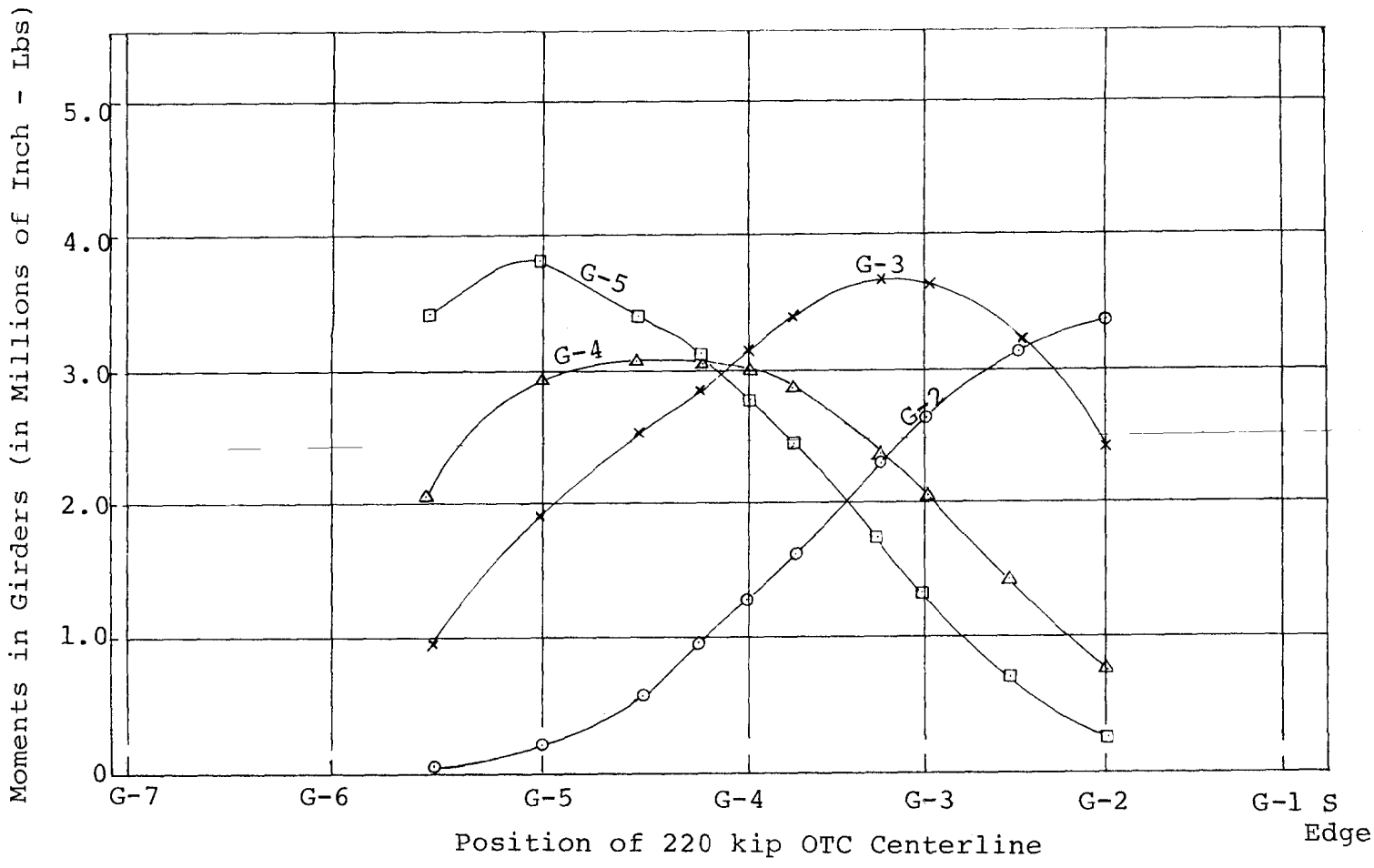

FIG. 42 MOMENT IN GIRDERS AT MIDSPAN DUE TO 220 k OVERLOAD TRUCK CRANE - DESIGN CONCRETE PROPERTIES - **UNCRACKED SLAB**

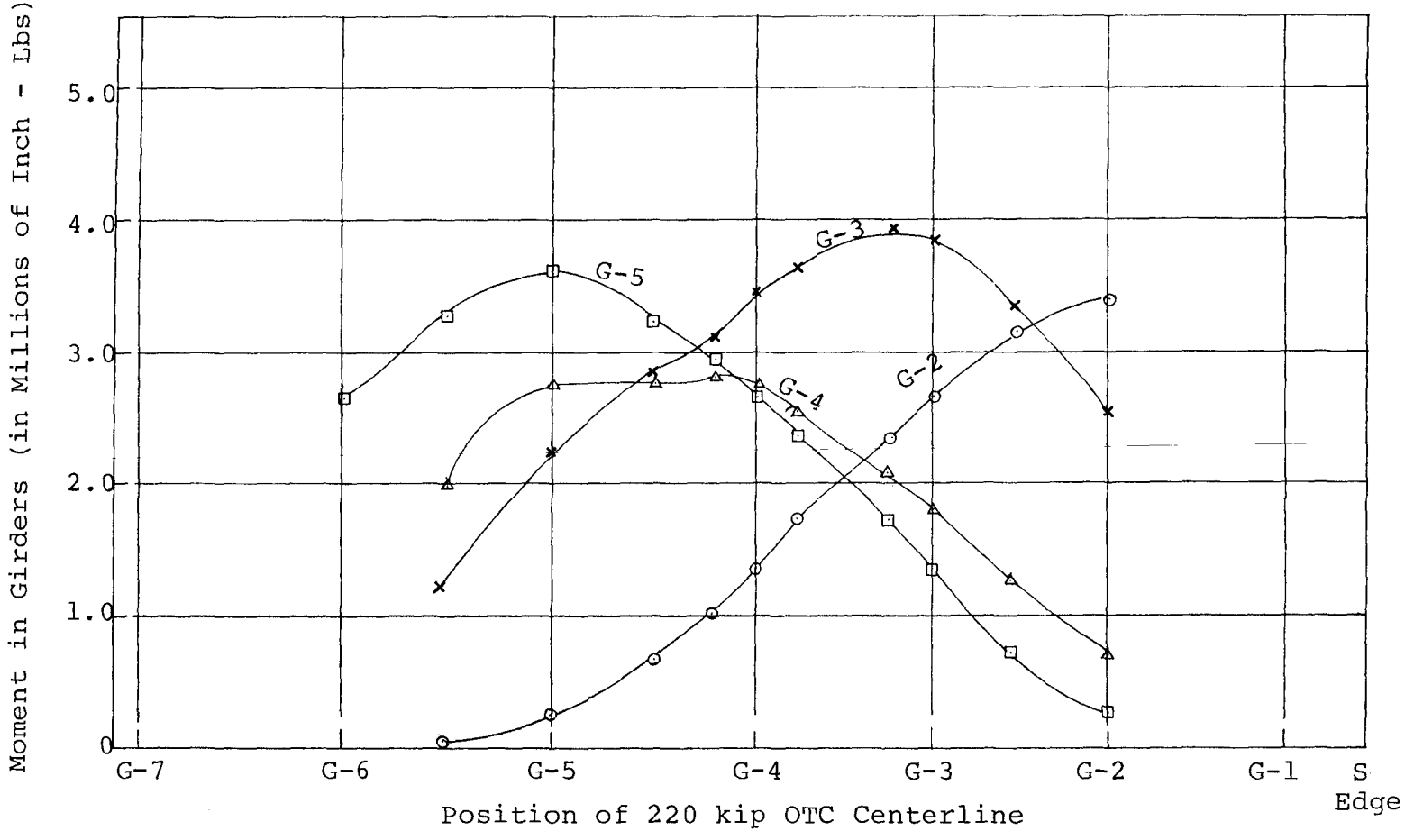

FIG. 43 MOMENT IN GIRDERS AT MIDSPAN DUE TO 220 k OVERLOAD TRUCK CRANE - FIELD CONCRETE PROPERTIES - UNCRACKED SLAB

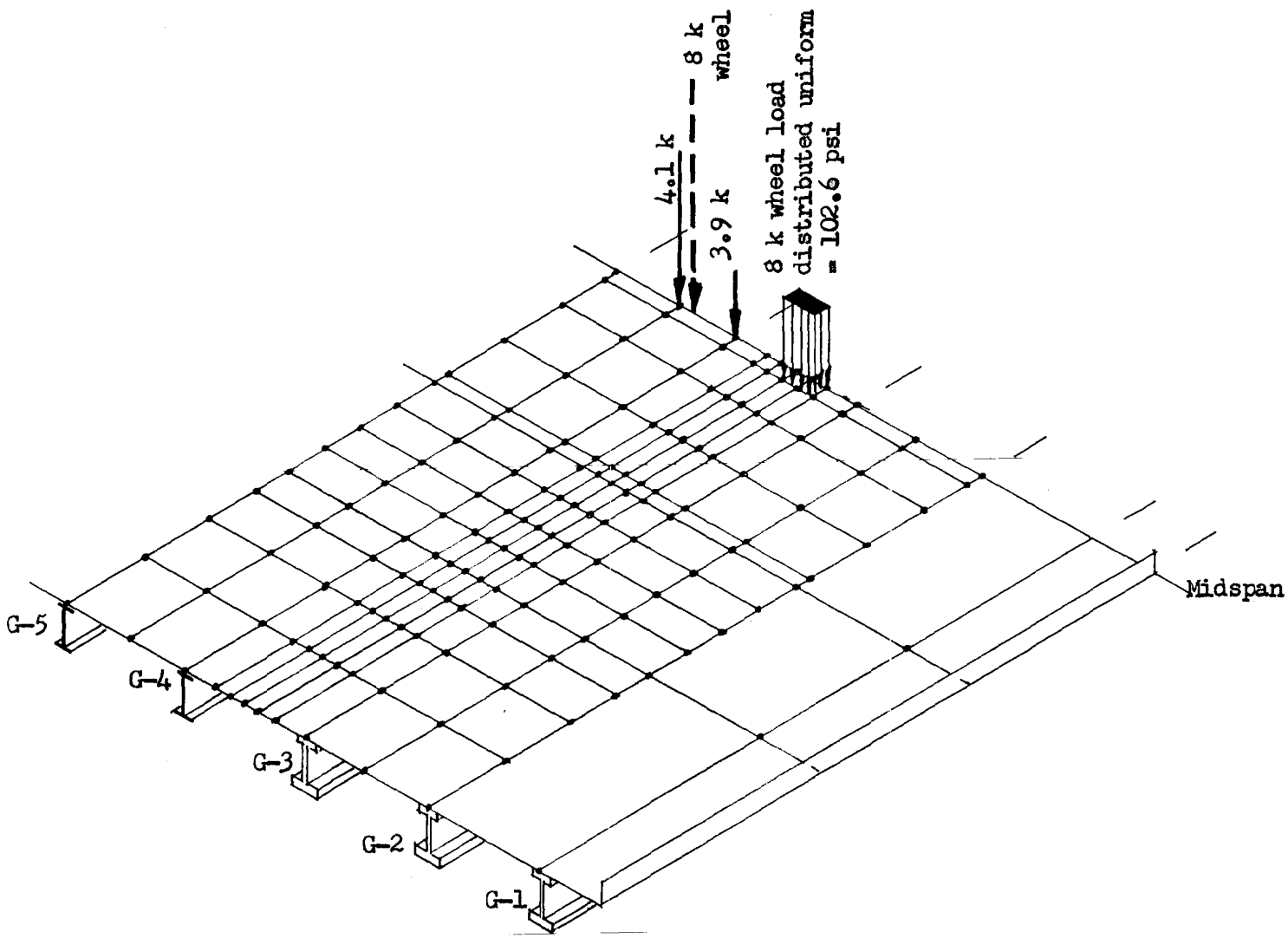

FIG. 44 TYPICAL DISTRIBUTION OF WHEEL LOADS TO GRID POINTS FOR MOMENTS IN SLAB DUE TO HS20-44 TRUCK LOAD

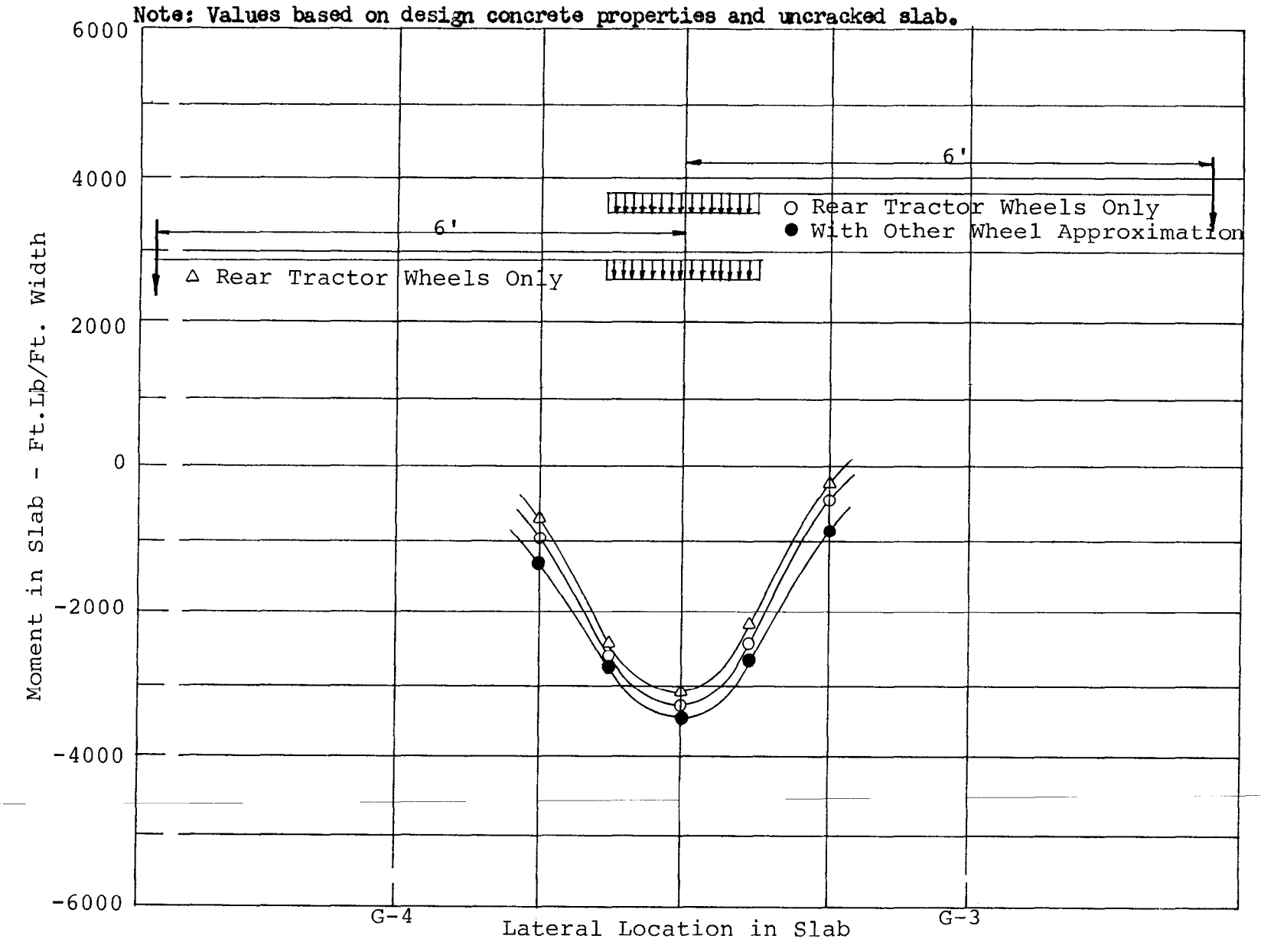

FIG. 45 VARIATION OF MOMENT IN SLAB CAUSED BY HS20-44 TRUCK LOAD AT SELECTED LOCATIONS

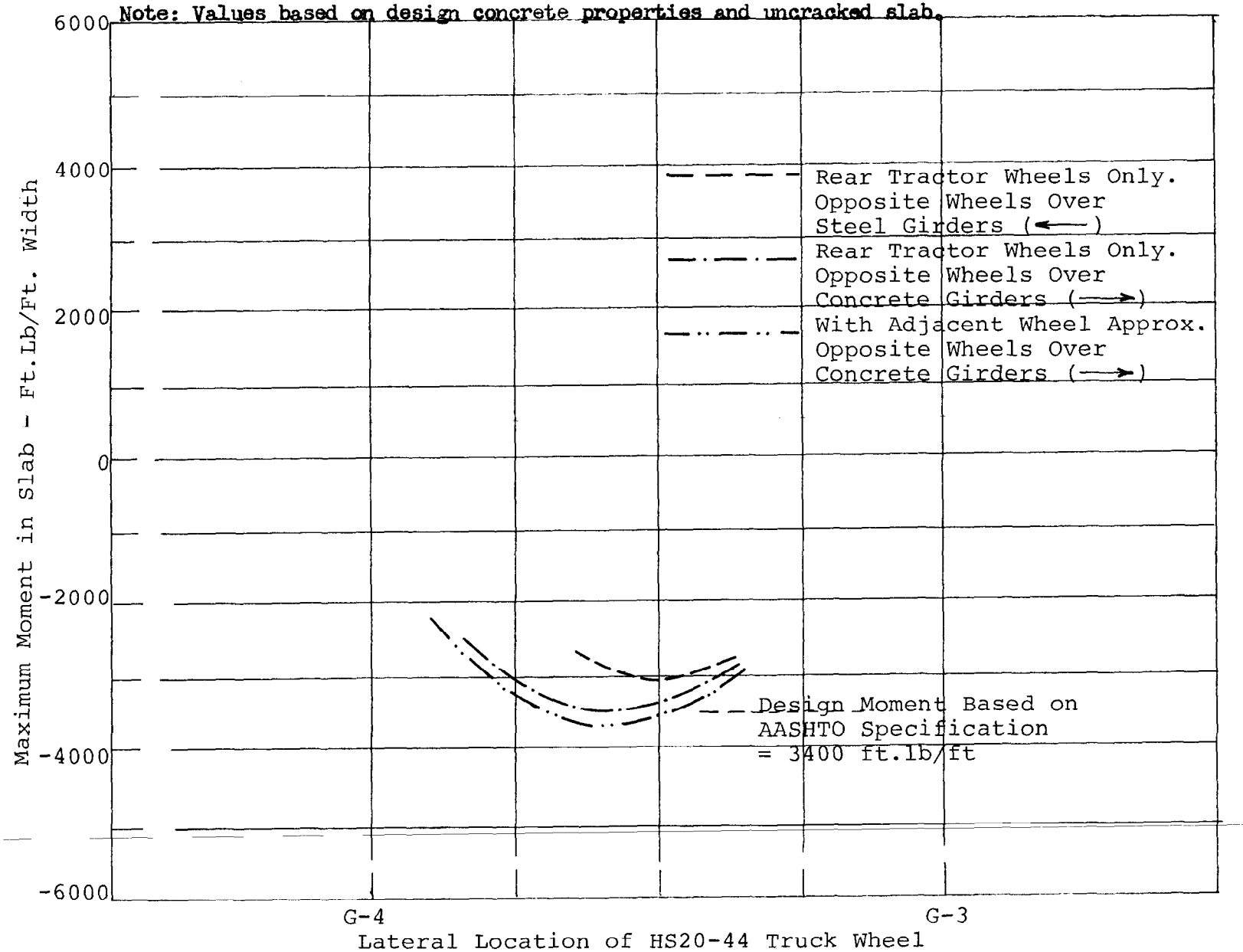

FIG. 46 VARIATION OF MAXIMUM MOMENT IN SLAB AS A FUNCTION OF HS20-44 TRUCK WHEEL LOCATION

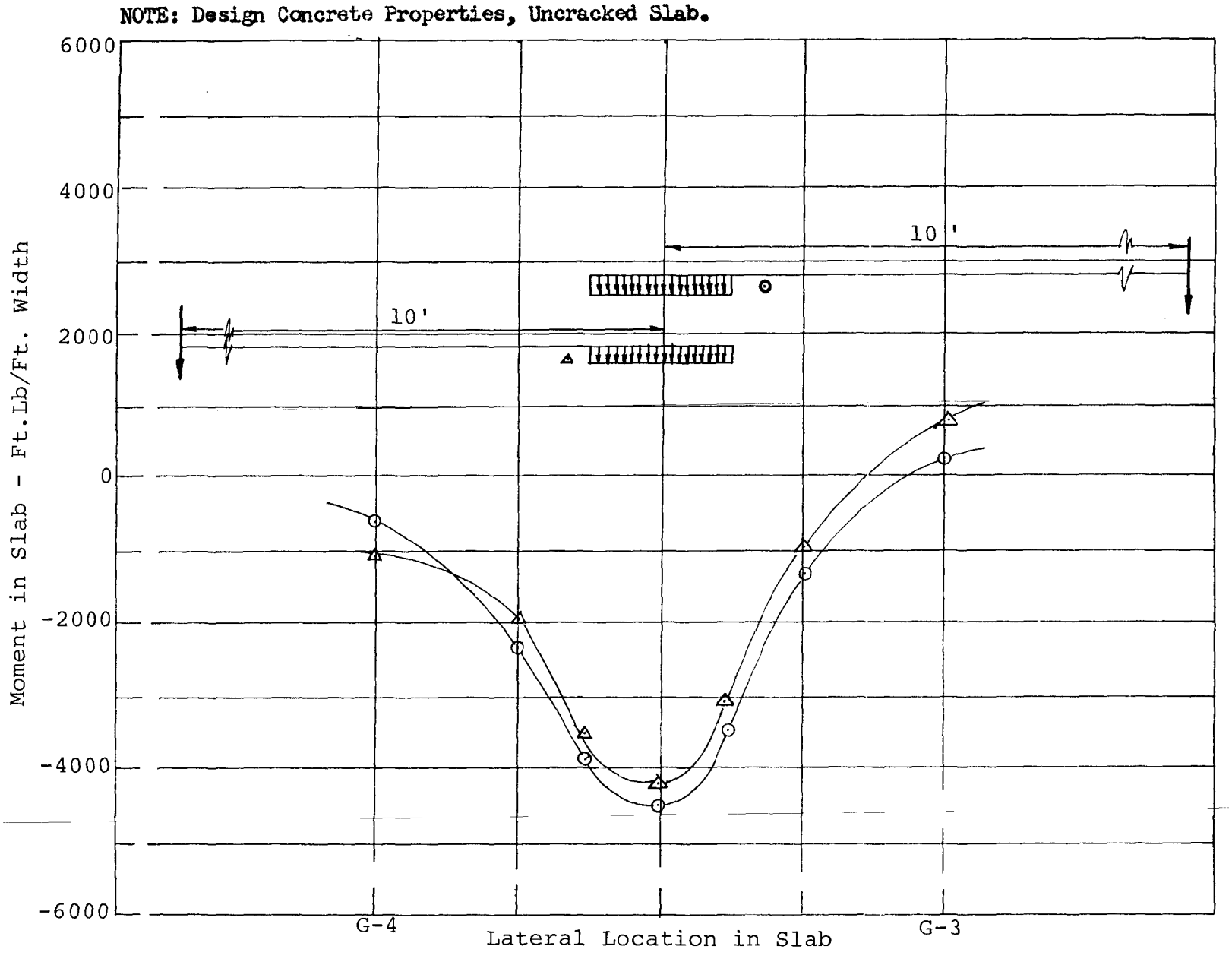

FIG. 47 VARIATION OF MOMENT IN SLAB CAUSED BY 220 k OVERLOAD TRUCK CRANE AT SELECTED POSITIONS

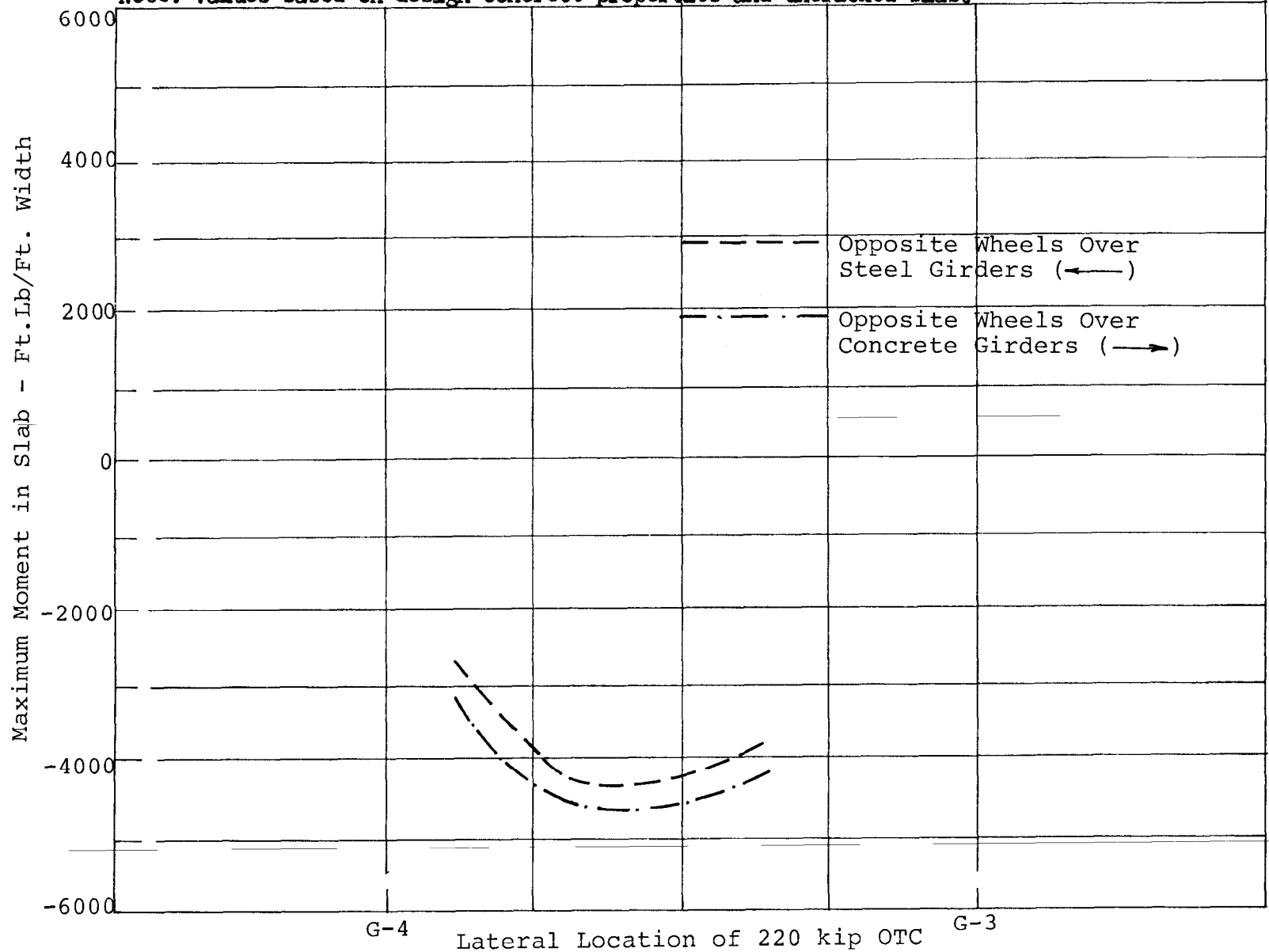

FIG.48 VARIATION OF MAXIMUM MOMENT IN SLAB AS A FUNCTION OF 220 k OVERLOAD TRUCK CRANE WHEEL LOCATION

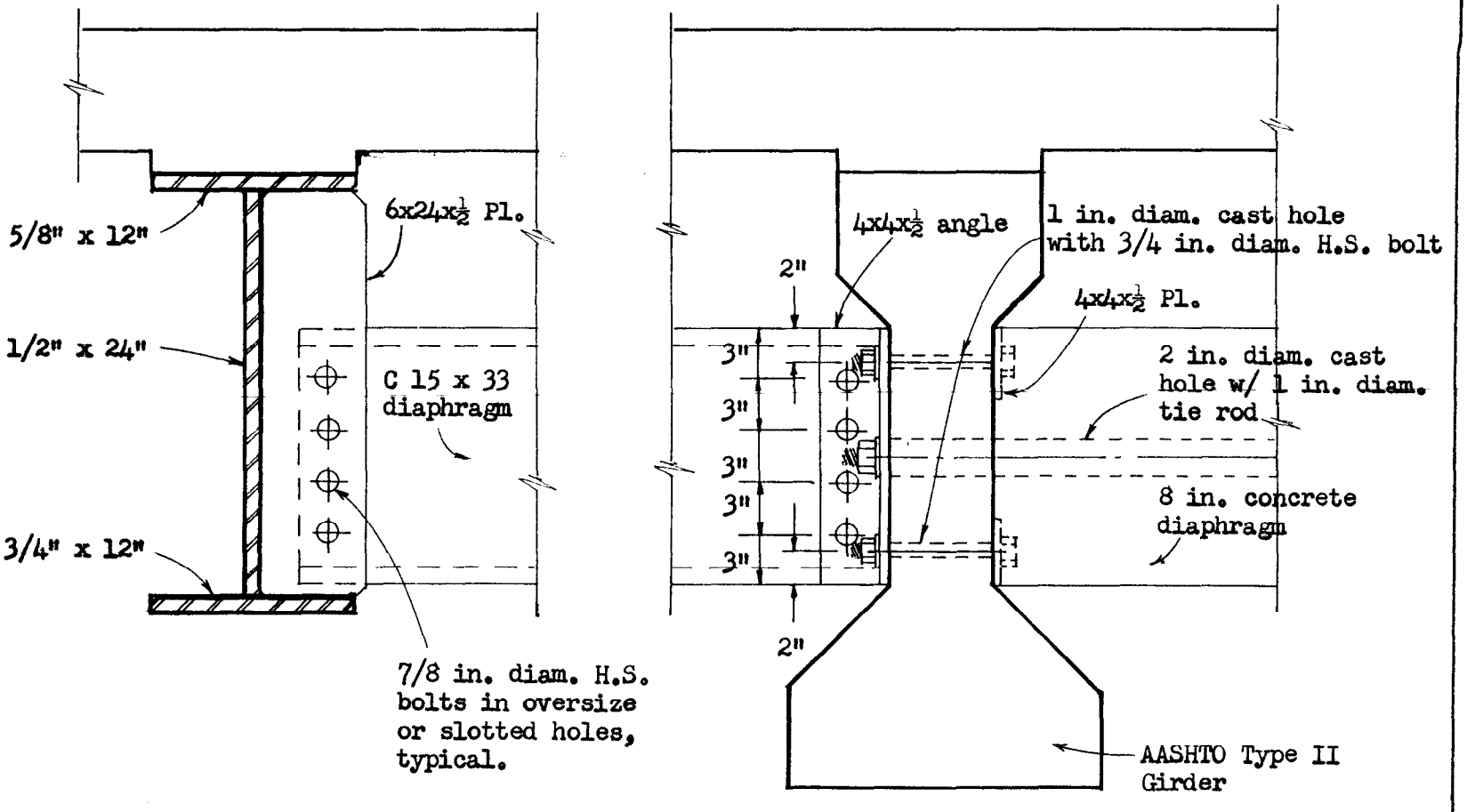

FIG. 49 DETAILS OF DIAPHRAGMS

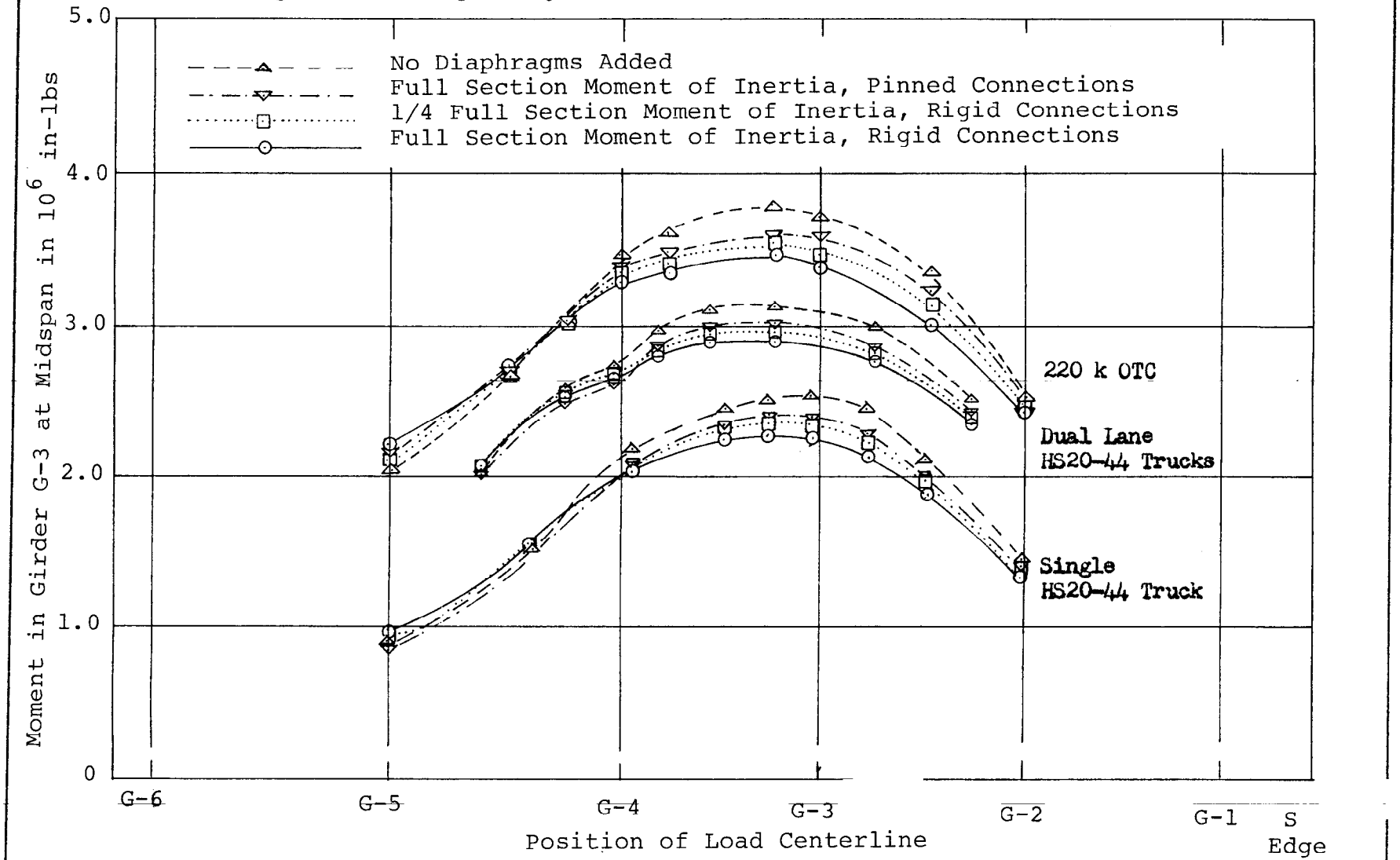

FIG. 50 EFFECT OF DIAPHRAGMS AT THIRD SPAN ON MAXIMUM MOMENT GIRDER G-3 FOR HS20-44 TRUCK LOAD AND 220 k OTC

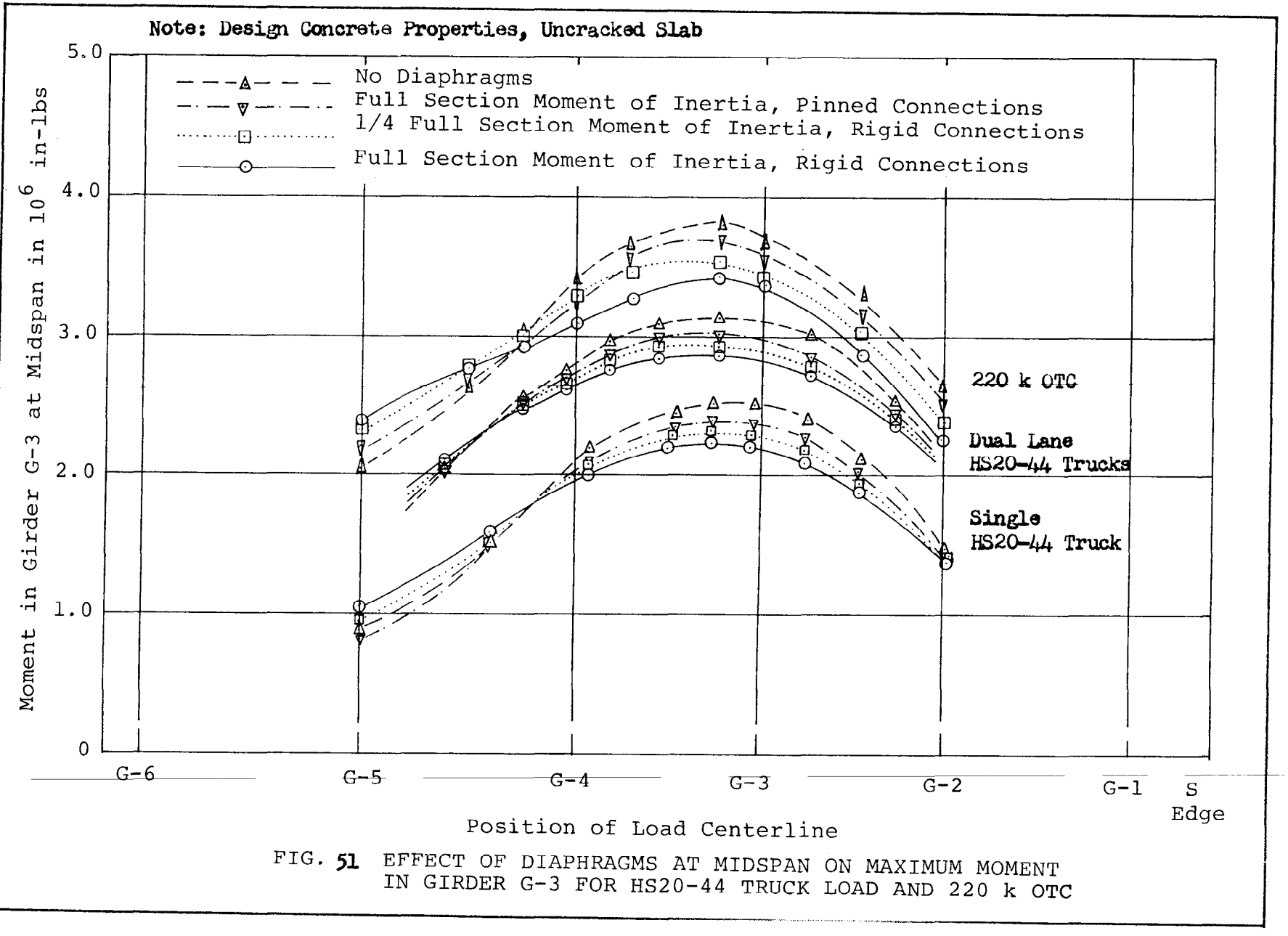

FIG. 51 EFFECT OF DIAPHRAGMS AT MIDSPAN ON MAXIMUM MOMENT IN GIRDER G-3 FOR HS20-44 TRUCK LOAD AND 220 k OTC

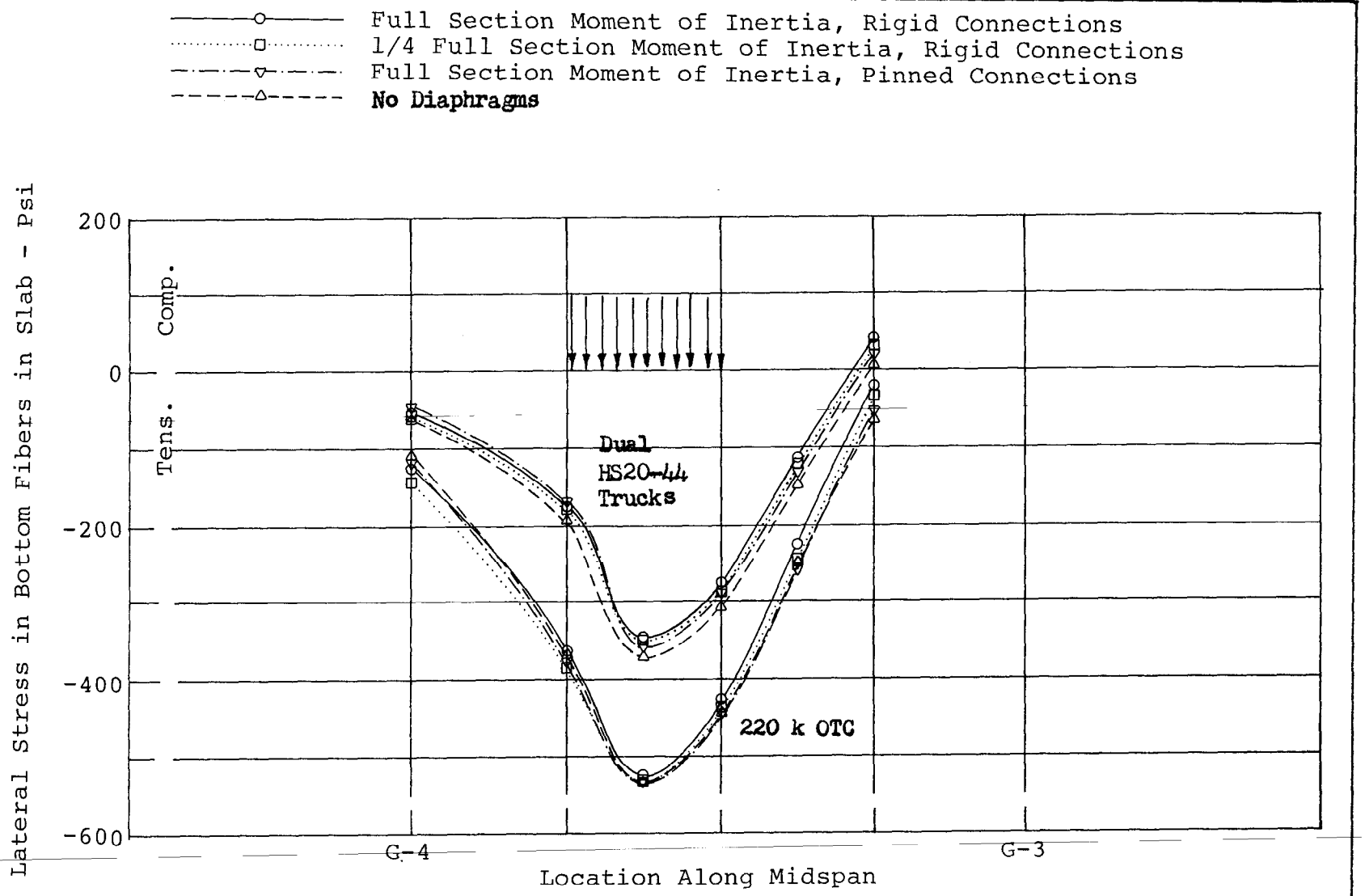

FIG. 52 EFFECT OF DIAPHRAGMS AT THIRD SPAN ON STRESSES IN SLAB FOR HS20-44 TRUCK LOAD AND 220 k OTC
DESIGN CONCRETE PROPERTIES, UNCRACKED SLAB

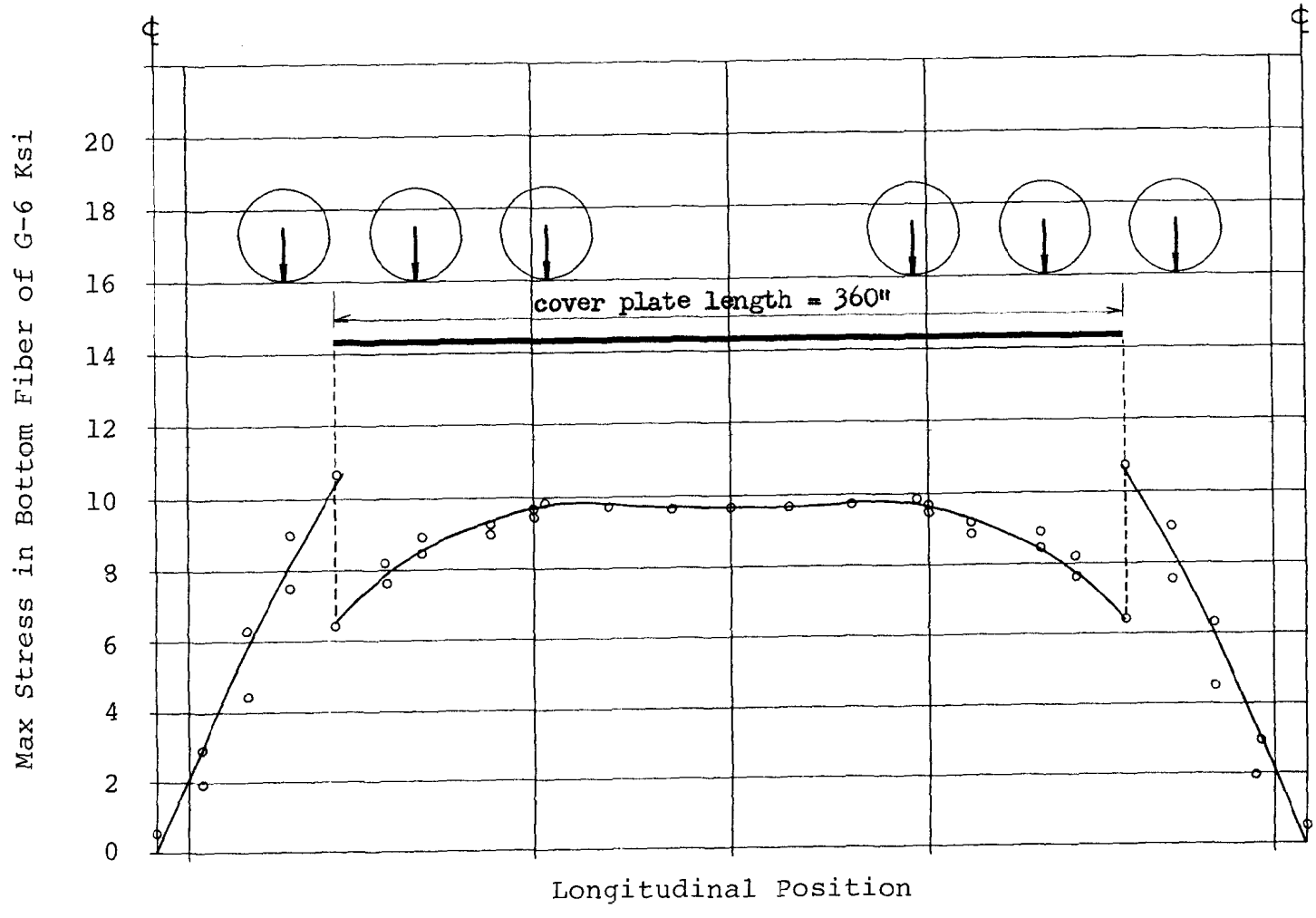

FIG. 53 TYPICAL STRESS DISTRIBUTION IN BOTTOM FIBERS OF GIRDER G-6 USING ROLLED BEAMS WITH COVERPLATES

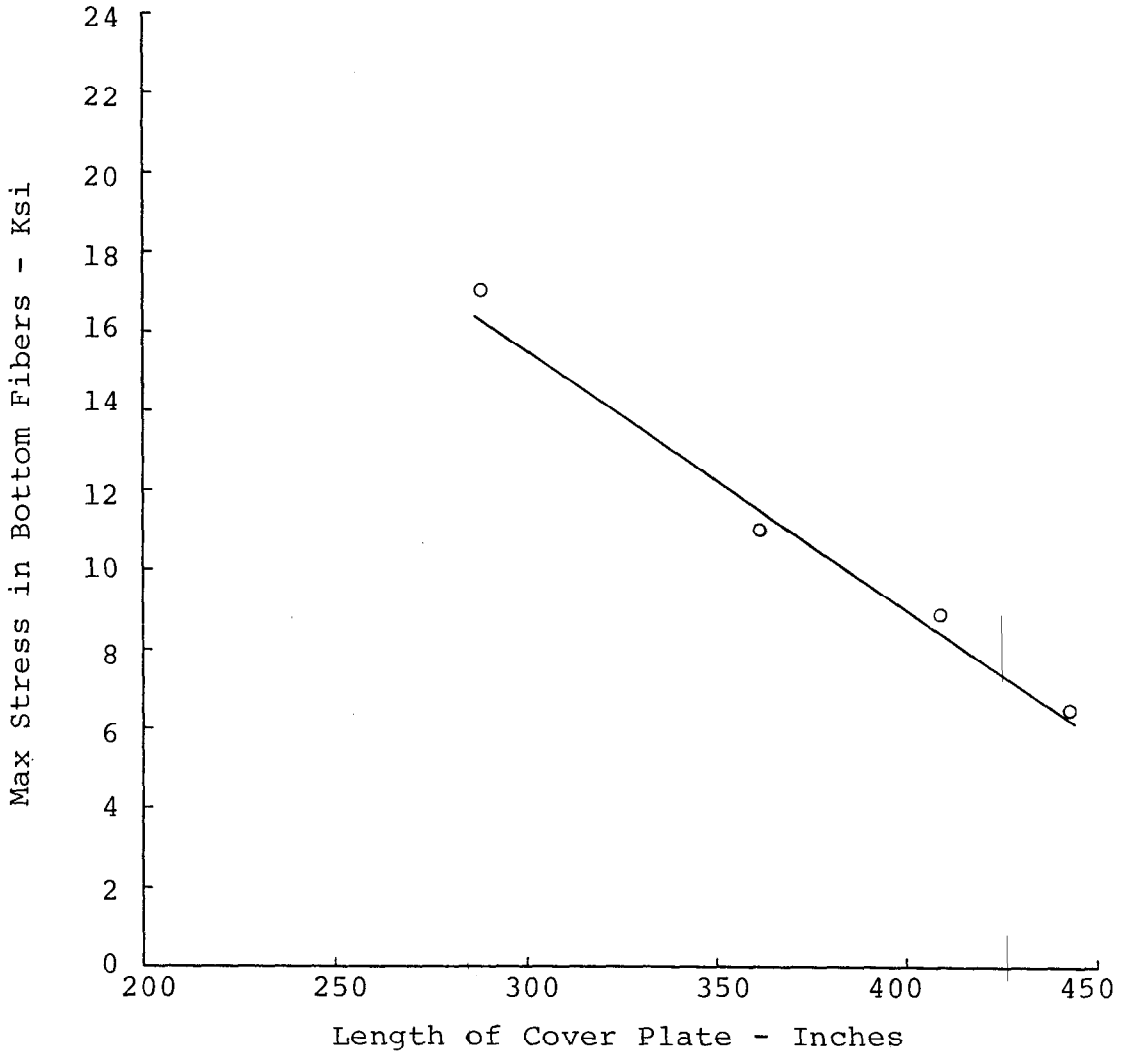

FIG. 54 EFFECT OF LENGTH OF COVER PLATE ON MAXIMUM STRESS IN BOTTOM FIBERS OF FLANGE OF BEAM AT END OF COVER PLATE

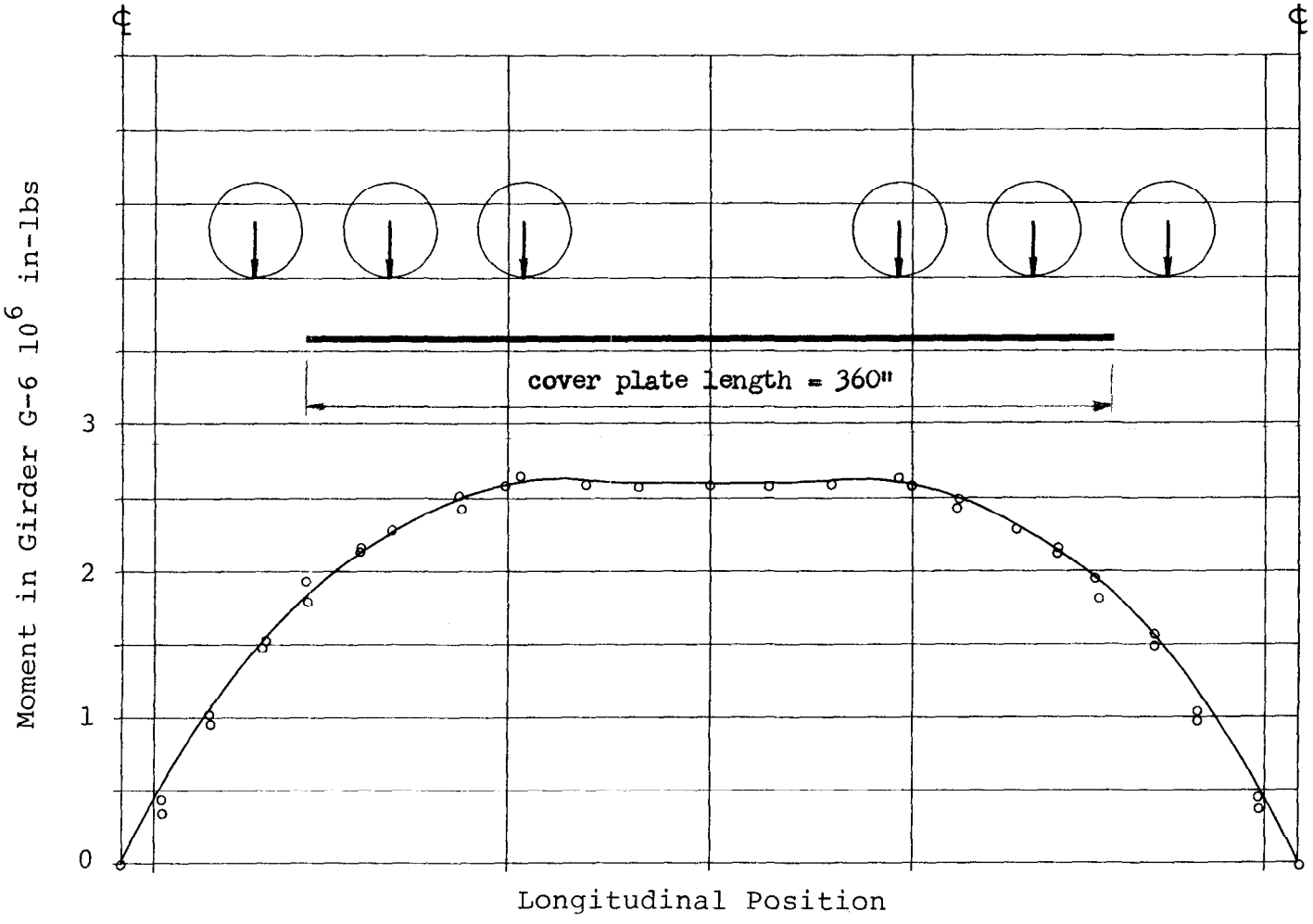

FIG. 55 TYPICAL MOMENT DISTRIBUTION FOR GIRDER G-6 WHEN USING ROLLED BEAMS WITH COVER PLATES

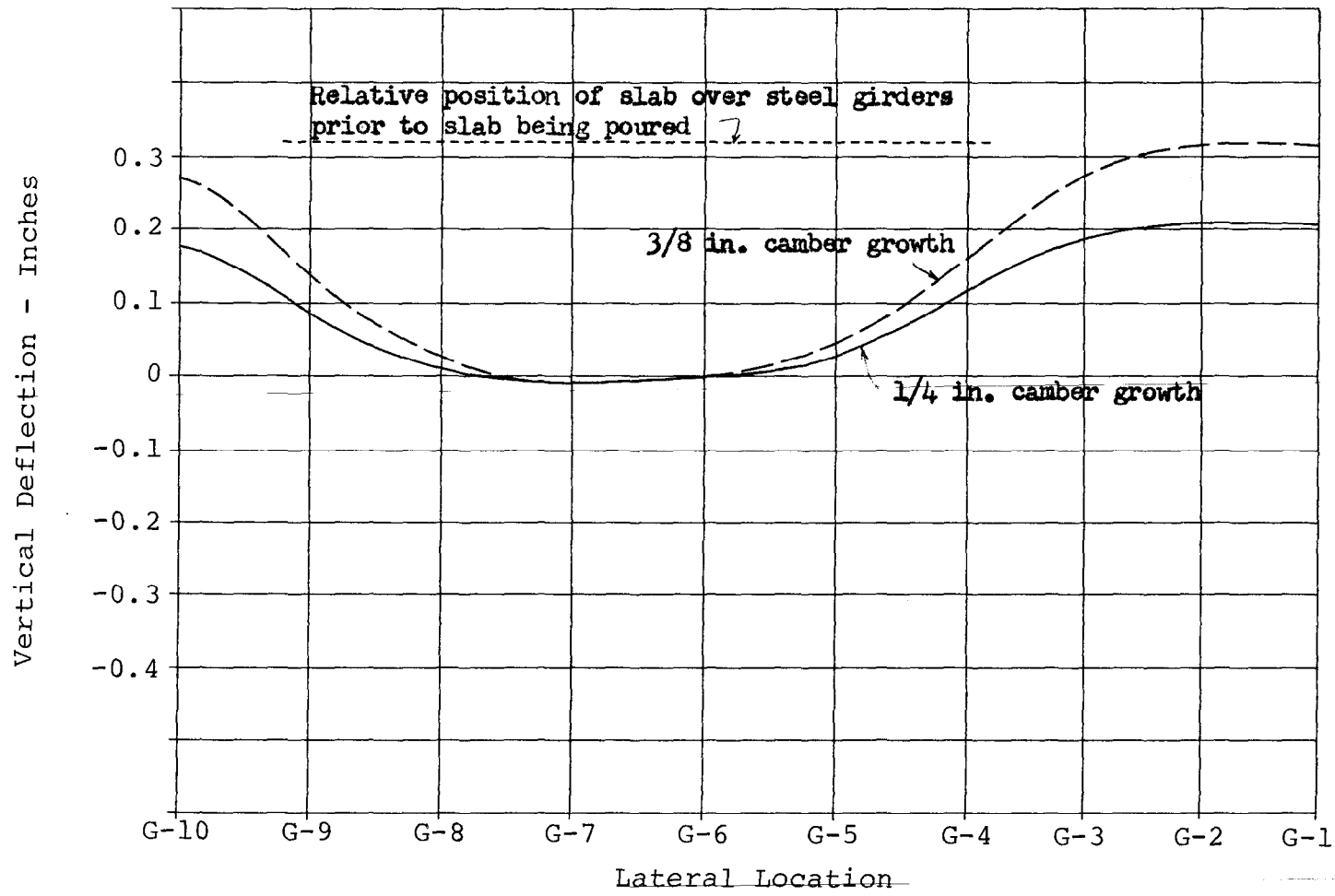

FIG. 56 VERTICAL DEFLECTION OF SLAB AT MIDSPAN DUE TO CAMBER GROWTH WHEN LOADED WITH DEAD WEIGHT OF SLAB
DESIGN CONCRETE PROPERTIES, UNCRACKED SLAB

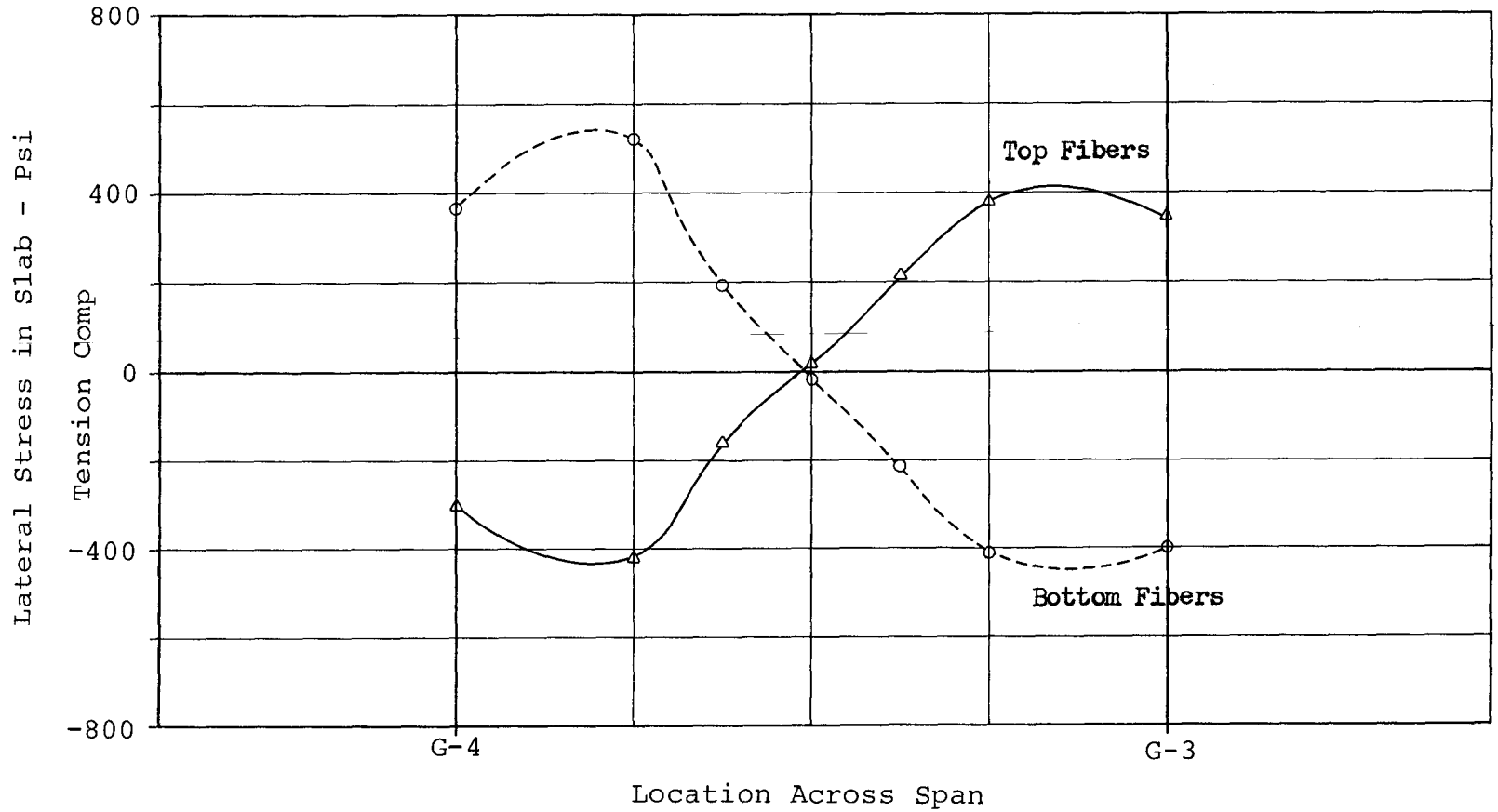

FIG. 57 EFFECT OF 0.1 IN. CONSOLIDATION OF NEOPRENE PAD ON LATERAL STRESSES IN SLAB AT END OF SPAN
DESIGN CONCRETE PROPERTIES, UNCRACKED SLAB

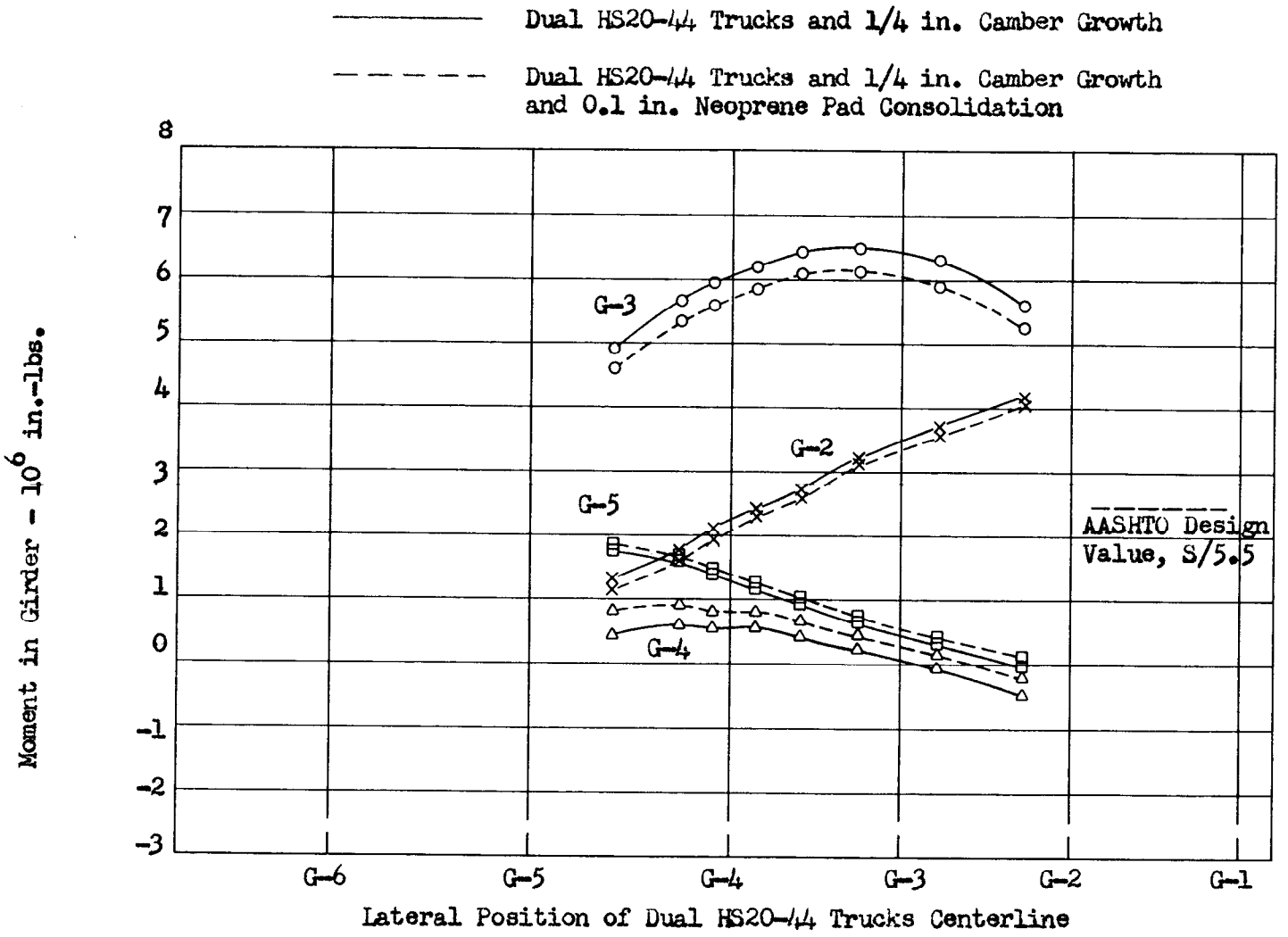

FIG. 58 COMBINED EFFECT ON THE MOMENT AT MIDSPAN IN COMPOSITE GIRDER DUE TO DUAL HS20-44 TRUCKS LOAD, 1/4 IN. CAMBER GROWTH, AND 0.1 IN. NEOPRENE PAD CONSOLIDATION - DESIGN CONCRETE PROPERTIES, UNCRACKED SLAB

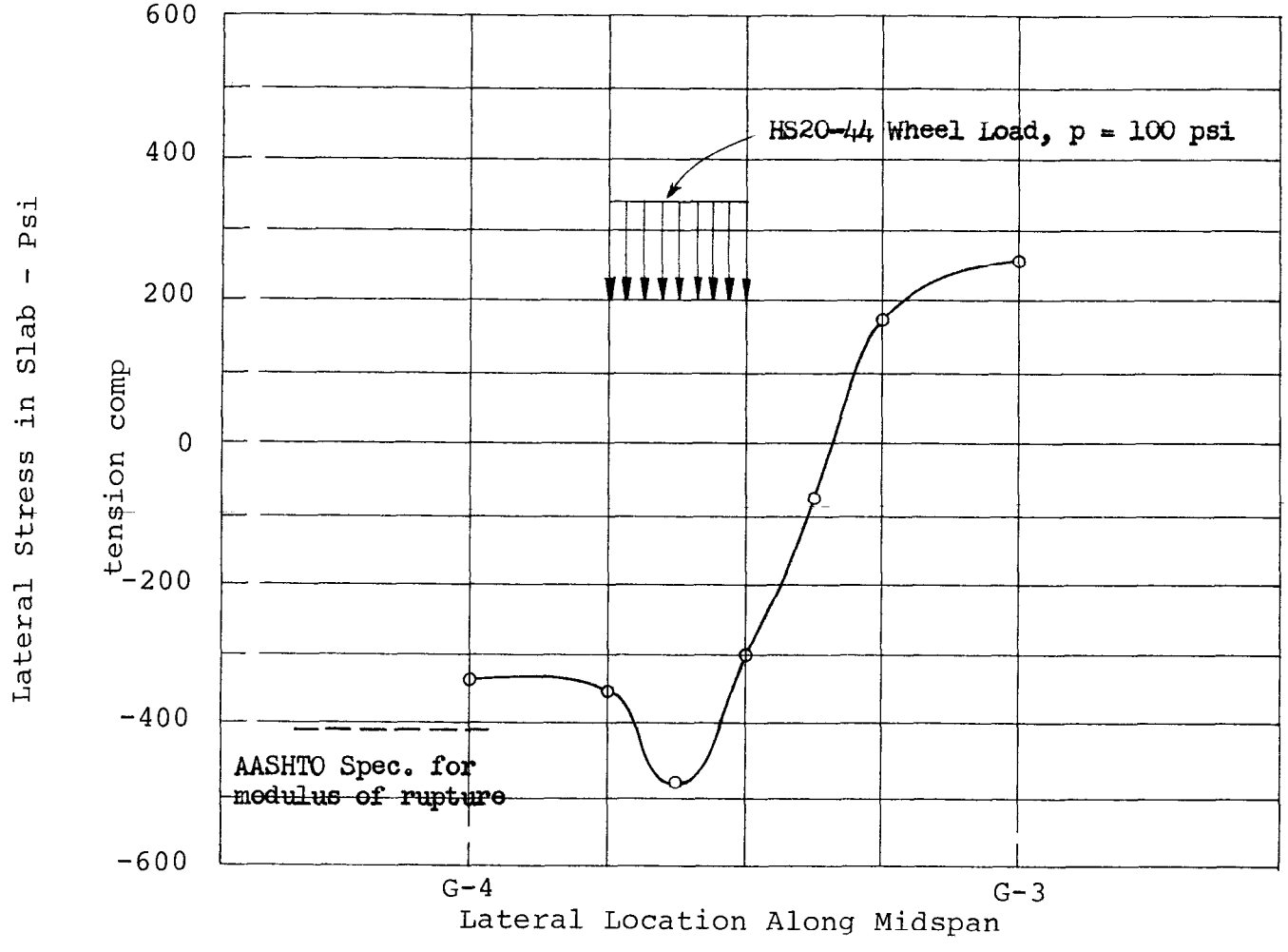

FIG. 59 COMBINED EFFECT ON LATERAL STRESSES IN BOTTOM FIBERS OF SLAB AT MIDSPAN DUE TO DUAL HS20-44 TRUCK LOAD, THREE HOURS OF SUNSHINE, 1/4 IN. CAMBER GROWTH, 0.1 IN. NEOPRENE PAD CONSOLIDATION, AND 30°F TEMPERATURE INCREASE OF STEEL GIRDERS DESIGN CONCRETE PROPERTIES, UNCRACKED SLAB

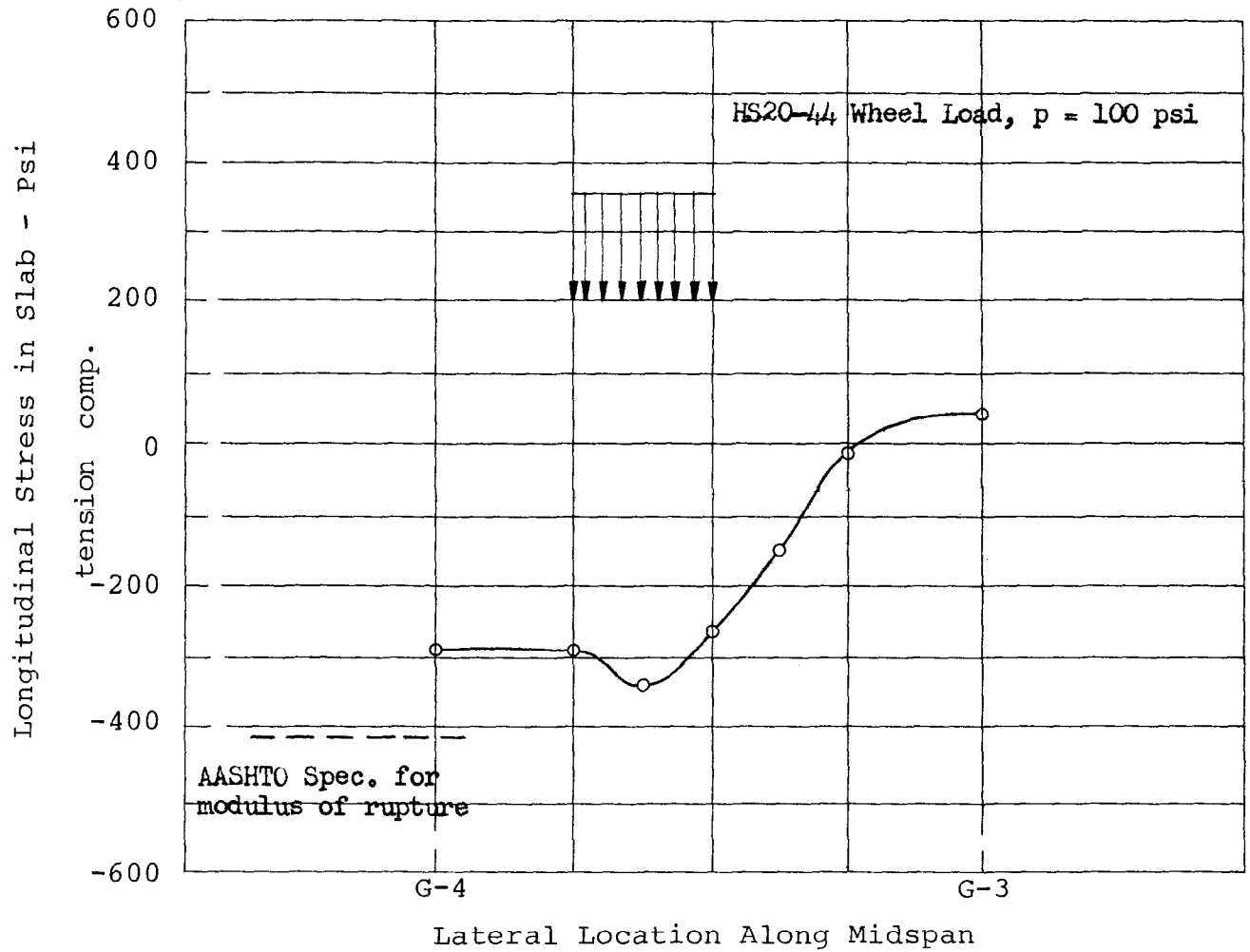

FIG. 60 COMBINED EFFECT ON LONGITUDINAL STRESSES IN BOTTOM FIBERS OF SLAB AT MIDSPAN DUE TO DUAL HS20-44 TRUCKS LOAD, THREE HOURS OF SUNSHINE, 1/4 IN. CAMBER GROWTH, 0.1 IN. NEOPRENE PAD CONSOLIDATION, AND 30 DEG. F TEMPERATURE INCREASE OF STEEL GIRDERS - DESIGN CONCRETE PROPERTIES, UNCRACKED SLAB

5. SUMMARY AND RECOMMENDATIONS

5.1 Summary

Extensive vertical deflections and certain horizontal deflections were measured for a span of the Bonnabel Overpass for loadings with live loads and thermal loads. The live loads consisted of nominal AASHTO HS20-44 trucks and a 220 k overload truck crane. The thermal loads consisted of ambient temperature changes and several hours of sunshine. The deflection measurements were made using dial indicators supported for the most part by stakes driven in the ground. The live load field test results are believed to accurately represent the deflection of the span. The small inconsistencies in the data were mainly due to hysteresis in the support system. The deflection measurements from the thermal load tests, while equally as accurate as those obtained for the live load tests, are not as useful for comparison because of the difficulties in defining ambient temperature conditions.

A span of the Bonnabel Overpass was modeled mathematically using the MSC/NASTRAN Finite Element Computer Program. Computer runs were made simulating all of the field test live load configurations and simulating the thermal loading conditions where practical.

Relative to comparison of computed deflections and field measured deflections under live load conditions, it is

believed that the only limitation to obtaining excellent agreement is the accurate definition of the computer input data. In the case of the Bonnabel Overpass, excellent agreement could be obtained by adjusting the computer model to account for lateral cracking of the slab and to account for less than rigid end conditions for the diaphragms.

It is believed that the MSC/NASTRAN computer program has certain limitations in so far as calculating the response of a structure such as the Bonnabel Overpass to ambient thermal conditions. The most severe limitation is that of defining the temperature input data required by the program. On the other hand, if the temperature distribution in the structure is well defined, NASTRAN can yield accurate information regarding thermally induced stresses in the structure.

The NASTRAN program was used to investigate seven areas relative to overpass design and mixed girder support systems. In addition, the effects of combining these areas, where appropriate, were investigated. One of the objectives of the overall project was to use the NASTRAN computer program to define potential problem areas for future study. No attempt has been made to investigate the areas completely nor to verify the validity of the individual computer solutions. Rather, the results are presented only to indicate trends and gross effects as predicted by the NASTRAN computer program. A summary of the more significant results of the computer study is given below.

In the mixed girder system the computer solution indicates that camber growth can have a very significant effect on the maximum moment in the adjacent concrete and steel girders. For the predicted amount of camber growth (1/4"), the resulting moment increase in the adjacent concrete girder is quite large and of the same order of magnitude as the AASHTO design moment due to live loads.

Ambient temperature changes appear to have relatively small effects on the stresses in the span superstructure; however, ambient temperature changes and direct sunshine on the top of the deck cause rather large tensile stresses in the slab. These stresses can routinely be as high as one-third the modulus of rupture for the concrete.

For the mixed girder system, the maximum moment due to live load in the concrete girder adjacent to the steel girders will be greater than the moment in the steel girder adjacent to the concrete girders. For the case of dual lane HS20-44 trucks on the Bonnabel Overpass, the moment in the adjacent concrete girder exceeds the AASHTO design value by 27% when design concrete properties are used and by 36% when field measured concrete properties are used.

Concrete diaphragms which are installed for the purpose of distributing moments between girders are more effective at mid-span than at the one-third span location. However, the diaphragms modeled herein would not be effective in distributing moments because the end connections are too flexible. Care should be exercised in placing rigid

diaphragms between the adjacent concrete and steel girders because of the probability of camber growth. An increase in rigidity in this case would further increase the moment due to camber growth in the adjacent concrete girder.

The neoprene bearing pads apparently have consolidated by approximately 0.1" and their modulus of elasticity increased several fold. The increase in modulus of elasticity would cause a corresponding increase in the shear modulus, which in turn would increase the forces on the bent caps. The field test results suggest that the opposing forces on each bent cap almost cancel each other and that the motions of the bent caps are dependent on the overall expansion of the complete overpass.

For the mixed girder system, the combination of live load and camber growth may cause severe overloading of the adjacent concrete girder. In the case of the Bonnabel Overpass, the computer results show that dual HS20-44 trucks live load and a 1/4" camber growth acting together will cause the maximum moment in the adjacent concrete girder to be approximately 100% greater than the AASHTO design value.

The computer results also show that a combination of live load and thermal effects, primarily sunshine effects, will cause large tensile stresses in the bottom fibers of the slab both in the lateral and longitudinal direction. For the case of the Bonnabel Overpass, these stresses are expected to frequently approach the modulus of rupture of the concrete.

5.2 Recommendations

Since the NASTRAN program can be used to model a range of mixed girder bridges, e.g., spans of 40 ft., 60 ft., and 80 ft.; and steel girder spacings of 4 ft., 7 ft., and 10 ft.; it is felt that provisions should be made to keep the NASTRAN program active and current and at the disposal of the State and the University.

With the NASTRAN program (or its equivalent) available, additional studies should be initiated into at least two areas. First, it is felt that the combination of live load and camber growth can overload the concrete girder adjacent to a steel girder in a mixed girder span, and that this combination should be further investigated, including the advisability of the use of diaphragms between the concrete and steel girders.

Secondly, it is felt that the combination of live load and thermal load can have a detrimental effect on the integrity of the deck slab, and that this combination should be further investigated.

Consideration should be given to future investigations addressing in more detail live load distribution and its relationship to AASHTO specifications. It is felt that it will be necessary to go beyond empirical computer studies to address live load distribution, and that major analytical work would be required.

APPENDIX A

USAGE OF MSC/NASTRAN COMPUTER PROGRAM AND GENERAL BRIDGE MODEL

A.1 Introduction

MSC/NASTRAN is a licensed, finite element computer program installed on selected mainframe computers. Like other similar programs, it is licensed on a yearly basis, with fees based on the amount of computer time used in running the program.

NASTRAN must be installed in a mainframe computer prior to its being able to be used in solving problems. This installation process can be complex because of peculiarities of the local computer system on which it is installed, as well as the size and complexity of the NASTRAN program itself.

In addition to developing and installing the NASTRAN program, other means of formulating a finite element bridge model were examined that would be consistent with the use of a mainframe program such as NASTRAN for the final computer model.

The program MSC/PAL was used to explore bridge modeling using the finite element approach. PAL is also supplied by the MSC Corporation, but it runs on an IBM PC or compatible computer. Its modeling capacity is much less than MSC/NASTRAN.

PAL has a feature which allows for the conversion of a PAL based finite element model to a NASTRAN based model. At first, it was thought that this might provide a useful means of developing the initial model in PAL on a microcomputer, then converting the model data to NASTRAN when increased capacity was required. However, after preliminary development using PAL, it was decided that writing the NASTRAN model over from the beginning was the most efficient method because of the severe limitations that PAL imposes on its models.

Another microcomputer program, PRENASTRAN, was briefly investigated. PRENASTRAN is designed to produce a NASTRAN model from user input data. Its limitations in selecting a bridge model prevented any serious use.

The NASTRAN program, leased from MSC Corporation, is separate from the input data for a bridge model developed under this project. The input data described below is specific to the bridge model. Finally, the NASTRAN program was "verified" by testing its results for simple structural situations for which analytical solutions could be calculated.

A.2 Description of Program

A.2.1 The Connected Node Finite Element Model Concept

The concept of the finite element, connected node model is that a continuous representation of physical structure is represented by a mathematical model that is divided into

segments, or elements. These elements are connected at specific points in space, called grid points.

The finite element model includes two major simplifications that lead to much of its power and widespread applicability. First, the elements are assumed to be connected only at the grid points; second, the "interior" of each finite element is only a mathematical approximation to the true physical phenomenon. The finite element model technique concentrates on insuring the accuracy of prediction at the grid points rather than the interior of the elements.

Finite element techniques, as embodied in programs such as NASTRAN, are highly developed and very accurate predictors of phenomenon modeled at the grid points. Furthermore, it is possible to place constraints on the motion of the grid points or the nature of the elements connecting the grid points in order to more closely approximate the true physical phenomenon.

In NASTRAN, a grid point may be constrained to move in only certain directions. It may be constrained not to rotate about certain axes. This ability to specify constraint directions gives a great deal of flexibility in defining the finite element model.

Judiciously used, grid point constraints can lead to model simplification when models are symmetric. For example, in the bridge model described in this report, symmetry and grid point constraints are used to reduce the

number of nodes necessary by almost half. As will be described in greater detail below, the centerline of the bridge between supports, and across the direction of traffic, is a line of symmetry if the bridge is loaded symmetrically about this centerline. Deflections on one side of the bridge centerline are symmetrically equal to bridge deflections on the other side of the bridge centerline. If the bridge supports are at the same level, the bridge at the centerline is exactly horizontal in the direction of the line of traffic. Hence, bridge grid points along the centerline may be "constrained" to be horizontal in the direction of traffic (not rotated), and so only one half of the bridge finite element model need be represented. This leads to a considerable saving in computing resources.

A.2.2 Structure of NASTRAN

The NASTRAN computer program is a very large program (over 500,000 lines of source code) which takes data on a specific finite element model as input. This data is known as an "input deck" and is specific to a particular model or structure. (The NASTRAN program itself does not change from one model to the next, only the data in the input deck does).

The individual lines of the data in the "input deck" are known as "cards," even though relatively few modern computer installations still use real computer punched cards stacked in decks. The terminology, however, survives. The

cards that will be referred to below are actually lines of data in datasets in computer memory, computer tape, or computer disks.

Before the user of the NASTRAN computer program can begin, it is assumed that he has developed a finite element model of the structure that he wishes to study; that is, a coordinate system is defined, grid points are located, and a set of modeling elements are connected between the grid points to model the structure. At this point, the user has enough data to begin to develop a NASTRAN data deck.

The user of the NASTRAN program must not only provide input data that describes the finite element model itself, but he must also provide input information that describes how the results of the program, the output data, will be presented. To allow efficient use of computer resources, the NASTRAN program allows for multiple load arrangements to be calculated for a single finite element model run.

NASTRAN organizes the input data deck into the following subsets:

1. Executive Control Deck

This deck contains a few data "cards" which describe the general type of data to follow. For example, it would include a SOL STATICS card to indicate a statics solution (rather than a dynamic analysis) is required.

2. Case Control Deck

This deck will include cards that describe the various loads to be applied to the finite element model. For example, if the finite element model is of a structure, several different structural loadings may be specified at this point so that each will be used in sequence with the same finite element model in one computer run.

The case control deck also includes cards that describe the output format that the user desires. For example, the user may specify that he wishes certain forces or moments printed out for a selected group of grid points. Graphical output may also be specified.

3. Bulk Data Deck

The bulk data deck contains all the information necessary to input the finite element model. Grid point locations in a global coordinate system, a list of elements and the grid points to which each connects, and material and dimensional properties of the elements are included in the bulk data deck. Also included are the data for the various load arrangements. NASTRAN also allows for group material properties to be specified; that is, mechanical properties of concrete can be specified on one card. The hundreds of elements which are made of concrete need only refer to the appropriate definition card--the properties need not be redefined for each concrete element.

A.2.3 NASTRAN Cards Useful for Bridge Modeling

The principal elements used in the modeling of the bridge are the bar, quad4, and elas2 elements. In the NASTRAN data deck, these elements are defined by related "cards;" for example, the bar element is described by the CBAR and PBAR cards, which describe the gridpoint connections and properties of the element respectively. (The cards are described in greater detail in the following section.)

The bar element is a prismatic element whose endpoint deflections are derived from classical beam theory. It is a simplified element in that the neutral axis and shear center coincide.

The quad4 element is a versatile plate and shell element with bending and membrane parts. The element is a quadrilateral in that it connects four neighboring nodes. Its connection and property cards are CQUAD4 and PSHELL. The quad4 element is used for modeling sections of the bridge deck.

Several cards that are useful for bridge modeling are described below. Following this card description will be an analysis of how some of these cards may be used in a simple bridge model.

GRID

The GRID card is used to identify the location of a grid point in space in a global coordinate system. If the

point is constrained to move in certain directions only, these directions are also specified on this card.

SET

The SET card is used to define subsets of grid points, model elements, load sets, temperature data, and constraint sets. Each set is assigned a unique number. These sets are used by many other cards to refer to selected groups of grid points or elements. For example, deflections may be printed out for a specified grid point set.

CBAR

The CBAR card describes the connection ("C") of a simple bar element between two grid points of a structural model. In the Bonnabel Overpass span model, the bar element is used to model the girders and diaphragms. The bar element properties ("P") are described by a PBAR card. One PBAR card may be referenced as the list of properties for many CBAR element connection cards. In the CBAR bulk data card, the associated grid points, offset of neutral axis from grid points, and appropriate PBAR card are referenced.

PBAR

The PBAR card lists the properties of a simple beam element, the bar, including material, cross sectional area, moments of inertia, torsional constants, and related properties. The grid point connections are described by the

CBAR card. The material properties are specified by referring to an associated MAT1 card.

MAT1

The MAT1 card defines material properties for cards that reference its identification number. The properties are for linear, isotropic materials, and include Young's modulus, shear modulus, Poisson's ratio, and related properties. This card is used by other cards such as PBAR as a reference for material properties. MAT1 (and MAT2) cards allow for linear thermal expansion but are otherwise temperature independent.

CQUAD4

The CQUAD4 card describes the connection of a quadrilateral plate element ("quad4") between four grid points. The quad4 element is used to model sections of the deck in the Bonnabel Overpass span model. The CQUAD4 card includes a list of the grid points connected, and the identification number of a PSHELL card which contains the properties of the plate, including the thickness.

PSHELL

The PSHELL card lists properties for the quad4 element used to model the sections of the bridge deck. The properties include material reference, bending stiffness, thickness, and related properties. The material properties

are determined by referring to an associated MAT2 card.

MAT2

The MAT2 card is used to define material properties for linear, temperature independent, anisotropic materials for two dimensional elements. For the overpass, this card is used to define material properties for the quad4 element, when cracked slab conditions are included.

CELAS2

The CELAS2 card is used to specify a single dimensional, elastic relationship, called a scalar spring model ("elas2"). In the model of the overpass span, it is used to model the vertical elastic properties of the supports. The CELAS2 card itself contains data listing the grid points that are connected by the elas2 element, and in which direction the elastic relationship is oriented.

RBAR

The RBAR card defines a rigid bar with six degrees of freedom at each end. Some of the degrees of freedom at each end may be constrained if the user wishes.

FORCE

The FORCE card specifies a force load vector at a grid point.

MOMENT

The MOMENT card will define a moment load at a grid point by specifying a vector.

LOAD

The LOAD card defines a static load as a set of forces and moments defined on grid points by the FORCE and MOMENT cards.

PLOAD2

The PLOAD2 card is used to define a static pressure load on a section of a quadrilateral or triangular element. This load is modeled as a uniform pressure over an entire quad4 element.

For the overpass span model, the PLOAD2 card is used to define the load exerted by the tires over the area of the tire prints, and to define the slab dead weight.

SUBCASE

The SUBCASE card is used to mark the beginning of a section of the case control deck containing cards relating to a single subcase. For the bridge model, subcases are used to describe different load locations.

SPC

An SPC card is used to define a single point constraint at a grid point. For example, this card may be used to

constrain a point to move only in the vertical or horizontal direction, or may constrain the point not to rotate about a given axis.

DISPLACEMENT

DISPLACEMENT is an output request card that is used in the Case Control Deck. Various options on this card allow the displacement output to be printed or plotted for all grid points, or a subset of the grid points.

ELSTRESS

The ELSTRESS card is used to control output of the element stresses of selected elements (defined by appropriate SET cards).

GPFORCE

The GPFORCE card is used to request a printout of the force balance at each of a set of grid points specified by parameters on the card.

GPSTRESS

The GPSTRESS card is used to produce a printout of stress at a grid point or a set of grid points.

TEMPD

The TEMPD card is used to define the temperature of all grid points not specified by other temperature definition cards.

TEMPP3

The TEMPP3 card is used to define a temperature field for a homogeneous plate element for the determination of thermal loading, temperature dependent material properties, and stress recovery. The temperature data is tabulated for the cross section. This card was used to define a temperature gradient in the deck for thermal effect studies described below.

TEMPRB

TEMPRB is used to define the temperature field for bar, beam, and other elements for determining thermal loading, temperature-dependent material properties, and stress recovery. This card was used in the bridge model to "simulate" girder camber growth by specifying a temperature gradient from the top to the bottom of the girder.

A.2.4 A Simple Bridge Span Model

A simple bridge span model will be discussed to show how the elements of NASTRAN are used to model it. Fig. A-1 shows the construction of the model.

The deck of the bridge is modeled by a pair of two quad4 elements. These elements are defined by the node numbers at the corners of the elements, so that the first element is defined by nodes 1-2-5-4 and the second by nodes 2-3-6-5. It can be noted that the nodes are located on the central plane of the deck. The thickness of the deck and

its static properties in various directions would be defined in the data deck.

The girders of the bridge are defined using the nodes of the deck, not separate nodes. The first girder (lower right) is composed of bar elements, the first connecting nodes 1 and 2, and the second connecting nodes 2 and 3. Since these girder elements do not occupy the same space as the deck, they are attached to the nodes by an offset distance separating the girder neutral axis from the grid point. This places the girder below the deck at the proper distance. Because of the continuity of the deflections of the finite element model, the two bar elements (1-2 and 2-3) model the continuous girder from node 1 to node 3. The second girder is modeled by two other bar elements in the same fashion, from 4 to 5 and from 5 to 6.

The supports of the bridge span at each end of each girder are modeled as separate springs in the vertical (z) and longitudinal (x) directions. To each of nodes 1, 3, 4, and 6 is attached a vertical spring to account for the vertical compliance of the supports. Hence, the bridge is imagined to rest on, or hang from, springs at the nodes at the ends of each girder. The elas2 element is used for the definitions of the spring elements. The vertical spring element is used to model the vertical compression of the neoprene pads. Even though the pads are at the bottom of the girders, their vertical deflections are in a direction that passes through the nodes at the ends of the girders,

and so the deflections may be modeled as if they occurred at those nodes.

The horizontal deflection of the neoprene pads is modeled by a spring element located in the horizontal direction parallel to the longitudinal axis of each girder. Because the deflection motion of the pads is not in line with the node at the end of the girder (and deck), a rigid bar connection was used in the modeling. This rigid bar (RBAR) is connected from the node at the end of the girder, for example, node 1, to another new node directly below it at a distance that corresponds to the bottom of the girder. An elastic element is connected to the node at the bottom of this bar that acts in the longitudinal (x) direction. The deflections modeled here arise from the curvature induced on the bottom surface of the girder by the load.

A diaphragm connection between two girders is modeled as a bar element connected between grid point nodes 2 and 5 with offsets. The offset positions the bar element at the centerline level of the diaphragm.

In NASTRAN, forces applied to a structure, such as F1 in the figure, can only be applied at the defined nodes. Hence, to model the correct application of F1, the model must be redefined with a node at its application point, or the force F1 must be resolved into equivalent forces at the surrounding nodes 1, 2, 4, and 5. Both methods were used in this modeling. The chief advantage of introducing additional nodes to the model is the increase in information

that can be obtained from the model, since the output of NASTRAN is generally restricted to forces and deflections at the node points. Since much of this project was concerned with the study of forces, moments, stresses, and deflections in the area between the neighboring steel and concrete girders, some of the models to be described contain additional nodes in this area to provide a finer resolution in the output data. However, no apparent increase in accuracy was observed as a result of the introduction of additional nodes.

To model the application of the load force through the tires of the trucks and the overload truck crane, the force of each tire was modeled as a uniform pressure over a specified area. This area corresponded closely to the shape and location of small quad4 elements used in the area of the bridge between the steel and concrete girders.

Finally, constraints were used to make the model more manageable. The supports at the fixed ends of the elastic elements are constrained so as not to move at all. Also, since all of the test loads on the bridge span were symmetric about the lateral centerline of the span (through nodes 2 and 5 of the model), it was decided to model only one half of the span. If the span in the Fig. A-1 were symmetrically loaded about the 2-5 centerline, then deflections would be symmetric about the 2-5 centerline as well. Maximum deflections would occur at 2 and 5, and the section of the span near 2 and 5 would be horizontal in the

longitudinal (x) direction. The span deflections can be modeled by only modeling one half of the span, and constraining the deflections of nodes 2 and 5 (all nodes on the centerline) to have no rotational deflection about the y axis as defined in Fig. A-1.

A.2.5 The Bonnabel Overpass Span Model

The coordinate system and node arrangement for the Bonnabel Overpass span model is shown in Fig. A-2. The x axis proceeds in the traffic direction, the y axis is perpendicular and across traffic, and the z axis is vertical. All dimensions are in inches. Coordinate dimensions are indicated along the edges of the span to locate each node.

Note that supports are modeled along the lower left side in the figure. The upper right side corresponds to the lateral centerline of the span. These nodes are not "supported," but are "constrained" to have no rotational deflection about the y axis. This effectively allows the modeling of symmetric loads on a symmetric span, while reducing the computational load almost in half.

Fig. A-3, similar to the preceding figure but without node numbers, shows the location and numbering of the principal elements connecting the nodes. These elements include the quad4 elements modeling the deck, the bar elements modeling the girders, and the bar elements modeling the diaphragms. Not shown are the elastic elements

supporting each end. The guard rails are included in the model.

A high node density is used to model the span deck between the steel and concrete girders. Additional nodes are also used to model the deck in the sections between concrete girders G-2 and G-3 and steel girders G-4 and G-5 to provide additional detail and allow an accurate positioning of the test loads.

The test loads are described as load sets in a subsequent section of this report. Each load set corresponds to the array of forces presented by the test loads through the tire prints.

A.2.6 Modeling Temperature Effects

Two temperature related effects were modeled using the NASTRAN model and the cards described in the previous section.

Effects on the bridge from large changes in temperature were studied. For example, if a weather front passed the overpass, the steel girders would heat up or cool off much faster than the concrete girders, leading to distortion of the deck and related stresses in the deck section between neighboring steel and concrete girders. This effect was modeled in the NASTRAN bridge model by declaring the steel girders to be a different temperature than the concrete girders. The TEMPRB card was used to impose different uniform temperatures on the girders.

The warming effect of sunshine on the deck was also modeled. The TEMPP3 card was used to model a temperature gradient in the deck from the top to the bottom to account for this effect. Different gradients were modeled to depict the gradual warming of the top surface of the deck relative to the bottom.

A.2.7 Modeling Camber Growth

Camber growth in concrete girders is an important consideration in the development of this model.

To simulate camber growth, a fictional temperature gradient is imposed on the concrete girders from top to bottom. This gradient was chosen to produce the appropriate camber in the girder. The resulting stress distribution in the deck was then studied. Although temperature distribution in the girder is "fictional," since it was chosen to produce the required amount of camber growth, the stresses in the deck and moments in the girders will model the actual stresses and moments due to camber growth in the girder.

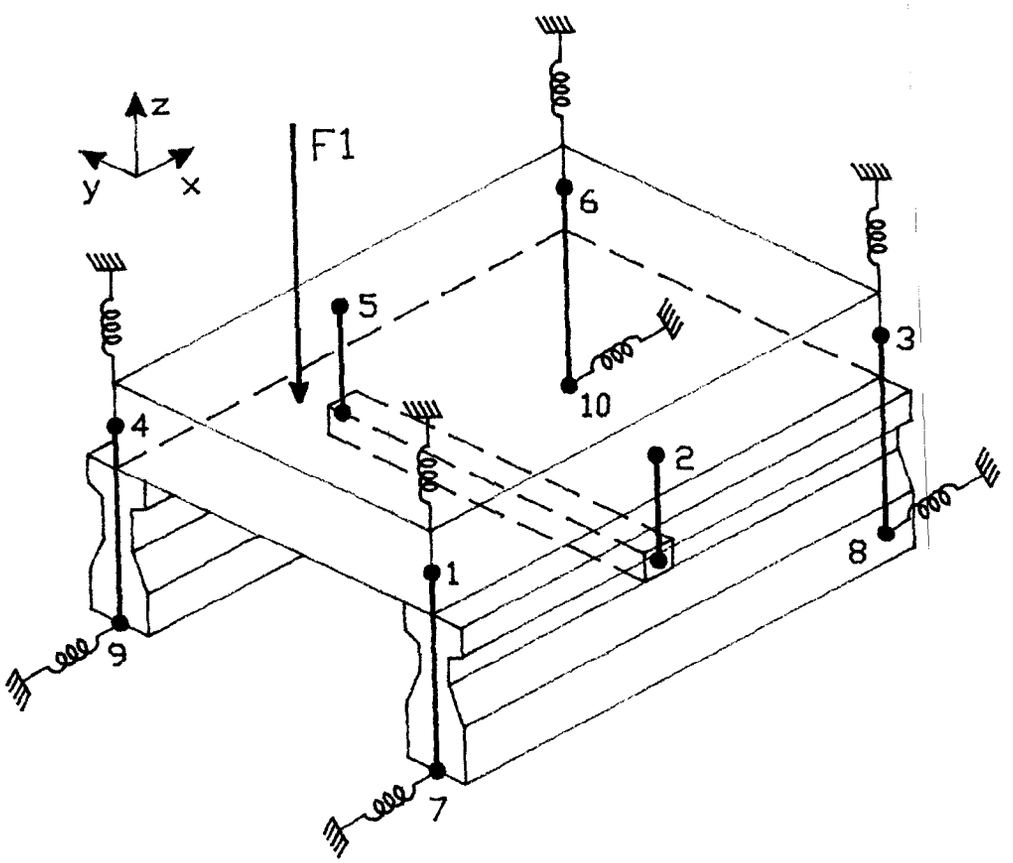

FIG. A-1 SIMPLE BRIDGE MODEL

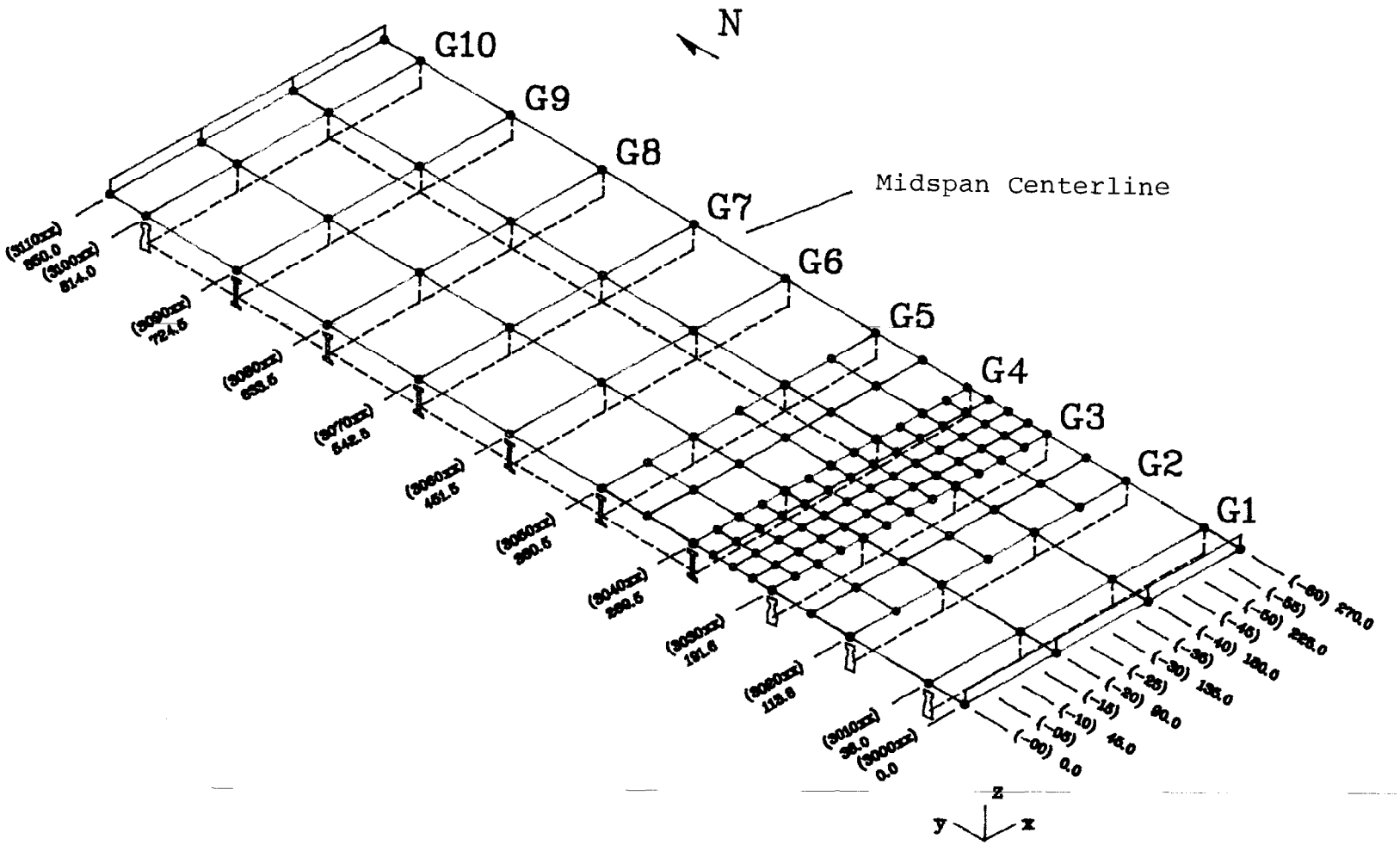

FIG. A-2 BRIDGE MODEL GRID PATTERN

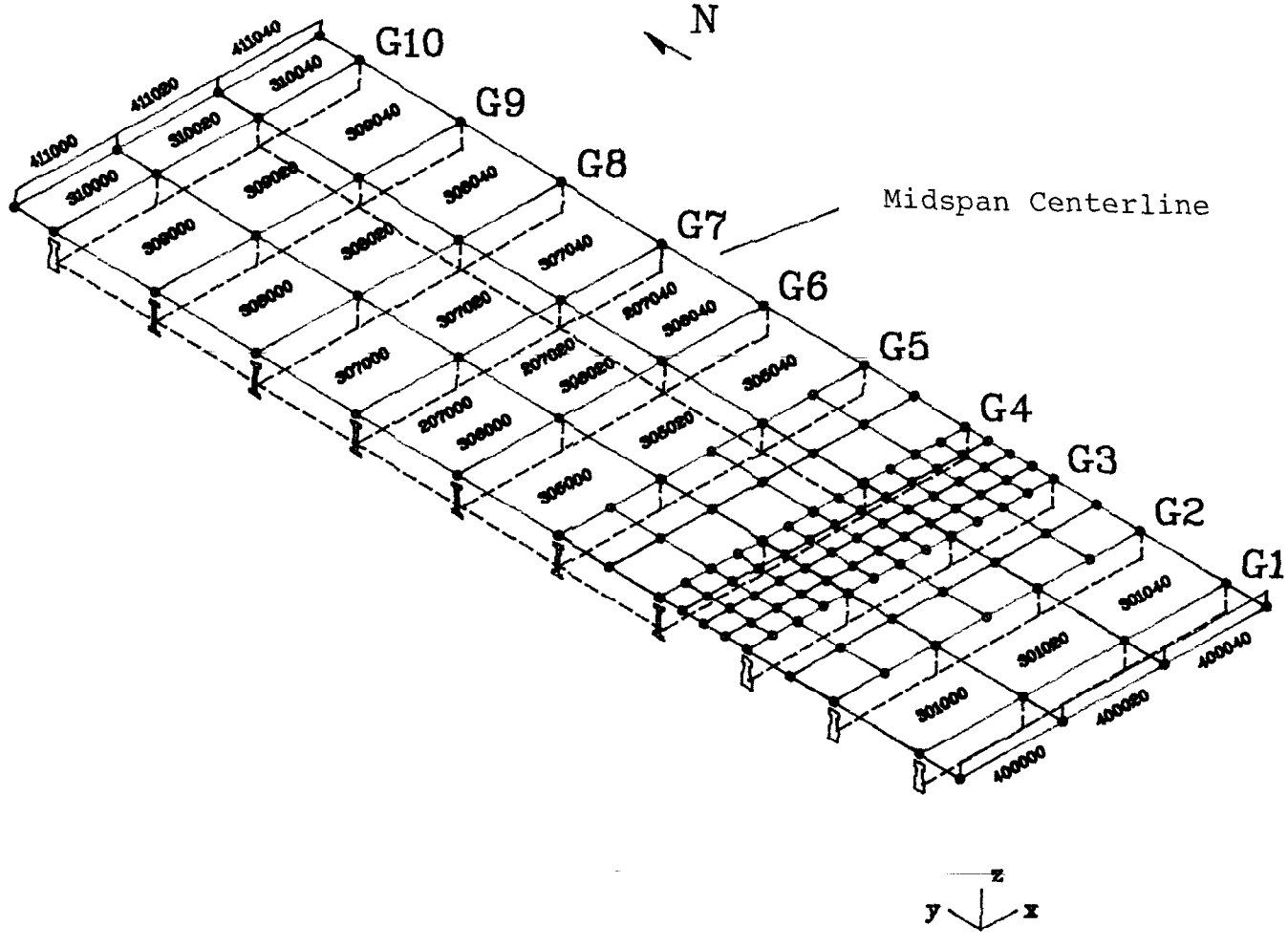

FIG. A-3 BRIDGE MODEL SELECTED ELEMENTS

This is the model which gave the best agreement with the overload truck crane field test results, as discussed in the previous section.

The results of the comparison under the nominal HS20-44 truck load are shown by Figs. 24, 25 and 26. It can be seen that the computed deflections agree very closely with the field test results. The maximum calculated deflections are within 5% of the maximum measured deflections and the shapes of the calculated and experimental deflection curves are similar.

3.4 Thermal Deflection Tests

In this section the results of the thermal deflection tests are discussed and certain computer results are compared with the field test data.

The NASTRAN computer program allows thermal loads to be applied by specifying temperature distributions in the structural elements. In terms of the model of the Bonnabel Overpass, a temperature gradient can be imposed through the slab from top to bottom and temperature changes can be imposed on the girders. However, the heat transfer analysis required to define these temperatures over a full diurnal cycle is beyond the scope of this investigation.

The computer comparison will be limited to a specific period of time during the field tests for which it is believed the element temperatures can be approximately specified. This is the period in the morning from sunrise

until about noon. Before this period there was a relatively long predawn period of approximately constant conditions.

This section also contains some observations relative to the effect of temperature variation on the Bonnabel Overpass.

3.4.1 Computer Comparison of Thermal Deflections

It can be seen from the thermal field test data that there is a period of several hours between about midnight and dawn when the temperature is approximately constant and the test span reaches a more or less stable condition. After sunrise, the structure starts to deflect upward at mid-span and continues to rise for several hours. An attempt has been made to model the overpass during this period using the NASTRAN computer program. As mentioned previously, defining the thermal loads for this situation is difficult and at best the results presented herein are only approximate; however, it is believed that some significant information is obtained.

During the period after the sun rises, the major thermal load on the span is caused by the radiant energy exchange on the top of the deck. Radiant energy is received both from direct sunshine and from sun rays reflected from the sky. This latter radiant energy is primarily reflected from water vapor and carbon dioxide. The amount of radiant energy received increases as the morning progresses, barring shading by clouds. Radiant energy is lost by the top of the

deck due to reradiation. As the deck heats up the amount of energy lost also increases. During the morning period the temperature of the top surface of the deck is slightly higher than ambient so that there is a small loss in thermal energy due to convection.

An average heat input to the top of the deck was estimated and this heat input was used to calculate temperature profiles through the slab at one hour intervals for four hours. These temperature profiles were used to specify the temperature gradients in the slab elements of the NASTRAN program.

During the same period of time the ambient temperature increased from approximately $63^{\circ}F$ to $80^{\circ}F$, which would cause the temperature of the girders to increase. The concrete girders have considerably more thermal mass than the steel girders, which means they will change temperature much more slowly. It is estimated that during the four-hour period under consideration the steel girders would increase in temperature in the order of five degrees, while the concrete girders would change only about one degree total. Temperatures for the steel and concrete girders are estimated at one-hour intervals for the four-hour period, and these values are used to specify the bulk temperature of the elements representing the girders.

The NASTRAN program is used to calculate the deflections caused by the thermal loads discussed above. The results are shown on Fig. 27. Fig. 28 shows the

computed deflections across mid-span after four hours of sunshine and the measured deflections at noon.

Considering the approximations made when defining the thermal inputs into the slab and girders, the agreement between the computer results and the field test data is close. It is believed that this agreement confirms the adequacy of the thermal input model used, this model being a relatively large heat input into the top of the slab and relative small heat input into the girders beneath the slab. The estimate that the rate of change of temperature of the steel girders is five times that of the concrete girders appears to be approximately correct for this configuration.

Changing the relative lateral stiffness of the slab, i.e., cracked versus uncracked, did not change the computer results noticeably. Thus the thermal test results can not be used to gain additional insight into the cracked condition of the slab.

The computer program used for the above analysis also calculated the change in length of the girders at the bottom fibers, as a function of temperature. These values can be compared with the measured values, as shown on Fig. 29. While the agreement between computer results and the field test data is far from ideal, the trends and overall effects appear to be similar.

In the predawn hours the vertical position of the span has become constant, and the lengths of both the concrete and steel girders are decreasing very slightly. This

probably indicates that the overall temperature of the span is uniform and almost constant. When the sun rises and the span starts to arch up at mid-span, the girders will be concave downward, which would tend to shorten the bottom fibers of the girders. On the other hand, the ambient temperature is increasing, which will cause the girders to increase in temperature and thus become longer. As mentioned above, the temperature of the steel girders will change more rapidly than the concrete girder. This result is observed in Fig. 29, where the length of the bottom fibers of the concrete girder, G-3, is remaining relatively constant and the length of bottom fibers of the steel girder, G-4, is increasing significantly.

It is believed that the NASTRAN computer program can accurately represent structures under thermal loading provided the temperature distributions can be specified and the structure can be correctly modeled. However, in the case of an overpass span subjected to atmospheric variations, as in the case herein, the program has some serious limitations. Even if the environmental conditions could be precisely defined, the heat transfer calculations required to specify element temperature distributions are formidable.

3.4-2 Girder-Bent Cap Motion

The longitudinal deflection measurements taken during the thermal field tests give some insight into the overall motion of the overpass. The results indicate that the

overpass expands and contracts as a unit and the motion of the bent caps and columns supporting the concrete girders are a function of the overall overpass design rather than being a function of the expansion and contraction of the individual simple span.

Fig. 29 shows the field measurements for the length of the concrete girder along the bottom fibers. The length measurement was made at approximately the same elevation as the neoprene bearing pad, thus the change in girder length relates to the relative motion of the neoprene pads. It can be seen that the concrete girder bottom fiber length is a minimum in the morning daylight hours and in the afternoon increases in length to reach a maximum in the early evening, with the total change in length being approximately 0.03 inches.

During the thermal deflection test discussed in Section 2.4, the longitudinal movements of the ends of girder G-3 with respect to the bent caps were measured. These measurements, shown on Fig. 16, show that as the concrete girder expands, the west end of the girder moves west with respect to the west bent cap and the east end of the girder moves east with respect to the east bent cap. The magnitude of each motion is approximately the same on each end indicating that the span maintains an approximately centered position between the bent caps.

Measurements of the motion of the bent caps with respect to the ground indicate that the bent caps are more

or less moving together; as the concrete girder length is increasing, both bent caps for the span investigated are moving east and as the length decreases both bent caps for the span investigated move back to the west. Further, measurements can be combined to obtain the net change in distance between the bent caps. As shown by the bottom curve of Fig. 29, the distance between the bent caps changes by only a small amount.

It is believed that the above motion as observed in the field can be explained by considering two apparent facts; namely, the neoprene bearing pads act as approximately linear springs in the longitudinal or shear direction, and each span of the overpass experiences more or less the same environmental conditions. Thus as each span expands and contracts by approximately the same amount, the longitudinal forces exerted by the spans on either side of a bent cap approximately balance out each other. If the abutments at each end of the overpass were perfectly rigid and each span reacted exactly the same, the bent caps would not move at all. However, differences in the environmental conditions of the spans, differences in thermal and elastic properties of the spans and differences in support stiffnesses may cause unbalanced loading on the bent caps.

Thus, it is believed that when neoprene bearing pads are used, the longitudinal loads on the supports are influenced to a great extent by the overall design of the structure and can not be determined by considering a single span.

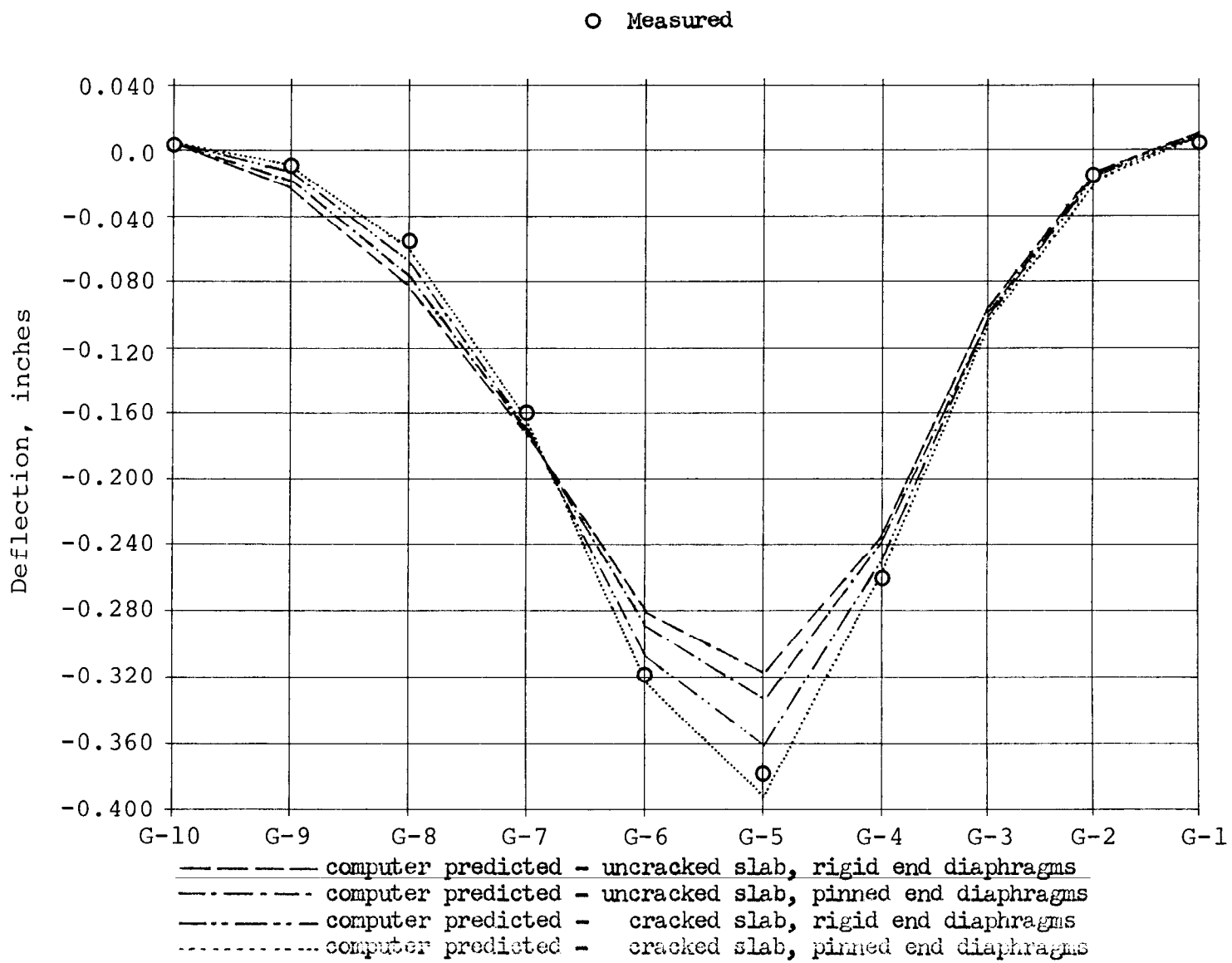

FIG. 18 SPAN TRANSVERSE CENTERLINE COMPUTER PREDICTED VS MEASURED DEFLECTIONS FOR OVERLOAD POSITION NO. 1

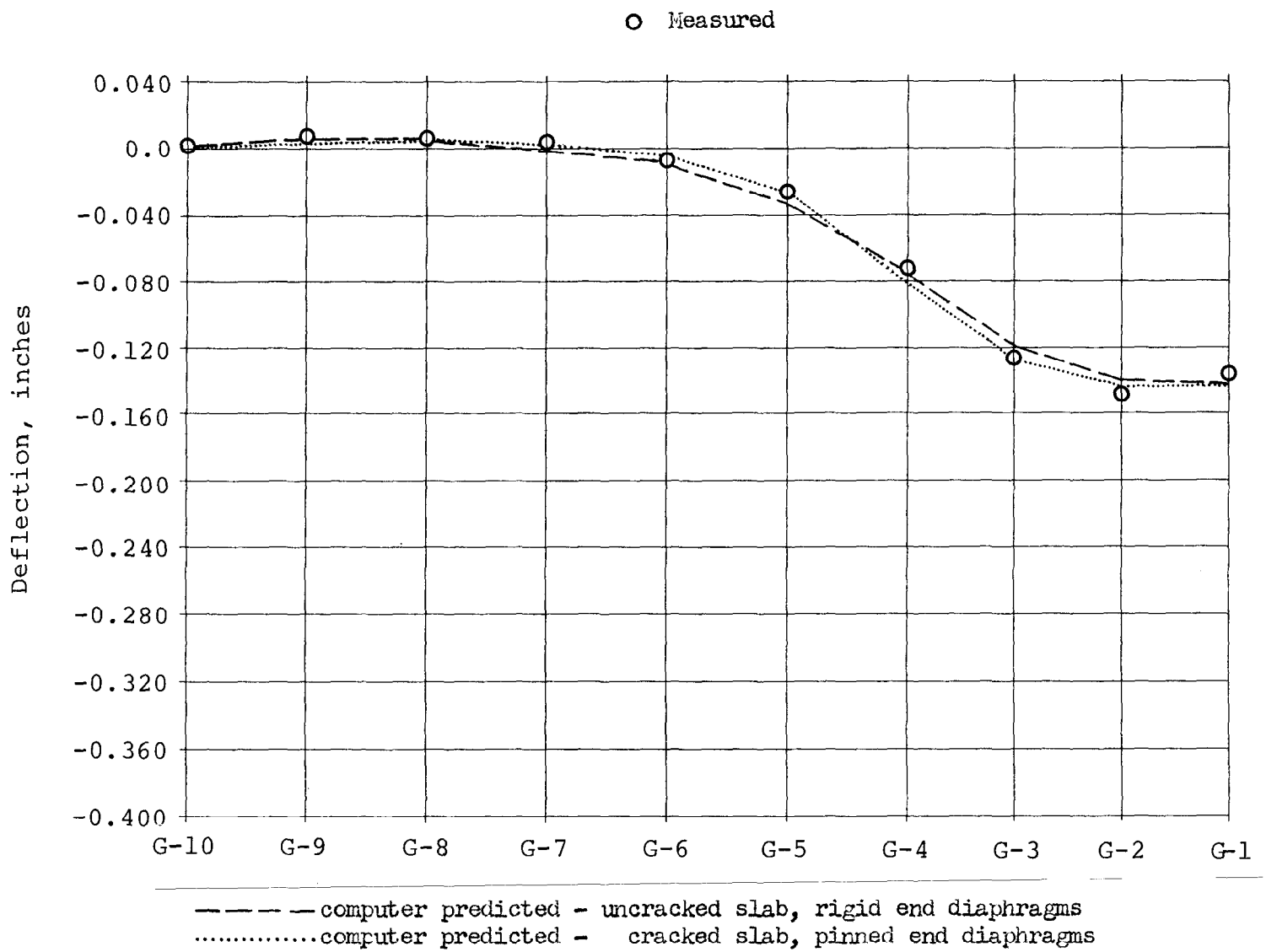

FIG. 19 SPAN TRANSVERSE CENTERLINE COMPUTER PREDICTED VS. MEASURED DEFLECTIONS FOR OVERLOAD POSITION NO. 2

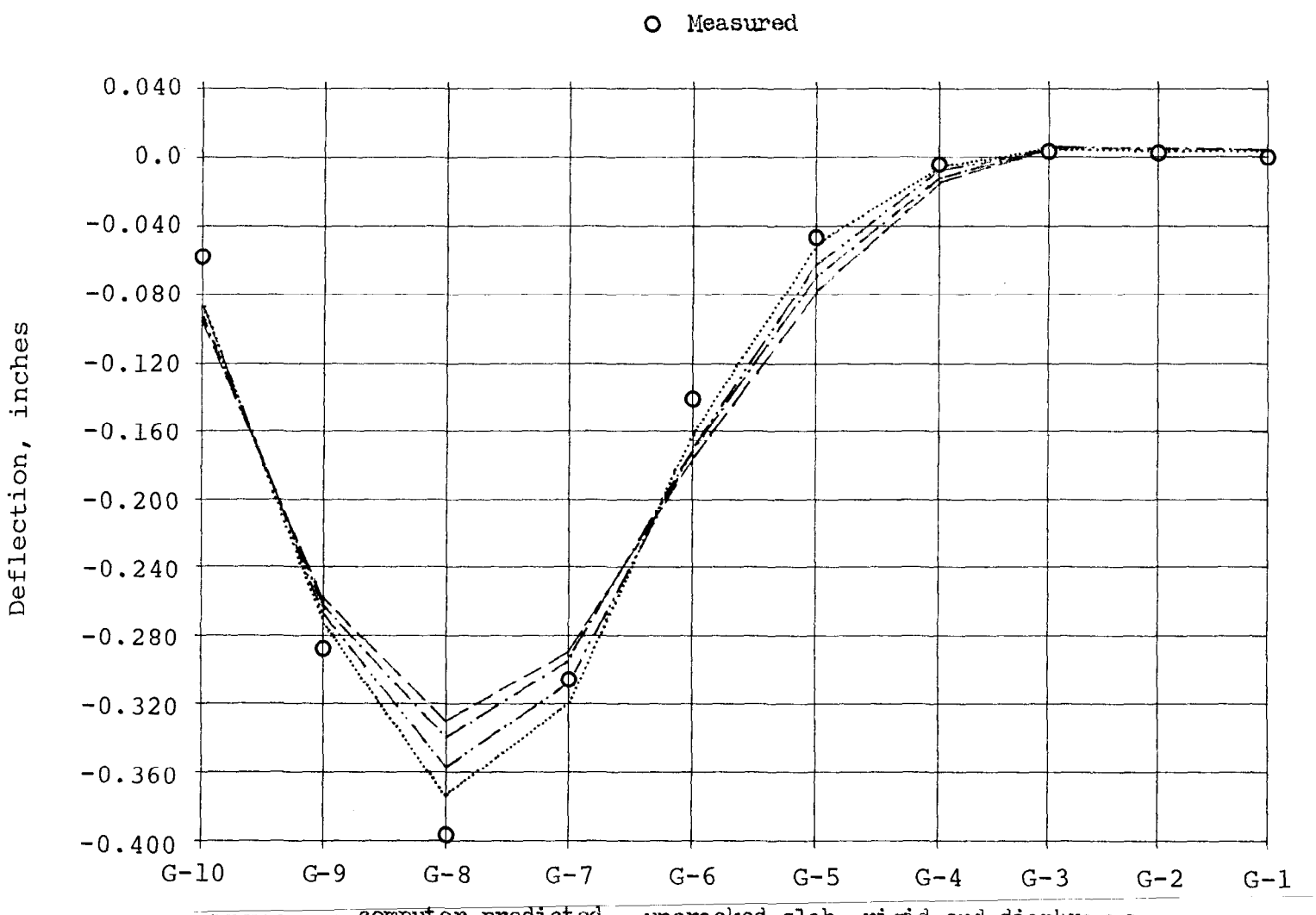

FIG. 20 SPAN TRANSVERSE CENTERLINE COMPUTER PREDICTED VS. MEASURED DEFLECTIONS FOR OVERLOAD POSITION NO. 3

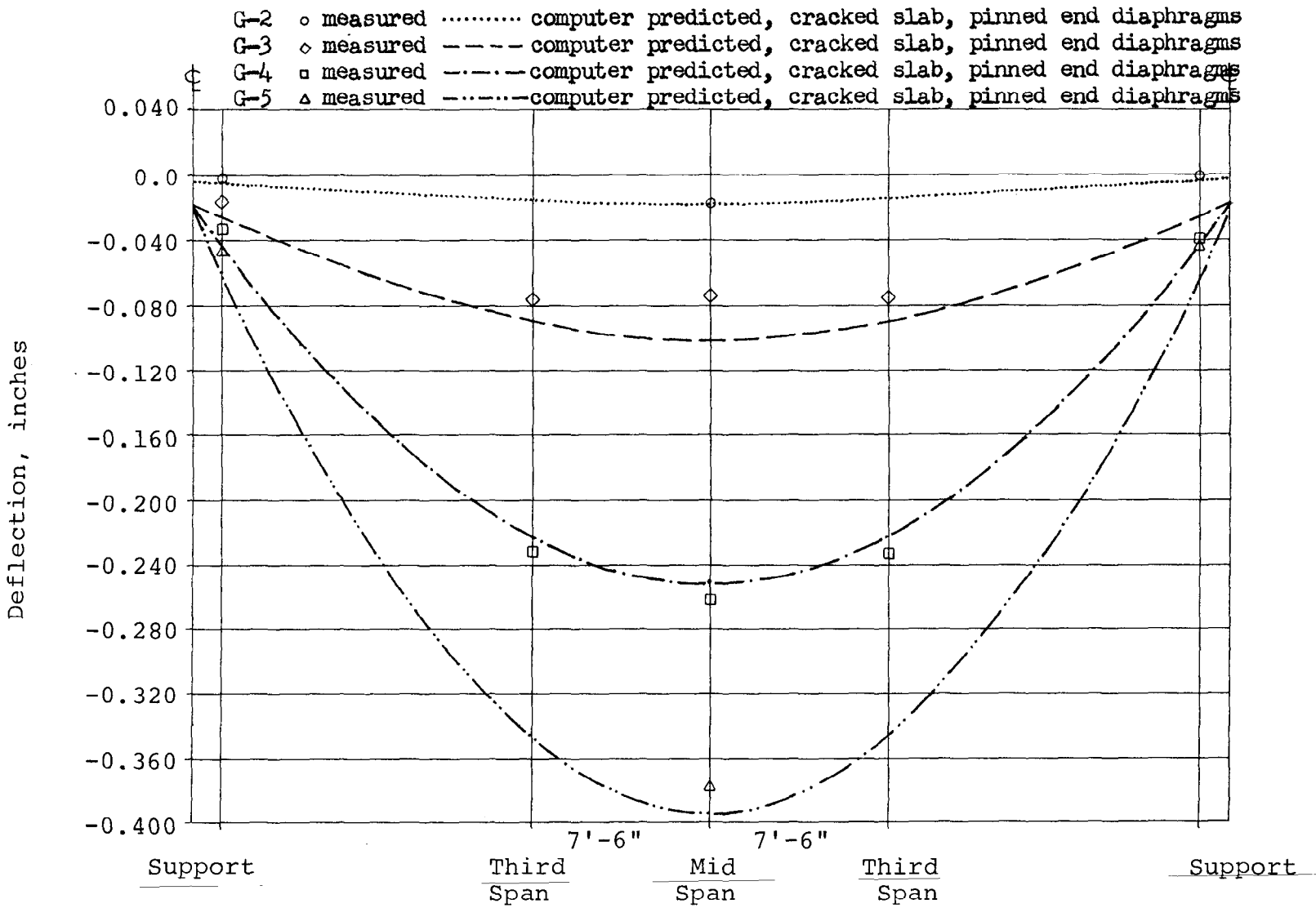

FIG. 21 COMPUTER PREDICTED VS. MEASURED LONGITUDINAL DEFLECTIONS FOR OVERLOAD POSITION NO. 1

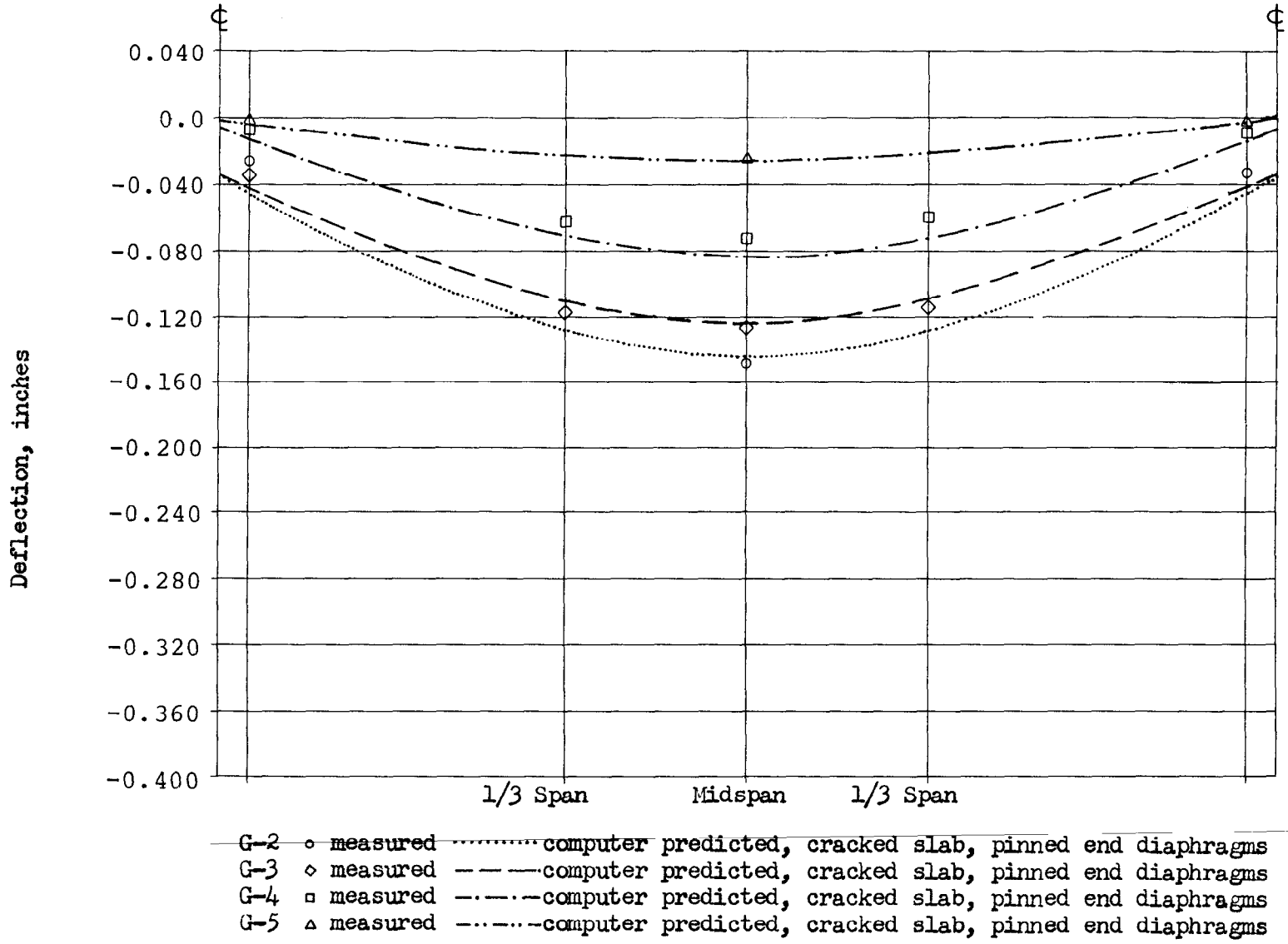

FIG. 22 COMPUTER PREDICTED VS. MEASURED LONGITUDINAL DEFLECTIONS FOR OVERLOAD POSITION NO. 2

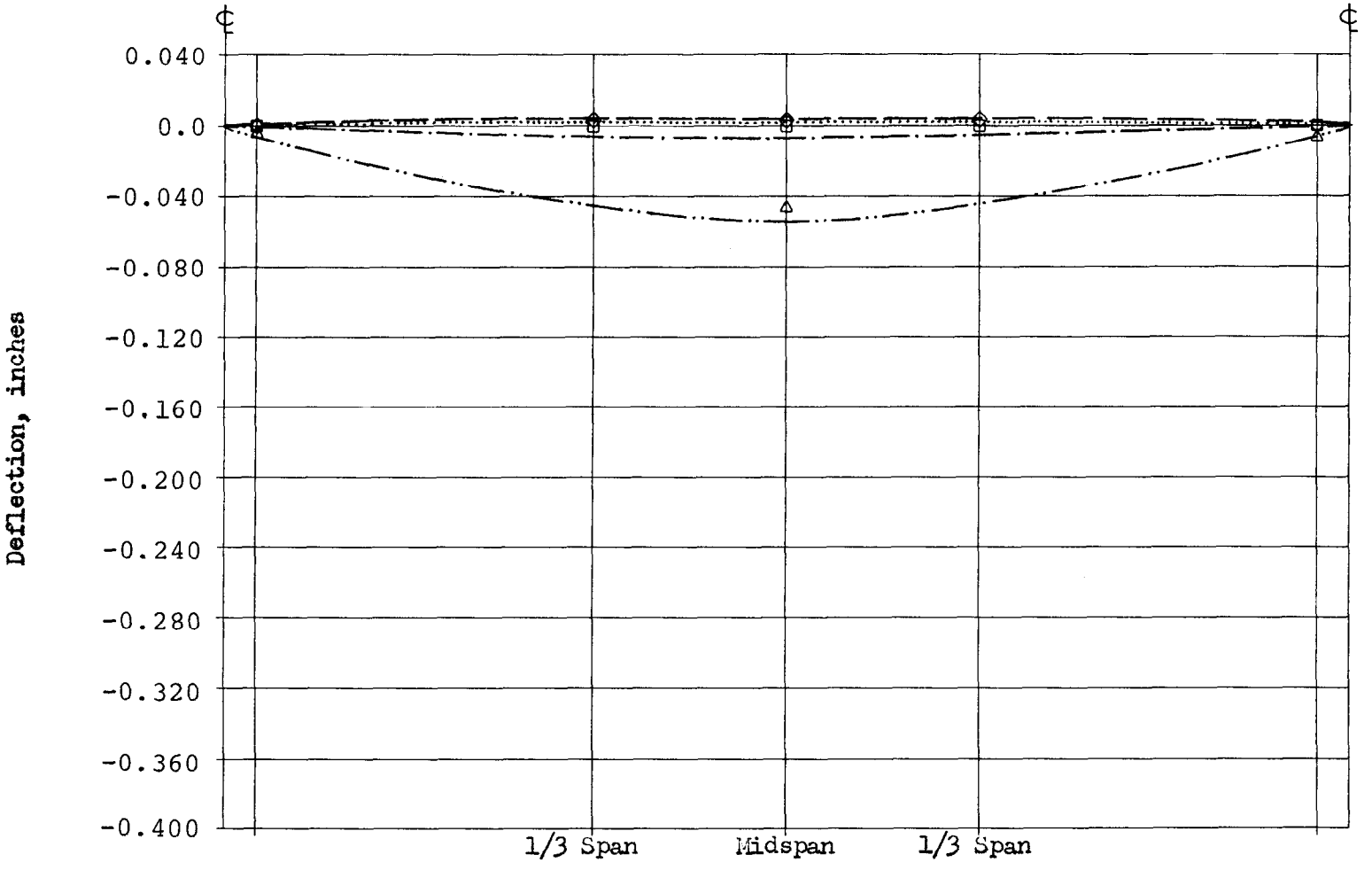

G-2 ○ measured ·····computer predicted, cracked slab, pinned end diaphragms
G-3 ◇ measured — — —computer predicted, cracked slab, pinned end diaphragms
G-4 □ measured —·—·—computer predicted, cracked slab, pinned end diaphragms
G-5 △ measured —··—··—computer predicted, cracked slab, pinned end diaphragms

FIG. 23 COMPUTER PREDICTED VS. MEASURED LONGITUDINAL DEFLECTIONS FOR OVERLOAD POSITION NO. 3

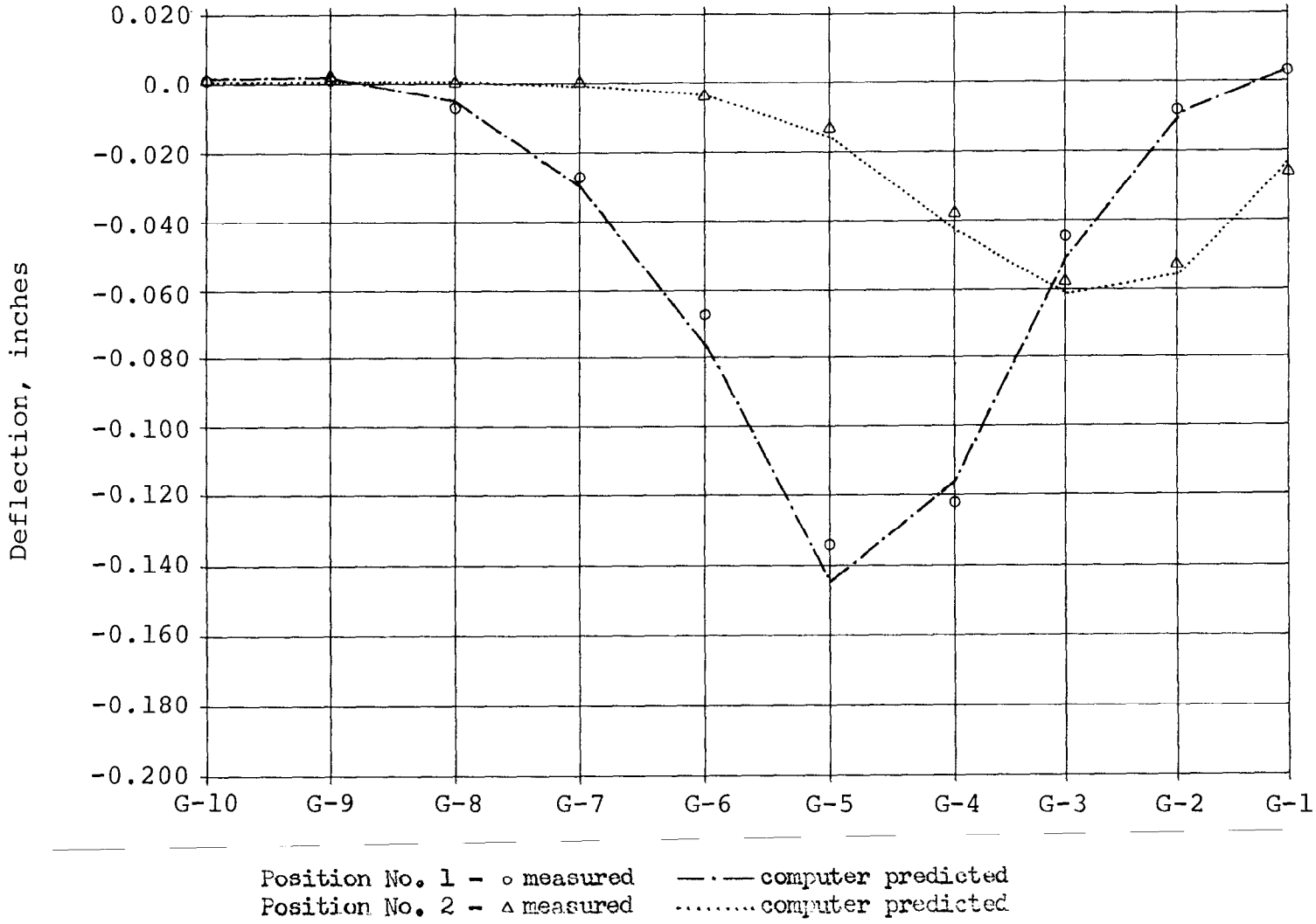

FIG. 24 SPAN TRANSVERSE CENTERLINE COMPUTER PREDICTED VS. MEASURED DEFLECTIONS FOR NOMINAL HS20-44 LOADING POSITION NO. 1 AND NO. 2

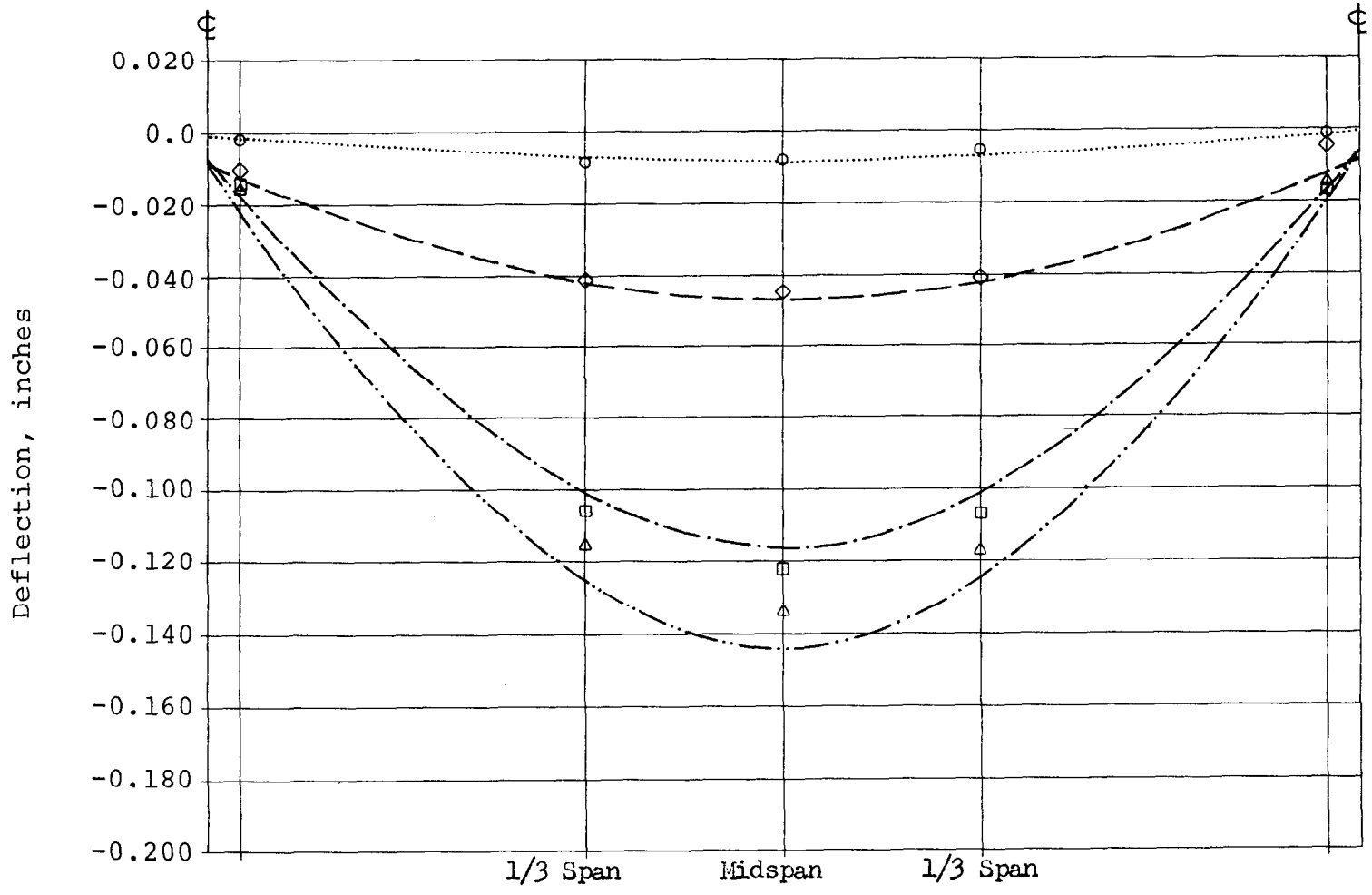

FIG. 25 COMPUTER PREDICTED VS. MEASURED LONGITUDINAL DEFLECTIONS FOR NOMINAL HS20-44 LOADING POSITION NO. 1

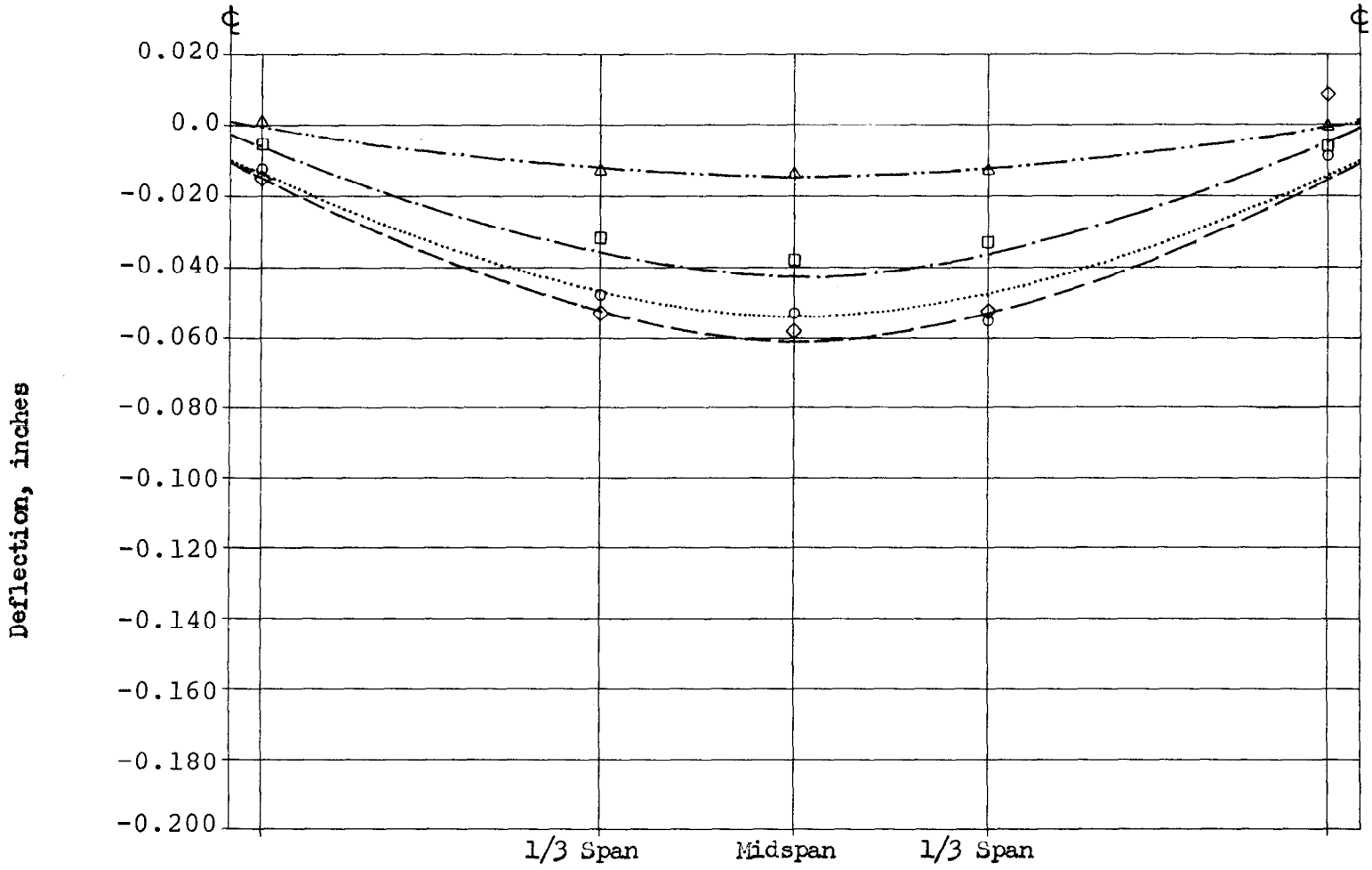

G-2 ○ measured ····· computer predicted, cracked slab, pinned end diaphragms
G-3 ◇ measured – – – computer predicted, cracked slab, pinned end diaphragms
G-4 □ measured –·–·– computer predicted, cracked slab, pinned end diaphragms
G-5 △ measured –···– computer predicted, cracked slab, pinned end diaphragms

FIG. 26 COMPUTER PREDICTED VS. MEASURED LONGITUDINAL DEFLECTIONS FOR NOMINAL HS20-44 LOADING POSITION NO. 2

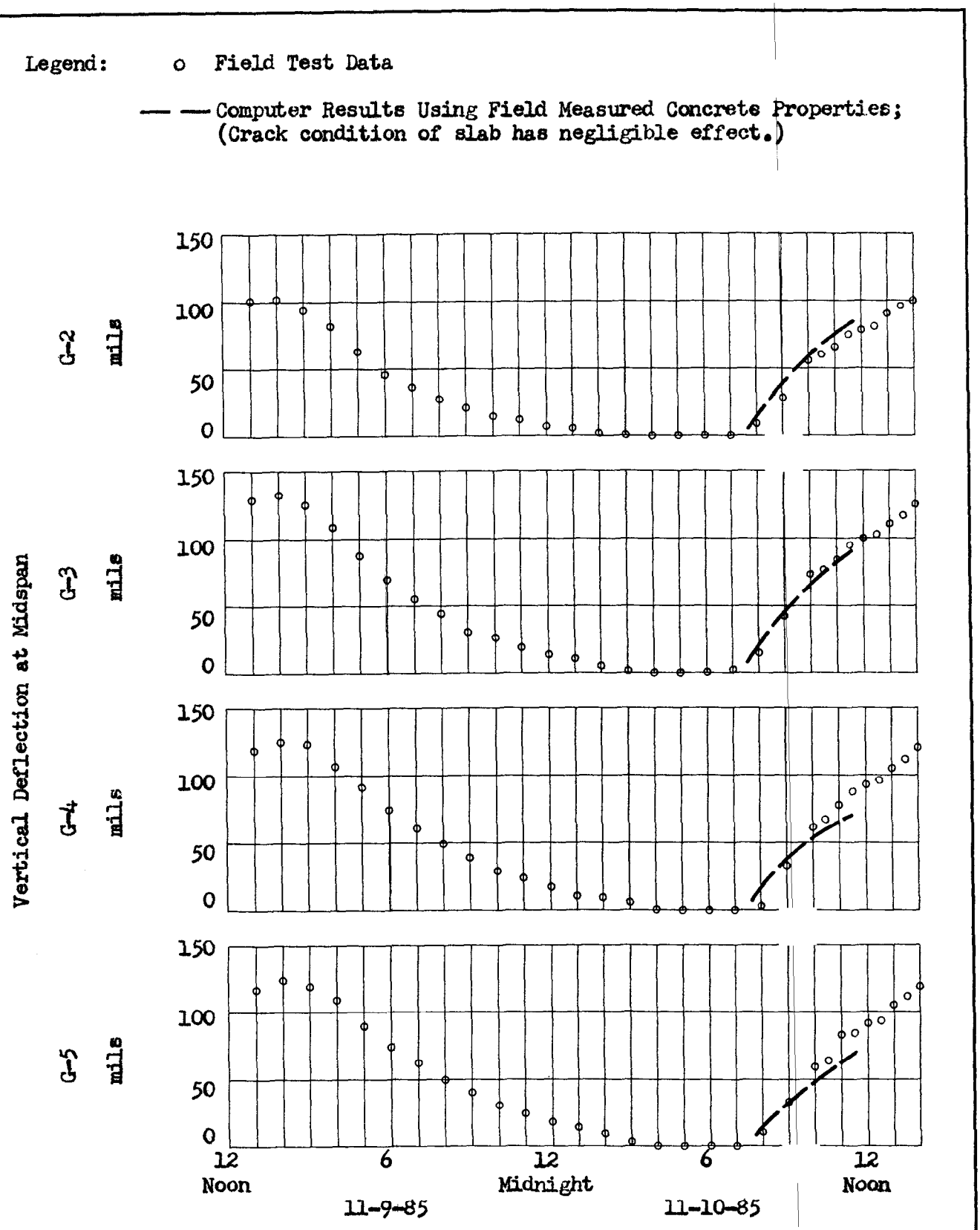

FIG. 27 COMPARISON OF TEMPERATURE INDUCED VERTICAL DEFLECTIONS AS A FUNCTION OF THE TIME OF DAY

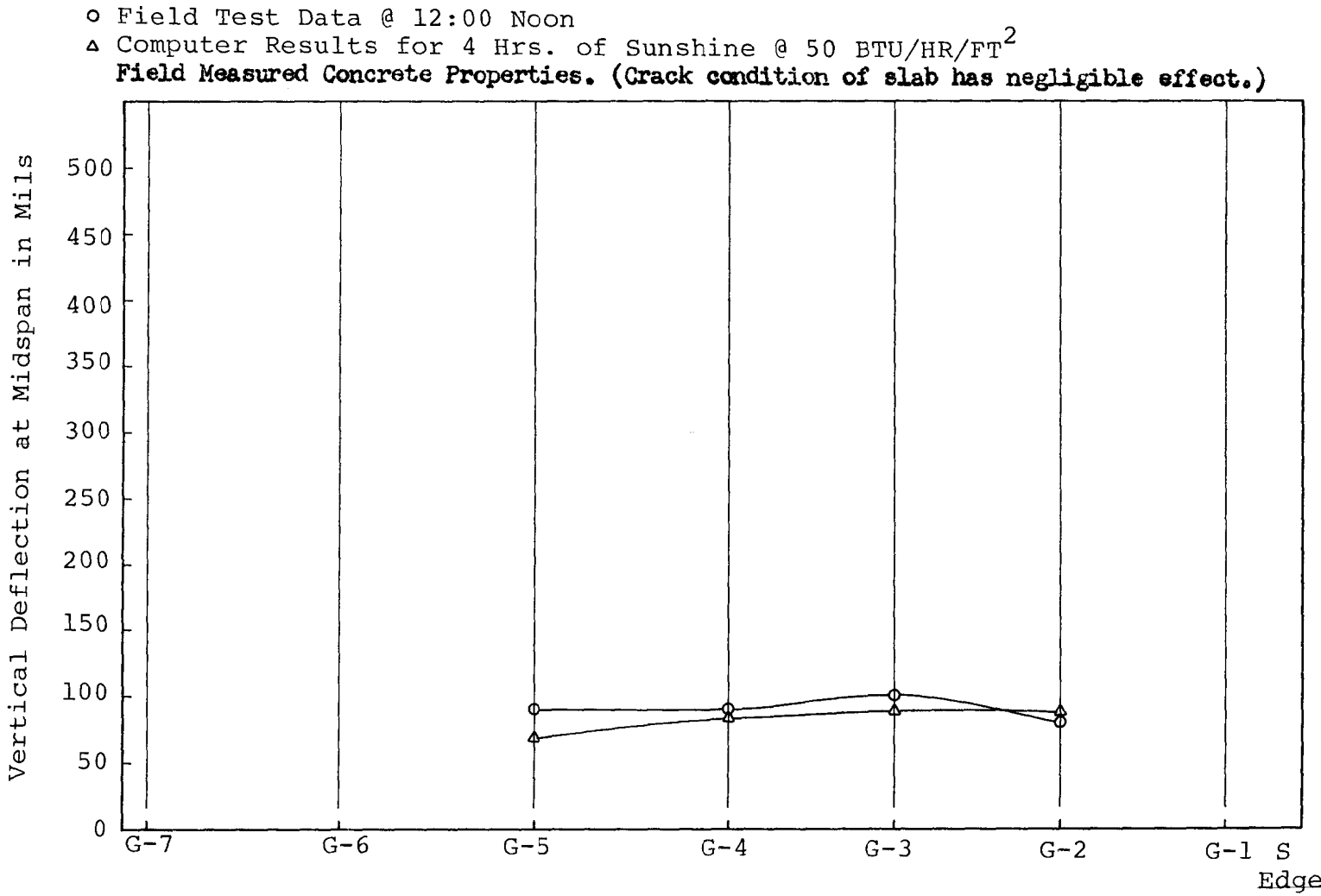

FIG. 28 COMPUTER PREDICTED DEFLECTIONS ACROSS TRANSVERSE CENTERLINE AFTER FOUR HOURS OF SUNSHINE VS. MEASURED DEFLECTIONS AT NOON

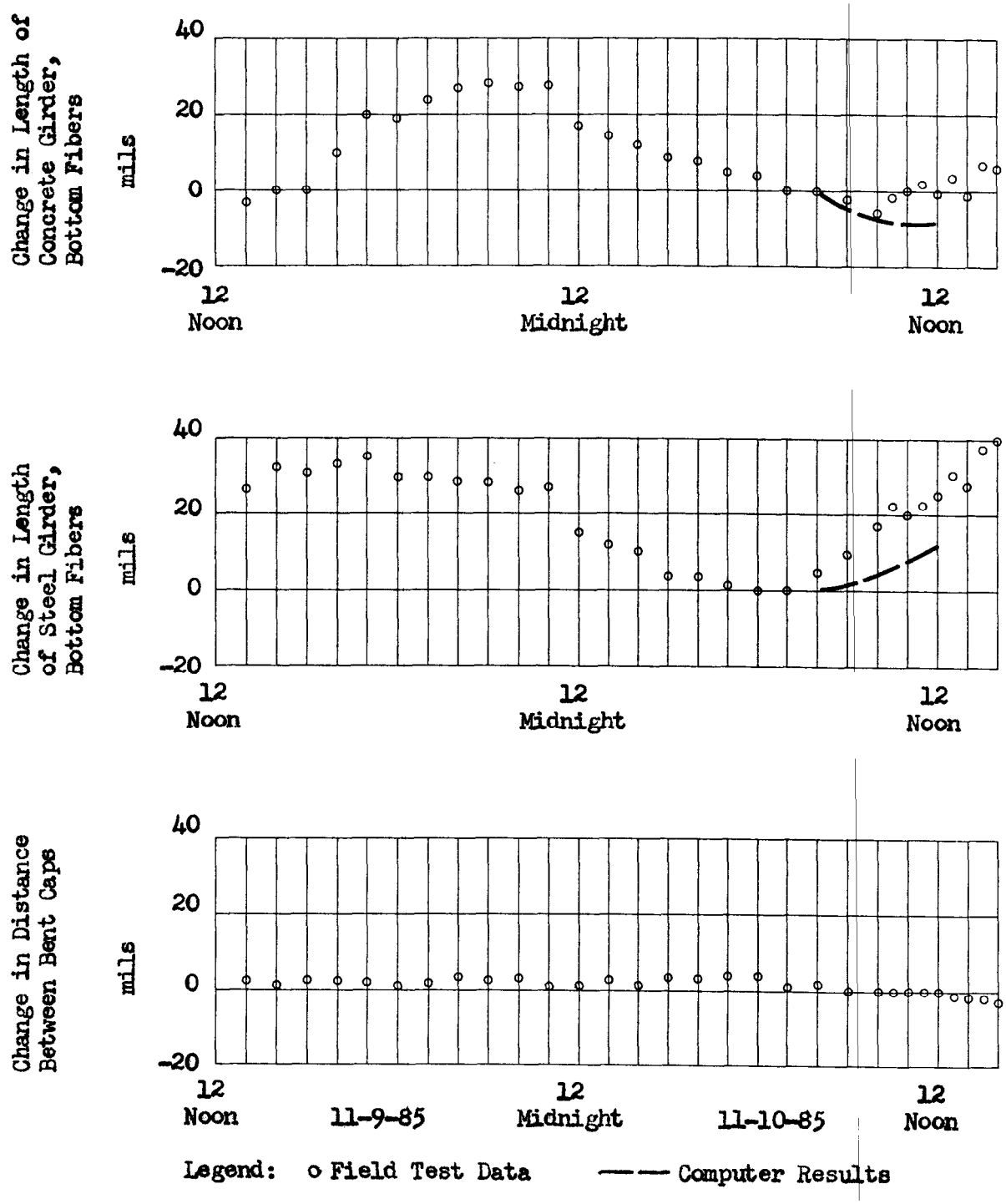

FIG. 29 COMPUTER PREDICTED LONGITUDINAL DEFLECTIONS AS A FUNCTION OF TEMPERATURE VS. MEASURED LONGITUDINAL DEFLECTIONS

4. INVESTIGATION OF MIXED GIRDER SUPPORT SYSTEM

4.1 Introduction

The computer model developed herein is used to investigate potential problem areas associated with mixed girder systems. The areas investigated are: camber growth, temperature effects, live load distribution, concrete diaphragms, rolled beams with cover plates, non-composite rolled beams and bearing movement effects. Finally, the combination of the above areas as appropriate are considered.

It is not the intent of these investigations to probe each area in great breadth nor to offer solutions to any problems uncovered but rather to determine on a gross scale which of the above effects could be a potential problem area.

The cases studied are limited to configurations similar to the Bonnabel Overpass and the computer models used are variations of the model developed for the Bonnabel Overpass. In all cases the model had a 45-ft, simply supported span with six steel girders in the interior, three concrete girders on the south side and one concrete girder on the north side. Also, in all cases symmetry about the mid-span is assumed. This means that the computer model is written for only half the span and a boundary condition of zero rotation about the lateral axis (y-axis) is applied at the

mid-span. The general layout of the model is shown on Fig. 30. The symmetry assumption saved considerable programming and machine time. In only one instance is the assumption suspected of affecting the results; that being when applying the HS20-44 live load to the determination of slab moments. In that situation the effect is investigated and is discussed under Section 4.4.

The following sections describe the model and loading configuration used and the results obtained for each of the potential problem areas investigated.

In this section when the term moment in a girder is used it means the moment about the lateral (y-direction) axis at mid-span in the composite girder-slab system. The term moment in the slab means the moment per unit width of slab about the longitudinal (x-direction) axis at mid-span.

4.2 Camber Growth

When camber growth occurs in prestressed concrete girders, they tend to arch in the center region. If these girders are located alongside steel girders which do not arch, then additional moments and stresses are caused in the concrete girders adjacent to the steel girders and in the section of slab between the concrete and steel girders. In this section these additional moments and stresses are investigated using the NASTRAN computer program.

The amount of camber growth to be expected for these prestressed girders was estimated using the AASHTO

prediction method. Fabrication and installation records were not available for individual girders, and thus camber growth was estimated based on average or specified values. The estimated camber growth based on this information is 1/4" at mid-span. Since this value is at best an average for many girders, it was decided to make computer runs simulating camber growths at mid-span of 1/8", 1/4" and 3/8".

The method used to simulate camber growth is to utilize the thermal aspects of the MSC/NASTRAN program. As discussed earlier, the bar element allows lateral thermal gradients across the element. In this case a positive thermal gradient is applied from bottom to top of the bar elements representing the concrete girders. When the girder is acting alone, the amount of arching at midspan is dependent only upon the magnitude of the temperature gradient imposed. On the other hand, when the girder is acting as a part of a composite beam with the slab in place, it is significant as to whether the gradient causes the bottom of the girder to contract or the top of the girder to expand. The model believed to best represent camber growth is one for which the top fibers of the girder experience little or no net creep and the bottom fibers experience the greatest compressive creep.

Thus the procedure for simulating camber growth is to first determine the linear temperature gradients required to cause 1/8", 1/4" and 3/8" growth at midspan, respectively,

for single girders acting alone. These gradients are then applied to the bar elements representing concrete girders in the total model and the bulk or average temperatures of the elements are specified so that the top of the girders will be at ambient or initial temperature.

As camber growth occurs in concrete girder G-3, which is adjacent to steel girder G-4, girder G-3 will carry a greater share of the dead weight of the slab, while girder G-4 will carry a lesser share of the dead weight of the slab. Also, the net shortening of the concrete girder caused by the compressive creep is being restrained by the slab and adjacent steel girder. This action causes a net tensile force on the girder in the axial direction, which decreases the amount of prestress compression in the bottom fibers of the girder.

Computer runs were made to investigate the stresses and moments in the adjacent concrete and steel girders caused by camber growth. Because of thermal and three dimensional effects as discussed above, there is no "simple moment" applicable to each individual girder. However, in order to compare the results obtained with applicable AASHTO design criteria, an equivalent moment is defined as being the moment required in order to cause the same stress in the bottom fiber of the respective girder. These moments are shown in Fig. 31. It will be observed that the computer program predicts that the moment at mid-span in the concrete girder increases significantly, while the moment in the

steel girder decreases significantly. The initial moments shown, i.e., the moments at zero camber growth, represent the moments due to the dead weight of the slab.

It should be pointed out that no correction has been made to the amount of camber growth caused by the added dead weight of the slab.

The lateral stresses at mid-span in the top and bottom fibers of the slab caused by camber growth are also shown on Fig. 32. It can be seen that the stresses are large near the girders and tend to be smaller in the center region of the slab. This is an advantage because, as will be seen later, the maximum stresses caused by live loads occur in the center region of the slab. Nevertheless, these moments and stresses are of significant magnitude, especially when it is observed that they are not considered in the design process.

4.3 Temperature Effects

The NASTRAN computer program is used to investigate the effect of ambient thermal changes upon the stresses in the section of slab between the concrete and steel girders and the stress in the adjacent concrete girder. Three conditions were investigated; these were a sudden increase in ambient temperature, a sudden decrease in ambient temperature, and a period of bright sunshine on the slab.

When a sudden change of the ambient temperature occurs, the various components of the structure will start to undergo a temperature change. The rate of change of the

bulk or average temperature is dependent upon the ratio of the surface area exposed to the atmosphere to the thermal mass of the component; the thermal mass being the product of the physical mass and the specific heat capacity. In the case of the Bonnabel Overpass, the rate of change in temperature of the steel girders would be five to ten times that of the slab and of the concrete girders. It is estimated that for normal diurnal changes in ambient temperature, the temperature of the steel girders will follow the ambient temperature to within a few degrees, while the concrete girders and slab will only change temperature by a total of a few degrees. This estimate does not include the effect on the slab of bright sunshine. This effect is considered later.

Since the purpose of these investigations is to identify gross problem areas rather than provide exact results, assumed values of 30°F sudden temperature increase and 40° sudden temperature decrease for the steel girders are used. These two conditions are modeled in the NASTRAN computer program by using the thermal expansion characteristics of the CBAR element. That is, a uniform bulk temperature change is imposed upon the bar elements representing the steel girders.

When a temperature increase is imposed on the steel girders, they will expand, tending to cause the center of the span to deform downward or sag near mid-span. On the other hand, the concrete girders which have experienced much

less bulk temperature increase will still be in their cambered profile. This condition will cause lateral moments and lateral stresses in the section of slab between the concrete and steel girders. The relative expansion of the steel girders will also cause a stretching of the slab and adjacent concrete girder in the longitudinal direction, which will cause longitudinal tension stresses in the slab and in the bottom fibers of the concrete girders.

The results of the computer study for the slab are shown on Figs. 33 and 34. Fig. 33 addresses lateral stresses and Fig. 34 addresses longitudinal stresses. It can be seen that for a $30^{o}F$ temperature increase maximum lateral tensile stresses of approximately 120 psi are caused in the top of the slab near girder G-3. The maximum longitudinal stress caused by this condition is approximately 150 psi in the bottom of the slab near girder G-4.

The computer analysis also shows that when a $30^{o}F$ sudden temperature increase is imposed on the steel girders, a tensile stress of approximately 240 psi is superimposed on the bottom fibers of concrete girder G-3.

When a temperature decrease is imposed on the steel girders, an opposite deflection occurs. The steel girders contract, tending to cause the span to arch upward near mid-span. This condition will likewise cause moments and lateral stresses in the section of slab between the concrete and steel girders. Referring to Fig. 33 again, it can be

seen that a $40^{\circ}F$ temperature decrease causes a lateral tensile stress of approximately 120 psi in the bottom of the slab near girder G-3 and a lateral tensile stress of approximately 180 psi in the top of the slab near girder G-4.

The contraction of the steel girder will cause the slab and concrete girders to be in longitudinal compression throughout, thus having minimal effect.

The stresses caused by temperature increases and decreases, as calculated in this section, probably represent extreme cases, because temperature changes of perhaps $50^{\circ}F$ in a one-hour period would be required. On the other hand, the calculations do show that these effects are significant when compared to the AASHTO design criteria. The design values are indicated on the graph.

When a span is subjected to a period of constant ambient temperature and no sunshine as might occur in the early morning hours, the slab and other components tend to reach a uniform temperature. If bright sunshine then impinges upon the deck, the slab will experience a radiant heat input, which will start to heat the top layer of the slab. With time, the heat will be conducted through the slab. After about three hours of sunshine on a slab of this thickness, the thermal gradient from top to bottom will be most severe and the temperature difference between the top and the bottom will be a maximum.

The thermal gradient was calculated for a constant radiant heat input of 50 Btu/hr/ft^2. This value is believed to be close to the maximum value which would be experienced in the early daylight hours. The calculated thermal gradient was imposed in the thickness direction of the quad4 plate elements used to model the slab.

Figs. 33 and 34 give the results of the computer analysis of this situation. The thermal expansion on the top of the slab places the bottom fibers of the slab in tension. It can be seen that both the lateral and longitudinal tensile stresses in the bottom of the slab are uniform across the section of slab between the concrete and steel girders, the lateral stress being about 100 psi and the longitudinal stress being about 70 psi. The stress in the longitudinal direction is less because the girders tend to restrain the expansion of the slab.

Sunshine on the top of the slab will cause small compressive stresses in the bottom fibers of the concrete girders.

It would appear from examining the graphs that the stresses caused by sunshine are not affected by the mixed girder configuration. However, these stresses do appear to be significant. In the lateral direction, the stress caused by sunshine is approximately 25% of the modulus of rupture and in the longitudinal direction the stress is approximately 20% of the modulus of rupture as given in the AASHTO specifications.

All of the computer results presented in this section are for the uncracked slab configuration and design concrete properties.

4.4 Live Load Distribution

The longitudinal moments in the girders at mid-span and the lateral moments in the section of slab between the steel and concrete girders caused by live loads were investigated.

Three different live load configurations were considered for determining the moments in the girders: a single AASHTO HS20-44 truck, dual lane AASHTO HS20-44 trucks and the 220k overload truck crane (OTC). Two different live load configurations were considered for determining the moments in the slab: a single AASHTO HS20-44 truck and the OTC. Since the maximum slab moments are primarily dependent on the tire print, it is not considered necessary to consider both the single and dual lane configurations for slab moment calculations.

For determining moments in the girders, the loads were centered on the span, as shown on Fig. 35, and for determining moments in the slab, the loads were placed with one wheel set at center span, as shown in Fig. 36. There are no significant differences in the girder moments caused by the two configurations, except as discussed below.

In order to facilitate use of the symmetrical computer model, certain wheel loads which would have negligible effect were omitted. For the case of finding moments in the

girders, the load due to the front wheels of the HS20-44 tractor truck were assumed to be negligible, because they are located very nearly over the support points. For the case of finding the moments in the slab, some loads were neglected for the basic investigation. The effect of this assumption was investigated and is discussed later.

For the case of calculating the moments in the slab due to the 220 k OTC, the load caused by all three opposite end axles was neglected. Two axles are off the span under consideration and the third axle is very near the support points.

The basic NASTRAN data deck for the Bonnabel Overpass with certain modifications, was used for this investigation. The only significant modification was to change the grid spacing in the longitudinal direction (x-coordinate) so that the vehicle axles were directly over the line of grid points.

Design properties of the concrete were used in the live-load investigation, except for a few runs made specific-ally to determine the effect of the concrete properties. Design concrete strengths were taken as 3000 psi for the slab and 5000 psi for the prestressed girders. Using the AASHTO equation, the corresponding values for Young's Modulus are 3.3×10^6 psi for the slab and 4.3×10^6 psi for the prestressed girders.

Two sets of computer runs were made for the purpose of investigating the effect of concrete properties. For these

runs concrete strengths more representative of those found in the field were used. Strengths of 6,800 psi for the slab and 8,500 psi for the prestressed girders were assumed, yielding values of Young's modulus of 5.0×10^6 psi for the slab and 5.6×10^6 psi for the prestressed girders. Poisson's ratio was assumed to be 0.15 in all cases.

4.4.1 Girder Moments HS20-44 Truck

Computer runs were made simulating the placing of a single HS20-44 truck at several different positions laterally across the span in the vicinity of the interface between the concrete and steel girders. All runs were made with the truck trailer centered on the span longitudinally, as illustrated on Figure 36. The longitudinal grid spacing was selected such that the wheel sets of the trailer would be over the line of the grid points. Further, in positioning the truck in the lateral direction, positions were chosen such that the wheel located between the concrete and steel girders would be directly over a grid point. For plate type elements point loads can be placed only at grid points; thus, for those cases where the wheel did not fall over a grid point, the wheel load was distributed to adjacent grid points assuming a linear distribution. The results of the computer study for the single HS20-44 truck are shown by the graphs of Figs. 37 and 38. These graphs show plots of the moment in the composite girders at mid-span as a function of position of a single HS20-44 truck

across the span. Results are shown for both design concrete properties and field measured concrete properties. An uncracked slab is assumed for both cases.

The magnitude of the moment at mid-span acting on the composite girder is a function of the vertical location of the lateral axis about which moments are taken. This is because there are longitudinal axial stresses in the girders caused by the interaction between girders. The moments in the girders as given herein are the moments about the neutral axis of each girder, calculated by assuming the composite section to be made up of the girder and the portion of the slab out to the mid-point between the adjacent girder on either side. The vertical location of the neutral axes will thus vary with type girder and with concrete properties. The moments for girders G-2 through G-5 are shown. These are the two concrete and two steel girders adjacent to the concrete-steel girder interface. Note that girder G-3, which is the concrete girder closest to the steel girders, carries approximately 12% more load than girder G-2.

On the other hand, the stiffer concrete girder tends to protect the nearest steel girder G-4. Girder G-4 carries about 20% less load than girder G-5. It is interesting to note that the maximum moment in steel girder G-5 is approximately the same as that in concrete girder G-2, even though the spacing of the steel girders is approximately 16% greater than that of the concrete girders.

A series of computer runs was made with two HS20-44 trucks side-by-side, simulating dual lane loading. The two trucks had a center-to-center spacing of 10 feet. As in the case of the single HS20-44 truck, the dual trucks were positioned at several different lateral locations in the vicinity of the interface between the concrete and steel girders. All computer runs were made with the truck trailers centered on the span longitudinally, as illustrated on Fig. 35.

Comments given in the previous discussion relative to load distribution at grid points and the neutral axes for girder moments are also applicable for this discussion.

The results of the study for the dual lane loading are given on the graphs of Figs. 39, 40 and 41. These graphs show plots of the moment in the composite girders at mid-span as a function of lateral position of the HS20-44 trucks. Results are shown for three concrete configurations: design concrete properties and uncracked slab, field concrete properties and uncracked slab, and field concrete properties and cracked slab. It can be seen that the maximum moment in girder G-3 exceeds the AASHTO design specification value in all cases, by approximately 28%, 35% and 45% respectively for the three concrete configurations given.

The results show that for dual lane loading the moment in girder G-2 also exceeds the AASHTO design value by a

significant amount. It appears that this girder is experiencing edge or end effects.

The data shows that the concrete girder protects the adjacent steel girder, G-4, causing it to carry much less than its share of the load.

4.4.2 Girder Moments - 220 k OTC:

Computer runs were made simulating placing of a 220 k OTC at several different positions laterally across the span in the vicinity of the interface between the concrete and steel girders. All runs were made with the OTC centered or straddling mid-span in the longitudinal direction, as indicated on Fig. 35. The OTC has three wheel sets or axles on both the front and rear and the longitudinal grid spacing was again selected so that each axle of the vehicle would be over a line of grid points. The OTC has a transverse wheel spacing of 10 ft, which means that when the wheels along one side are positioned over the region between the concrete and steel girders, the wheels on the other side may be outside the fine grid region and consequently these wheels may not be over a line of grid points. In this case a linear distribution was used to distribute the load to the neighboring grid points.

The results of the computer study are shown by the graphs of Figs. 42 and 43. The graphs show moments in the composite girders at mid-span as a function of position of the 220 k OTC centerline across the span. Results are shown

for design concrete properties and for field measured concrete properties. An uncracked slab is assumed in both cases. It can be seen that girder G-3, the concrete girder next to the steel girders, carries about 10% to 15% more load than the adjacent concrete girder G-2.

Also it can be seen that the concrete girder again protects the nearest steel girder, G-4, causing girder G-4 to carry about 25% less load than G-5.

4.4.3 Slab Moments - HS20-44 Truck:

Computer runs were made to investigate the moments in the section of the slab between the concrete and steel girders caused by a single HS20-44 truck load. The output was limited to the moments along mid-span. The truck was positioned longitudinally, with one wheel set over mid-span, as shown on Fig. 36, and was positioned at several locations across the span.

For cases involving the determination of slab moments, it was decided that the load of the wheel on the section of slab between the concrete and steel girders would be modeled using a uniform pressure load. The longitudinal grid spacing was thus selected so that the plate elements along mid-span would be approximately the size of the tire contact area given in the AASHTO specification. The details of a typical loading case are shown by Fig. 44. It will be noted that two additional lines of longitudinal grid points have been included so as to better define the moment curves.

Four runs were made to investigate the effect of neglecting the remaining wheels of the tractor-trailer configuration. The worst configuration was assumed to be the case where the rear wheels of the tractor are over mid-span, the front wheels of the tractor are 14 feet ahead of mid-span, and the rear wheels of the trailer are 14 feet before mid-span. Since the computer model required symmetrical loading, the above configuration was approximated by averaging the 4 k front wheel load of the tractor and the 16 k rear wheel load of the trailer and placing 10 k at each wheel location to either side of mid-span. This case could then be simulated by the symmetrical computer model by placing 10 k at the location of the front wheels, as they are shown on Fig. 36. The results of the computer study relative to moments in the slab caused by the HS20-44 truck load are shown by the graphs of Figs. 45 and 46. The significant output from the NASTRAN computer program for this situation is stress in the slab top and bottom fibers. Flexural theory was used to convert these stresses to equivalent moments per unit width assuming design concrete properties and a full depth uncracked slab.

Fig. 45 shows how the moment varies across the section of slab between the concrete and steel girders for several representative loading positions. The maximum lateral moment resulting from each loading position was determined graphically and cross plotted to obtain the graph of Fig. 46.

This second graph shows the maximum moment as a function of the position of the truck wheel across the slab.

It can be noted that the presence of the additional wheel loads 14 feet forward and aft of the mid-span wheel load increases the moment in the slab by approximately 5%.

The maximum moment in the slab is seen to be very near 3400 ft-lb/ft, which would be the design value based on the AASHTO specifications. This would indicate that the present slab design criteria, as given in Section 3.24.3.1 of the 1985 AASHTO specifications, are adequate for spans similar to the Bonnabel Overpass when loaded with an HS20-44 truck.

4.4.4 Slab Moments - 220 k OTC:

Computer runs were made to investigate the moments in the section of slab between the concrete and steel girders caused by the 220 k OTC. The OTC was positioned longitudinally with the center axle of one of the three-axle sets over mid-span and was positioned at several locations laterally across the span.

The load of the wheel which is located at mid-span and on the section of slab between the concrete and steel girders was again modeled using a uniform pressure load. The details of this loading were described in the previous section.

All loads due to the wheels on the opposite end of the OTC were neglected, because two axles are off the span under

investigation and the third is approximately over the supports.

The results of the computer study relative to the moments in the slab caused by the 220 k OTC is shown by the graphs of Figs. 47 and 48. As described earlier, the moments were obtained from stress data output.

Fig. 47 shows how the moment varies across the section of slab between the concrete and steel girders for two representative loading positions. The remaining loading position data were omitted to avoid confusion. The maximum moment resulting from each loading position was determined graphically and cross plotted to obtain the graph of Fig. 48. This graph shows the maximum moment as a function of the position of the OTC wheel across the slab.

It can be seen that the maximum moment in the slab is approximately 4700 ft-lb/ft, and it occurs when the wheels on the opposite side are over the concrete girders. The value of 4700 ft-lb/ft is approximately 40% higher than the value obtained using the AASHTO criteria.

4.5 Concrete Diaphragms

A series of computer runs was made in order to determine the effect on girder moments and slab stresses of adding diaphragms between the concrete girders and between the concrete and steel girders. Two configurations for diaphragm locations were considered. These were placing diaphragms at the third spans and placing diaphragms at the

mid-spans. The existing Bonnabel Overpass and the basic computer model have diaphragms at the third span between the steel girders.

The designs of the diaphraghms used are shown on Fig.49. Between the concrete girders, a cast reinforced concrete diaphragm is used. The diaphragm is attached to the girders by means of a 1" diameter tie rod. Between the concrete and steel girders, a C15 x 33 steel channel diaphragm is used. On the concrete girder end, the channel is bolted to a steel angle bracket, which is in turn bolted to the concrete girder. On the steel girder end, the channel is bolted to a steel plate, which has been welded to the steel girder.

In order to obtain an estimate of the end fixity conditions which should be used to represent the actual field situation, a uniform moment along the diaphragm was assumed. For this situation it is estimated that the angular rotation at each end resulting from the type end connection is in the order of four times the angular deflection that occurs along the remainder of the diaphragm. It is thus deduced that the effective stiffness of the diaphragms is at most one fourth of the stiffness of a rigid end diaphragm. For the steel diaphragms the rotation could be much higher if the bolts slide in the slotted bolt holes. Sliding of the bolts in the bolt holes is not considered in the analysis. Computer runs were made for three different diaphragm end connection configurations and for no diaphragms. The three end connection configurations

represent a very rigid condition, a very flexible condition and an intermediate condition. The intermediate condition is believed to approximate the actual situation. The computer inputs for the three configurations were, respectively, diaphragms with full section moments of inertia and rigid end connections, diaphragms with full section moments of inertia and pinned end conditions, and diaphragms with one quarter of the full section moment of inertia and rigid end connections.

The effects of adding the diaphragms on the maximum moments in girder G-3 are shown by Figs. 50 and 51. It can be seen that as the load is positioned at various locations across the span, there will be a maximum moment value for each diaphragm configuration. It can be seen that the effect of the increasing diaphragm stiffness is to reduce the maximum moment in the girder. If the diaphragm could be installed with perfectly rigid end connections, the maximum moment would be reduced by 10%-12%; however, under actual end fixity conditions the reduction is believed to be less than 10% and may be as low as 5%.

It can be observed that from the standpoint of reducing the moments in girder G-3, one diaphragm at midspan is just as effective as two diaphragms located one at each third span point.

It was found that the diaphragms have even less effect on the slab stresses. This can be seen in Fig. 52, which shows that the maximum stress in the slab is reduced about

8% by diaphragms with perfectly rigid end connections but is only reduced about 4% for the case believed to represent the actual end conditions.

4.6 Rolled Beams with Cover Plates

The computer input data deck representing the Bonnabel Overpass was modified so that all steel beams would be rolled beams with welded coverplates. The rolled beam used was a W 24 x 62 with a section major moment of inertia of 1540 in^4 and a section cross section area of 18.0 in^2. The coverplate was 1/2" x 9" plate.

The span was loaded using the 220 k overload truck crane (OTC), assuming 18.3 k per wheel. The vehicle was centered longitudinally over mid-span. Three lateral loading positions were considered; these being the vehicle centered over (straddling) girder G-6, the vehicle centered between girders G-5 and G-6, and the north wheels of the vehicle directly over girder G-6. Although the differences were small, the case where the vehicle is centered over the girder gave the maximum stresses in the bottom fibers of the girder, and this is the case presented.

Fig. 53 shows a typical curve of stress distribution in the bottom fibers along the length of the girder. The magnitude of the stress along the center portion of the girder is approximately constant and independent of the overall length of the coverplate. At each end of the

coverplate there will be a step increase in stress as shown on the graph.

Computer runs were made for a range of coverplate lengths. Fig. 54 shows how the peak stress at the end of the coverplate varies with coverplate length. It will be noted that for the case of the Bonnabel Overpass symmetrically loaded with the 220 k OTC, the coverplates must be almost 400 inches long (75% of total length) before the stress level at the end of the coverplate drops below the value at mid-span.

Fig. 55 shows the moment distribution along the composite section made up of the steel girder and the associated strip of the concrete slab. The moments acting on this composite section are not values which can be obtained as a direct output from the NASTRAN computer program. To obtain these moments it is necessary to define a composite section and determine a neutral axis location in the traditional manner. The stress data output from the computer can then be used to "work backwards" to obtain the moment distribution for the composite section.

On the stress and moment curves of Figs. 53 and 55 there are two values for each location (some are coincident). This is because the computer model for the girder is made up of a number of bar elements and the NASTRAN program gives output stresses for each end of each bar. Thus for each location where two bar elements attach to a single grid point, two stress values are given.

4.7 Non-Composite Rolled Beams

In this investigation the NASTRAN input data deck for the Bonnabel Overpass is modified so that all steel girders are replaced with non-composite rolled beams. The purpose of this investigation is to determine if camber growth in the concrete girders will cause the slab to separate from the non-composite steel girders. The beams are W27 x 146 with a section major moment of inertia of 5430 in^4 and a cross-section area of 42.7 in^2.

The non-composite configuration is modeled by using a double row of GRID points along each steel girder, one row being attached to the slab and the other row being attached to the girders. Corresponding grid points between the slab and girders are connected using a rigid RBAR element. This element can be programmed so that the grid points are rigidly connected in the vertical direction but are free to move relative to each other in the lateral and longitudinal direction and in the three rotational directions. (MSC has developed a non-linear element called CGAP which allows modeling of surfaces which may come into contact. Documentation was not available on this element in time for it to be used on this project).

The modified model is loaded to simulate camber growth by the same method used in Section 4.2. Fig. 56 shows the vertical deflection of the slab at mid-span caused by camber growth. Curves are shown on the graph for camber growths of 1/4 inch and 3/8 inch. Also shown on the graph is a

dotted line indicating the relative position the slab over the steel girders would have prior to the slab being poured. This line represents the fact that steel girders will deflect downward approximately 0.3 inches when the slab is poured. Thus the slab over the steel girders must be raised by that amount before the slab loses contact with the non-composite girders.

It can be seen from the graph that a camber growth of 3/8 inch will cause the slab in the vicinity of G-4 to raise up by only about 0.2 inches; thus the slab will not lose contact with the non-composite steel girder. It appears that a camber growth of approximately 5/8 inch would be required before the slab lifted off the adjacent non-composite girder.

5.8 Bearing Movement Effects

The original Bonnabel Overpass was constructed using self-lubricated bronze bearing shoes to support the steel girders. These shoes allow sliding motion in the longitudinal direction, rocking motion about the lateral axes and are inelastic in the vertical direction. When the Bonnabel Overpass was widened, neoprene pads were used to support the prestressed concrete girders. These pads, compared to the bronze shoes, are considered to be less rigid in the vertical direction and to impose higher loads on the supporting structure in the longitudinal direction.

The purpose of this section is to investigate some of the consequences of using the neoprene pads.

As was discussed in Section 3.5, a new neoprene pad representative of those used in the Bonnabel Overpass widening was tested in compression. The elastic constant in the vertical direction for this new pad was found to be 0.5 x 10^6 lb/in. Also, the new pad has an uncompressed thickness of 1.1 inches. The dead load on each of these pads when in service is approximately 23,000 pounds, which would cause a compression of about 0.05 inches, so that the thickness of the pads under load would be about 1.05 inches. It was found, however, that the neoprene pads which were installed at the time of the widening are presently about 0.9 inches in thickness, indicating that these pads have experienced considerable creep and consolidation.

Examination of the load test data of sections 2.2 and 2.3 show that both the supports for the steel girders and the supports for the concrete girders are deflecting vertically under load. Elastic constants were deduced from these results to be used in the computer comparison of Sections 3.2 and 3.3. The values used were 1.4 x 10^6 pounds per inch for the steel girder supports and 1.0 x 10^6 pounds per inch for the concrete girder supports. It is noted that the elastic constant of 1.0 x 10^6 pounds per inch for the concrete girder supports includes the effect of both the soil elasticity and the neoprene pad elasticity, and yet it is still twice the elastic constant of a new neoprene pad.

This indicates that the elastic constants of the in-place pads have increased several fold.

One of the most severe consequences of having used the neoprene pads would result from the more than 0.1 inches consolidation of the pad. Assuming the bent caps did not move vertically, this would mean the concrete girders have moved vertically with respect to the steel girders and would thus place a significant bending load on the slab. This load would be the greatest at the end of the span. A computer analysis was made to investigate the effect of this bending. Fig. 57 shows the computed lateral stress in the top and bottom fibers of the slab at the end of the span due to imposing a 0.1 inch vertical displacement downward on girders G-1, G-2 and G-3. It can be seen that the tension stresses in both the top and bottom of the slab are large and are nearing the magnitude which would cause cracks, even without the effect of any other loading.

The computer program was also used to investigate the longitudinal forces on the bent caps caused by thermal contraction and expansion of the span superstructure. The magnitude of these forces are directly dependent on the amount of relative movement of the bent caps and the shear modulus of the neoprene pad. The results of Section 3.4 show that the distance between adjacent bent caps is very nearly constant and the span remains centered between the caps. Thus for this analysis it can be assumed that the neoprene pad supports are fixed.

As discussed above, the elastic constant of the in-place pads appears to have increased several fold, and thus Young's modulus would be much larger than the value for virgin neoprene. This means that the shear modulus has also increased several fold.

In this investigation the properties of new neoprene are used to obtain a base value for the longitudinal forces on the bent caps. Runs were made for $+40^{\circ}F$ and $-40^{\circ}F$ temperature change of the entire span superstructure. It was found that a temperature change of $40^{\circ}F$ causes a longitudinal force of 10,000 pounds at each neoprene pad. The resulting stresses in the bottom fibers of the concrete girders would be 30 psi tension for a $40^{\circ}F$ temperature decrease and 30 psi compression for a $40^{\circ}F$ temperature increase.

Again, these are the forces and stresses assuming virgin neoprene properties. The longitudinal force and stress would be approximately proportional to the shear modulus, thus it is believed that the actual values would be several times the value given above.

It is suspected that the neoprene pads are not performing as intended. The pads have consolidated significantly, possibly causing cracking of the slab near the ends of the span and the pads may have become more or less inelastic, causing abnormally high longitudinal forces on the bent caps.

4.9 Combined Effects

In this section the effects on girder moments and slab stresses of combined loading are considered. The loads used consist of linear combinations of the individual loads as appropriate, which are discussed in earlier sections of this chapter. It is not the intent of this section that all combinations be studied nor that the maximum moments and stresses due to combined loading be determined, but rather to present representative combinations to indicate whether or not problem areas may exist.

The loading situations which the computer solutions indicate as having large effects on girder moments are live loads and camber growth. Neoprene pad consolidation has a lesser effect on girder moments. Computer solutions were obtained for the moments at mid-span due to these combined loads using the Bonnabel Overpass Model, with an uncracked slab configuration and design concrete properties. Girder moments were determined for two combined loading situations: for dual HS20-44 trucks liveload and 1/4" camber growth; and for dual HS20-44 trucks live load, 1/4" camber growth and -0.1" neoprene pad consolidation.

As was discussed in section 4.2, three dimensional and thermal effects make it necessary to further define the meaning of the moment in the composite girder. The term "moment in girder" as used in this section means the equivalent moment which would produce the same stress in the bottom fibers of the girders.

The computer results for the two load cases described above are shown on Fig. 58. The moments at mid-span in girders G-2 through G-5 are plotted versus the lateral position of the dual HS20-44 trucks centerline. It can be seen that the moment in girder G-3, the concrete girder adjacent to the steel girders, is very large, being approximately twice the AASHTO design value given by S/5.5. Note that these moment values do not include the effect of the initial weight of the slab but only the effect of live load, camber growth and pad consolidation.

It can be seen from the graph that the effect on girder moment of neoprene pad consolidation is relatively small and only affects girders G-3 and G-4. Pad consolidation causes a slight decrease in the maximum moment in G-3 and a slight increase in G-4. It will also be observed that the moment in G-4 is negative for some loading situations and reaches a maximum value of only one third of the design value, even when the dual HS20-44 trucks are directly over that girder.

As was discussed in Section 4.2, no correction is made for the effect on camber growth of the added dead weight caused by camber growth. Nevertheless, the computer solution indicates that a combination of live loads and camber growth could cause serious overloading in the adjacent concrete girder for mixed girder configurations.

A series of computer runs was made to determine the effect on slab tensile stresses of a combination of all those loads believed to be significant. The loads which

cause tensile stresses in the bottom fibers of the slab are live load, sunshine on the slab, camber growth, neoprene pad consolidation, and expansion of the steel girders due to temperature increase. All of these loads were input into the computer and an output was obtained which combines dual HS20-44 live load, 3 hours of sunshine, 1/4" camber growth, -0.1" neoprene pad consolidation and 30^{o}F temperature increase of steel girders. The results of these computer runs for one HS20-44 loading position are shown in Figs. 59 and 60. Fig. 59 shows the lateral stress in the bottom fibers of the slab along the mid-span, and Fig. 60 shows the longitudinal stress in the bottom fibers of the slab along mid-span. It can be observed that at a location underneath the tire print, the tensile stress in the lateral direction exceeds the AASHTO specified value for modulus of rupture for plain concrete.

The tension stresses discussed above are caused primarily by live load and sunshine and are thus not unique to the mixed girder situation. The sunshine loading situation used herein assumes a rather modest heat input rate, and it is believed probable that conditions conducive to causing cracking of the bottom of the slab frequently occur over the entire span. This belief is corroborated by the comparison of computer predictions with field test results, as discussed in Sections 3.2 and 3.3.

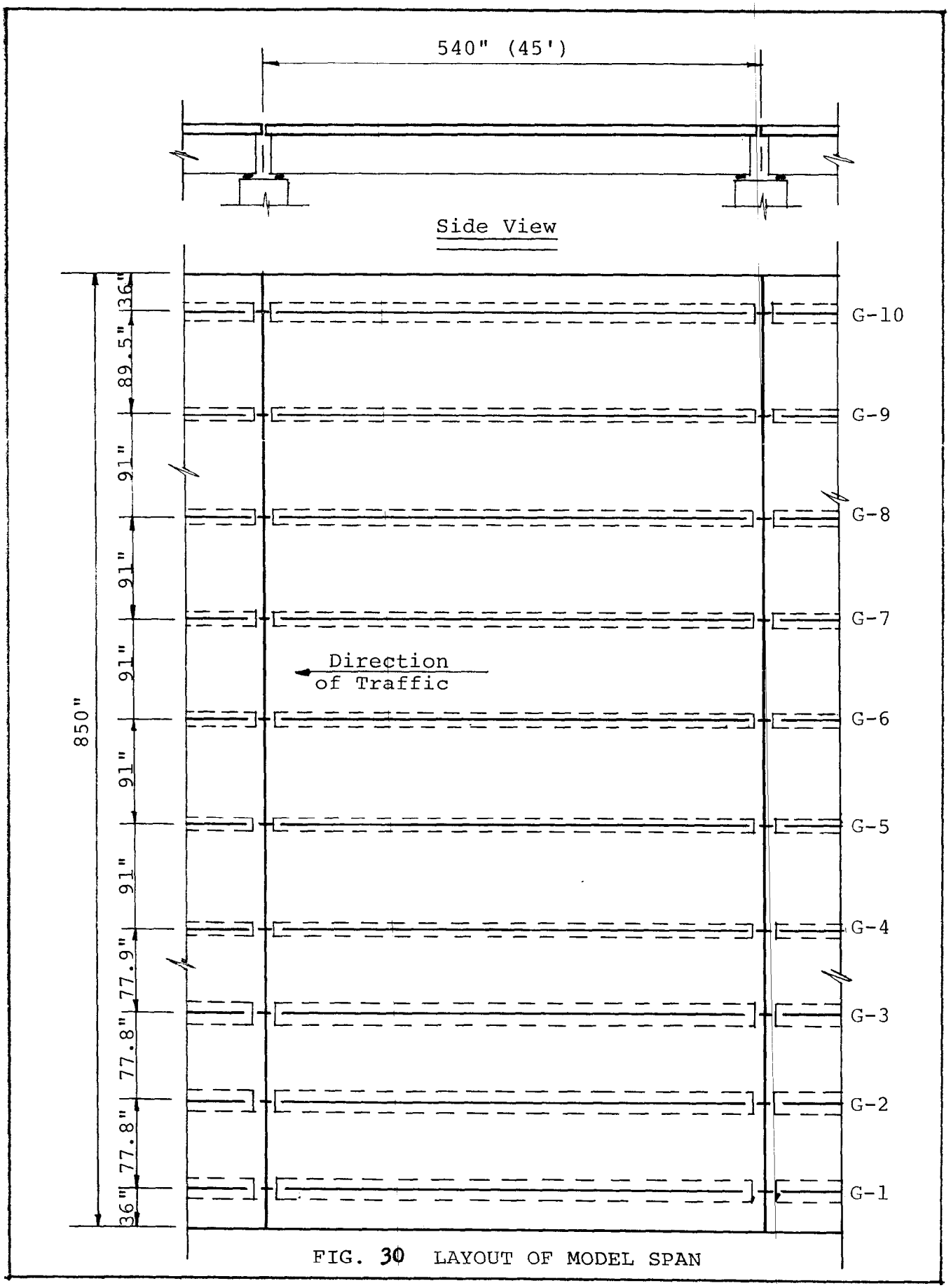

FIG. 30 LAYOUT OF MODEL SPAN

Note: See Section 4.2 for definition of moment as plotted on this figure.

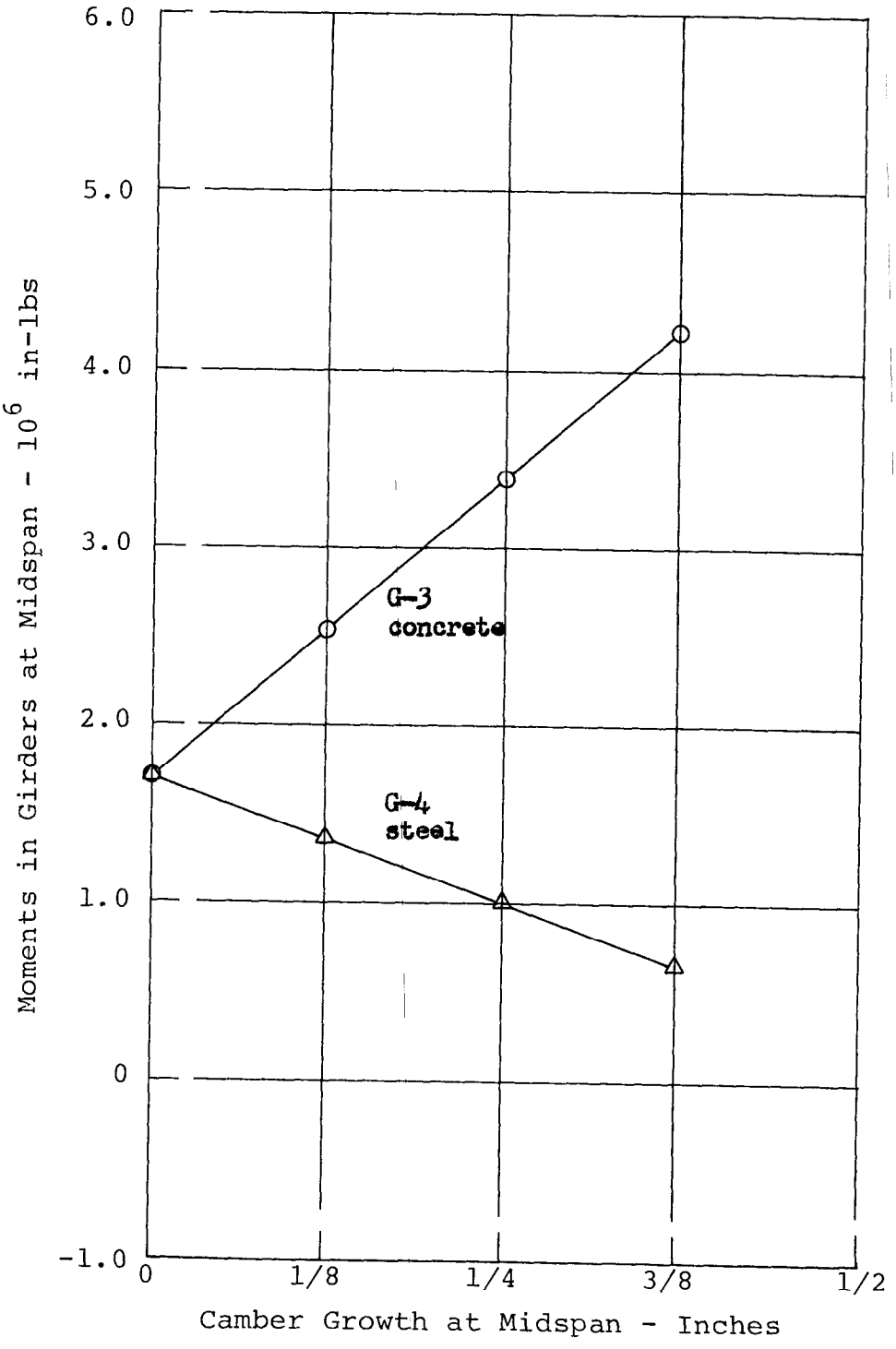

FIG. 31 EFFECT OF CAMBER GROWTH ON MOMENT AT MIDSPAN IN ADJACENT CONCRETE AND STEEL COMPOSITE GIRDERS

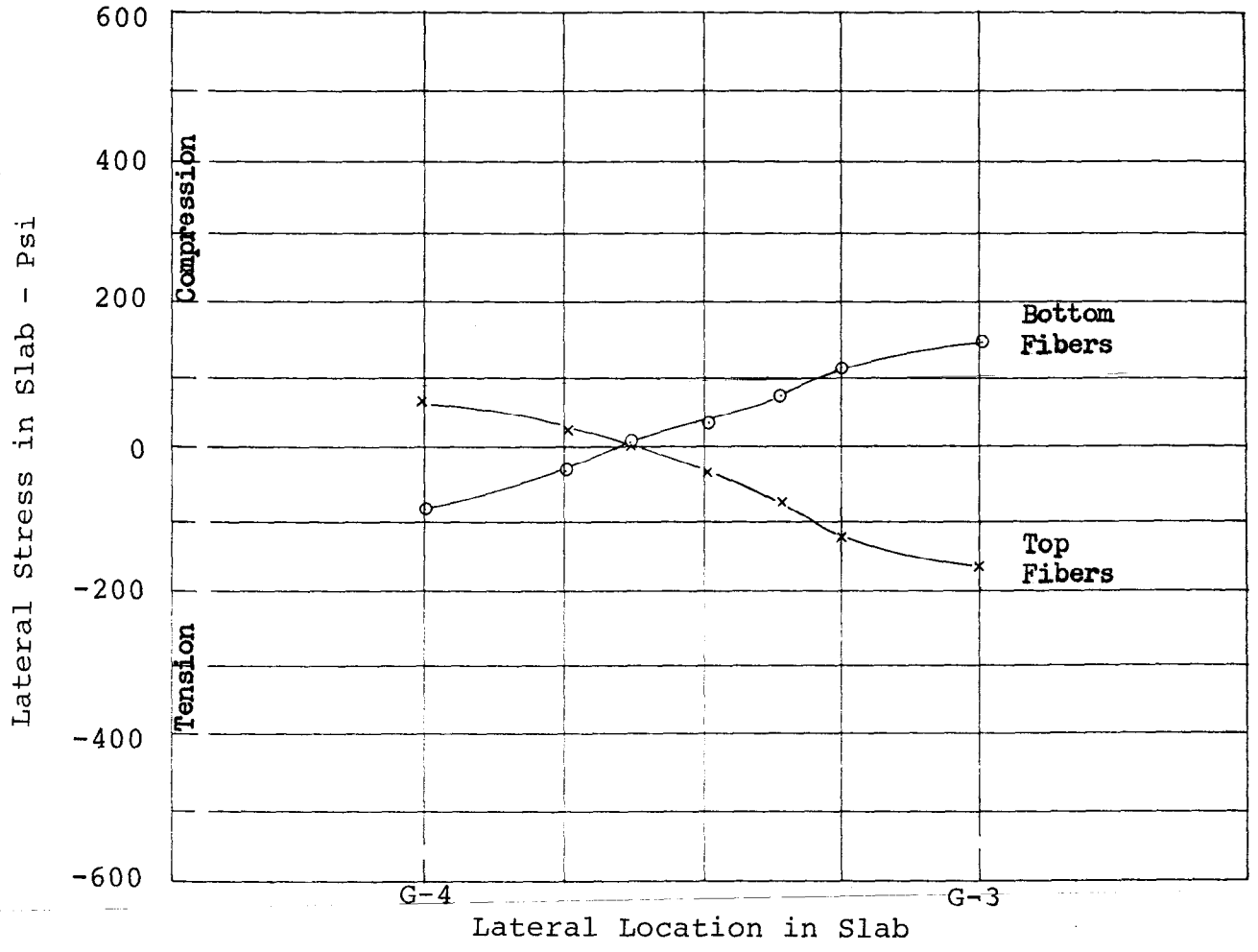

FIG. 32 LATERAL STRESS IN TOP AND BOTTOM FIBERS OF SLAB AT MIDSPAN DUE TO 1/4 IN. CAMBER GROWTH

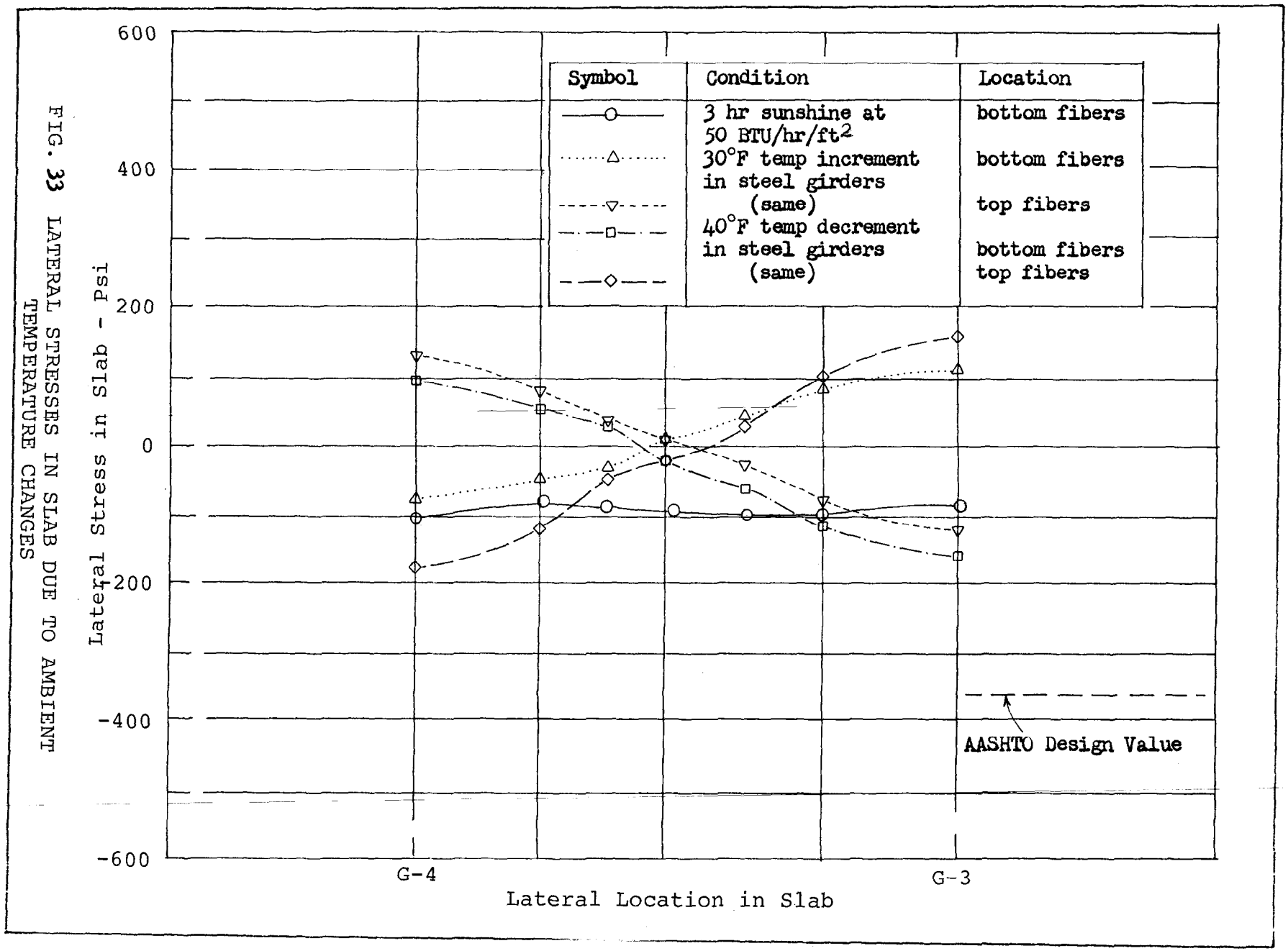

FIG. 33 LATERAL STRESSES IN SLAB DUE TO AMBIENT TEMPERATURE CHANGES

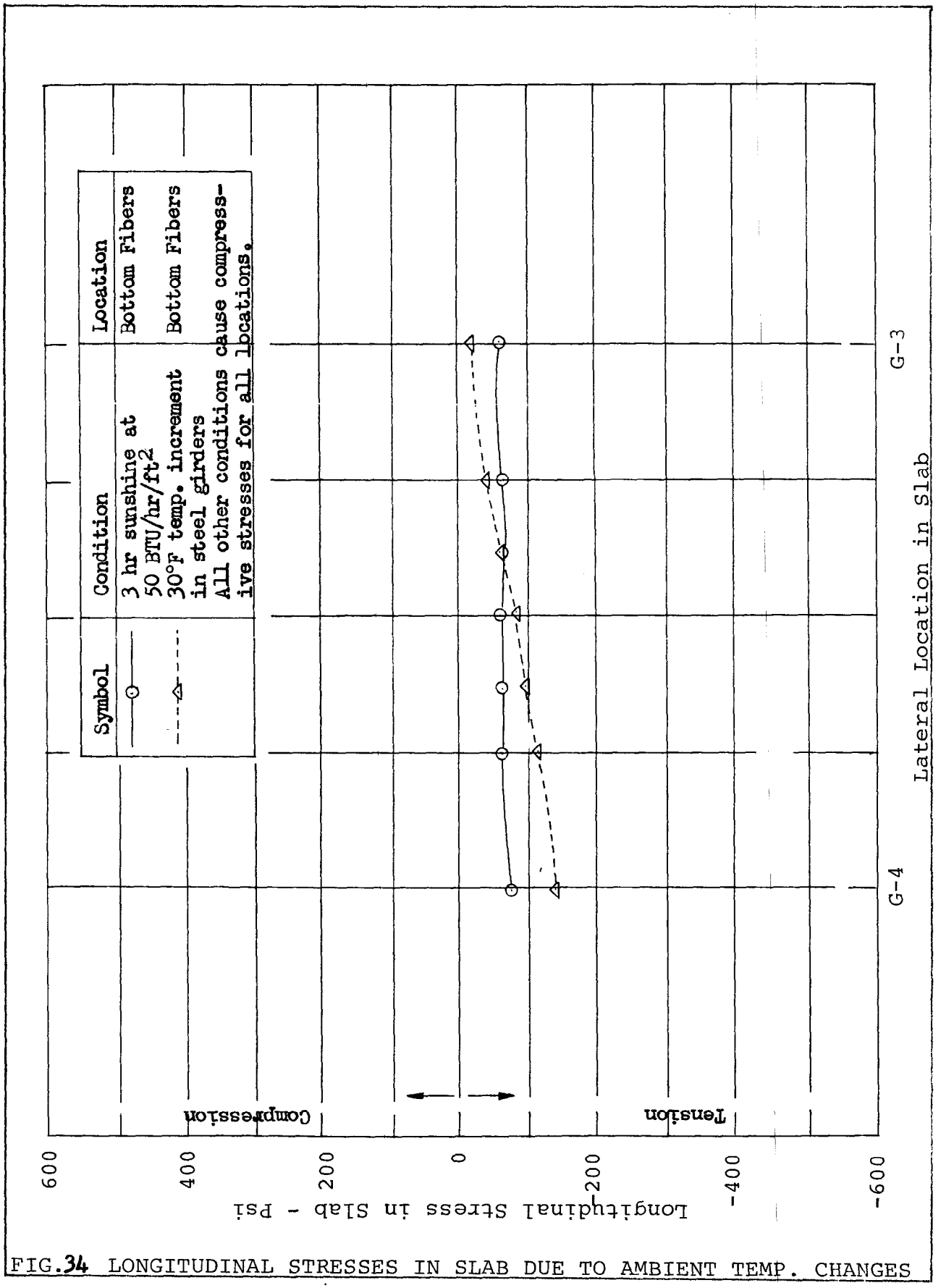

FIG.34 LONGITUDINAL STRESSES IN SLAB DUE TO AMBIENT TEMP. CHANGES

Note: There is no significant difference in the maximum girder moment caused by the load configuration shown on this figure, and that shown on Fig. 36.

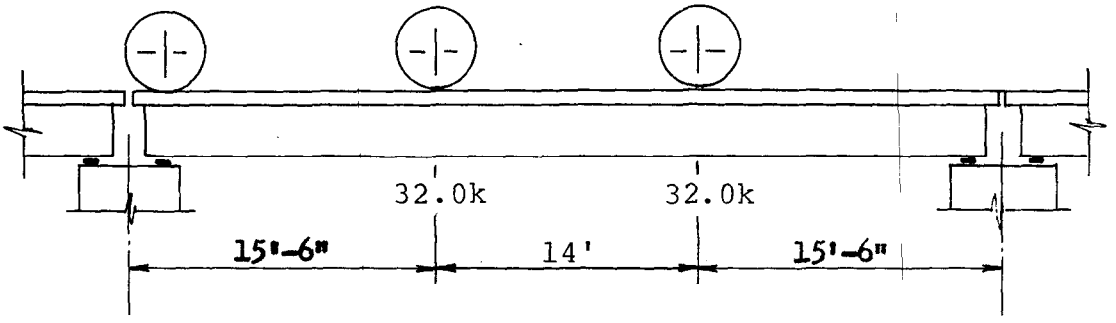

(1) HS20-44 Truck

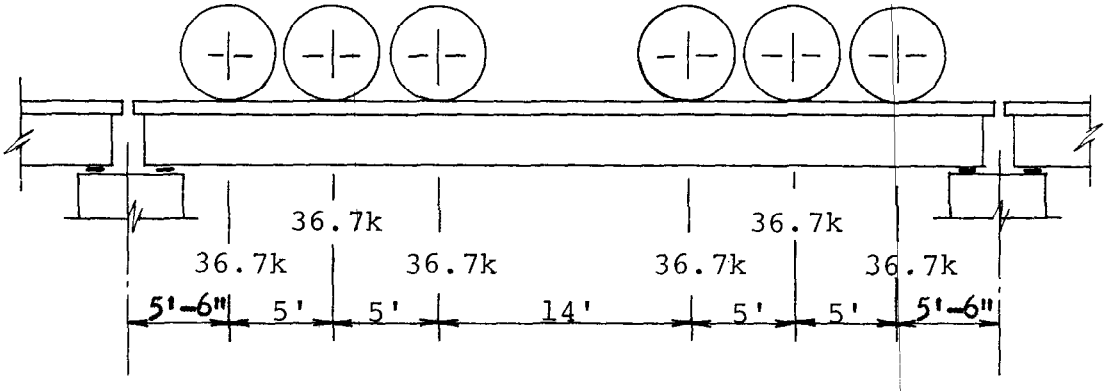

(2) 220k Overload Truck Crane

FIG. 35 LIVE LOAD LOCATION FOR DETERMINING LONGITUDINAL MOMENT IN GIRDERS

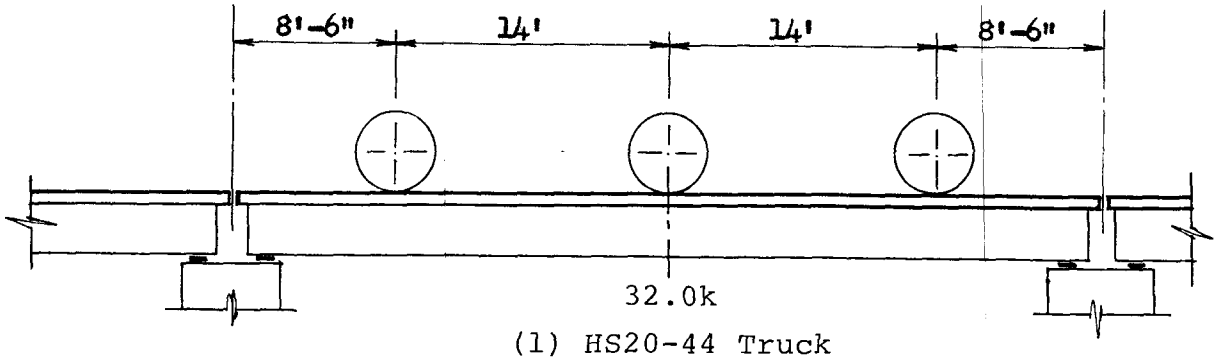

(1) HS20-44 Truck

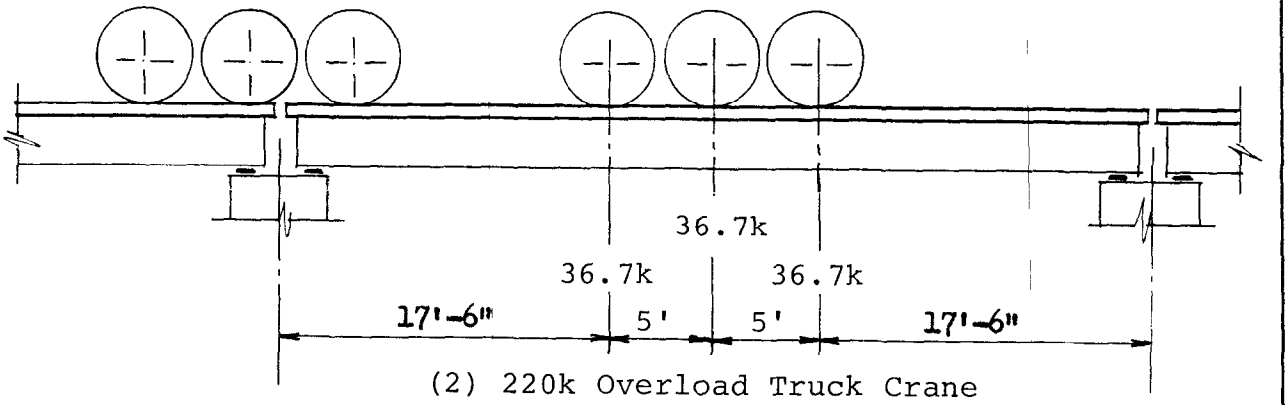

(2) 220k Overload Truck Crane

FIG. 36 LIVE LOAD LOCATION FOR DETERMINING LATERAL MOMENT IN SLAB

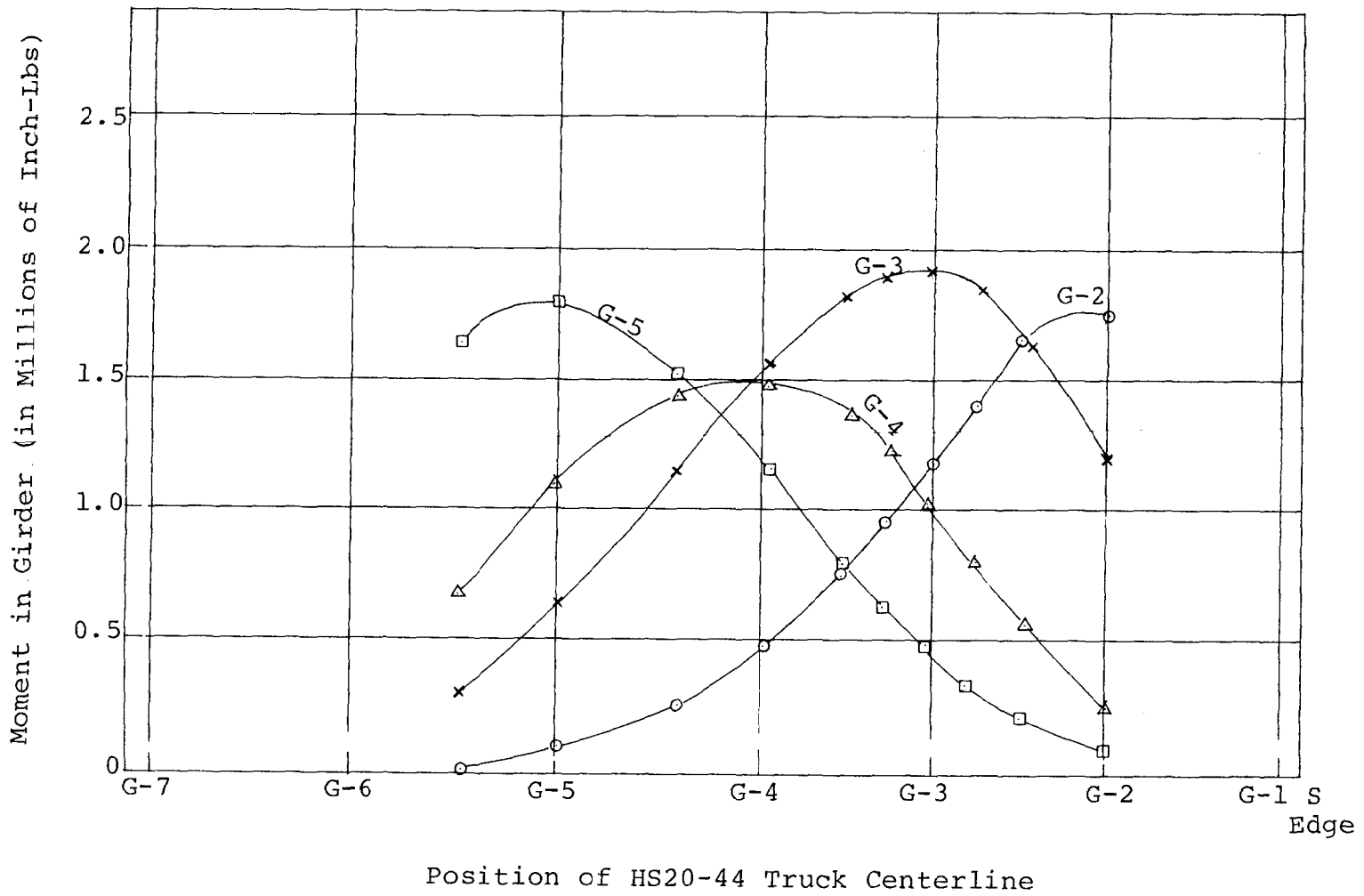

FIG. 37 MOMENT IN GIRDERS AT MIDSPAN DUE TO HS20-44 TRUCK LOAD - DESIGN CONCRETE PROPERTIES
- UNCRACKED SLAB

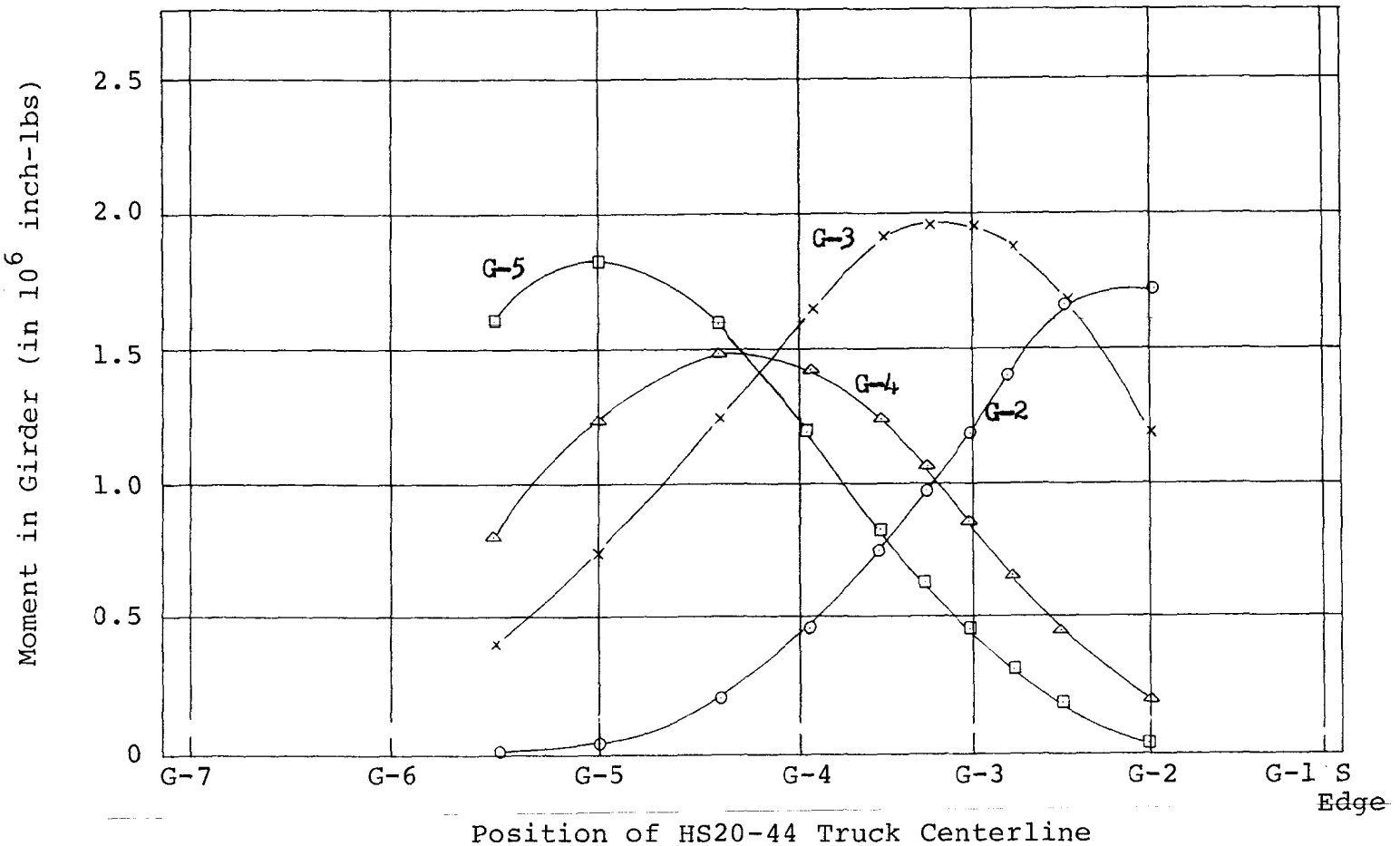

FIG. 38 MOMENT IN GIRDERS AT MIDSPAN DUE TO HS20-44 TRUCK LOAD - FIELD CONCRETE PROPERTIES - UNCRACKED SLAB

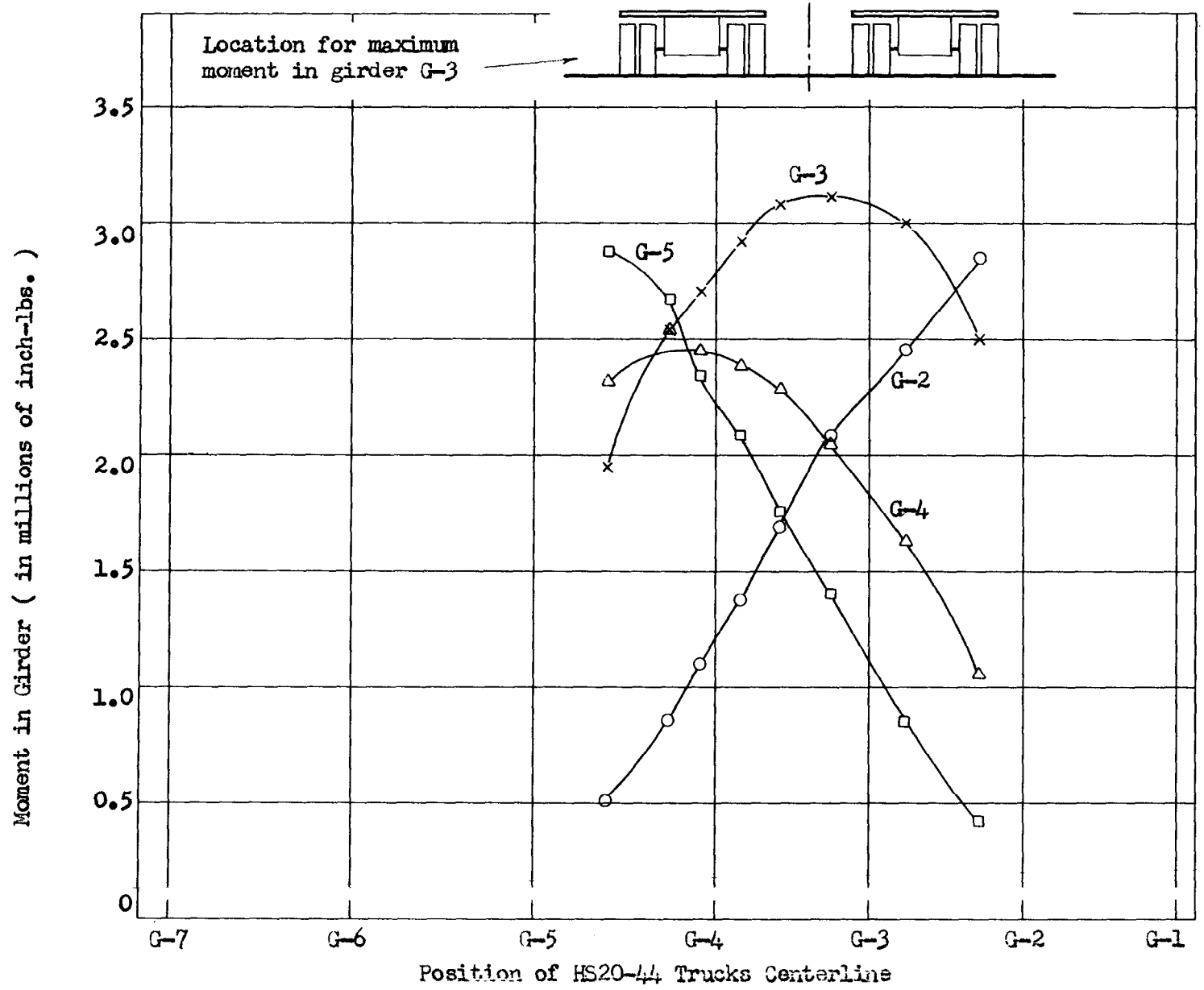

FIG. 39 MOMENT IN GIRDERS AT MIDSPAN DUE TO TWO HS20-44 TRUCKS SIDE BY SIDE - DESIGN CONCRETE PROPERTIES UNCRACKED SLAB

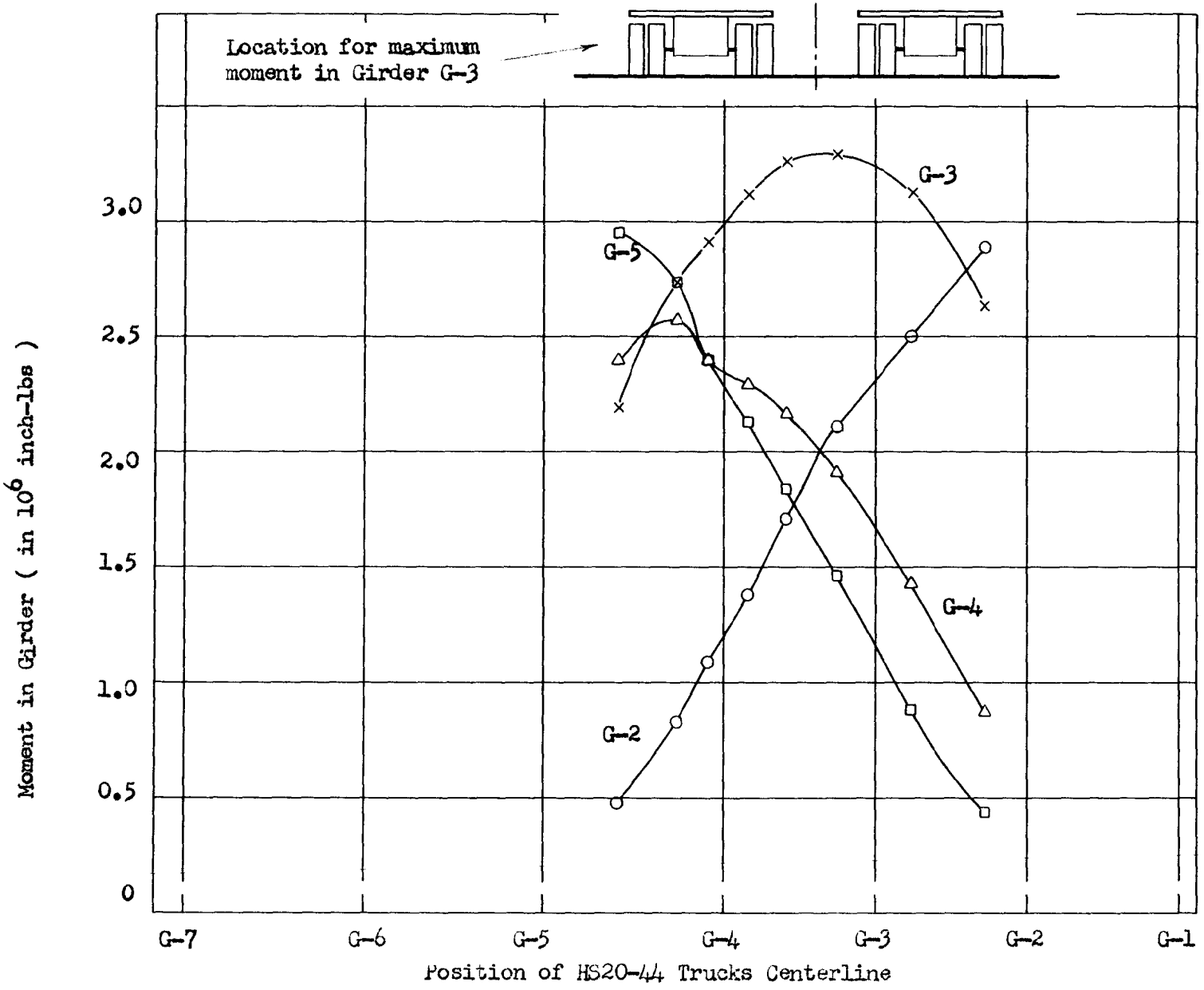

FIG. 40 MOMENT IN GIRDERS AT MIDSPAN DUE TO TWO HS20-44 TRUCKS SIDE BY SIDE - FIELD CONCRETE PROPERTIES UNCRACKED SLAB

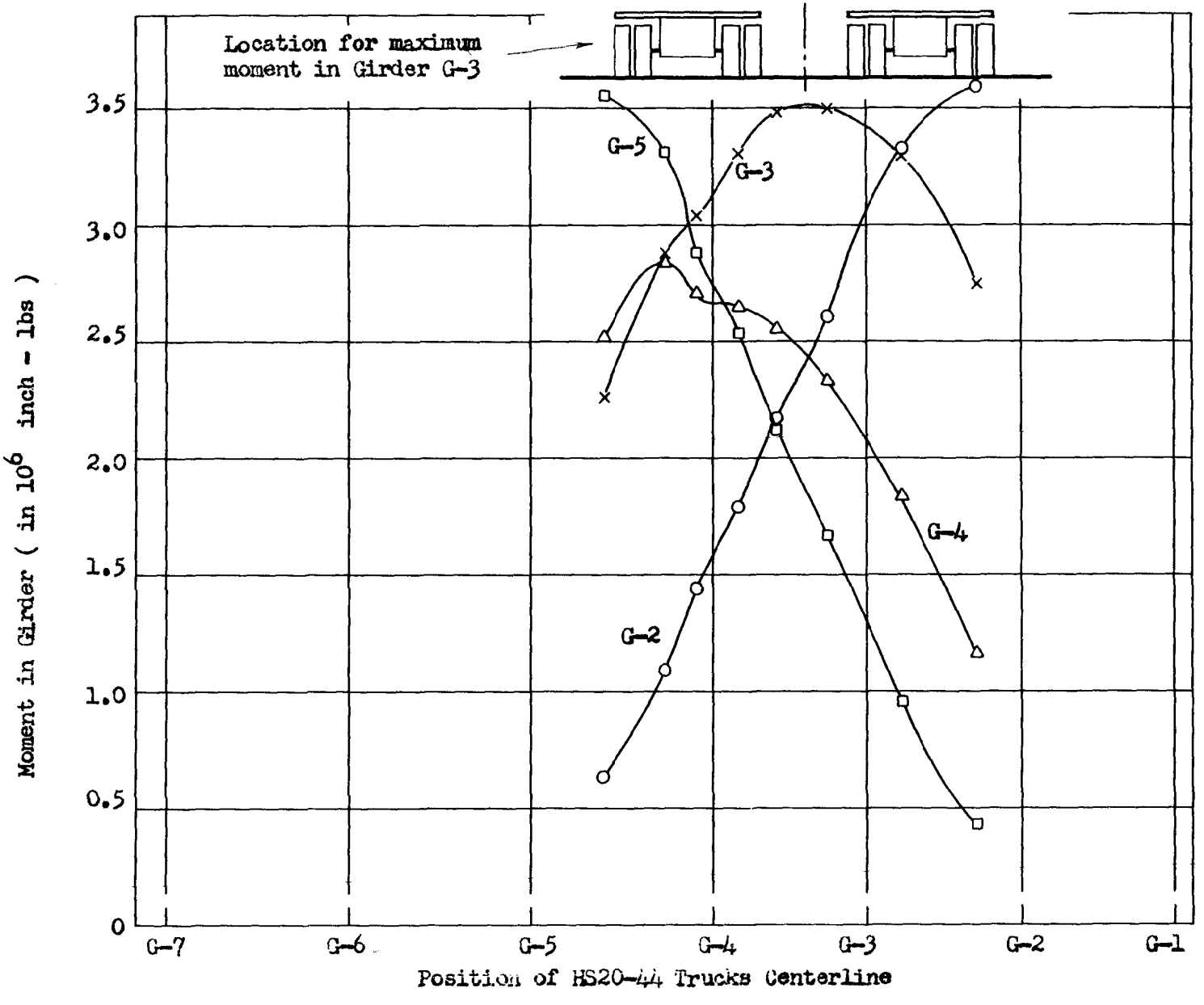

FIG. 41 MOMENT IN GIRDERS AT MIDSPAN DUE TO TWO HS20-44 TRUCKS SIDE BY SIDE - FIELD CONCRETE PROPERTIES BOTH OLD AND NEW SLAB CRACKED

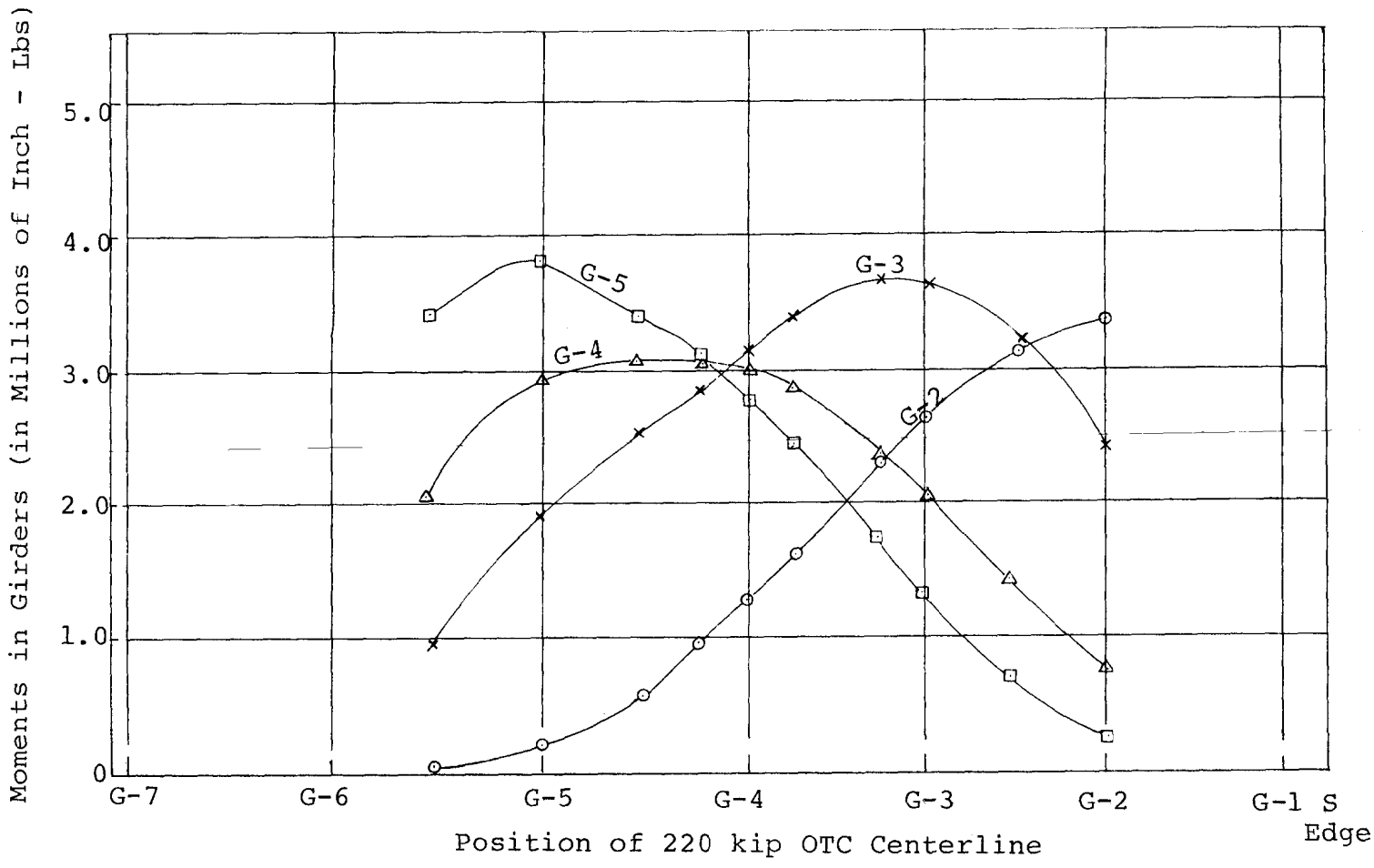

FIG. 42 MOMENT IN GIRDERS AT MIDSPAN DUE TO 220 k OVERLOAD TRUCK CRANE - DESIGN CONCRETE PROPERTIES - **UNCRACKED SLAB**

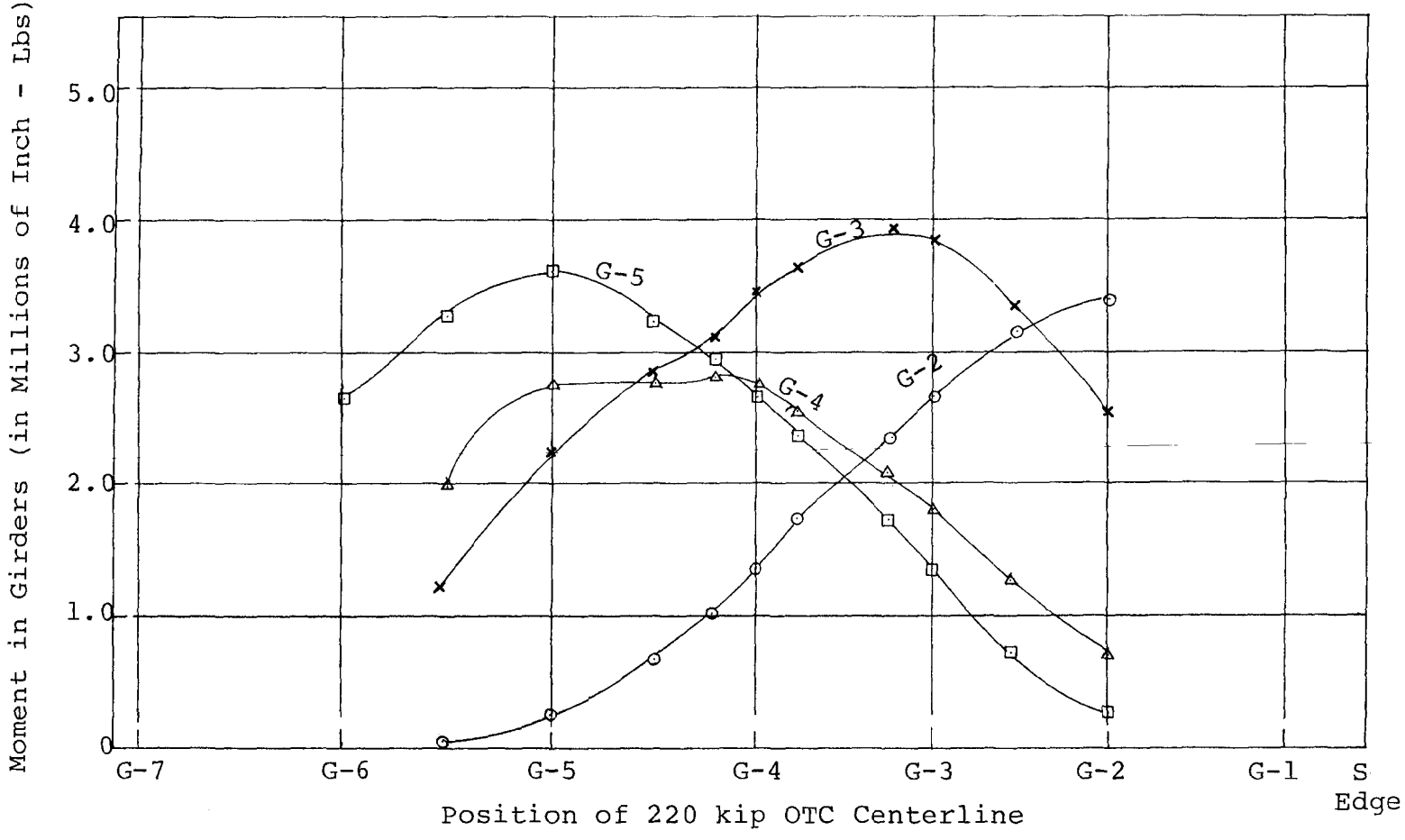

FIG. 43 MOMENT IN GIRDERS AT MIDSPAN DUE TO 220 k OVERLOAD TRUCK CRANE - FIELD CONCRETE PROPERTIES - UNCRACKED SLAB

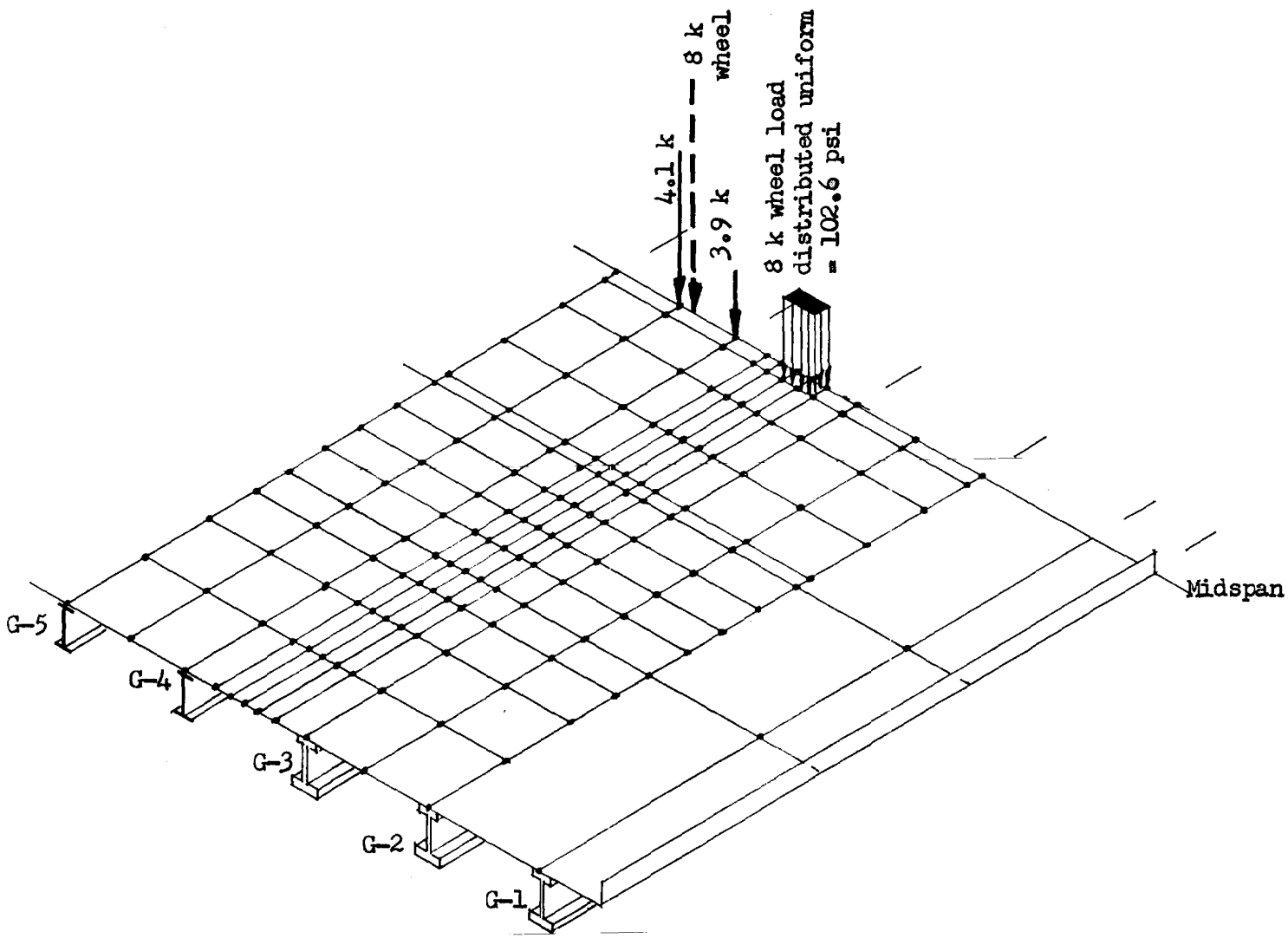

FIG. 44 TYPICAL DISTRIBUTION OF WHEEL LOADS TO GRID POINTS FOR MOMENTS IN SLAB DUE TO HS20-44 TRUCK LOAD

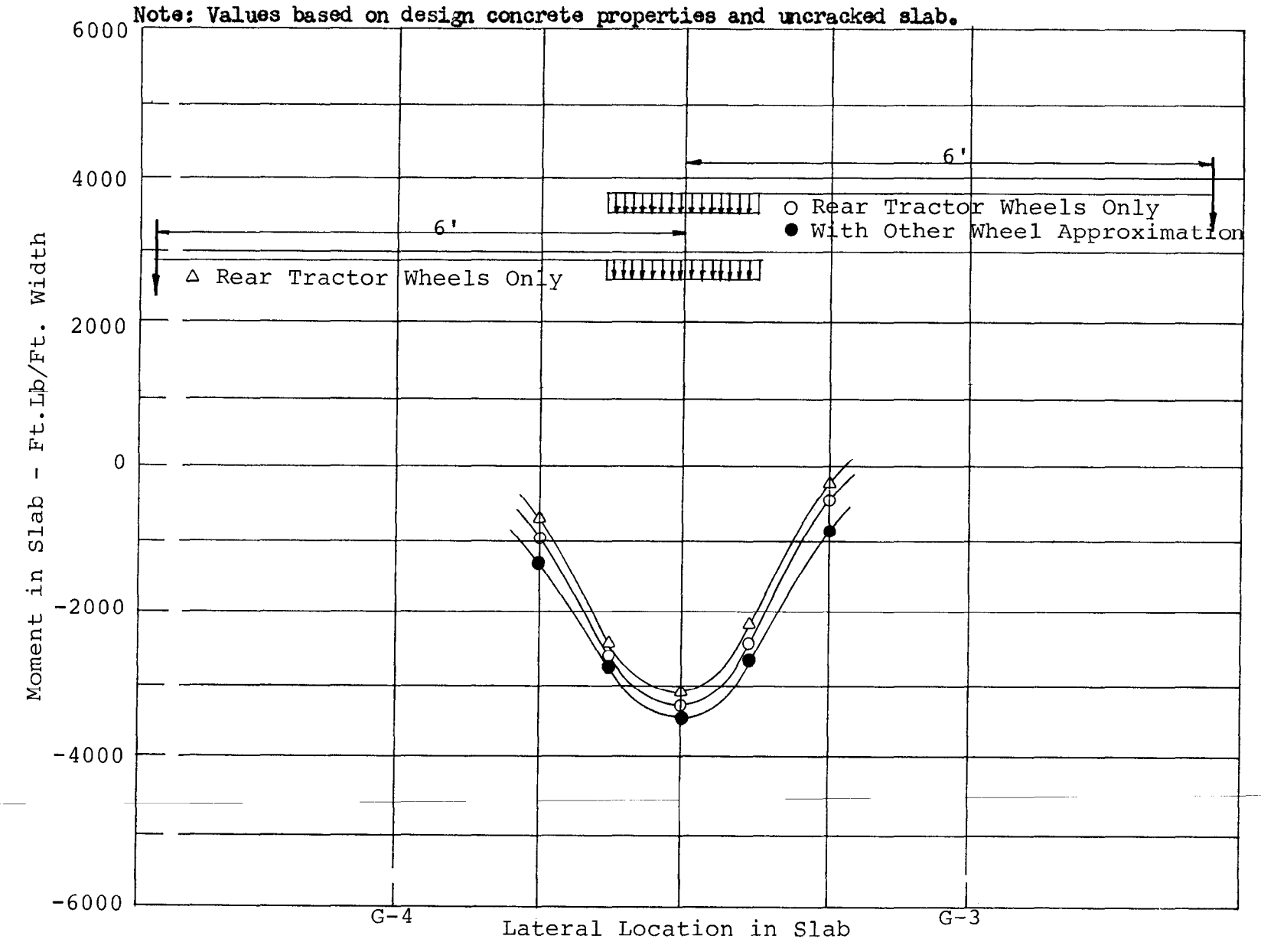

FIG. 45 VARIATION OF MOMENT IN SLAB CAUSED BY HS20-44 TRUCK LOAD AT SELECTED LOCATIONS

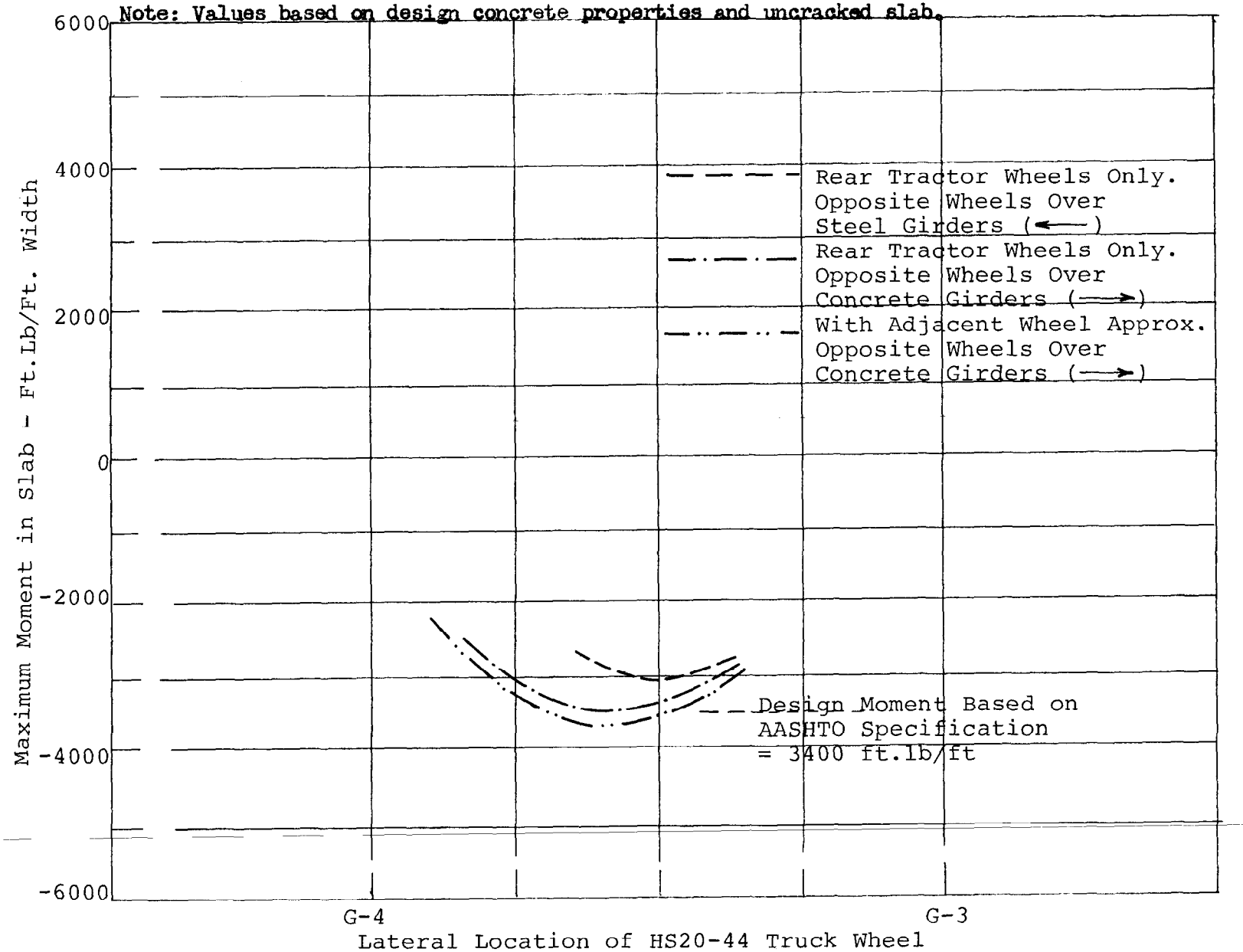

FIG. 46 VARIATION OF MAXIMUM MOMENT IN SLAB AS A FUNCTION OF HS20-44 TRUCK WHEEL LOCATION

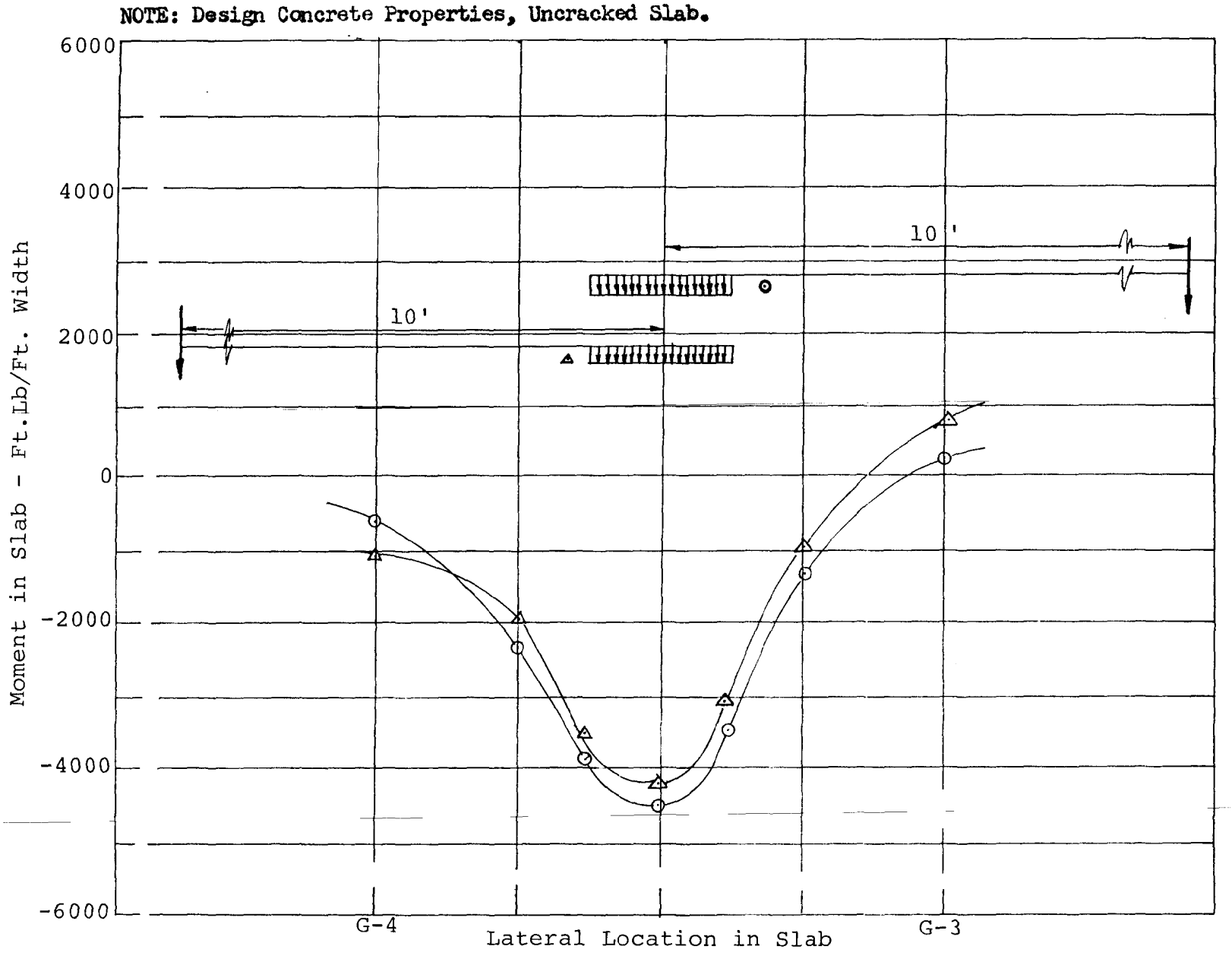

FIG. 47 VARIATION OF MOMENT IN SLAB CAUSED BY 220 k OVERLOAD TRUCK CRANE AT SELECTED POSITIONS

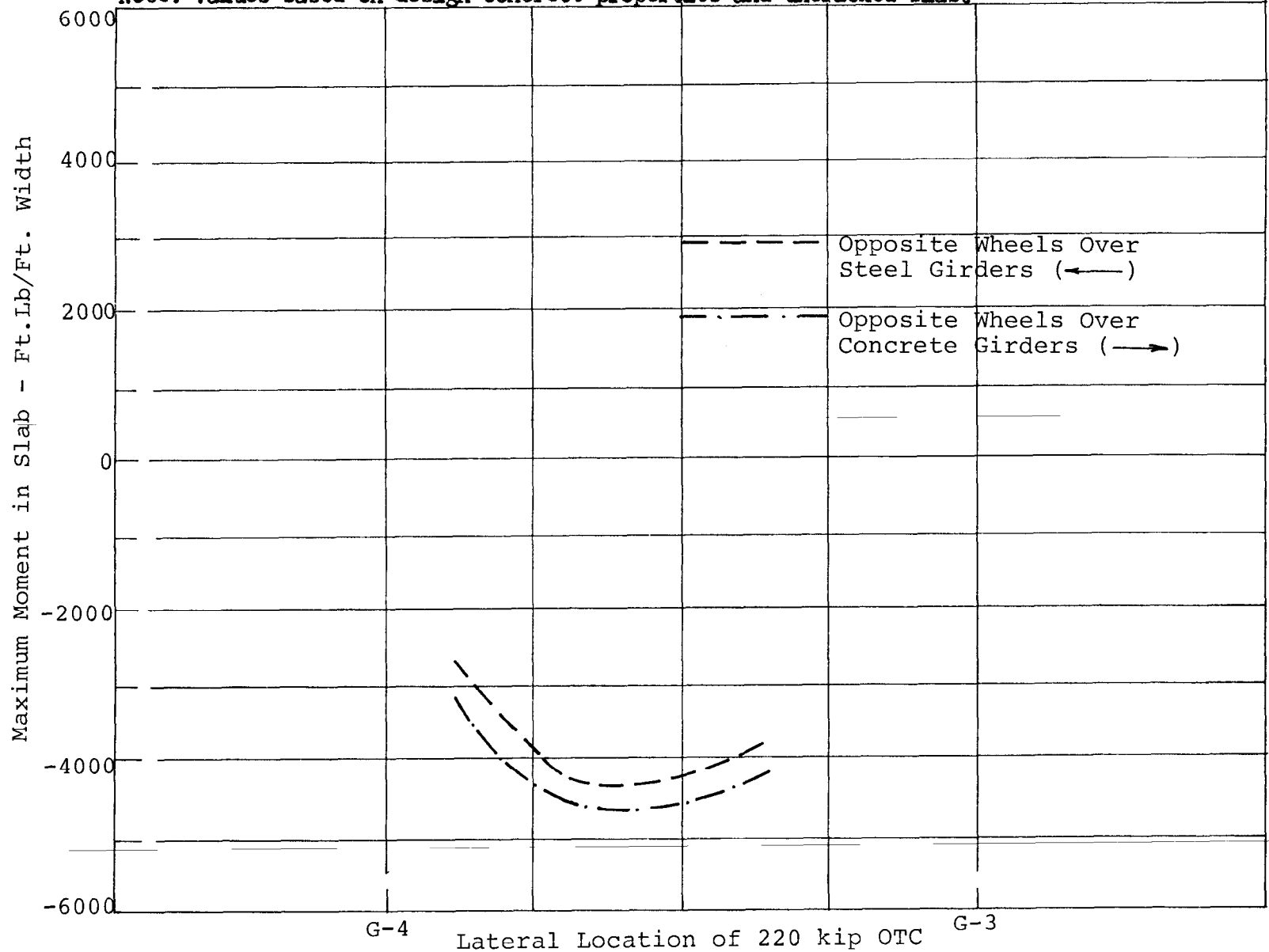

FIG.48 VARIATION OF MAXIMUM MOMENT IN SLAB AS A FUNCTION OF 220 k OVERLOAD TRUCK CRANE WHEEL LOCATION

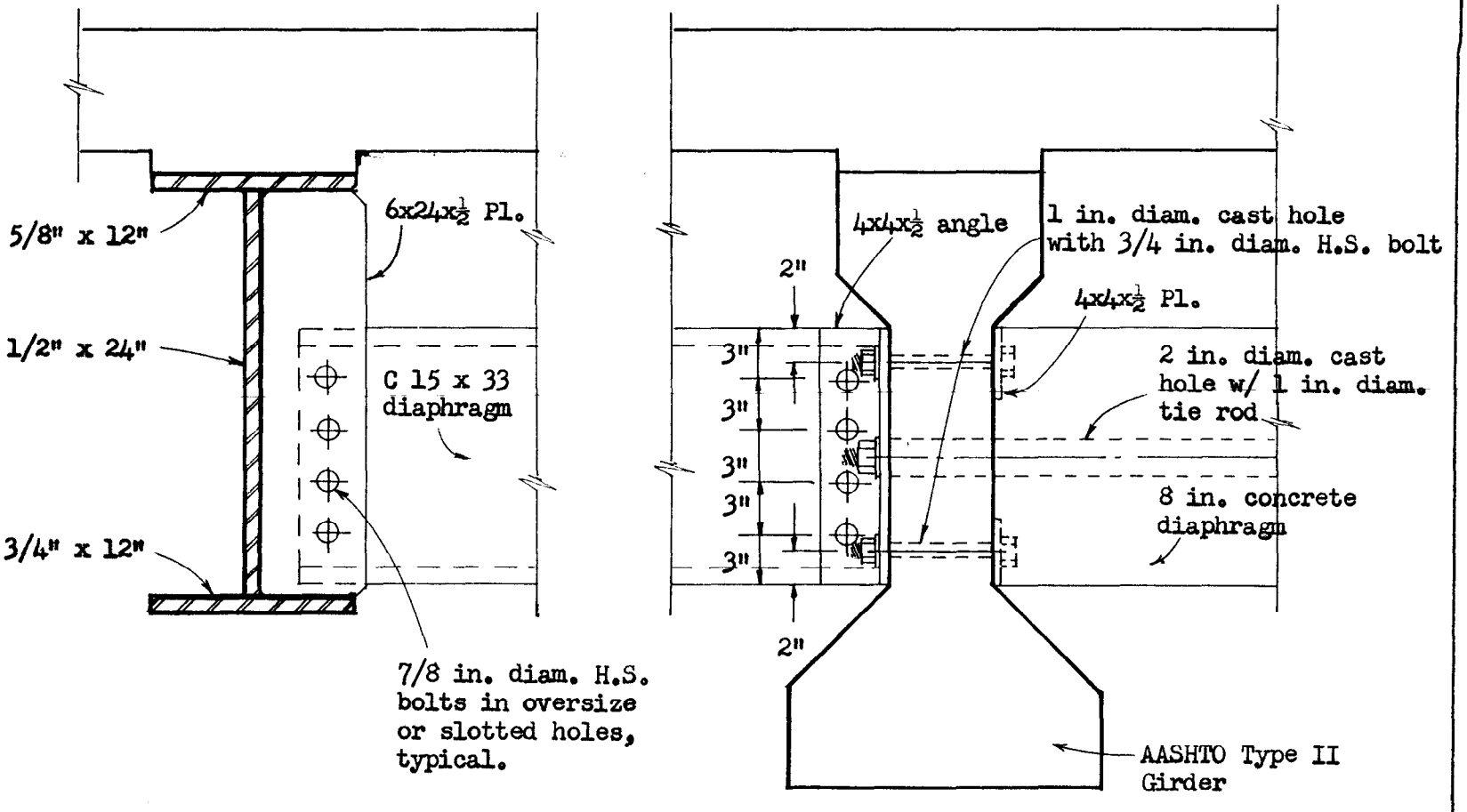

FIG. 49 DETAILS OF DIAPHRAGMS

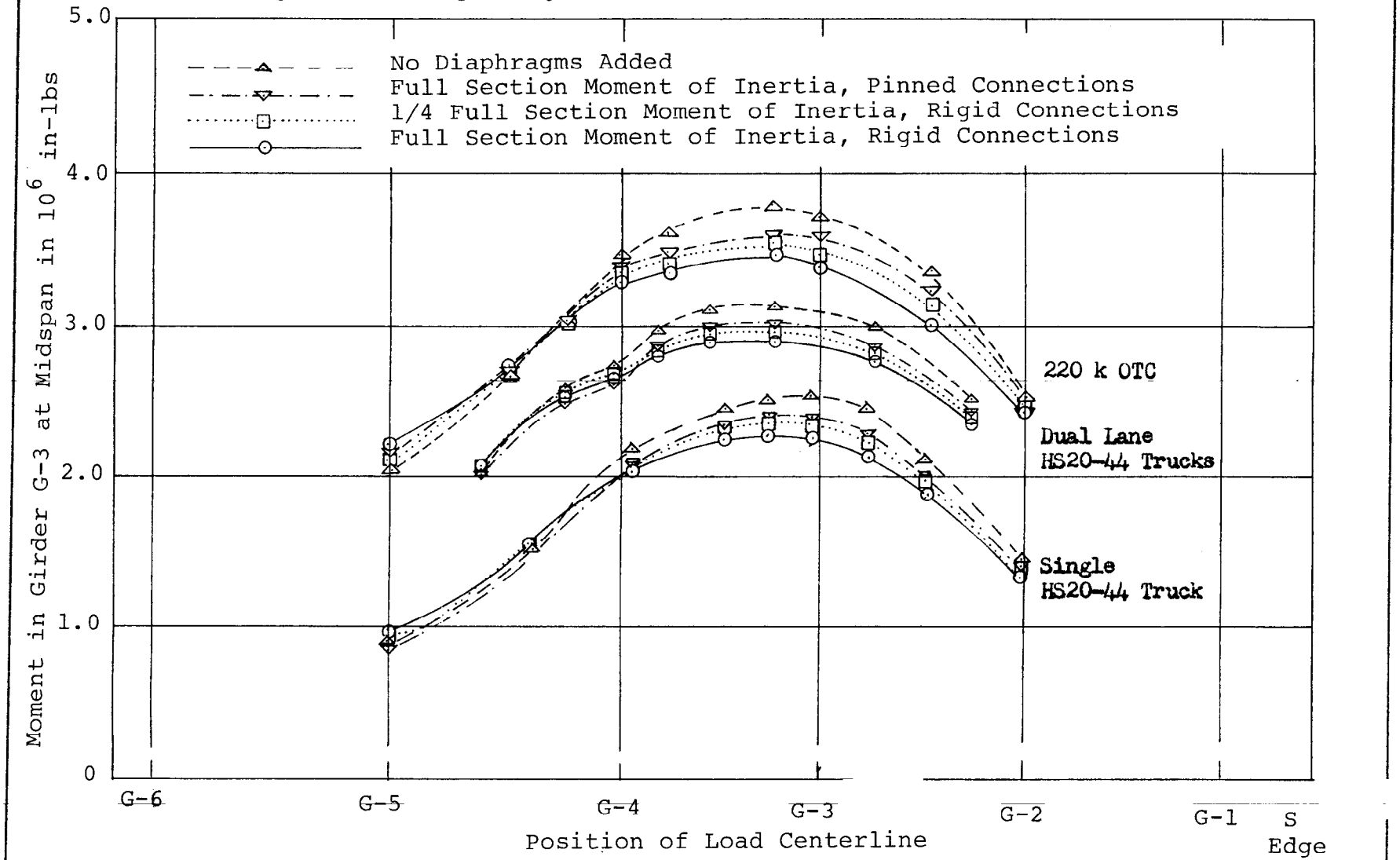

FIG. 50 EFFECT OF DIAPHRAGMS AT THIRD SPAN ON MAXIMUM MOMENT GIRDER G-3 FOR HS20-44 TRUCK LOAD AND 220 k OTC

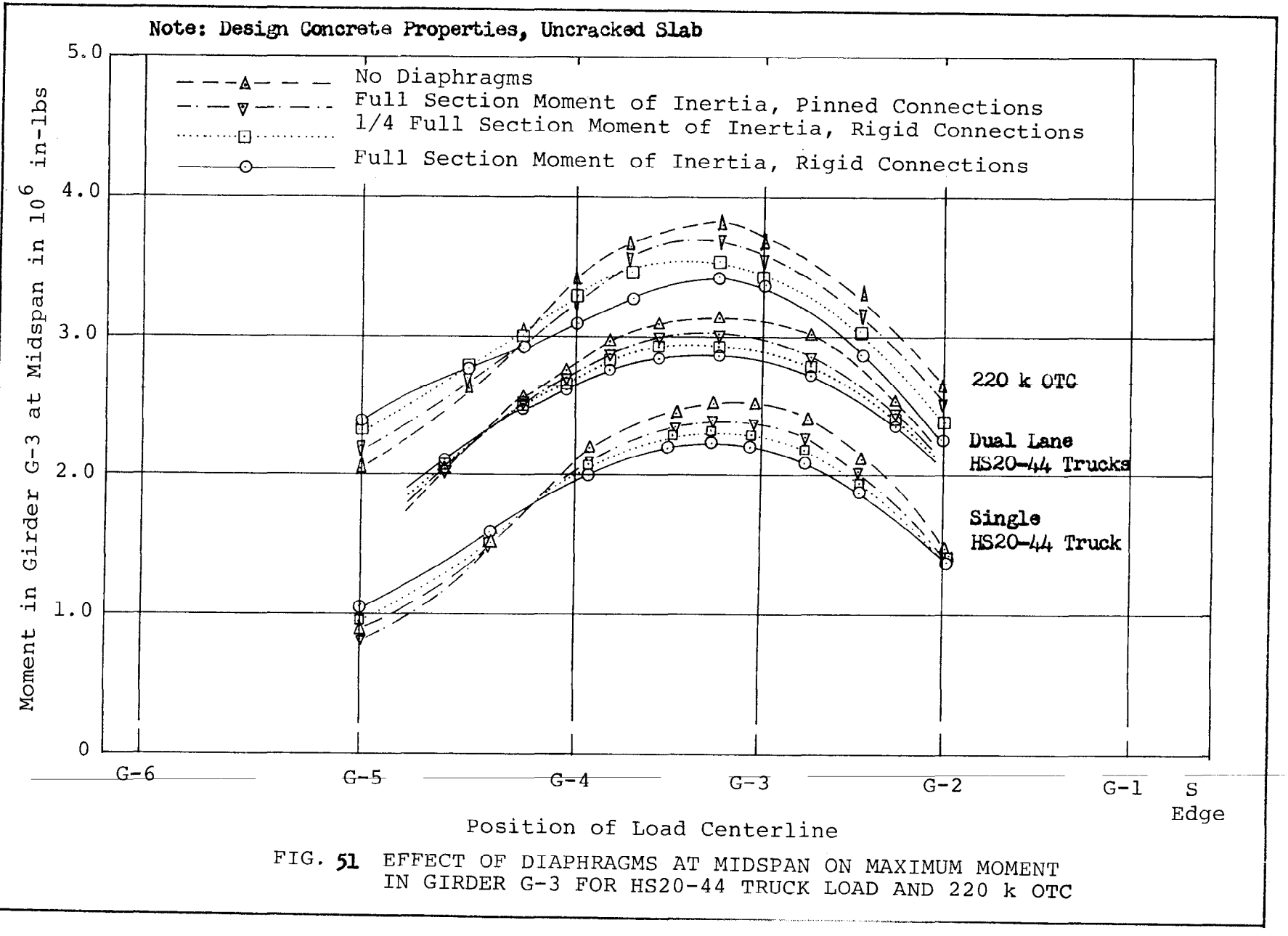

FIG. 51 EFFECT OF DIAPHRAGMS AT MIDSPAN ON MAXIMUM MOMENT IN GIRDER G-3 FOR HS20-44 TRUCK LOAD AND 220 k OTC

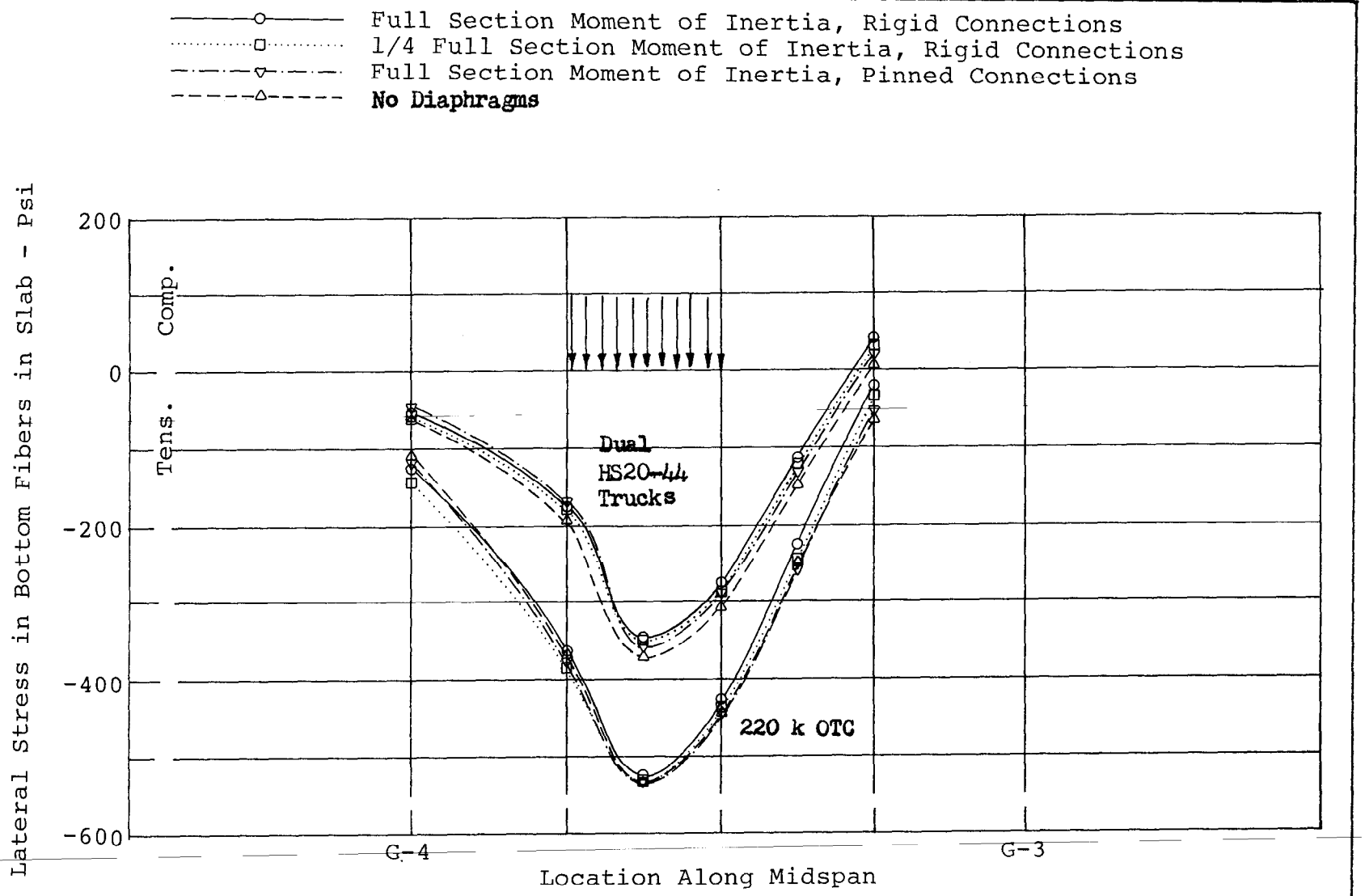

FIG. 52 EFFECT OF DIAPHRAGMS AT THIRD SPAN ON STRESSES IN SLAB FOR HS20-44 TRUCK LOAD AND 220 k OTC
DESIGN CONCRETE PROPERTIES, UNCRACKED SLAB

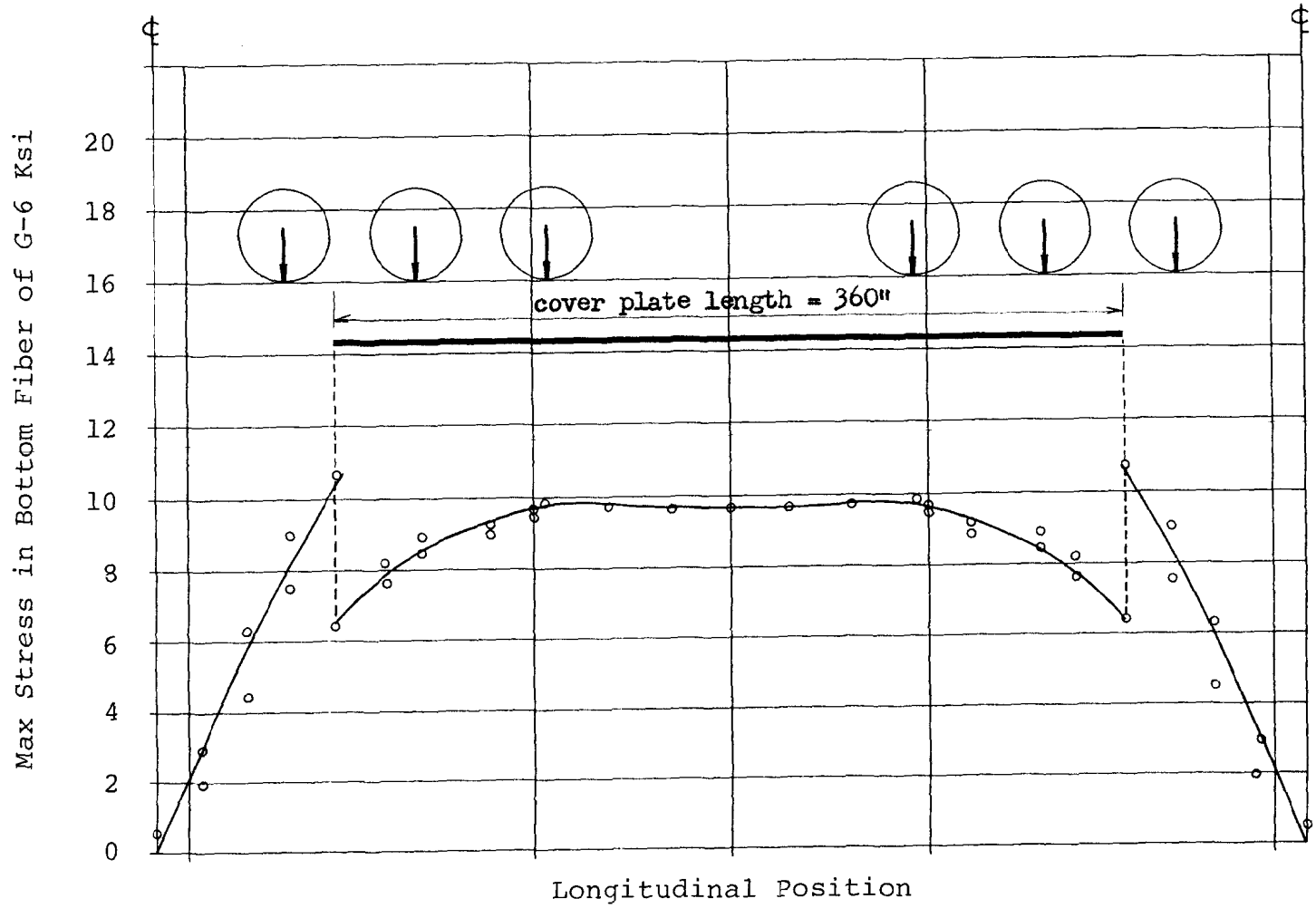

FIG. 53 TYPICAL STRESS DISTRIBUTION IN BOTTOM FIBERS OF GIRDER G-6 USING ROLLED BEAMS WITH COVERPLATES

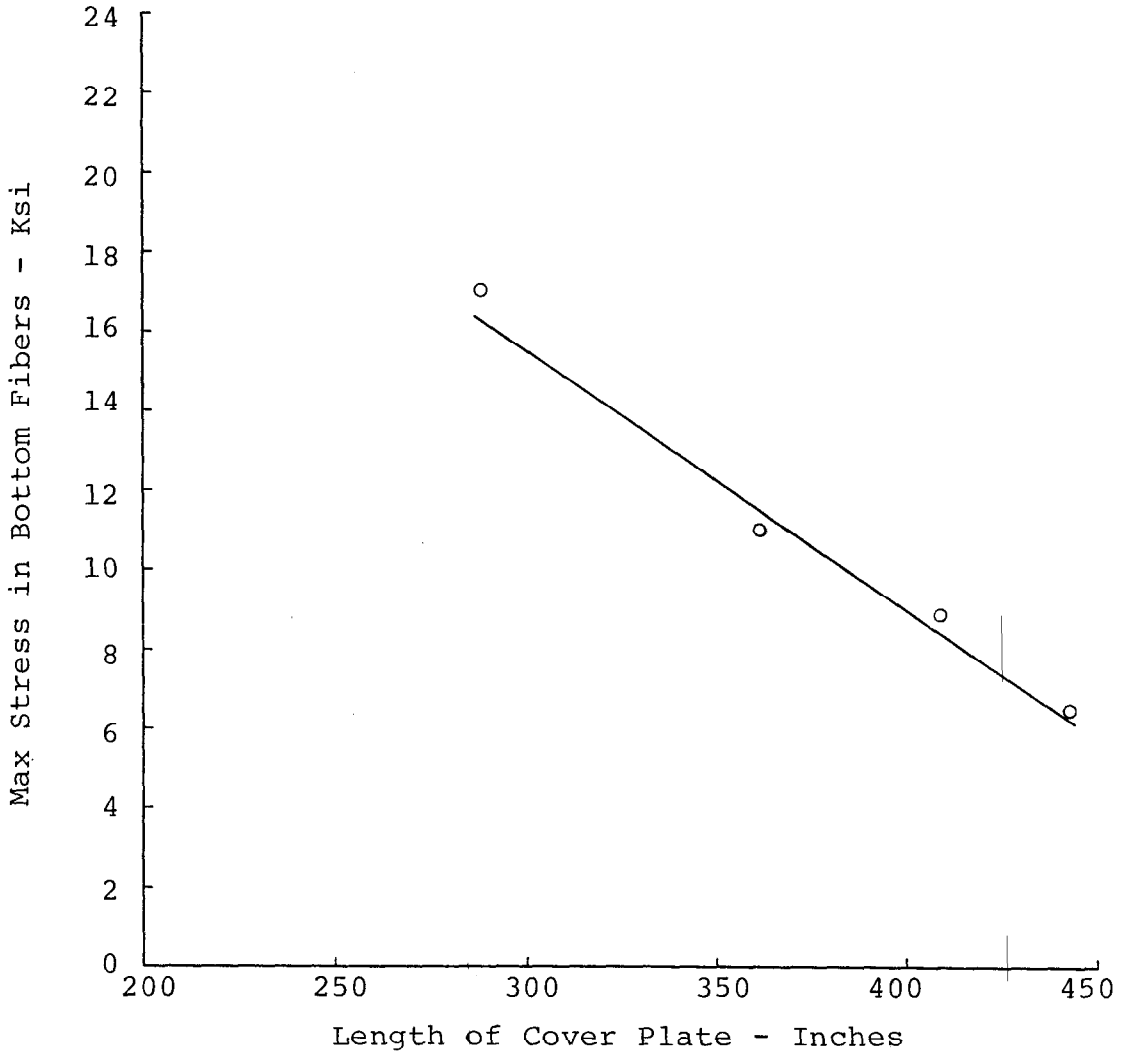

FIG. 54 EFFECT OF LENGTH OF COVER PLATE ON MAXIMUM STRESS IN BOTTOM FIBERS OF FLANGE OF BEAM AT END OF COVER PLATE

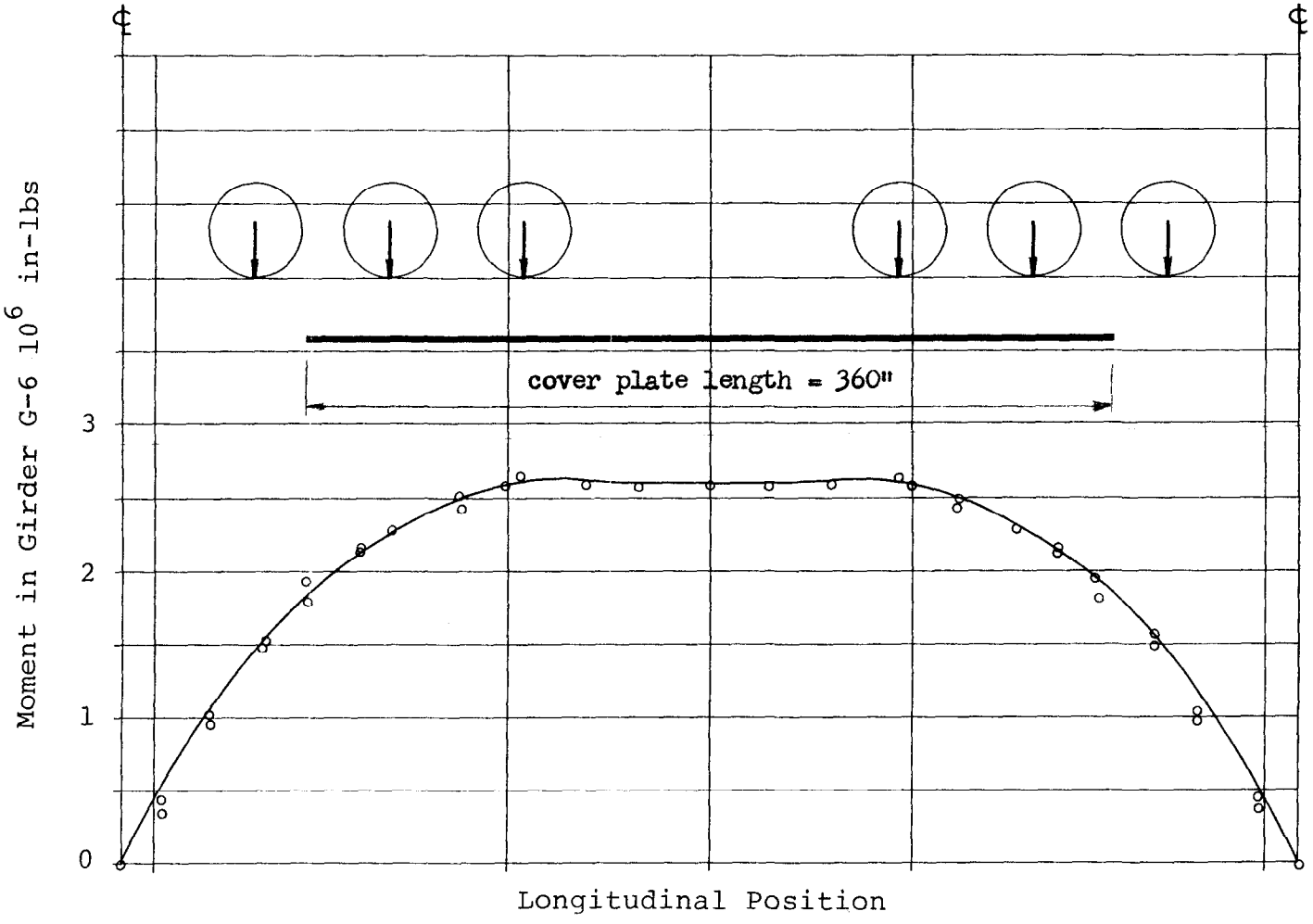

FIG. 55 TYPICAL MOMENT DISTRIBUTION FOR GIRDER G-6 WHEN USING ROLLED BEAMS WITH COVER PLATES

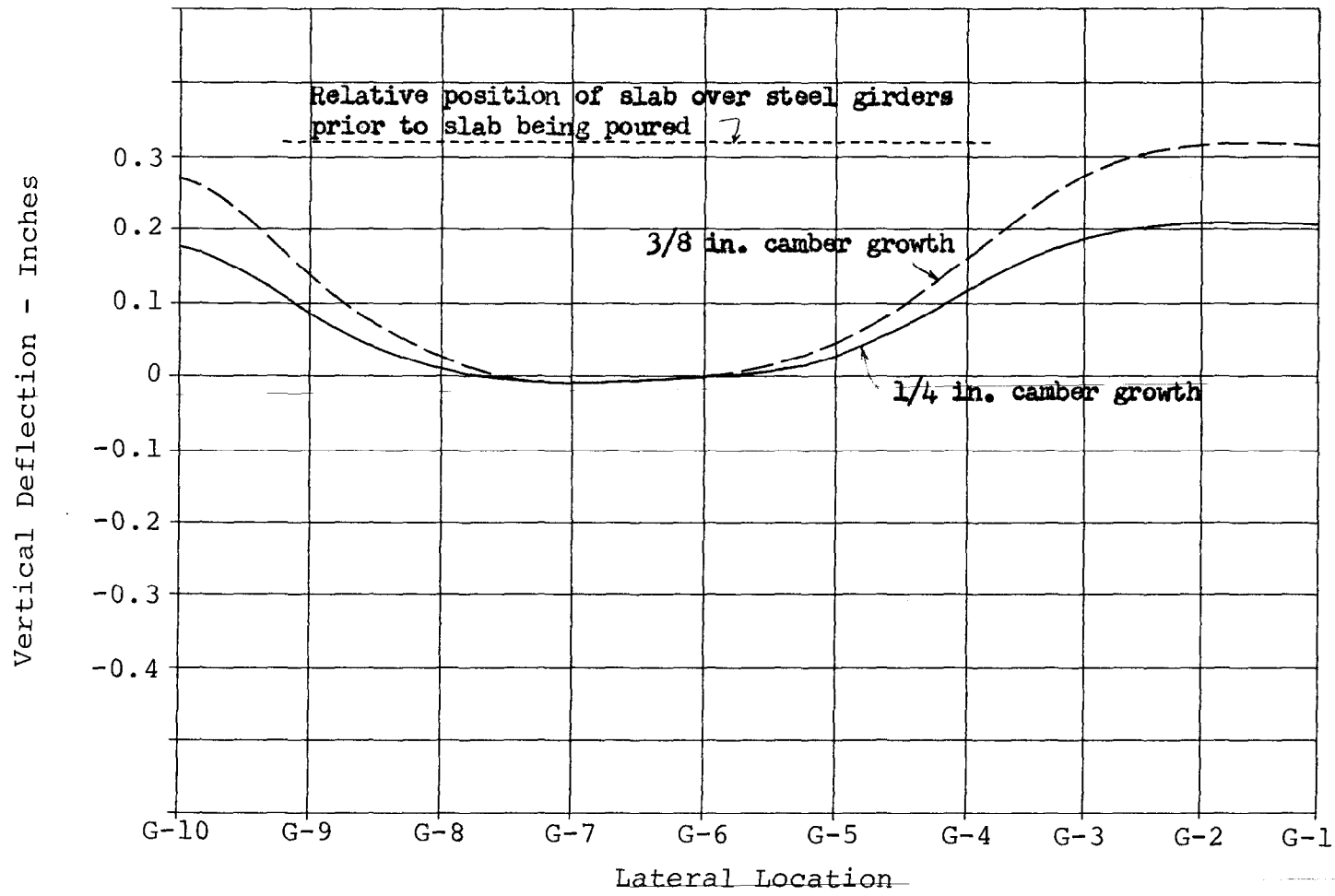

FIG. 56 VERTICAL DEFLECTION OF SLAB AT MIDSPAN DUE TO CAMBER GROWTH WHEN LOADED WITH DEAD WEIGHT OF SLAB
DESIGN CONCRETE PROPERTIES, UNCRACKED SLAB

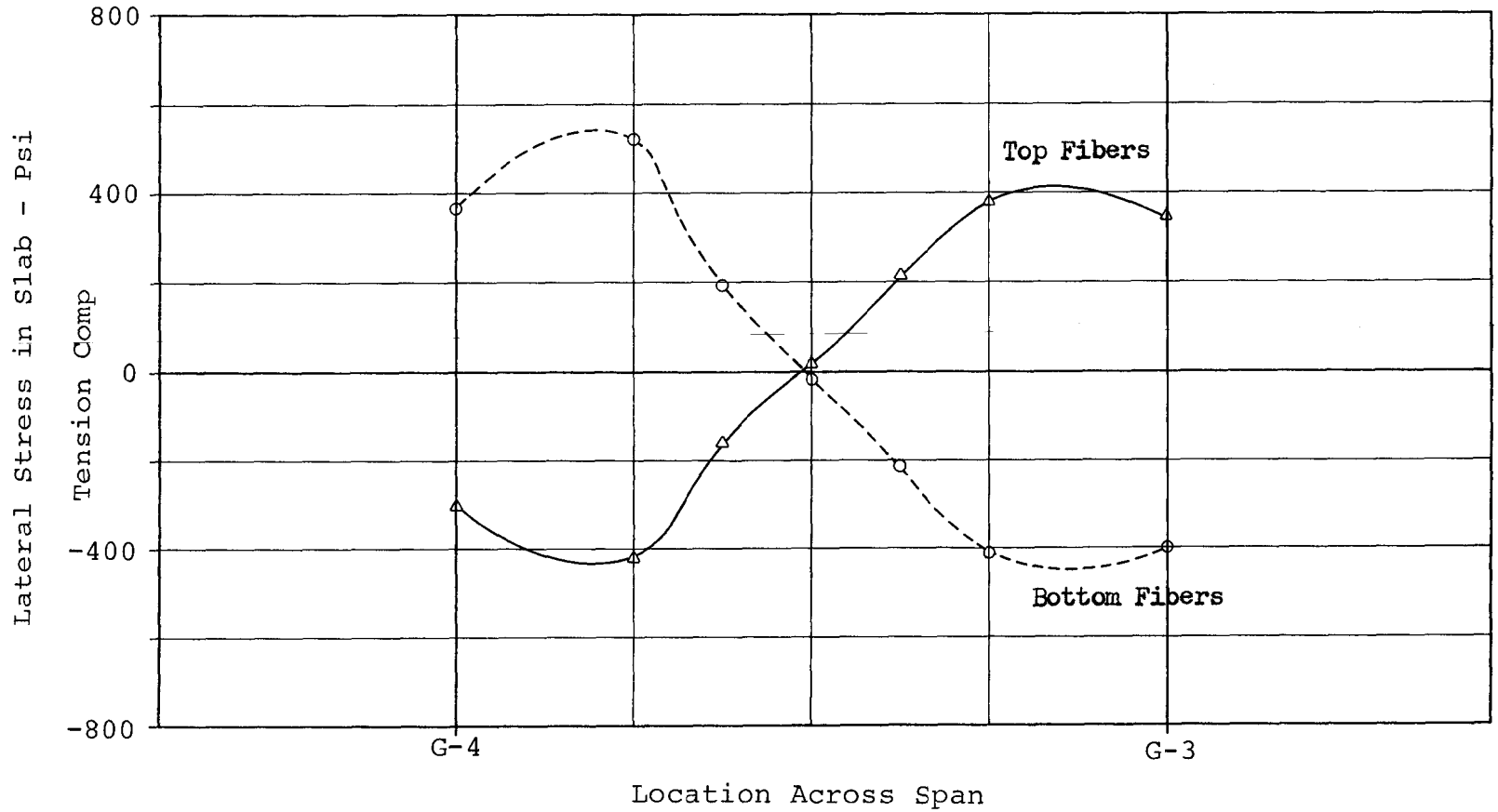

FIG. 57 EFFECT OF 0.1 IN. CONSOLIDATION OF NEOPRENE PAD ON LATERAL STRESSES IN SLAB AT END OF SPAN
DESIGN CONCRETE PROPERTIES, UNCRACKED SLAB

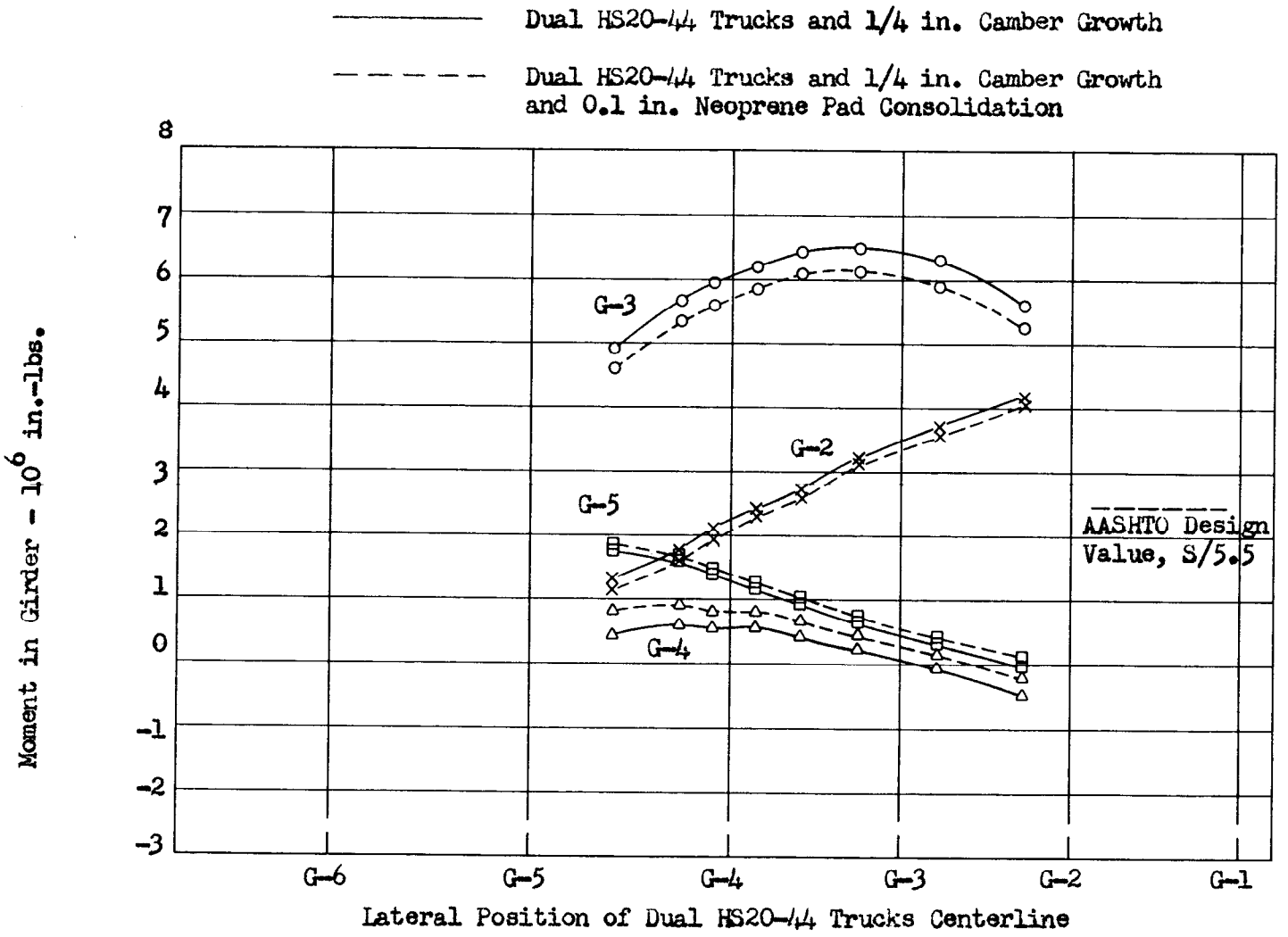

FIG. 58 COMBINED EFFECT ON THE MOMENT AT MIDSPAN IN COMPOSITE GIRDER DUE TO DUAL HS20-44 TRUCKS LOAD, 1/4 IN. CAMBER GROWTH, AND 0.1 IN. NEOPRENE PAD CONSOLIDATION - DESIGN CONCRETE PROPERTIES, UNCRACKED SLAB

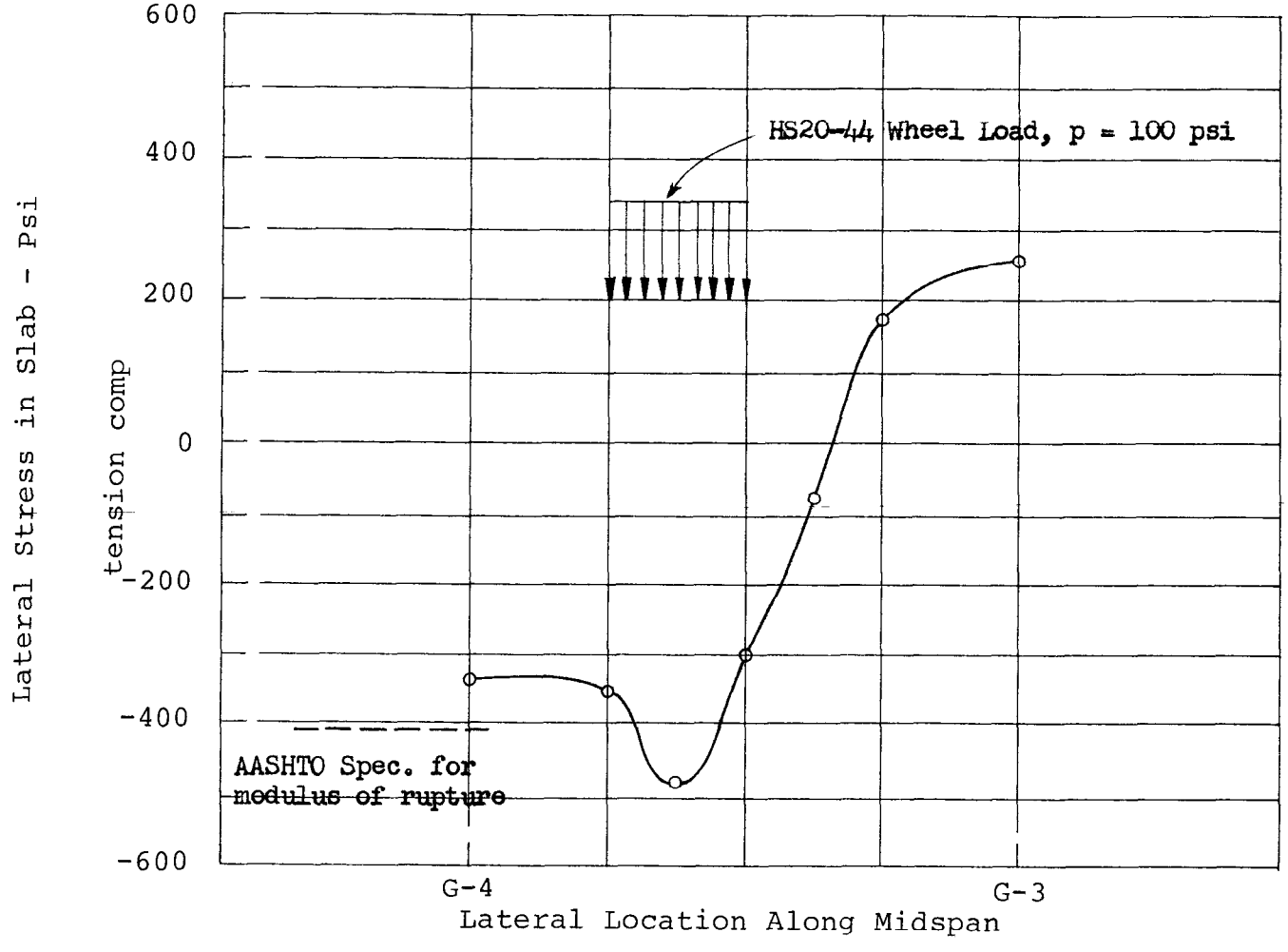

FIG. 59 COMBINED EFFECT ON LATERAL STRESSES IN BOTTOM FIBERS OF SLAB AT MIDSPAN DUE TO DUAL HS20-44 TRUCK LOAD, THREE HOURS OF SUNSHINE, 1/4 IN. CAMBER GROWTH, 0.1 IN. NEOPRENE PAD CONSOLIDATION, AND 30°F TEMPERATURE INCREASE OF STEEL GIRDERS DESIGN CONCRETE PROPERTIES, UNCRACKED SLAB

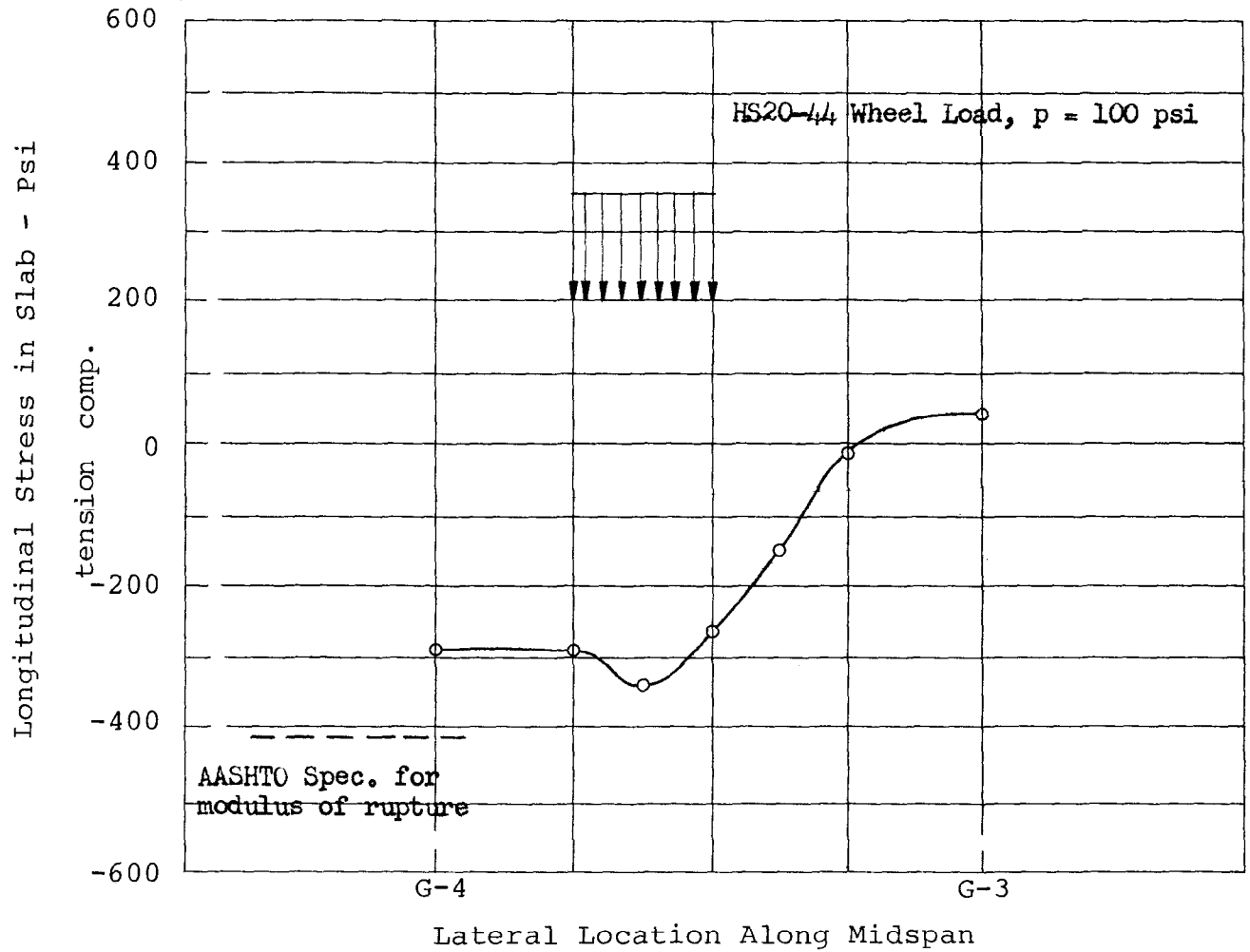

FIG. 60 COMBINED EFFECT ON LONGITUDINAL STRESSES IN BOTTOM FIBERS OF SLAB AT MIDSPAN DUE TO DUAL HS20-44 TRUCKS LOAD, THREE HOURS OF SUNSHINE, 1/4 IN. CAMBER GROWTH, 0.1 IN. NEOPRENE PAD CONSOLIDATION, AND 30 DEG. F TEMPERATURE INCREASE OF STEEL GIRDERS - DESIGN CONCRETE PROPERTIES, UNCRACKED SLAB

5. SUMMARY AND RECOMMENDATIONS

5.1 Summary

Extensive vertical deflections and certain horizontal deflections were measured for a span of the Bonnabel Overpass for loadings with live loads and thermal loads. The live loads consisted of nominal AASHTO HS20-44 trucks and a 220 k overload truck crane. The thermal loads consisted of ambient temperature changes and several hours of sunshine. The deflection measurements were made using dial indicators supported for the most part by stakes driven in the ground. The live load field test results are believed to accurately represent the deflection of the span. The small inconsistencies in the data were mainly due to hysteresis in the support system. The deflection measurements from the thermal load tests, while equally as accurate as those obtained for the live load tests, are not as useful for comparison because of the difficulties in defining ambient temperature conditions.

A span of the Bonnabel Overpass was modeled mathematically using the MSC/NASTRAN Finite Element Computer Program. Computer runs were made simulating all of the field test live load configurations and simulating the thermal loading conditions where practical.

Relative to comparison of computed deflections and field measured deflections under live load conditions, it is

believed that the only limitation to obtaining excellent agreement is the accurate definition of the computer input data. In the case of the Bonnabel Overpass, excellent agreement could be obtained by adjusting the computer model to account for lateral cracking of the slab and to account for less than rigid end conditions for the diaphragms.

It is believed that the MSC/NASTRAN computer program has certain limitations in so far as calculating the response of a structure such as the Bonnabel Overpass to ambient thermal conditions. The most severe limitation is that of defining the temperature input data required by the program. On the other hand, if the temperature distribution in the structure is well defined, NASTRAN can yield accurate information regarding thermally induced stresses in the structure.

The NASTRAN program was used to investigate seven areas relative to overpass design and mixed girder support systems. In addition, the effects of combining these areas, where appropriate, were investigated. One of the objectives of the overall project was to use the NASTRAN computer program to define potential problem areas for future study. No attempt has been made to investigate the areas completely nor to verify the validity of the individual computer solutions. Rather, the results are presented only to indicate trends and gross effects as predicted by the NASTRAN computer program. A summary of the more significant results of the computer study is given below.

In the mixed girder system the computer solution indicates that camber growth can have a very significant effect on the maximum moment in the adjacent concrete and steel girders. For the predicted amount of camber growth (1/4"), the resulting moment increase in the adjacent concrete girder is quite large and of the same order of magnitude as the AASHTO design moment due to live loads.

Ambient temperature changes appear to have relatively small effects on the stresses in the span superstructure; however, ambient temperature changes and direct sunshine on the top of the deck cause rather large tensile stresses in the slab. These stresses can routinely be as high as one-third the modulus of rupture for the concrete.

For the mixed girder system, the maximum moment due to live load in the concrete girder adjacent to the steel girders will be greater than the moment in the steel girder adjacent to the concrete girders. For the case of dual lane HS20-44 trucks on the Bonnabel Overpass, the moment in the adjacent concrete girder exceeds the AASHTO design value by 27% when design concrete properties are used and by 36% when field measured concrete properties are used.

Concrete diaphragms which are installed for the purpose of distributing moments between girders are more effective at mid-span than at the one-third span location. However, the diaphragms modeled herein would not be effective in distributing moments because the end connections are too flexible. Care should be exercised in placing rigid

diaphragms between the adjacent concrete and steel girders because of the probability of camber growth. An increase in rigidity in this case would further increase the moment due to camber growth in the adjacent concrete girder.

The neoprene bearing pads apparently have consolidated by approximately 0.1" and their modulus of elasticity increased several fold. The increase in modulus of elasticity would cause a corresponding increase in the shear modulus, which in turn would increase the forces on the bent caps. The field test results suggest that the opposing forces on each bent cap almost cancel each other and that the motions of the bent caps are dependent on the overall expansion of the complete overpass.

For the mixed girder system, the combination of live load and camber growth may cause severe overloading of the adjacent concrete girder. In the case of the Bonnabel Overpass, the computer results show that dual HS20-44 trucks live load and a 1/4" camber growth acting together will cause the maximum moment in the adjacent concrete girder to be approximately 100% greater than the AASHTO design value.

The computer results also show that a combination of live load and thermal effects, primarily sunshine effects, will cause large tensile stresses in the bottom fibers of the slab both in the lateral and longitudinal direction. For the case of the Bonnabel Overpass, these stresses are expected to frequently approach the modulus of rupture of the concrete.

5.2 Recommendations

Since the NASTRAN program can be used to model a range of mixed girder bridges, e.g., spans of 40 ft., 60 ft., and 80 ft.; and steel girder spacings of 4 ft., 7 ft., and 10 ft.; it is felt that provisions should be made to keep the NASTRAN program active and current and at the disposal of the State and the University.

With the NASTRAN program (or its equivalent) available, additional studies should be initiated into at least two areas. First, it is felt that the combination of live load and camber growth can overload the concrete girder adjacent to a steel girder in a mixed girder span, and that this combination should be further investigated, including the advisability of the use of diaphragms between the concrete and steel girders.

Secondly, it is felt that the combination of live load and thermal load can have a detrimental effect on the integrity of the deck slab, and that this combination should be further investigated.

Consideration should be given to future investigations addressing in more detail live load distribution and its relationship to AASHTO specifications. It is felt that it will be necessary to go beyond empirical computer studies to address live load distribution, and that major analytical work would be required.

APPENDIX A

USAGE OF MSC/NASTRAN COMPUTER PROGRAM AND GENERAL BRIDGE MODEL

A.1 Introduction

MSC/NASTRAN is a licensed, finite element computer program installed on selected mainframe computers. Like other similar programs, it is licensed on a yearly basis, with fees based on the amount of computer time used in running the program.

NASTRAN must be installed in a mainframe computer prior to its being able to be used in solving problems. This installation process can be complex because of peculiarities of the local computer system on which it is installed, as well as the size and complexity of the NASTRAN program itself.

In addition to developing and installing the NASTRAN program, other means of formulating a finite element bridge model were examined that would be consistent with the use of a mainframe program such as NASTRAN for the final computer model.

The program MSC/PAL was used to explore bridge modeling using the finite element approach. PAL is also supplied by the MSC Corporation, but it runs on an IBM PC or compatible computer. Its modeling capacity is much less than MSC/NASTRAN.

PAL has a feature which allows for the conversion of a PAL based finite element model to a NASTRAN based model. At first, it was thought that this might provide a useful means of developing the initial model in PAL on a microcomputer, then converting the model data to NASTRAN when increased capacity was required. However, after preliminary development using PAL, it was decided that writing the NASTRAN model over from the beginning was the most efficient method because of the severe limitations that PAL imposes on its models.

Another microcomputer program, PRENASTRAN, was briefly investigated. PRENASTRAN is designed to produce a NASTRAN model from user input data. Its limitations in selecting a bridge model prevented any serious use.

The NASTRAN program, leased from MSC Corporation, is separate from the input data for a bridge model developed under this project. The input data described below is specific to the bridge model. Finally, the NASTRAN program was "verified" by testing its results for simple structural situations for which analytical solutions could be calculated.

A.2 Description of Program

A.2.1 The Connected Node Finite Element Model Concept

The concept of the finite element, connected node model is that a continuous representation of physical structure is represented by a mathematical model that is divided into

segments, or elements. These elements are connected at specific points in space, called grid points.

The finite element model includes two major simplifications that lead to much of its power and widespread applicability. First, the elements are assumed to be connected only at the grid points; second, the "interior" of each finite element is only a mathematical approximation to the true physical phenomenon. The finite element model technique concentrates on insuring the accuracy of prediction at the grid points rather than the interior of the elements.

Finite element techniques, as embodied in programs such as NASTRAN, are highly developed and very accurate predictors of phenomenon modeled at the grid points. Furthermore, it is possible to place constraints on the motion of the grid points or the nature of the elements connecting the grid points in order to more closely approximate the true physical phenomenon.

In NASTRAN, a grid point may be constrained to move in only certain directions. It may be constrained not to rotate about certain axes. This ability to specify constraint directions gives a great deal of flexibility in defining the finite element model.

Judiciously used, grid point constraints can lead to model simplification when models are symmetric. For example, in the bridge model described in this report, symmetry and grid point constraints are used to reduce the

number of nodes necessary by almost half. As will be described in greater detail below, the centerline of the bridge between supports, and across the direction of traffic, is a line of symmetry if the bridge is loaded symmetrically about this centerline. Deflections on one side of the bridge centerline are symmetrically equal to bridge deflections on the other side of the bridge centerline. If the bridge supports are at the same level, the bridge at the centerline is exactly horizontal in the direction of the line of traffic. Hence, bridge grid points along the centerline may be "constrained" to be horizontal in the direction of traffic (not rotated), and so only one half of the bridge finite element model need be represented. This leads to a considerable saving in computing resources.

A.2.2 Structure of NASTRAN

The NASTRAN computer program is a very large program (over 500,000 lines of source code) which takes data on a specific finite element model as input. This data is known as an "input deck" and is specific to a particular model or structure. (The NASTRAN program itself does not change from one model to the next, only the data in the input deck does).

The individual lines of the data in the "input deck" are known as "cards," even though relatively few modern computer installations still use real computer punched cards stacked in decks. The terminology, however, survives. The

cards that will be referred to below are actually lines of data in datasets in computer memory, computer tape, or computer disks.

Before the user of the NASTRAN computer program can begin, it is assumed that he has developed a finite element model of the structure that he wishes to study; that is, a coordinate system is defined, grid points are located, and a set of modeling elements are connected between the grid points to model the structure. At this point, the user has enough data to begin to develop a NASTRAN data deck.

The user of the NASTRAN program must not only provide input data that describes the finite element model itself, but he must also provide input information that describes how the results of the program, the output data, will be presented. To allow efficient use of computer resources, the NASTRAN program allows for multiple load arrangements to be calculated for a single finite element model run.

NASTRAN organizes the input data deck into the following subsets:

1. Executive Control Deck

This deck contains a few data "cards" which describe the general type of data to follow. For example, it would include a SOL STATICS card to indicate a statics solution (rather than a dynamic analysis) is required.

2. Case Control Deck

This deck will include cards that describe the various loads to be applied to the finite element model. For example, if the finite element model is of a structure, several different structural loadings may be specified at this point so that each will be used in sequence with the same finite element model in one computer run.

The case control deck also includes cards that describe the output format that the user desires. For example, the user may specify that he wishes certain forces or moments printed out for a selected group of grid points. Graphical output may also be specified.

3. Bulk Data Deck

The bulk data deck contains all the information necessary to input the finite element model. Grid point locations in a global coordinate system, a list of elements and the grid points to which each connects, and material and dimensional properties of the elements are included in the bulk data deck. Also included are the data for the various load arrangements. NASTRAN also allows for group material properties to be specified; that is, mechanical properties of concrete can be specified on one card. The hundreds of elements which are made of concrete need only refer to the appropriate definition card--the properties need not be redefined for each concrete element.

A.2.3 NASTRAN Cards Useful for Bridge Modeling

The principal elements used in the modeling of the bridge are the bar, quad4, and elas2 elements. In the NASTRAN data deck, these elements are defined by related "cards;" for example, the bar element is described by the CBAR and PBAR cards, which describe the gridpoint connections and properties of the element respectively. (The cards are described in greater detail in the following section.)

The bar element is a prismatic element whose endpoint deflections are derived from classical beam theory. It is a simplified element in that the neutral axis and shear center coincide.

The quad4 element is a versatile plate and shell element with bending and membrane parts. The element is a quadrilateral in that it connects four neighboring nodes. Its connection and property cards are CQUAD4 and PSHELL. The quad4 element is used for modeling sections of the bridge deck.

Several cards that are useful for bridge modeling are described below. Following this card description will be an analysis of how some of these cards may be used in a simple bridge model.

GRID

The GRID card is used to identify the location of a grid point in space in a global coordinate system. If the

point is constrained to move in certain directions only, these directions are also specified on this card.

SET

The SET card is used to define subsets of grid points, model elements, load sets, temperature data, and constraint sets. Each set is assigned a unique number. These sets are used by many other cards to refer to selected groups of grid points or elements. For example, deflections may be printed out for a specified grid point set.

CBAR

The CBAR card describes the connection ("C") of a simple bar element between two grid points of a structural model. In the Bonnabel Overpass span model, the bar element is used to model the girders and diaphragms. The bar element properties ("P") are described by a PBAR card. One PBAR card may be referenced as the list of properties for many CBAR element connection cards. In the CBAR bulk data card, the associated grid points, offset of neutral axis from grid points, and appropriate PBAR card are referenced.

PBAR

The PBAR card lists the properties of a simple beam element, the bar, including material, cross sectional area, moments of inertia, torsional constants, and related properties. The grid point connections are described by the

CBAR card. The material properties are specified by referring to an associated MAT1 card.

MAT1

The MAT1 card defines material properties for cards that reference its identification number. The properties are for linear, isotropic materials, and include Young's modulus, shear modulus, Poisson's ratio, and related properties. This card is used by other cards such as PBAR as a reference for material properties. MAT1 (and MAT2) cards allow for linear thermal expansion but are otherwise temperature independent.

CQUAD4

The CQUAD4 card describes the connection of a quadrilateral plate element ("quad4") between four grid points. The quad4 element is used to model sections of the deck in the Bonnabel Overpass span model. The CQUAD4 card includes a list of the grid points connected, and the identification number of a PSHELL card which contains the properties of the plate, including the thickness.

PSHELL

The PSHELL card lists properties for the quad4 element used to model the sections of the bridge deck. The properties include material reference, bending stiffness, thickness, and related properties. The material properties

are determined by referring to an associated MAT2 card.

MAT2

The MAT2 card is used to define material properties for linear, temperature independent, anisotropic materials for two dimensional elements. For the overpass, this card is used to define material properties for the quad4 element, when cracked slab conditions are included.

CELAS2

The CELAS2 card is used to specify a single dimensional, elastic relationship, called a scalar spring model ("elas2"). In the model of the overpass span, it is used to model the vertical elastic properties of the supports. The CELAS2 card itself contains data listing the grid points that are connected by the elas2 element, and in which direction the elastic relationship is oriented.

RBAR

The RBAR card defines a rigid bar with six degrees of freedom at each end. Some of the degrees of freedom at each end may be constrained if the user wishes.

FORCE

The FORCE card specifies a force load vector at a grid point.

MOMENT

The MOMENT card will define a moment load at a grid point by specifying a vector.

LOAD

The LOAD card defines a static load as a set of forces and moments defined on grid points by the FORCE and MOMENT cards.

PLOAD2

The PLOAD2 card is used to define a static pressure load on a section of a quadrilateral or triangular element. This load is modeled as a uniform pressure over an entire quad4 element.

For the overpass span model, the PLOAD2 card is used to define the load exerted by the tires over the area of the tire prints, and to define the slab dead weight.

SUBCASE

The SUBCASE card is used to mark the beginning of a section of the case control deck containing cards relating to a single subcase. For the bridge model, subcases are used to describe different load locations.

SPC

An SPC card is used to define a single point constraint at a grid point. For example, this card may be used to

constrain a point to move only in the vertical or horizontal direction, or may constrain the point not to rotate about a given axis.

DISPLACEMENT

DISPLACEMENT is an output request card that is used in the Case Control Deck. Various options on this card allow the displacement output to be printed or plotted for all grid points, or a subset of the grid points.

ELSTRESS

The ELSTRESS card is used to control output of the element stresses of selected elements (defined by appropriate SET cards).

GPFORCE

The GPFORCE card is used to request a printout of the force balance at each of a set of grid points specified by parameters on the card.

GPSTRESS

The GPSTRESS card is used to produce a printout of stress at a grid point or a set of grid points.

TEMPD

The TEMPD card is used to define the temperature of all grid points not specified by other temperature definition cards.

TEMPP3

The TEMPP3 card is used to define a temperature field for a homogeneous plate element for the determination of thermal loading, temperature dependent material properties, and stress recovery. The temperature data is tabulated for the cross section. This card was used to define a temperature gradient in the deck for thermal effect studies described below.

TEMPRB

TEMPRB is used to define the temperature field for bar, beam, and other elements for determining thermal loading, temperature-dependent material properties, and stress recovery. This card was used in the bridge model to "simulate" girder camber growth by specifying a temperature gradient from the top to the bottom of the girder.

A.2.4 A Simple Bridge Span Model

A simple bridge span model will be discussed to show how the elements of NASTRAN are used to model it. Fig. A-1 shows the construction of the model.

The deck of the bridge is modeled by a pair of two quad4 elements. These elements are defined by the node numbers at the corners of the elements, so that the first element is defined by nodes 1-2-5-4 and the second by nodes 2-3-6-5. It can be noted that the nodes are located on the central plane of the deck. The thickness of the deck and

its static properties in various directions would be defined in the data deck.

The girders of the bridge are defined using the nodes of the deck, not separate nodes. The first girder (lower right) is composed of bar elements, the first connecting nodes 1 and 2, and the second connecting nodes 2 and 3. Since these girder elements do not occupy the same space as the deck, they are attached to the nodes by an offset distance separating the girder neutral axis from the grid point. This places the girder below the deck at the proper distance. Because of the continuity of the deflections of the finite element model, the two bar elements (1-2 and 2-3) model the continuous girder from node 1 to node 3. The second girder is modeled by two other bar elements in the same fashion, from 4 to 5 and from 5 to 6.

The supports of the bridge span at each end of each girder are modeled as separate springs in the vertical (z) and longitudinal (x) directions. To each of nodes 1, 3, 4, and 6 is attached a vertical spring to account for the vertical compliance of the supports. Hence, the bridge is imagined to rest on, or hang from, springs at the nodes at the ends of each girder. The elas2 element is used for the definitions of the spring elements. The vertical spring element is used to model the vertical compression of the neoprene pads. Even though the pads are at the bottom of the girders, their vertical deflections are in a direction that passes through the nodes at the ends of the girders,

and so the deflections may be modeled as if they occurred at those nodes.

The horizontal deflection of the neoprene pads is modeled by a spring element located in the horizontal direction parallel to the longitudinal axis of each girder. Because the deflection motion of the pads is not in line with the node at the end of the girder (and deck), a rigid bar connection was used in the modeling. This rigid bar (RBAR) is connected from the node at the end of the girder, for example, node 1, to another new node directly below it at a distance that corresponds to the bottom of the girder. An elastic element is connected to the node at the bottom of this bar that acts in the longitudinal (x) direction. The deflections modeled here arise from the curvature induced on the bottom surface of the girder by the load.

A diaphragm connection between two girders is modeled as a bar element connected between grid point nodes 2 and 5 with offsets. The offset positions the bar element at the centerline level of the diaphragm.

In NASTRAN, forces applied to a structure, such as F1 in the figure, can only be applied at the defined nodes. Hence, to model the correct application of F1, the model must be redefined with a node at its application point, or the force F1 must be resolved into equivalent forces at the surrounding nodes 1, 2, 4, and 5. Both methods were used in this modeling. The chief advantage of introducing additional nodes to the model is the increase in information

that can be obtained from the model, since the output of NASTRAN is generally restricted to forces and deflections at the node points. Since much of this project was concerned with the study of forces, moments, stresses, and deflections in the area between the neighboring steel and concrete girders, some of the models to be described contain additional nodes in this area to provide a finer resolution in the output data. However, no apparent increase in accuracy was observed as a result of the introduction of additional nodes.

To model the application of the load force through the tires of the trucks and the overload truck crane, the force of each tire was modeled as a uniform pressure over a specified area. This area corresponded closely to the shape and location of small quad4 elements used in the area of the bridge between the steel and concrete girders.

Finally, constraints were used to make the model more manageable. The supports at the fixed ends of the elastic elements are constrained so as not to move at all. Also, since all of the test loads on the bridge span were symmetric about the lateral centerline of the span (through nodes 2 and 5 of the model), it was decided to model only one half of the span. If the span in the Fig. A-1 were symmetrically loaded about the 2-5 centerline, then deflections would be symmetric about the 2-5 centerline as well. Maximum deflections would occur at 2 and 5, and the section of the span near 2 and 5 would be horizontal in the

longitudinal (x) direction. The span deflections can be modeled by only modeling one half of the span, and constraining the deflections of nodes 2 and 5 (all nodes on the centerline) to have no rotational deflection about the y axis as defined in Fig. A-1.

A.2.5 The Bonnabel Overpass Span Model

The coordinate system and node arrangement for the Bonnabel Overpass span model is shown in Fig. A-2. The x axis proceeds in the traffic direction, the y axis is perpendicular and across traffic, and the z axis is vertical. All dimensions are in inches. Coordinate dimensions are indicated along the edges of the span to locate each node.

Note that supports are modeled along the lower left side in the figure. The upper right side corresponds to the lateral centerline of the span. These nodes are not "supported," but are "constrained" to have no rotational deflection about the y axis. This effectively allows the modeling of symmetric loads on a symmetric span, while reducing the computational load almost in half.

Fig. A-3, similar to the preceding figure but without node numbers, shows the location and numbering of the principal elements connecting the nodes. These elements include the quad4 elements modeling the deck, the bar elements modeling the girders, and the bar elements modeling the diaphragms. Not shown are the elastic elements

supporting each end. The guard rails are included in the model.

A high node density is used to model the span deck between the steel and concrete girders. Additional nodes are also used to model the deck in the sections between concrete girders G-2 and G-3 and steel girders G-4 and G-5 to provide additional detail and allow an accurate positioning of the test loads.

The test loads are described as load sets in a subsequent section of this report. Each load set corresponds to the array of forces presented by the test loads through the tire prints.

A.2.6 Modeling Temperature Effects

Two temperature related effects were modeled using the NASTRAN model and the cards described in the previous section.

Effects on the bridge from large changes in temperature were studied. For example, if a weather front passed the overpass, the steel girders would heat up or cool off much faster than the concrete girders, leading to distortion of the deck and related stresses in the deck section between neighboring steel and concrete girders. This effect was modeled in the NASTRAN bridge model by declaring the steel girders to be a different temperature than the concrete girders. The TEMPRB card was used to impose different uniform temperatures on the girders.

The warming effect of sunshine on the deck was also modeled. The TEMPP3 card was used to model a temperature gradient in the deck from the top to the bottom to account for this effect. Different gradients were modeled to depict the gradual warming of the top surface of the deck relative to the bottom.

A.2.7 Modeling Camber Growth

Camber growth in concrete girders is an important consideration in the development of this model.

To simulate camber growth, a fictional temperature gradient is imposed on the concrete girders from top to bottom. This gradient was chosen to produce the appropriate camber in the girder. The resulting stress distribution in the deck was then studied. Although temperature distribution in the girder is "fictional," since it was chosen to produce the required amount of camber growth, the stresses in the deck and moments in the girders will model the actual stresses and moments due to camber growth in the girder.

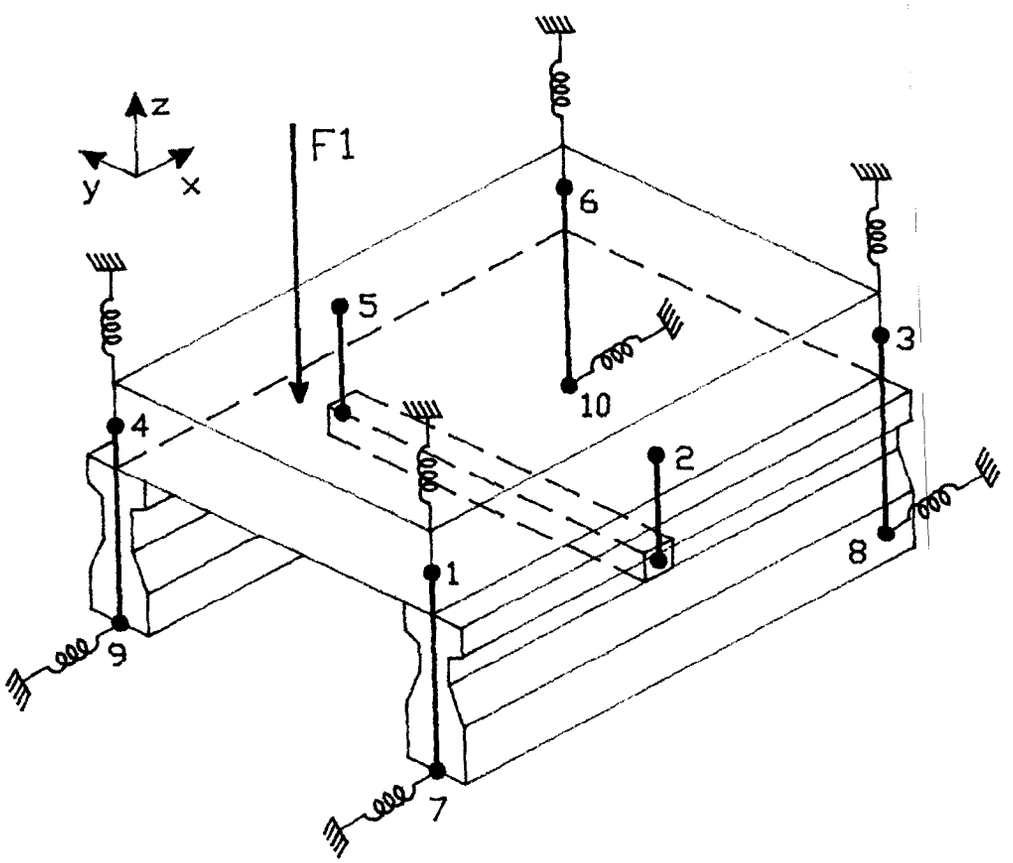

FIG. A-1 SIMPLE BRIDGE MODEL

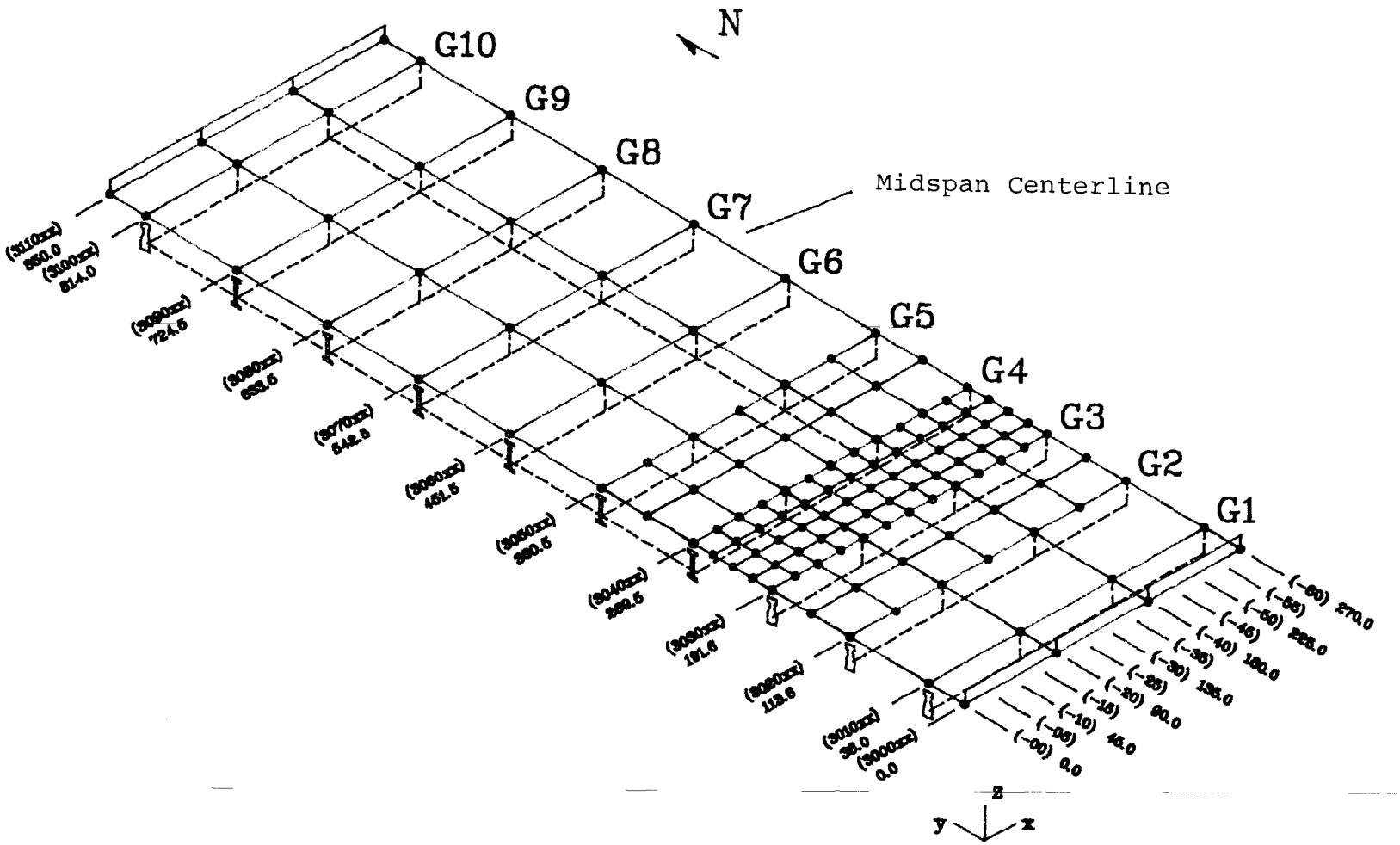

FIG. A-2 BRIDGE MODEL GRID PATTERN

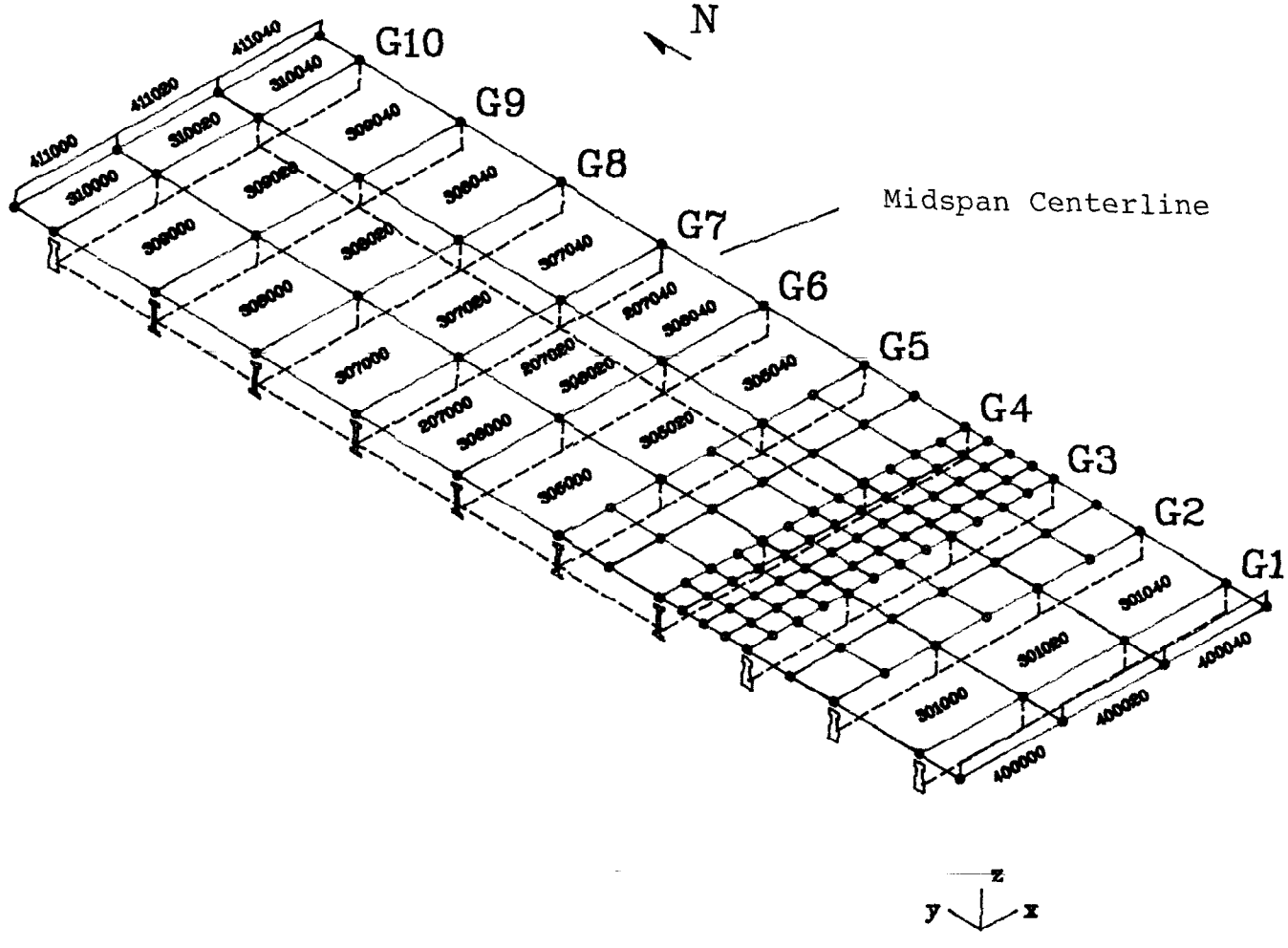

FIG. A-3 BRIDGE MODEL SELECTED ELEMENTS